Aus der
Klinik für Strahlentherapie und Radioonkologie
des Universitätsklinikums Bonn
Direktorin: Univ.-Prof. Dr. med. Eleni Gkika

Verträglichkeit und Wirksamkeit akzelerierter und zielgerichteter strahlentherapeutischer Behandlungskonzepte in der Neuroonkologie

Habilitationsschrift
zur Erlangung der venia legendi
der Hohen Medizinischen Fakultät
der Rheinischen Friedrich-Wilhelms-Universität Bonn
für das Lehrgebiet
„Experimentelle Strahlentherapie“

Vorgelegt von
Dr. med. Julian Philipp Layer
Wissenschaftlicher Mitarbeiter
an der Rheinischen Friedrich-Wilhelms-Universität Bonn

Bonn 2024
Online veröffentlicht 2026

Die folgend aufgelisteten sechs Originalarbeiten liegen dieser kumulativen Habilitationsschrift, welche die wesentlichen Ergebnisse der Publikationen zusammenfasst und diskutiert, zugrunde.

1. Giordano FA*, **Layer JP***, Leonardelli S*, Friker LL, Turiello R, Corvino D, Zeyen T, Schaub C, Mueller W, Sperk E, Schmeel LC, Sahm K, Oster C, Kebir S, Hambsch P, Pietsch T, Bisdas S, Platten M, Glas M, Seidel C, Herrlinger U*, Hölzel M*. L-RNA aptamer-based CXCL12 inhibition combined with radiotherapy in newly-diagnosed glioblastoma: dose escalation of the phase I/II GLORIA trial. Nat Commun. 2024 May 28;15(1):4210. DOI: 10.1038/s41467-024-48416-9

   (*Impact factor 2022: 16.6*)

2. Hamed M*, Potthoff AL*, **Layer JP**, Koch D, Borger V, Heimann M, Scafa D, Sarria GR, Holz JA, Schmeel FC, Radbruch A, Güresir E, Schäfer N, Schuss P, Garbe S, Giordano FA, Herrlinger U, Vatter H, Schmeel LC*, Schneider M*. Benchmarking Safety Indicators of Surgical Treatment of Brain Metastases Combined with Intraoperative Radiotherapy: Results of Prospective Observational Study with Comparative Matched-Pair Analysis. Cancers (Basel). 2022 Mar 16;14(6):1515. DOI: 10.3390/cancers14061515

   (*Impact factor: 5.2*)

3. **Layer JP***, Hamed M*, Potthoff AL, Dejonckheere CS, Layer K, Sarria GR, Scafa D, Koch D, Köksal M, Kugel F, Grimmer M, Holz JA, Zeyen T, Friker LL, Borger V, Schmeel FC, Weller J, Hölzel M, Schäfer N, Garbe S, Forstbauer H, Giordano FA, Herrlinger U, Vatter H, Schneider M*, Schmeel LC*. Outcome assessment of intraoperative radiotherapy for brain metastases: results of a prospective observational study with comparative matched-pair analysis. J Neurooncol. 2023 Aug;164(1):107-116. DOI: 10.1007/s11060-023-04380-w

   (*Impact factor 2022: 3.9*)

4. **Layer JP**, Shiban E, Brehmer S, Diehl CD, de Castro DG, Hamed M, Dejonckheere CS, Cifarelli DT, Friker LL, Herrlinger U, Hölzel M, Vatter H, Schneider M, Combs SE, Schmeel LC, Cifarelli CP, Giordano FA, Sarria GR*, Kahl KH*. Multicentric assessment of safety and efficacy of combinatorial adjuvant brain metastasis treatment by intraoperative radiotherapy and immunotherapy. Int J Radiat Oncol Biol Phys. 2024 Apr 1;118(5):1552-1562. DOI: 10.1016/j.ijrobp.2024.01.009

   (*Impact factor 2022: 7.0*)

5. **Layer JP**, Layer K, Sarria GR, Röhner F, Dejonckheere CS, Friker LL, Zeyen T, Koch D, Scafa D, Leitzen C, Köksal M, Schmeel FC, Schäfer N, Landsberg J, Hölzel M, Herrlinger U, Schneider M, Giordano FA, Schmeel LC. Five-Fraction Stereotactic Radiotherapy for Brain Metastases—A Retrospective Analysis. Curr Oncol. 2023; 30(2):1300-1313. DOI: 10.3390/curroncol30020101

   (*Impact factor 2022: 2.6*)

6. Dejonckheere CS*, **Layer JP***, Hamed M, Layer K, Glasmacher A, Friker LL, Potthoff AL, Zeyen T, Scafa D, Koch D, Garbe S, Holz JA, Kugel F, Grimmer M, Schmeel FC, Gielen GH, Forstbauer H, Vatter H, Herrlinger U, Giordano FA, Schneider M, Schmeel LC, Sarria GR. Intraoperative or postoperative stereotactic radiotherapy for brain metastases: time to systemic treatment onset and other patient-relevant outcomes. J Neurooncol. 2023 Sep;164(3):683-691. DOI: 10.1007/s11060-023-04464-7

   (*Impact factor 2022: 3.9*)

* Geteilte Erst-/Letztautorenschaft

Datum des Habilitationskolloquiums: 30.01.2025

Aus Gründen der besseren Lesbarkeit wird auf den folgenden Seiten ausschließlich das generische Maskulinum verwendet. Sämtliche Personenbezeichnungen gelten gleichermaßen für alle Geschlechter.

Inhaltsverzeichnis

Gewidmet meiner Frau Katharina

„I will love you as a drawer loves a secret compartment, and as a secret compartment loves a secret, and as a secret loves to make a person gasp...
I will love you until all such compartments are discovered and opened, and all the secrets have gone gasping into the world."
Lemony Snicket, The Beatrice Letters

1. Abkürzungsverzeichnis

BHS	Blut-Hirn-Schranke
CEST	*Chemical exchange saturation transfer*
CT	Computertomographie
CTCAE	*Common Terminology Criteria for Adverse Events*
CTV	*Clinical target volume*
DSC	Perfusionsbildgebung (*dynamic susceptibility contrast*)
DWI	Diffusionsbildgebung (*diffusion weighted imaging)*
EBRT	Perkutane Bestrahlung (*external beam radiotherapy*)
EQD2	2 Gy-Äquivalenzdosis (*equivalent dose of 2 Gy*)
FSRT	Fraktionierte stereotaktische Strahlentherapie
GBM	Glioblastom
GTV	*Gross tumor volume*
ICI	Immuncheckpointinhibitor
IGRT	Bildgeführte Strahlentherapie (*image guided* radiotherapy)
IMRT	Intensitätsmodulierte Radiotherapie
IORT	Intraoperative Radiotherapie
MGMT	O6-Methylguanin-DNA-Methyltransferase
MRT	Magnetresonanztomographie
NOX-A12	Olaptesed pegol
OAR	Risikoorgan (*organ at risk)*
OS	Gesamtüberleben (*overall survival*)
PFS	Progressionsfreies Überleben (*progression-free survival*)
PTV	*Planning target volume*
RBE	Relative biologische Effektivität
RN	Radionekrose
RNA	Ribonukleinsäure (*ribonucleic acid*)
SBRT	Stereotaktische Bestrahlung (*stereotactic body radiotherapy*)
SRS	Stereotaktische Radiochirurgie (*stereotactic radiosurgery)*
SOC	*Standard of care*
TME	Tumormikromilieu (*tumor microenvironment*)

TMZ	Temozolomid
TT	Zielgerichtete Therapie (*targeted therapy*)
$V_{100\%}$	Volumen mit Dosisbelastung mit 100% der Verschreibung
WBRT	Ganzhirnbestrahlung (*whole brain radiotherapy)*
WHO	Weltgesundheitsorganisation (*World Health Organization*)
ZNS	Zentrales Nervensystem

2. Einleitung

2.1 Klassifikation maligner Hirntumoren

Hirntumoren werden im Hinblick auf ihre Ätiologie unterschieden in primäre, sogenannte hirneigene Tumoren und sekundäre, metastatische Hirntumoren. Die Histologie, Therapie und Prognose primärer und sekundärer Hirntumoren unterscheiden sich mitunter erheblich. Gemeinsam haben die Hirntumoren jedoch die klinische Symptomatik, die primär von Lokalisation, Größe und Wachstumsgeschwindigkeit der Läsionen abhängig ist. In Bezug auf ihren zellulären Ursprung werden primäre Hirntumoren grob unterschieden in gliale und nicht-gliale Tumoren und in Bezug auf ihre Dignität in maligne und benigne Tumoren (Louis *et al.*, 2021). Hirnmetastasen weisen ebenfalls verschiedene zugrundeliegende Entitäten auf, werden grundsätzlich jedoch den malignen Hirntumoren zugeordnet. Die Diagnostik der Wahl zur weiteren Abklärung ist die Durchführung einer (neuro-)radiologischen Bildgebung mittels Computertomographie (CT) oder besser Magnetresonanztomographie (MRT) und die Verknüpfung der Ergebnisse mit anamnestischen und klinischen Befunden (Suh *et al.*, 2020). Neben behandlungsbedürftigen malignen Prozessen wie höhergradigen Gliomen oder Metastasen kommen auch Lymphome und zahlreiche benigne intrazerebrale Befunde differentialdiagnostisch in Betracht. So können die prognostisch ebenfalls ungünstigen Lymphome bildgebend wie primäre Hirntumoren erscheinen, sprechen in der Regel initial jedoch rasch auf eine Kortisontherapie an (Ferreri *et al.*, 2023). Benigne Hirntumoren gehen mit einer deutlich geringer ausgeprägten Wachstumsdynamik und damit auch einem latenteren klinischen Verlauf einher, wobei in vielen Fällen dennoch eine Notwendigkeit zur medizinischen Intervention besteht (Ogasawara *et al.*, 2021). Auch wenn sich insbesondere durch moderne Bildgebung mittels dünnschichtiger MRT-Sequenzen bereits wichtige Hinweise ergeben, kann eine definitive Zuordnung der Tumorentität erst nach histologischer Sicherung im Rahmen einer chirurgischen Biopsie oder Resektion erfolgen. Bei Vorliegen eines hochgradigen Glioms oder einer zerebralen Metastasierung solider Tumoren besteht eine Indikation zur zeitnahen zerebralen Strahlentherapie, wobei eine ganze Reihe strahlentherapeutischer Verfahren, Techniken

und Dosierungsschemata sowie gegebenenfalls deren Kombination mit Systemtherapien zur Anwendung kommen kann.

2.2 Primäre Hirntumoren - Das Glioblastom

Das Glioblastom (GBM) ist der häufigste maligne primäre Hirntumor des Erwachsenen und geht mit einer schlechten Prognose einher. Während eine Erkrankung in prinzipiell jeder Altersgruppe möglich ist, sind die meisten Patienten über 55 Jahre alt (Ostrom *et al.*, 2019). Männer sind relativ gesehen häufiger betroffen als Frauen. Der einzige wissenschaftlich anerkannte Risikofaktor für die GBM-Entstehung ist eine vorhergehende Bestrahlung im Kopf/Hals-Bereich. Demgegenüber suggerieren verfügbare epidemiologische Daten einen protektiven Effekt von Erkrankungen aus dem atopischen Formenkreis (Ostrom et al, 2019). Der biologische Hintergrund der Erkrankung ist insgesamt noch unzureichend verstanden und Gegenstand gegenwärtiger wissenschaftlicher Diskussionen. Aktuelle Konzepte postulieren eine Gliomentstehung aus neuroglialen Stammzellen oder Progenitorzellen aus dem Bereich der Subventrikularzone des Gehirns (Lee *et al.*, 2018; Jung *et al.*, 2019). Pathologisch charakterisiert sich das GBM als diffuses astrozytäres Gliom mit Vorliegen einer Trias aus mikrovaskulären Gefäßproliferaten, Nekrosearealen sowie gegebenenfalls spezifischen molekularen Auffälligkeiten (Weller *et al.*, 2021). Die diagnosebestimmende *World Health Organization* (WHO)-Klassifikation für Tumoren des zentralen Nervensystems (ZNS) wurde im Jahr 2021 erheblich überarbeitet, um den zwischenzeitlich neugewonnenen molekulargenetischen Erkenntnissen und ihren prognostischen Implikationen Rechnung zu tragen (Louis *et al.*, 2021). Hierdurch ergaben sich zahlreiche Verschiebungen in der diagnostischen Einteilung von Gliomen, was letztlich zu einer deutlich strengeren Grenzziehung prognostisch günstiger Gliome zum Glioblastom führte. So wurden etwa IDH-mutierte Gliome grundsätzlich aufgrund ihrer therapeutisch adressierbaren Mutation (Melinghoff *et al.*, 2023) und des vorteilhafteren klinischen Verlaufs ausgegliedert und von den GBM abgegrenzt (Reuss, 2023). Studien, die auf älteren Versionen der WHO-Klassifikation basieren, sind insofern nur noch eingeschränkt mit neueren Daten auf Grundlage der aktuellen Klassifikation vergleichbar. Gliome mit prognostisch günstigeren molekularen Eigenschaften waren Teil älterer Studienkohorten und können daher zu einer

Heterogenität der Studienpopulation erheblich beitragen und die Bewertung der Ergebnisse deutlich erschweren.

Das GBM zeichnet sich ferner molekularpathologisch und -genetisch intra- wie auch interindividuell durch eine erhebliche, zudem auch dynamische Heterogenität aus (Wang *et al.*, 2022; Eisenbarth und Wang, 2023). Forschungsbemühungen der vergangenen Jahre zielten auf eine Charakterisierung der wichtigsten GBM-Subtypen ab (Aldape *et al.*, 2015). Der proneurale Subtyp ist der häufigste in jungen Erwachsenen und geht mit einer CDK4- und PDGFRa-Amplifikation einher. Der klassische Subtyp ist mit einer EGFR-Amplifikation und einem homozygoten CDKN2A- oder CDKN2B-Verlust assoziiert. Der häufig einen NF1-Verlust aufweisende mesenchymale Subtyp wird mit einem besonders aggressiven Verlauf sowie einer Tumorinfiltration durch Makrophagen in Verbindung gebracht. Faktisch finden sich dynamische Mischbilder der genannten Subtypen und außerhalb experimentaltherapeutischer Ansätze ergeben sich hieraus bislang keine spezifischen Implikationen. Zahlreiche aktuelle Studien versuchen jedoch, molekulargenetische Auffälligkeiten und Tumorphänotypen therapeutisch zu adressieren (Alexander *et al.*, 2018; Le Rhun *et al.*, 2019; Wick *et al.*, 2019).

Standardtherapie des GBM ist die maximale chirurgische Resektion, gefolgt von einer Radiotherapie oder Radiochemotherapie (Weller *et al.*, 2021). Der bislang einzige etablierte prädiktive Biomarker im GBM ist der O6-Methylguanin-DNA-Methyltransferase (MGMT)-Promotor-Methylierungsstatus. Ca. 40% bis 50% aller Patienten weisen eine MGMT-Promotor-Methylierung auf (Hegi *et al.*, 2005). Diese Patienten profitieren erheblich stärker von einer systemischen Chemotherapie mit Temozolomid (TMZ) und überleben die Erkrankung im Durchschnitt etwa 50% länger (Hegi *et al.*, 2005; Stupp *et al.*, 2009). Bei hohem Patientenalter kann bei Vorliegen einer MGMT-Promotor-Methylierung auf eine Bestrahlung verzichtet und eine alleinige TMZ-Therapie durchgeführt werden (Wick *et al.*, 2012). Jüngere MGMT-Promotor-methylierte Patienten in hinreichend gutem Allgemeinzustand können zusätzlich von einer Ergänzung des Alkylans Lomustin im Rahmen der Radiochemotherapie profitieren (Herrlinger *et al.*, 2019). Der Nutzen der TMZ-Therapie in MGMT-Promotor-unmethylierten GBM-Patienten ist hingegen umstritten. Eine *Post-hoc*-Analyse gemäß der aktualisierten WHO-Klassifikation als GBM definierter Fälle aus der nach damaliger Definition bei

anaplastischen Astrozytomen durchgeführten CATNON-Studie zweifelt gar generell die Wirksamkeit der TMZ-Therapie im GBM an (Tesileanu *et al.*, 2022). Eine Ergänzung elektrischer Wechselfelder (*tumor treating fields*) nach Abschluss der Radiochemotherapie zeigte in der Erstlinie ein verbessertes Gesamtüberleben und ist zwar noch kein SOC, stellt aber die jüngste Neuerung in den etablierten Verfahren dar (Stupp *et al.*, 2017). Zahlreiche Studien mit neuen therapeutischen Ansätzen sind in den vergangenen Jahren gescheitert, darunter auch viele Medikamente insbesondere aus dem Bereich der Immuntherapien, die sich in anderen Tumorentitäten als überaus wirksam erwiesen (Reardon *et al.*, 2020; Lim *et al.*, 2022; Omuro *et al.*, 2023). Ausweislich aktueller Krebsregisterdaten bleibt die Erkrankung letztlich trotz aller therapeutischen Bemühungen infaust und weist eine Fünfjahresüberlebensrate von deutlich unter 10% auf (Ostrom *et al.*, 2019). Aufgrund dieser sehr eingeschränkten klinischen Perspektiven empfiehlt auch die deutsche Leitlinie für Gliome ausdrücklich, einen Einschluss insbesondere der MGMT-Promotor-unmethylierten Patienten in Studien zu prüfen (Wick *et al.*, 2021).

2.3 Sekundäre Hirntumoren - Hirnmetastasen

Bis zu 40% aller Patienten mit soliden malignen Tumoren beklagen im Laufe ihrer Erkrankung eine zerebrale Metastasierung (Cagney *et al.*, 2017). Da sich die Gesamtprognose der Erkrankungen in vielen Fällen durch die verbesserten systemtherapeutischen Behandlungsoptionen mit zielgerichteten Therapien (*targeted therapies*, TTs) und insbesondere den neuen immuntherapeutischen Ansätzen wie Immuncheckpointinhibitoren (ICIs) verbessert hat (Antonia *et al.*, 2018; Haslam und Prasad; 2019), ist ein indirekter Nebeneffekt dieses Fortschritts auch eine durch den protrahierten Verlauf bedingt steigende Inzidenz zerebraler Metastasen (Nayak *et al.*, 2012; Davis *et al.*, 2012). Ein weiterer Grund für steigende Inzidenzen sind die verbesserten Detektionsraten durch immer breiter verfügbare und technologisch fortschrittlichere Bildgebungsverfahren (Bernstock *et al.*, 2022). Die Tumorentitäten, die absolut betrachtet am häufigsten intrazerebral metastasieren, sind das Lungenkarzinom, das Maligne Melanom, das Mammakarzinom und das Nierenzellkarzinom (Lamba *et al.*, 2021). Während Hirnmetastasen unter Ausnutzung der heutzutage gegebenen medizinischen Therapieoptionen nicht notwendigerweise einen relevanten Einfluss auf

das Gesamtüberleben ausüben (Yamamoto *et al.*, 2012; Nieder *et al.*, 2022), ist ihre lokale Behandlung in vielen Fällen unabdingbar, um einer neurologischen Verschlechterung und der damit einhergehenden, potenziell erheblichen Einschränkung der Lebensqualität (Schödel *et al.*, 2013; Verhaak *et al.*, 2019) vorzubeugen. Die Prognose von zerebral metastasierten Patienten ist abhängig von tumorspezifischen Faktoren wie dem Allgemeinzustand, dem Alter, der Anzahl der zerebralen Metastasen sowie dem extrazerebralen Ausbreitungsstatus und insgesamt weitgehend infaust (Sperduto *et al.*, 2011). Eine Auswertung von knapp 10.000 Datensätzen von Patienten mit zerebraler Metastasierung unterschiedlicher Entitäten ergab ein medianes Gesamtüberleben (*overall survival*, OS) nach Diagnosestellung von weniger als vier Monaten (Lamba *et al.*, 2021). Auch bei synchroner zerebraler Metastasierung lag das mediane OS entitätsunabhängig unter zwölf Monaten (Cagney *et al.*, 2017).

Tumorzellen müssen zur Absiedelung einer zerebralen Metastase nach Zurücklegen großer Strecken über die Blutgefäße und Anheftung an die zerebralen Endothelzellen letztlich die Blut-Hirn-Schranke (BHS) durchqueren. Dies gelingt durch Expression von speziellen Proteinprogrammen zur Adhäsion, Extravasation, Proteolyse, Migration, Immunzellinteraktion und Proliferation (Eichler *et al.*, 2011). Mit Erweiterung der therapeutischen Handlungsspielräume durch Etablierung neuer, gegen diese Programme zielgerichteter Substanzklassen oder versierterer strahlentherapeutischer Techniken haben sich auch die Behandlungsmöglichkeiten für Hirnmetastasen verbessert. Zerebrale Metastasierungswege stellen jedoch weiterhin eine besondere Herausforderung für die klinischen Behandler dar. Es kommt häufig zu einem zum Gesamterkrankungsstatus diskrepanten lokalen Therapieansprechen (Seute *et al.*, 2006; Mehta *et al.*, 2009). Hierfür gibt es verschiedene Gründe. So verhindert die BHS in bestimmten Fällen eine suffiziente intrazerebrale Wirksamkeit zahlreicher Wirkstoffe (Di Giacomo *et al.*, 2019). Ferner bedingt eine erworbene Therapieresistenz aufgrund der häufig mehreren vorhergehenden Therapielinien möglicherweise eine Resistenz (Brastianos *et al.*, 2015). Zuletzt ist eine unabhängige, vom Primarius abweichende molekulargenetische Evolution von zerebralen Metastasen beschrieben, die einerseits eine Notwendigkeit für lokalspezifische systemtherapeutische Schritte nahelegt (Brastianos *et al.*, 2015) und andererseits Implikationen für die Wirksamkeit strahlentherapeutischer Behandlungskonzepte haben kann.

2.4 Lokale Standardtherapieverfahren

Die lokale Therapie von malignen Hirntumoren ist von zahlreichen Faktoren abhängig und letztlich sind Entscheidungen interdisziplinär sowie in gemeinsamer Abstimmung mit dem Patienten zu treffen. Insbesondere der klinische Allgemeinzustand des Patienten, die lokale Symptomatik, Größe und anatomische Lage der Läsion sind zu berücksichtigen. Falls sicher durchführbar, ist bei großen oder klinisch symptomatischen (Aizer *et al.*, 2022) sowie auch bei solitären Raumforderungen (Lamba *et al.*, 2019) eine chirurgische Resektion indiziert. Auch bei Unsicherheit bezüglich der Entität oder, genereller, der Dignität der Läsion sollte zwecks histologischer Sicherung eine Probenentnahme erfolgen, die gegebenenfalls dann auch als vollständige Resektion durchgeführt werden kann (Aizer *et al.*, 2022). Eine möglichst umfassende Resektion des Tumorgewebes ist grundsätzlich sowohl beim GBM als auch bei Hirnmetastasen anzustreben (Weller *et al.*, 2021; Aizer *et al.*, 2022) und beim GBM unbestritten prognostisch bedeutsam (Stummer *et al.*, 2009). Mit einer chirurgischen Resektion von Hirnmetastasen lässt sich gemäß der aktuellen Literaturlage eine Lokalkontrollrate von ca. 40% bis 50% nach einem Jahr erzielen (Mahajan *et al.*, 2017; Churilla *et al.*, 2019). Für das Glioblastom besteht neben dem positiven Effekt auf die lokale Tumorkontrolle auch ein erwiesener positiver Einfluss auf das Gesamtüberleben (Karschnia *et al.*, 2023). Für die Relevanz der kompletten Resektion von Hirnmetastasen für das OS finden sich hingegen widersprüchliche Angaben (Jünger *et al.*, 2021; Baumgart *et al.*, 2023).

Eine vermutete Ursache für die häufige lokale Tumorrekurrenz nach Resektion von Hirnmetastasen ist der intraoperativ nicht darstellbare Verbleib mikroskopischer Tumorreste im Bereich der Resektionshöhle. Diesbezüglich stellt die Strahlentherapie eine ideale Ergänzung zur chirurgischen Resektion dar, da sie bei adjuvanter Anwendung großflächig und ohne dimensionale Limitationen verbliebene Tumorzellen unschädlich machen kann. Dies zeigt sich auch in den lokalen Kontrollraten, die durch eine adjuvante perkutane Bestrahlung (*external beam radiotherapy*, EBRT) abhängig insbesondere von der Größe der Läsionen und dem gewählten strahlentherapeutischen Verfahren auf ca. 70 bis 85% ansteigen (Kocher *et al.*, 2011; Mahajan *et al.*, 2017; Lehrer *et al.*, 2019; Eitz *et al.*, 2020). Falls die oben genannten Gründe für eine unmittelbare Resektion von Hirnmetastasen nicht vorliegen, sollte dem Patienten unabhängig von der Anzahl der

Läsionen eine definitive Bestrahlung angeboten werden. Auch diese erzielt eine sehr gute lokale Kontrolle von bis zu 90% in einem Jahr bei guter Verträglichkeit (Minniti *et al.*, 2011; Yamamoto *et al.*, 2014; Minniti *et al.*, 2016). Bezüglich der Zielvolumendefinition und der Dosisverschreibung ergeben sich regional und institutionell erhebliche Unterschiede. Insbesondere gibt es bisher noch keine evidenzbasierte allgemeingültige Empfehlung für die strahlentherapeutische Behandlung von Hirnmetastasen. Bis in die 2010er Jahre wurde die adjuvante und auch definitive Bestrahlung von Hirnmetasten in aller Regel in Form einer Ganzhirnbestrahlung (*whole brain radiotherapy*, WBRT) durchgeführt. Trotz vergleichbarer Lokalkontrollraten und insgesamt überzeugender distanter intrazerebraler Kontrolle (Brown *et al.*, 2017) wurde dieser Behandlungspfad mittlerweile größtenteils verlassen, da zahlreiche Studien eine unterlegene Toxizität insbesondere mit einem erheblichen negativen Einfluss der WBRT auf die Neurokognition (Chang *et al.*, 2009; Kocher *et al.*, 2011; Brown *et al.*, 2017) und die Lebensqualität (Mulvenna *et al.*, 2016) nachweisen konnten. Stattdessen zogen modernere, zielgerichtetere Verfahren wie die stereotaktische Radiochirurgie (*stereotactic radiosurgery*, SRS) und die fraktionierte stereotaktische Strahlentherapie (*fractionated stereotactic radiotherapy*, FSRT) ein, die mit erheblich höheren technischen Anforderungen und höherem planerischem Aufwand einhergehen. Technisch betrachtet kann hierdurch selbst bei deutlich über zwölf Hirnmetastasen noch auf eine WBRT verzichtet werden (Becker *et al.*, 2023). Während in den USA die einzeitige SRS sowohl im adjuvanten (Brown *et al.*, 2017) als auch im definitiven (Minniti *et al.*, 2011; Lehrer *et al.*, 2019) Setting präferiert wird, ist das Bild in Europa etwas uneinheitlicher und vielfältiger. Die SRS ist hier ebenfalls die primäre Behandlungsoption für die definitive Bestrahlung kleiner Läsionen, wird jedoch in aller Regel nicht für eine adjuvante Bestrahlung genutzt. Hier setzt man ebenso wie für größere Läsionen vielmehr auf die FSRT, die in einem Rahmen von ca. drei (Doré *et al.*, 2017; Minniti *et al.*, 2016; Eitz *et al.*, 2020) bis maximal zwölf Fraktionen (Putz *et al.*, 2022) appliziert wird. Generell sind größere Läsionen sowie geringere Strahlendosen im Randbereich mit einer reduzierten Lokalkontrolle assoziiert (Vogelbaum *et al.*, 2006; Han *et al.*, 2012).

Auch beim GBM verbessert die adjuvante EBRT die lokale Kontrolle und zusätzlich auch das Gesamtüberleben selbst in fragilen Patientensubgruppen (Keime-Guibert *et al.*, 2007). Anders als bei der Behandlung von Hirnmetastasen ist jedoch aufgrund der

Tumoraggressivität, der Migrationsneigung der Gliomzellen und der diffusen Infiltration in den Übergangsbereichen zum gesunden Gewebe beim GBM unabhängig von den ohnehin häufig bereits größeren GTV ein signifikant erweiterter Sicherheitssaum für das CTV zu berücksichtigen (Nyazi *et al.*, 2023). Für die strahlentherapeutische Primärtherapie eignet sich daher am besten ein normofraktionierter (Stupp *et al.*, 2009) oder bei älteren Patienten in reduziertem Allgemeinzustand ein milde hypofraktionierter (Perry *et al.*, 2017) Ansatz. FSRT und SRS kommen hingegen bevorzugt in Rezidivsituationen zum Einsatz, in denen die Strahlentherapie ebenfalls einen sehr hohen Stellenwert hat (Minniti *et al.*, 2021; Tsien *et al.*, 2023).

2.5 Alternative intrakavitäre strahlentherapeutische Lokalverfahren

Eine Reihe intrakavitärer strahlentherapeutischer Behandlungsverfahren steht als Alternative für die oben genannten perkutanen Techniken zur Verfügung. Als eine mögliche intrakavitäre Behandlungsform ist eine dauerhafte Implantation radioisotopischer *Seeds* im Rahmen der Resektion möglich. Diese birgt bei vergleichbaren Tumorkontrollraten jedoch neben dem immanenten Risiko einer Dislokation oder arterieller Verschlüsse (Bernstein *et al.*, 1993) insbesondere ein erhebliches Risiko für symptomatische postradiogene Veränderungen (Huang *et al.*, 2009). Ebenso geht die selten angewandte Brachytherapie zerebraler Metastasen bei vergleichbarer Effektivität mit erhöhten Risiken für eine Radionekrose (RN) einher (Chitti *et al.*, 2020).

In den vergangenen Jahren kam als weitere therapeutische Alternative die intraoperative Bestrahlung (*intraoperative radiotherapy*, IORT) hinzu. In der Bestrahlung des lokalisierten Mammakarzinoms konnte für die IORT in einer randomisierten Phase 3-Studie die Nichtunterlegenheit gegenüber der EBRT bei guter Verträglichkeit nachgewiesen werden (Vaidya et al, 2010). Prinzipiell eignen sich die lokalen Begebenheiten des Tumorbetts nach Resektion einer Hirnmetastase technisch betrachtet ebenfalls sehr gut für eine IORT. Hierfür gab es hingegen bislang nur wenige, teils nicht *Peer Review*-geprüfte Auswertungen kleiner retrospektiver Kohorten mit sehr geringer Evidenz, die jedoch eine mit einer EBRT vergleichbare Wirksamkeit nahelegten (Brehmer *et al.*, 2018; Cifarelli *et al.*, 2019; Kahl *et al.*, 2021). Für das Glioblastom wird aufgrund vielversprechender Phase 2-Daten (Giordano *et al.*, 2019) derzeit eine multizentrische

Phase 3-Studie durchgeführt, um das Potenzial der IORT im Sinne einer Dosiseskalation vor leitliniengerechter EBRT zu eruieren (NCT02685605). Häufig genannte Vorteile der IORT sind die unmittelbare lokale Tumorzelleradikation, die Vermeidung zusätzlicher Behandlungstermine und dezidiert lokal begrenzte Wirksamkeit. Bei der IORT handelt es sich anders als bei der EBRT, die üblicherweise mit einer Photonenenergie im Bereich von 6 bis 10 MeV appliziert wird, um eine niedrigenergetische Bestrahlungstechnik mit 50 kV. Umgebende Risikoorgane (*organs at risk*, OARs) werden aufgrund des resultierenden extrem steilen Dosisgradienten geringer belastet als bei der EBRT (Herskind *et al.*, 2017). Der an die anatomischen Begebenheiten angepasste und für die IORT von Hirntumoren in aller Regel sphärische Applikator wird noch im Rahmen der Operation nach vollständiger Resektion des Tumors und Blutungsstillung in den Operationssitus eingebracht. Ziel ist die vollständige und unmittelbare Umschließung des Applikators durch die Resektionsränder. Sodann erfolgt eine Dosisverordnung von in der Regel 20 bis 30 Gy auf die Oberfläche, wobei die gegenüber der EBRT insbesondere auf der Oberfläche erhöhte relative biologische Effektivität (RBE) der Strahlung zu beachten ist (Schneider *et al.*, 2013). Eine Verordnungsdosis von 30 Gy entspricht unter Berücksichtigung der RBE einer EQD2 bei einem $\alpha / \beta = 3$ von über 250 Gy auf der Applikatoroberfläche, was eine deutlich höhere lokale Dosis als bei einer EBRT darstellt. Nachteilig ist hingegen die ungenauere Bestimmung der örtlichen Dosisprofile und Gewebebelastungen, da diese auf Tiefendosisprofilen beruht, sich jedoch intraoperativ nur auf Grundlage einer präoperativen MRT mittels Neuronavigation orientiert werden kann. Neben der exakten Positionierung des Applikators ist auch der Umschließungsgrad des Applikators durch angrenzendes Gewebe für die Tiefe klinisch nur abschätzbar. Eine aktuelle Studie unserer Klinik (Grimmer *et al.*, 2024) untersucht daher derzeit die Möglichkeit einer intraoperativ bildgeführten Strahlentherapie (*image guided radiotherapy*, IGRT). Die Behandlungszeit einer IORT beträgt abhängig von der gewählten Applikatorgröße und der Dosisverordnung ca. zehn bis 45 Minuten. Es ergeben sich keine weiteren Termine, wodurch Patienten bei verringertem persönlichem Aufwand auch potenziell früher konsekutiven Therapien zugeführt werden können.

2.6 Verträglichkeit der intrazerebralen Strahlentherapie - Die Radionekrose und Pseudoprogression als primäre Therapiekomplikationen

Strahlung stört die Proliferation und Differenzierung neuronaler Zellen, verursacht vaskuläre Schäden mit konsekutiver Ischämie sowie Flüssigkeitsaustritt in die Extrazellulärmatrix und bedingt eine intrazerebrale Inflammationsreaktion (Wilke *et al.*, 2018). Insbesondere durch die technischen Innovationen der vergangenen 20 Jahre mit zumindest in der westlichen Welt weitgehend flächendeckender Einführung der IGRT und der intensitätsmodulierten Radiotherapie (IMRT) hat sich neben der Effektivität auch das Nebenwirkungs- und Komplikationsprofil der Strahlentherapie im Kopfbereich entscheidend verbessert (De Ruysscher *et al.*, 2019). Die Abkehr von der WBRT und die Hinwendung zu immer präziseren fokalen Bestrahlungen mittels SRS und FSRT begründet weiterhin die heutzutage sehr gute Verträglichkeit der Bestrahlung von Hirntumoren (Brown *et al.*, 2016). Abseits von niedriggradigen und transienten Symptomen wie Nausea oder Cephalgien sind vor allem postradiogene Veränderungen des Gehirns von besonderer Relevanz. Infolge hochdosierter Bestrahlung von Hirnmetastasen kommt es in ca. 5 bis 25% der Fälle zu einer fokalen RN (Bloningen *et al.*, 2010; Kohutek *et al.*, 2015; Minniti *et al.*, 2011). Typischerweise tritt die RN drei bis zwölf Monate nach Abschluss einer Bestrahlung auf, jedoch sind auch Verläufe mit jahrelanger Latenz beschrieben (Kargiotis *et al.*, 2010).

Pathophysiologisch liegt der RN am ehesten eine multifaktorielle Genese zugrunde (Vellayappan *et al.*, 2018). Die radiogene Destruktion der BHS verursacht eine verstärkte vaskuläre Gefäßpermeabilität und kapilläre Durchlässigkeit. Über unter anderem TNFα und IL-1β vermittelte Signalkaskaden kommt es zu einer Inflammation sowie Verengung und fibrinoiden Nekrose kleiner Gefäße, was letztlich auch eine Apoptose neuronaler Zellen verursacht. Durch die resultierende Hypoxie folgt zusätzlich eine Freisetzung von HIF1α und VEGF. Die VEGF-vermittelte Angiogenese führt zur Bildung vermehrt defekter, relativ permeabler Gefäße, was wiederum zu einer Verstärkung des zerebralen Ödems beiträgt (Nordal *et al.*, 2004). Die glialen Zellen werden zudem unmittelbar durch eine postradiogene Demyelinisierung geschädigt (Panagiotakos *et al.*, 2007).

Oft sind RNs asymptomatisch und treten als Zufallsbefund bzw. Differentialdiagnose der Verlaufsbildgebung zutage. Bei Symptomatik kann eine medikamentöse Therapie der RN

mittels Dexamethason oder bei Therapieversagen auch Bevacizumab angezeigt sein (Tye *et al.*, 2014). Schwerste Verläufe können eine chirurgische Resektion erforderlich machen, sind jedoch insgesamt selten. Frühzeitige medizinische Intervention kann das *Outcome* der RN verbessern (Pan *et al.*, 2022). Besonders problematisch ist die Entstehung einer RN aufgrund der häufig nicht gegebenen Unterscheidbarkeit ihres MRT-morphologischen Korrelats mit einer Progression der Tumorerkrankung (Vellayappan *et al.*, 2018; Ma *et al.*, 2019). Es besteht daher das Risiko, dass wirksame Therapien vorzeitig aufgrund einer Fehleinschätzung des Bildbefundes abgesetzt werden.

Unscharf abgegrenzt von der RN ist die sogenannte Pseudoprogression, die in aller Regel früher auftritt und häufiger einen selbstlimitierten Verlauf zeigt. Auch ihr liegt eine inflammatorische *Response* des TME auf eine Bestrahlung mit Ausbildung größenprogredienter Ödeme und zunehmender Kontrastmittelaufnahme zugrunde (Parvez *et al.*, 2014). *High Grade*-Gliome sind in erhöhtem Maße von diesen Pseudoprogressionen betroffen. Im GBM kommt es unter einer Radiochemotherapie mit TMZ in den ersten drei Monaten nach Abschluss der *Radiatio* in über 20% der Fälle zu einer Pseudoprogression (Brandsma *et al.*, 2008), wobei selbst im Rahmen von Studien mit dezidierten Bildgebungsprotokollen Pseudoprogressionen mitunter übersehen werden (Zeyen *et al.*, 2023). Vorübergehend zunehmende Kontrastmittelaufnahme wird sogar in bis zu 50% der Fälle beschrieben (Ellingson *et al.*, 2017). Die jüngst aktualisierte Version der *Response Assessment in Neuro-Oncology (RANO) criteria for high grade glioma 2.0* berücksichtigt das häufige Auftreten einer Pseudoprogression nach einer Strahlentherapie und definiert daher erstmalig nicht das postoperative, sondern das nach Abschluss der Strahlentherapie entstandene MRT als Baseline-Scan zur Beurteilung des künftigen Therapieansprechens. Ferner wird in den ersten zwölf Wochen nach Bestrahlung bei Nachweis einer Progression zunächst eine Therapiefortführung und eine Wiederholung der MRT nach mindestens vier Wochen empfohlen, bevor eine endgültige Beurteilung des Ansprechens erfolgt (Wen *et al.*, 2023). In Rezidivsituationen zeigt sich, unabhängig vom weiterhin unklaren Nutzen in Bezug auf primäre klinische Endpunkte, eine deutlich verbesserte Verträglichkeit einer *in field*-Re-Bestrahlung des GBM durch parallele Gabe von Bevacizumab (Tsien *et al.*, 2023).

Während die Einführung fortschrittlicher Diagnostik wie der diffusionsgewichteten MRT-Bildgebung (*diffusion weighted imaging,* DWI) (Detsky *et al.*, 2017), der Perfusions-MRT (*dynamic susceptibility contrast,* DSC) (Morabito *et al.*, 2019), der bislang noch nicht routinemäßig eingesetzten *chemical exchange saturation transfer* (CEST)-MRT (Zaiss *et al.*, 2015; von Knebel Doeberitz *et al.*, 2023) und insbesondere der Aminosäuren-Positronenemissionstomographie (Terakawa *et al.*, 2008) die Empfindlichkeit für die Differentialdiagnosen einerseits verbessert hat, nimmt die Inzidenz der RN andererseits möglicherweise auch aufgrund der häufigeren Kombination einer Bestrahlung von Hirnmetastasen mit Chemotherapien (Ruben *et al.*, 2006) und TTs wie ICIs (Martin *et al.*, 2018; Kim *et al.*, 2021) weiterhin zu. Auch höhere bzw. wiederholte Strahlendosen verursachen in Abhängigkeit vom bestrahlten Volumen in erhöhtem Maße RNs (Sneed *et al.*, 2015). Die RN und Pseudoprogression sind damit direkte Antagonisten des Therapieziels einer, soweit verträglich, sowohl auf die Intensität als auch die Therapiedauer maximal eskalierten und multimodalen Tumortherapie. Strahlentherapeutische Dosiskonzepte wie auch innovative systemische Kombinationspartner müssen auf das Risiko für relevante postradiogene Veränderungen sorgsam und frühzeitig überprüft werden, um Pseudoprogressionen wie auch RNs als solche zu identifizieren und Risikogruppen gegebenenfalls bereits präventiv medikamentös behandeln zu können, ohne onkologische Therapieziele zu gefährden.

2.7 Ziel der Arbeit

Ziel dieser Arbeit ist die wissenschaftliche Auswertung verschiedener innovativer strahlentherapeutischer Therapiekonzepte bei Hirntumoren, die eine Verkürzung der Behandlungszeit oder eine Kombination der Bestrahlung mit zielgerichteten Therapien zum gemeinsamen Ziel haben. Hierbei sollen neben den vordringlich relevanten Endpunkten der klinischen Effektivität auch sekundäre Endpunkte wie kurz- und langfristige Nebenwirkungsprofile, die Verträglichkeit mit den immer wichtigeren systemischen TTs und patientenzentrierte Behandlungsperspektiven charakterisiert werden. Abschließend sollen mögliche Prädiktoren für ein Therapieansprechen und die Verträglichkeit der Therapien diskutiert werden.

3. Ergebnisse

3.1 Giordano FA*, Layer JP*, Leonardelli S*, Friker LL, Turiello R, Corvino D, Zeyen T, Schaub C, Mueller W, Sperk E, Schmeel LC, Sahm K, Oster C, Kebir S, Hambsch P, Pietsch T, Bisdas S, Platten M, Glas M, Seidel C, Herrlinger U*, Hölzel M*. L-RNA aptamer-based CXCL12 inhibition combined with radiotherapy in newly-diagnosed glioblastoma: dose escalation of the phase I/II GLORIA trial. Nat Commun. 2024 May 28;15(1):4210.

Hintergrund und Zielsetzung der Arbeit: Das GBM geht insbesondere bei Nicht-Vorliegen einer MGMT-Promotor-Methylierung mit einer sehr schlechten Prognose einher. Eine nachgewiesen wirksame systemische Behandlungsmöglichkeit gibt es für diese Patienten nicht. Die Standardtherapie besteht aus einer möglichst kompletten Tumorresektion gefolgt von einer adjuvanten Bestrahlung. Das durch postradiogene Hypoxie verstärkt sezernierte Chemokin CXCL12 begünstigt die Rezidiventstehung durch Induktion einer Revaskularisierung des Tumors. Ziel dieser Arbeit war daher die klinische Anwendung eines CXCL12-Inhibitors in Ergänzung zur Strahlentherapie sowie die translationale Erforschung möglicher Marker für ein Ansprechen auf diese Kombinationstherapie.

Methoden und Ergebnisse: Im Dosiseskalationsteil der Phase 1/2-GLORIA-Studie wurden insgesamt zehn Patienten mit erstdiagnostiziertem, inkomplett oder gar nicht reseziertem und MGMT-Promotor-unmethyliertem GBM durch eine kombinierte Bestrahlung und CXCL12-Inhibition mit dem Aptamer Olaptesed pegol (NOX-A12) behandelt. Es ergaben sich keine dosislimitierenden Toxizitäten oder therapieassoziierte Todesfälle. Die Behandlung war sicher durchführbar und gut verträglich. MRT-morphologisch zeigte sich in neun von zehn Patienten ein Therapieansprechen in Bezug auf RANO-Kriterien wie auch in DWI- und DSC-MRT-Auswertungen. Eine höhere Häufigkeit CXCL12-exprimierender Endothel- und Gliomzellen („EG12-*Score*“) war bei GLORIA-Patienten, jedoch nicht bei SOC-Fällen, signifikant mit einem besseren PFS assoziiert. Bei medianer Teilung der Patientenkohorte in $EG12^{high}$ und $EG12^{low}$ GBM zeigte sich ein signifikant überlegenes PFS und ein Trend zu einem verbesserten OS für Patienten mit $EG12^{high}$ GBM.

Schlussfolgerungen: Die Studienergebnisse suggerieren eine klinische Wirksamkeit der Kombinationstherapie aus Bestrahlung und NOX-A12 in einer durch einen hohen EG12-*Score* geprägten Patientensubgruppe und betonen die Notwendigkeit einer fortgeführten und weitergehenden Charakterisierung des GBM-Tumormikromilieus. Die dargestellten Entdeckungen bilden die Basis für eine vertiefte Untersuchung dieses Biomarker-stratifizierten Behandlungskonzepts im GBM.

nature communications

Article

https://doi.org/10.1038/s41467-024-48416-9

L-RNA aptamer-based CXCL12 inhibition combined with radiotherapy in newly-diagnosed glioblastoma: dose escalation of the phase I/II GLORIA trial

Received: 29 September 2023

Accepted: 30 April 2024

Published online: 28 May 2024

Check for updates

A list of authors and their affiliations appears at the end of the paper

The chemokine CXCL12 promotes glioblastoma (GBM) recurrence after radiotherapy (RT) by facilitating vasculogenesis. Here we report outcomes of the dose-escalation part of GLORIA (NCT04121455), a phase I/II trial combining RT and the CXCL12-neutralizing aptamer olaptesed pegol (NOX-A12; 200/400/600 mg per week) in patients with incompletely resected, newly-diagnosed GBM lacking MGMT methylation. The primary endpoint was safety, secondary endpoints included maximum tolerable dose (MTD), recommended phase II dose (RP2D), NOX-A12 plasma levels, topography of recurrence, tumor vascularization, neurologic assessment in neuro-oncology (NANO), quality of life (QOL), median progression-free survival (PFS), 6-months PFS and overall survival (OS). Treatment was safe with no dose-limiting toxicities or treatment-related deaths. The MTD has not been reached and, thus, 600 mg per week of NOX-A12 was established as RP2D for the ongoing expansion part of the trial. With increasing NOX-A12 dose levels, a corresponding increase of NOX-A12 plasma levels was observed. Of ten patients enrolled, nine showed radiographic responses, four reached partial remission. All but one patient (90%) showed at best response reduced perfusion values in terms of relative cerebral blood volume (rCBV). The median PFS was 174 (range 58-260) days, 6-month PFS was 40.0% and the median OS 389 (144-562) days. In a post-hoc exploratory analysis of tumor tissue, higher frequency of $CXCL12^{+}$ endothelial and glioma cells was significantly associated with longer PFS under NOX-A12. Our data imply safety of NOX-A12 and its efficacy signal warrants further investigation.

Glioblastoma (GBM) is the most common malignant primary brain tumor in adults and is associated with a dismal prognosis[1]. Standard-of-care (SOC) treatment consists of maximum-feasible resection, external-beam radiotherapy (RT), and adjuvant therapy with temozolomide (TMZ)[2,3]. Tumors exhibiting unmethylated O^6-methylguanine DNA methyltransferase (MGMT) promoters are inherently resistant to chemotherapy[4], resulting in a median progression-free survival (PFS) of 4-5 months and a median overall survival (OS) of 10-15 months[5–8]. Beside age and clinical performance, the extent of tumor resection is an independent prognostic factor[9–11]. It is estimated that patients with completely resected tumors have a 61% higher likelihood of surviving 1 year than those with incomplete resection[12].

e-mail: Frank.Giordano@umm.de; michael.hoelzel@ukbonn.de

Residual tumor cells, along with their unique post-radiotherapeutic tumor microenvironment, efficiently restore the therapy-depleted vasculature via vasculogenesis[13]. In contrast to angiogenesis, which is characterized by VEGF-mediated local sprouting of pre-existing vessels[14,15], vasculogenesis occurs de novo and is mediated by progenitor bone marrow-derived cells (BMDC)[16–21]. Recruitment of such BMDC occurs towards a gradient of the CXCR4/CXCR7 ligand CXCL12 (also known as SDF-1), which is induced through hypoxia-driven activation of HIF1α[17,22–24]. Besides its crucial role in attracting pro-vasculogenic BMDC, CXCL12 is also suspected to, under certain circumstances, repel or sequester T cells[25–27], promote invasion of GBM cells, and decrease apoptosis[28,29].

Preclinical studies have shown improved intracranial tumor control in orthotopic GBM models after irradiation and subsequent inhibition of CXCR4 with the bicyclam derivative plerixafor[30]. Clinical safety of plerixafor after RT was recently reported in a phase I/II trial with 20 GBM patients as defined by the now outdated 2016 CNS WHO classification[31]. This trial also included patients with fully resected GBMs and more favorable molecular subtypes (IDH-mutant, MGMT methylated). Median PFS and OS compared favorably to historical data, and recurrence predominantly occurred outside of the irradiated areas, in line with the notion that $CXCR4^+/CXCR7^+$ cells play a key role in restoration of the local post-radiation vasculature leading to recurrence[31]. As treatment was non-continuous, but abrogated after just 28 days, the effects of CXCR4 blockade may conceptually not have been fully exploited. Furthermore, its impact on poor-outcome GBM remains unclear. Targeting CXCL12 with the pegylated L-RNA aptamer olaptesed pegol (NOX-A12) was highly effective in an autochthonous rat brain tumor model mimicking a highly treatment-refractory GBM[32]. In this model, RT plus NOX-A12 significantly reduced tumor burden and resulted in sustained complete regressions. Due to its non-natural enantiomeric configuration, NOX-A12 harbors very low immunogenic potential[33] while exhibiting a high affinity and specificity to its target[34]. To assess the clinical safety and efficacy of RT combined with NOX-A12, we conducted an open-label, multicentric phase I/II trial.

Here, we report on the results of the dose escalation part of this trial and on post-hoc analyses of tumor tissue biomarker-dependent outcomes.

Results

Trial design, enrollment, and patient characteristics

The GLORIA trial (NCT04121455) is a multicentric phase I/II trial conducted to assess the safety and efficacy of RT combined with continuous i.v. treatment with NOX-A12 in newly diagnosed, incompletely resected, or biopsied GBM (CNS WHO grade 4) lacking MGMT promoter methylation (Fig. 1a). The trial consists of a completed NOX-A12 dose escalation part reported here, and multiple expansion arms with additional treatment schemes that are ongoing and, thus, not reported here. In the dose-escalation part, NOX-A12 was administered in a modified 3 + 3 rule-based design with escalating dose levels (DLs) of 200, 400, and 600 mg NOX-A12 per week. The primary endpoint of the trial was safety. Secondary endpoints included maximum tolerable dose (MTD), recommended phase II dose (RP2D), NOX-A12 plasma levels, topography of recurrence, tumor vascularization, neurologic assessment in neuro-oncology (NANO), quality of life (QOL), median PFS, 6-months PFS and OS. In addition, tumor tissue obtained during surgery was analyzed as an exploratory post-hoc analysis by multiplexed immunofluorescence (mIF) imaging.

Between September 2019 and September 2021, three patients were enrolled at each DL. One patient of DL 3 dropped out early and was replaced to ensure safety data quality, hence a total of ten patients were treated with RT and NOX-A12 (Fig. 1b). The median age at diagnosis was 65 years (range 43–79 years). Eight of ten patients had undergone partial resection, two were not amenable to resection and received biopsy only. Seven patients received normofractionated and three hypofractionated RT (Table 1).

Pharmacokinetics and safety

NOX-A12 plasma levels reached a stable steady-state after approximately one week in all patients and surpassed 1.5 μM, which was considered to be the minimum plasma level required for disrupting CXCL12-mediated migration while minimizing bone marrow cell mobilization[34]. With increasing NOX-A12 DLs, a corresponding increase of NOX-A12 plasma levels was observed, in excess of CXCL12 levels (Fig. 2a). The median treatment time with NOX-A12 was 23.2 (12.3-48.1) weeks. Treatment was discontinued due to the end of treatment (EOT) as per protocol in two patients, suspected progressive disease (PD) in seven patients, and patient decision in one case. No patient discontinued treatment due to adverse events (AEs). In shared decision-making, the last patient enrolled continued treatment as per protocol beyond regular EOT after 26 weeks and also PD until a clinical deterioration in week 48. Treatment with RT and NOX-A12 was safe and well tolerated. No dose-limiting toxicities (DLTs) and no treatment-related deaths were observed. Thus, the MTD has not been reached and 600 mg per week of NOX-A12 is the RP2D also being taken forward into the ongoing expansion part of the trial. Out of 171 AEs, 13 (7.6%) were considered solely related to NOX-A12 (Table 2). Of all grade ≥2 adverse events ($n = 84$), 4 (4.7%) were considered to be NOX-A12-related, including one grade 3 AE at DL 3 (elevation of gamma-glutamyltransferase). Of note, this patient had idiopathic grade 1 elevated serum levels at baseline and suffered from an unrelated acute-on-chronic sigmoid diverticulitis soon after the AE. The majority of AEs were of grade 1 (50.9%) and were either unrelated or related to the GBM and RT. The most common treatment-emergent AEs (TEAEs, $n = 160$) were headaches which had been reported for a total of six patients with a maximum grading of grade 2 (Supplementary Fig. 1a). Increase of the alanine aminotransferase was the only treatment-related AE (TRAE) that occurred in three patients and did not exceed grade 2 (Supplementary Fig. 1b). Complete AE listings are summarized in Supplementary Data 1. TEAEs and TRAEs are provided in full in Supplementary Data 2–3 and Supplementary Tables 1–2, respectively.

Radiographic response

All ten patients enrolled in the dose-escalation part of the trial were considered for the response analysis. As an exemplary responsive patient, C1-003 was treated with NOX-A12 continuously for 26 weeks as per protocol, reaching partial remission (PR) in week 9 and relapsed at the EOT as confirmed in a significantly aggravated MRI scan in week 33 (Fig. 2b). Under NOX-A12, nine patients (90%) showed radiographic response in terms of MRI lesion sizes in at least one timepoint of follow-up. Eight of the nine patients (89%) with target lesions (TLs) at baseline MRI assessment showed a TL response during NOX-A12 therapy, with four (44%) reaching PR as per radiologic mRANO criteria, i.e., ≥50% reduction in sum of the products of the longest perpendicular diameters (SPD) (Fig. 2c). Of these, two patients each were treated at DL 1 and DL 3, respectively. All three patients of DL 1 and all four of DL 3 reached ≥50% size reduction of at least one non-target lesion (NTL). In three cases, two at DL 1 and one at DL 3, at least one NTL disappeared completely (Fig. 2d). Advanced MRI parameters, including perfusion and diffusion assessment, were performed to investigate anti-vasculogenic effects. Under NOX-A12, all but one patient (90%) showed at best response reduced perfusion values in terms of relative cerebral blood volume (rCBV) (Supplementary Fig. 2) and threshold-calculated high fractional tumor burden (FTB^{high}) with a median best response of −19.7% (24.0 to −55.5%) and −38.0% (9.3 to −100%) (Fig. 2e) indicating efficacy of the CXCL12 inhibitor therapy. In line with this, apparent diffusion coefficient (ADC) values were improved in 9 patients (90%) with a median best response of 29.2%

https://doi.org/10.1038/s41467-024-48416-9

a

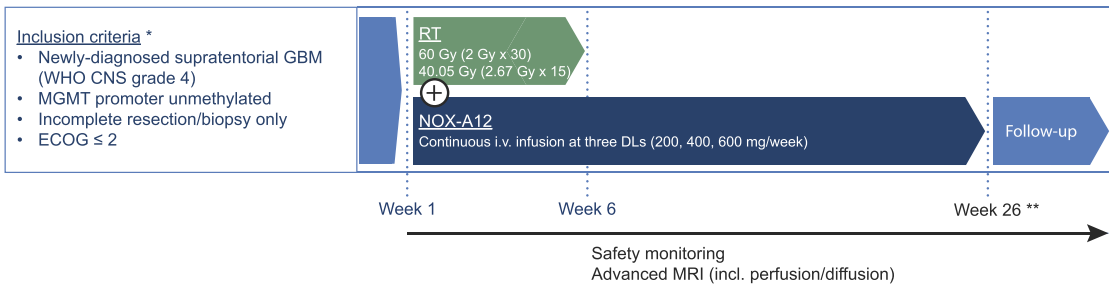

Primary endpoint:	Safety (incidence of adverse events)
Secondary endpoint:	NOX-A12 plasma levels, imaging parameters, PFS, OS *
Exploratory endpoints:	Multiplexed immunofluorescence imaging (CODEX®) - assessment of tissue biomarkers

b

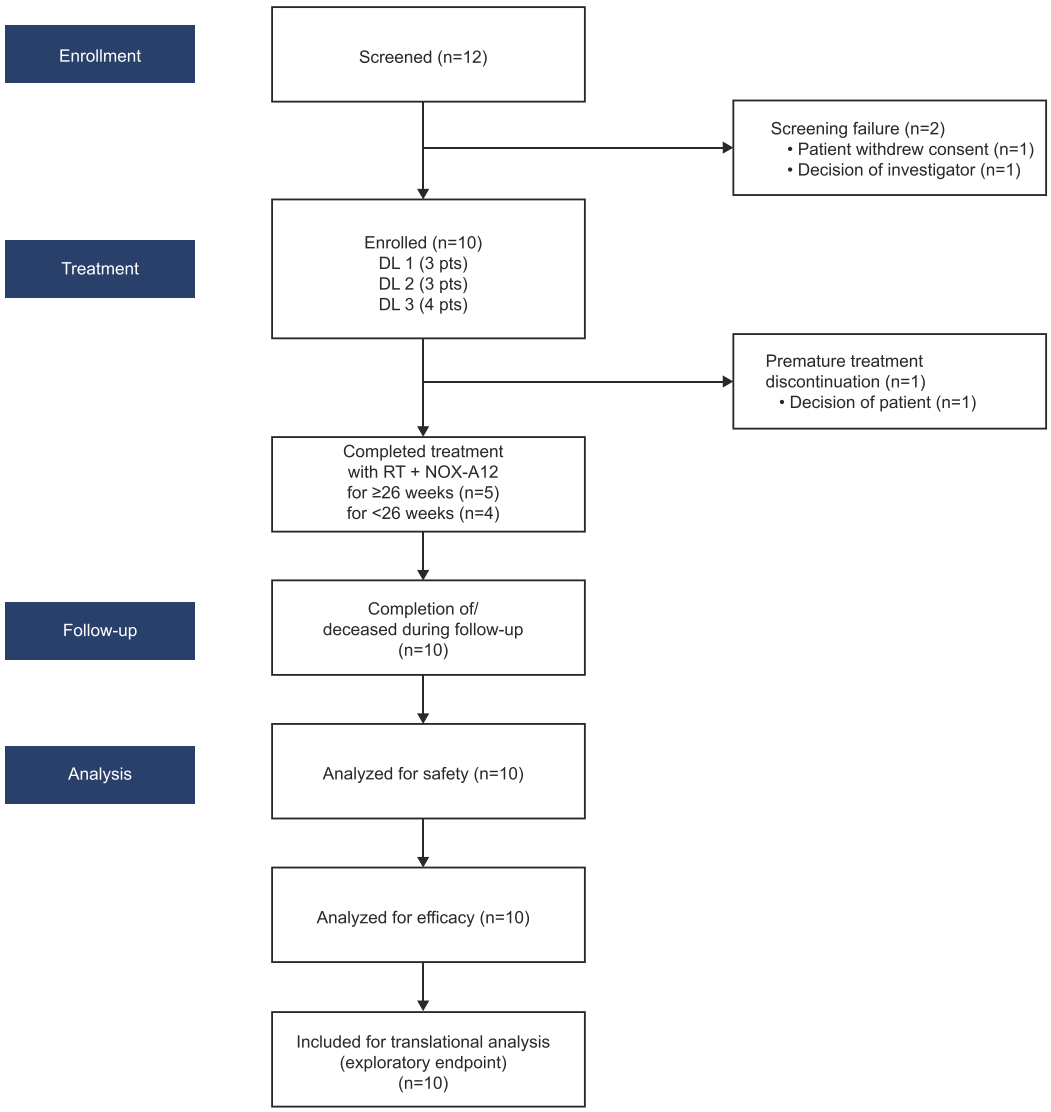

Fig. 1 | Study outline of the GLORIA trial. a Graphical overview of the study. GLORIA is a multicentric phase I/II trial conducted to assess the safety and efficacy of RT combined with escalating DLs of continuous i.v. treatment with NOX-A12 in newly diagnosed, incompletely resected, or biopsied GBM (CNS WHO grade 4) lacking MGMT promoter methylation ($n = 10$). *A complete and more detailed list of eligibility criteria and outcome measures is provided under ClinicalTrials.gov Identifier: NCT04121455. **End of treatment: 26 weeks as per protocol; treatment continuation beyond 26 weeks per investigator's choice if the patient has clear clinical benefit. **b** Flow chart of the study. CODEX® CO-Detection by indEXing, DL dose level, ECOG Eastern Cooperative Oncology Group performance score, GBM glioblastoma, MGMT O^6-methylguanine DNA methyltransferase, MRI magnetic resonance imaging, NOX-A12 olaptesed pegol, OS overall survival, PFS progression-free survival, RT radiotherapy.

Table 1 | GLORIA cohort patient characteristics (*n* = 10)

Variable	*n* (%)	Median (range)
Gender		
Male	7 (70)	
Female	3 (30)	
Age (years)		65 (43–79)
ECOG score		
0	7 (70)	
1	3 (30)	
Baseline NANO score		0 (0–4)
Resection status		
Incomplete Resection	8 (80)	
Biopsy	2 (20)	
Methylation status		
Methylated	0 (0)	
Unmethylated	10 (100)	
Residual tumor volume (cc)		4.3 (2.5–34.1)
Weeks post surgery		4.6 (3.9–7.1)
Tumor localization		
Frontal lobe	4 (40)	
Temporal lobe	5 (50)	
Parietal lobe	3 (30)	
Occipital lobe	2 (20)	
Radiotherapy		
Normofractionated	7 (70)	
Hypofractionated	3 (30)	

(−15.2 to 161.8%) (Fig. 2f). NANO, QOL, and topography of recurrence were secondary endpoints but are not reported here.

Clinical endpoints

The median PFS of the entire GLORIA cohort was 174 days (range 58–260 days), 6-month PFS 40.0%, and the median OS 389 days (144–562 days; Supplementary Fig. 3). This high variability prompted us to initiate a post-hoc exploratory analysis to search for potential biomarkers that correlate with NOX-A12 treatment responses focusing on CXCL12, the target of NOX-A12.

Biomarker-dependent survival analysis

Analyzing publicly available single-cell RNA sequencing (scRNAseq) data from human GBM[35] showed the highest level and frequency of *CXCL12* mRNA expression in endothelial cells, followed by pericytes, myeloid (macrophages, microglia), and glioma cells (Fig. 3a, Supplementary Fig. 4). Therefore, we decided to assess total and cell-type specific CXCL12 protein expression in pre-treatment tumor samples obtained from GLORIA patients ($n = 10$) in a posthoc translational analysis. As an external control, pre-treatment tumor samples from an independent cohort of GBM patients with comparable clinical and histological features treated with SOC ($n = 22$; patient characteristics in Supplementary Table 3) were equally analyzed (Fig. 3b). We selected a panel of six antibodies validated for formalin-fixed paraffin-embedded (FFPE) tissue sections to identify endothelial cells (E; CD31), pericytes (P; α-SMA), macrophages (Mϕ)/microglia (M; CD68), glioma cells (G; GFAP), proliferating cells (Ki-67) and CXCL12$^+$ cells alongside 4′,6-diamidino-2-phenylindole (DAPI) as nuclear stain (Fig. 3c). For mIF imaging we employed co-detection by indexing (CODEX®), a well-established technology for profiling the tumor microenvironment of different tumor types including GBM[36,37]. Following image raw data processing, DAPI signals were used for automated nuclear segmentation with a custom-trained deep learning neural network algorithm implemented within the HALO® AI analysis software. Subsequent cell-type assignment was based on marker expression (e.g., CD31 for endothelial cells). Lastly, the CXCL12 expression status was determined in a cell-type-specific manner (Supplementary Fig. 5, Methods). Samples of both the GLORIA and the SOC cohort were stained, imaged, and analyzed under the same conditions and settings, with all tumor areas being verified independently by two neuropathologists. Example images of CXCL12$^+$ cell populations and H&E staining of the analyzed tumor areas are shown in Fig. 3c. All side-by-side illustrations of the analyzed areas in mIF staining and corresponding H&E staining are provided in Supplementary Fig. 6.

In total, we analyzed more than six million single cells with an average of 189,000 cells per sample (Supplementary Data 4). Consistent with scRNAseq data by Abdelfattah et al.[34], mIF revealed that the frequency of CXCL12$^+$ cells was highest in endothelial cells (E12), followed by pericytes (P12), Mϕ/microglia (M12) and glioma cells (G12) (Fig. 3d). As CXCL12 promotes post-radiogenic vasculogenesis and recurrence in preclinical models[30], we next asked whether CXCL12 positivity might be predictive for NOX-A12 treatment responses.

While a PFS event was definable for nine of the GLORIA patients, one patient was censored for PFS as per the statistical analysis plan (for details, see patient narratives in Supplementary Note 1). We noted a significant positive correlation between the frequency of CXCL12$^+$ cells (total cells) and PFS in the GLORIA cohort (Spearman's rank correlation, $r_s = 0.712$, $p = 0.039$). This correlation was absent in the SOC cohort ($r_s = -0.251$, $p = 0.259$, Fig. 3e). Analyzing CXCL12 positivity per individual cell types, we detected significant positive correlations for frequency of CXCL12$^+$ endothelial cells (E12; $r_s = 0.695$, $p = 0.046$) and of CXCL12$^+$ glioma cells (G12; $r_s = 0.712$, $p = 0.039$) with PFS of patients enrolled in the GLORIA trial, while not reaching significance for frequency of CXCL12$^+$ Mϕ/microglia (M12; $r_s = 0.458$, $p = 0.223$) and CXCL12$^+$ pericytes (P12; $r_s = 0.559$, $p = 0.126$) (Fig. 3f). Importantly, we found no significant correlations between any of the cell-type specific frequencies of CXCL12$^+$ cells and PFS of the SOC cohort, including E12 ($r_s = 0.015$, $p = 0.946$) and G12 ($r_s = -0.261$, $p = 0.240$).

Both endothelial cells (E12) and glioma cells (G12) showed a significant correlation with PFS. While endothelial cells showed the highest relative CXCL12 positivity, the total number of endothelial cells was roughly twelve times lower than that of glioma cells. Therefore, we reasoned that combining E12 and G12 with approximately equal weights could embrace independent biological mechanisms and, thus, improve the correlation with NOX-A12 treatment responses. Consequently, we calculated the mean of the median-centered values of E12 and G12, resulting in a combined EG12 score that can hence adopt negative and positive values (Supplementary Fig. 7 and Supplementary Table 4). Here, the combined EG12 score strongly correlated with PFS ($r_s = 0.865$; $p = 0.005$; Fig. 4a) of the GLORIA patients. Again, in the SOC cohort, we found no significant correlation between the EG12 score and PFS ($r_s = -0.133$; $p = 0.556$; Fig. 4b). There was no significant correlation between the EG12 score and OS in the GLORIA cohort and the SOC cohort, but a positive and negative trend, respectively (Supplementary Fig. 8). Next, we used the EG12 score to divide the patients of the GLORIA and the SOC cohort by an unbiased median classifier into EG12^{high} and EG12^{low} subgroups. With a median PFS of 183 vs. 92 days, EG12^{high} patients in the GLORIA cohort had a significantly longer PFS than EG12^{low} patients (HR 0.12 (95% confidence interval (CI) 0.01–0.81); log-rank test, $p = 0.031$; Fig. 4c). We also detected a trend for prolonged OS for E12^{high} over E12^{low} GLORIA patients (median OS 481 vs. 338 days; HR 0.25 (95% CI 0.03–1.17); log-rank test, $p = 0.075$; Fig. 4d). In the SOC cohort, no significant difference was measured in PFS (median PFS 118 vs. 136 days; HR 1.25 (95% CI 0.51–3.12); log-rank test, $p = 0.628$; Fig. 4e) or OS (median OS 328 vs. 288 days; HR 1.30 (95% CI 0.53–3.25); log-rank test, $p = 0.568$; Fig. 4f) between E12^{high} patients and E12^{low} patients.

https://doi.org/10.1038/s41467-024-48416-9

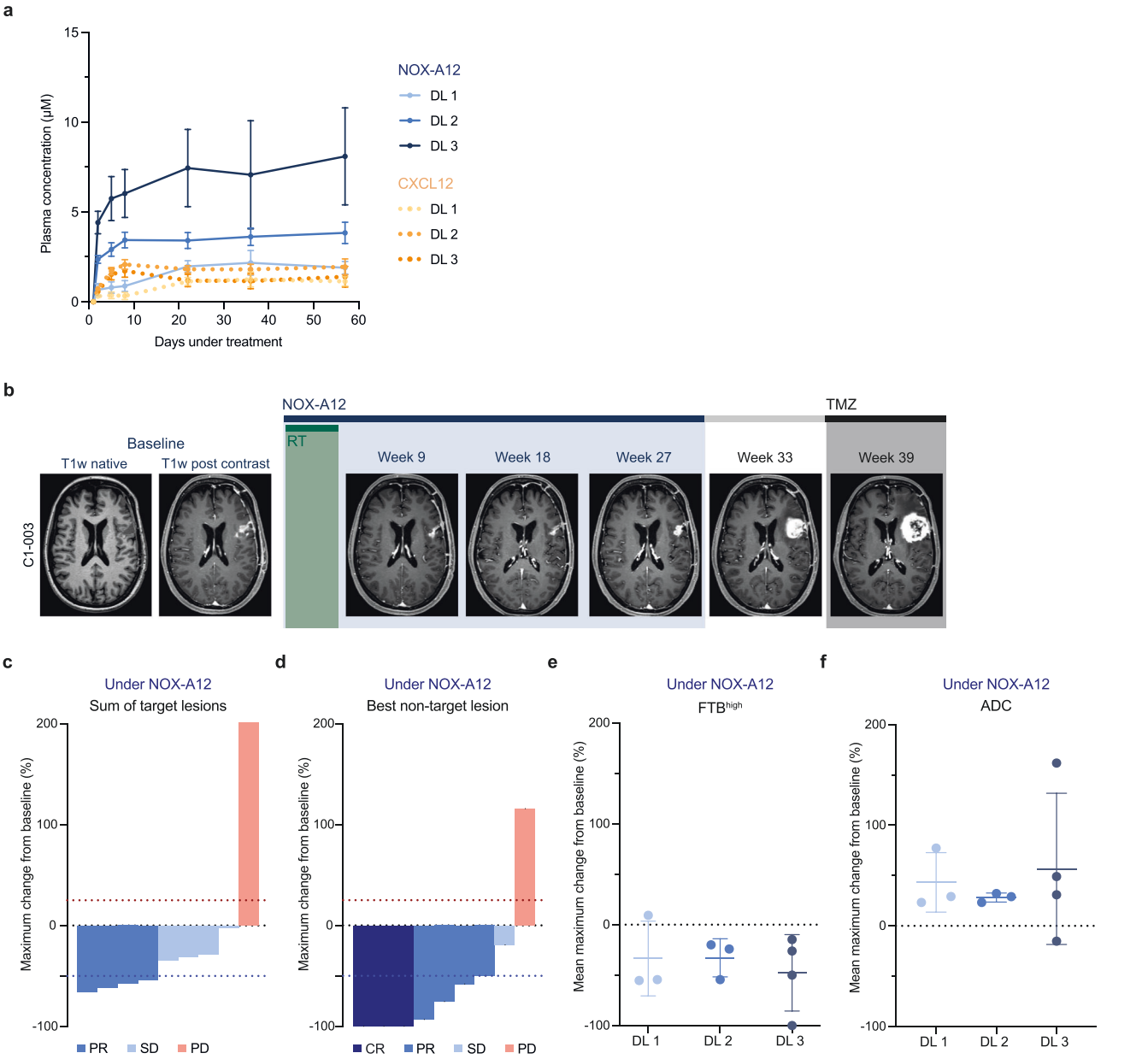

Fig. 2 | Treatment with RT and NOX-A12 is safe and shows radiographic responses in conventional and advanced MRI. a Serial plasma NOX-A12 (blue, full lines) and CXCL12 (orange, dashed lines) concentrations (µM) over treatment time (days) in respective GLORIA DLs ($n = 10$) indicated by color coding. Error bars indicate the standard error of the mean. **b** Representative illustration of the treatment course of a responding patient. Patient C1-003 was treated with RT (6 weeks; 2 Gy ad 60 Gy) and continuous NOX-A12 infusion for 26 weeks as per protocol, reaching partial remission in week 9. The patient relapsed at the end of NOX-A12 treatment (week 27) and deteriorated both before and after the initiation of TMZ. **c**, **d** Waterfall plots for best radiographic response as per mRANO under NOX-A12 (maximum change from baseline) of the sum of target lesion SPD (T1 Gd MRI) (**c**) and the best responding non-target lesion SPD (T1 Gd MRI) (**d**). Colors from blue to red indicate CR, PR, SD, and PD for each patient. As per mRANO, red dotted line indicates 25% increase (PD), blue dotted line indicates −50% decrease (PR). **e**, **f** Dot plots depicting mean maximum change from baseline under NOX-A12 for FTB^{high} (**e**) and ADC (**f**) of patients in the respective DLs (color-labeling in blue; 200 ($n = 3$), 400 ($n = 3$), 600 mg/week ($n = 4$)). Error bars indicate mean and standard deviation. Source data are provided as a Source Data file. ADC apparent diffusion coefficient, CR complete response, DL dose level, FTB^{high} high fractional tumor burden, GBM glioblastoma, mRANO modified Criteria for Radiographic Response, NOX-A12 olaptesed pegol, PD progressive disease, PR partial response, RT radiotherapy, SD stable disease, SPD sum of product of perpendicular diameters, TMZ temozolomide.

Discussion

In our study, we report the safety of RT and NOX-A12 in newly diagnosed, chemotherapy-resistant GBM meeting the primary endpoint of the trial. In addition, post-hoc tumor tissue analyses suggest improved clinical efficacy of this CXCL12-inhibiting L-RNA aptamer in a subgroup of patients characterized by a high frequency of CXCL12 positivity of endothelial and glioma cells.

Our trial supports previous findings that GBM recurrence after RT may be promoted by CXCL12-driven vasculogenesis[30,38–40]. We also demonstrated colocalization of CXCL12 with $CD31^+$ endothelial cells and $GFAP^+$ tumor (glioma) cells, in particular, identifying these cell populations as important sources of CXCL12. Our results are supported by a recent preclinical study that identified high endothelial CXCL12 expression as a key chemokine involved in pro-tumorigenic remodeling

Table 2 | GLORIA trial adverse events by CTCAE grade and indication of relationships

Adverse events	*n* (%)
CTCAE grade	
Grade 1	87 (50.9)
Grade 2	59 (34.5)
Grade 3	24 (14.0)
Grade 4	1 (0.6)
Grade 5	0 (0)
Relationship	
No relationship	81 (47.4)
Related to GBM	43 (25.1)
Related to RT	20 (11.7)
Related to RT & GBM	6 (3.5)
Related to NOX-A12	13 (7.6)
yGT elevation	1 (0.6)
ALT elevation	3 (1.8)
Leukocytosis	3 (1.8)
Constipation	3 (1.8)
Dyspnea	1 (0.6)
Paresthesia	1 (0.6)
Pyrexia	1 (0.6)
Related to NOX-A12 & GBM	4 (2.3)
Related to NOX-A12 & RT	2 (1.2)
Related to NOX-A12 & RT & GBM	2 (1.2)
Total events	171 (100)

ALT alanine aminotransferase, *CTCAE* common terminology criteria for adverse events, *yGT* gamma-glutamyltransferase.

of the glioma microenvironment[41]. In addition, our approach also underscores the value of single-cell analyses at spatial resolution to identify microenvironmental mechanisms that determine disease prognosis and recurrence as recently shown[42,43].

Categorizing patients by their EG12 score in a low and high subgroup can potentially cause bias and overestimation of the observed effect[44]. Inherent with the design of early-phase clinical trials, only ten patients were treated with NOX-A12, and thus, our results will need further confirmation in larger cohorts. This future investigation will then also allow for gender-based assessments that were not feasible given the present patient numbers. The small cohort size may also explain why the difference between the OS of patients with $EG12^{high}$ versus $EG12^{low}$ tumors did not reach statistical significance. Specifically, since salvage treatments with variable efficiency[45,46] were not pre-specified in the trial protocol and hence individual management after recurrence varied from best supportive care only (three patients) to anticancer therapies, including TMZ (six patients), bevacizumab (five patients), CCNU (four patients), regorafenib (two patients), or re-irradiation (two patients), which may have impacted OS.

Insufficient crossing of the blood–brain barrier is a frequent limitation of novel drugs targeting brain tumors[47]. However, tissue penetration is not a prerequisite for NOX-A12 efficacy. NOX-A12 neutralizes CXCL12 in the blood, and it also releases and sequesters CXCL12 bound to glycosaminoglycans on the surface of tumor endothelial cells at the interface between the blood system and tumor cells[48]. Thereby, NOX-A12 disrupts CXCL12-dependent recruitment of circulating BMDC to the hypoxic tumor tissue, which prevents restoration of the tumor vasculature and hence restrains tumor cell growth in preclinical models[49,50]. Our study confirms in humans that NOX-A12 treatment indeed detaches and sequesters CXCL12, as we detected a profound accumulation of the chemokine in the plasma reaching concentrations in the low micromolar range.

The mode of action of NOX-A12 strongly suggests that ongoing and uninterrupted treatment is crucial to prevent recurrence, as only the initial RT leads to devascularization of the tumor microenvironment, and an interruption of NOX-A12 infusions is likely to allow for rapid reconstitution of CXCL12 gradients and sequential vasculogenesis within few weeks[30]. Therefore, NOX-A12 effects on GBM control were possibly not fully exploited due to treatment interruptions or curtailments, especially in some of the responding patients. Notably, in some patients, NOX-A12 treatment was discontinued prematurely as a consequence of a misinterpretation of pseudo-progression (as observed and pathology-confirmed in patient C1-001).

The DLs selected for the GLORIA trial were supported by safety and efficacy considerations, as a NOX-A12 dose of 200 mg/week is expected to result in pharmacologically relevant mean plasma levels at steady state. Accordingly, NOX-A12 treatment resulted in excess of drug over target plasma levels in all DLs, which might explain the lack of a dose-dependency in this trial. The highest DL of 600 mg NOX-A12/week was safe and well tolerated. It is, therefore, the RP2D and also the DL being taken forward into expansion. While the GLORIA trial recruited only patients lacking MGMT methylation due to ethical reasons (no proven benefit of SOC with TMZ), there is no mechanistic reason to question the mode of action of NOX-A12 in MGMT methylated GBM. Thus, confirmation trials are now warranted that will continue to assess patient outcomes stratified by their EG12 score rather than other factors.

In conclusion, our results emphasize the need for further characterization of the GBM microenvironment to identify additional druggable targets and provide a rationale to intensify the in-depth investigation of a potential biomarker-stratified treatment of GBM with RT and CXCL12-directed therapy.

Methods

Trial design and oversight

GLORIA (SNOXA12C401, 2018-004064-62, NCT04121455) is a multicentric phase I/II study of RT in combination with NOX-A12 in first-line partially resected or unresected GBM (CNS WHO grade 4) patients with unmethylated MGMT promoter. The trial consisted of an initial dose-escalation arm (reported here) and additional expansion arms that evaluate NOX-A12 in combination with other drugs (follow-up ongoing). The first patient was enrolled on 23 September 2019. The last patient of the dose-escalation arm was enrolled on September 2, 2021.

The trial was first registered on EudraCT upon approval by the German authority (Bundesinstitut für Arzneimittel und Medizinprodukte (BfArM)) in May 2019 (https://www.clinicaltrialsregister.eu/ctr-search/trial/2018-004064-62/DE). The dose escalation was designed as a modified 3 + 3 rule-based design according to Le Tourneau et al.[51] with three successional cohorts consisting of three patients each. Patients of DL 1 were to be treated with a weekly dose of 200 mg, DL 2 with a weekly dose of 400 mg, and DL 3 with a weekly dose of 600 mg NOX-A12. After 4 weeks of treatment of the first patient of DL 1, the data safety monitoring board (DSMB) reviewed all DLTs, AEs, and relevant laboratory values. During the following ten weeks of treatment, the DSMB was kept informed continuously about all DLTs and SAEs, and, at the end of this period, reviewed all DLTs, AEs, and relevant laboratory values, including NOX-A12 plasma concentrations prior to enrollment of the next two patients of this DL. The evaluation was repeated prior to enrolling patients in DL 2 and after patients 2 and 3 received at least four weeks of treatment. The same procedures were performed prior to the enrollment of further patients in DL 2 and DL 3. If none of the three patients in any DL experienced a DLT, another three patients were to be treated at the next higher DL. However, if one of the three patients in a DL experienced a DLT, three more patients

https://doi.org/10.1038/s41467-024-48416-9

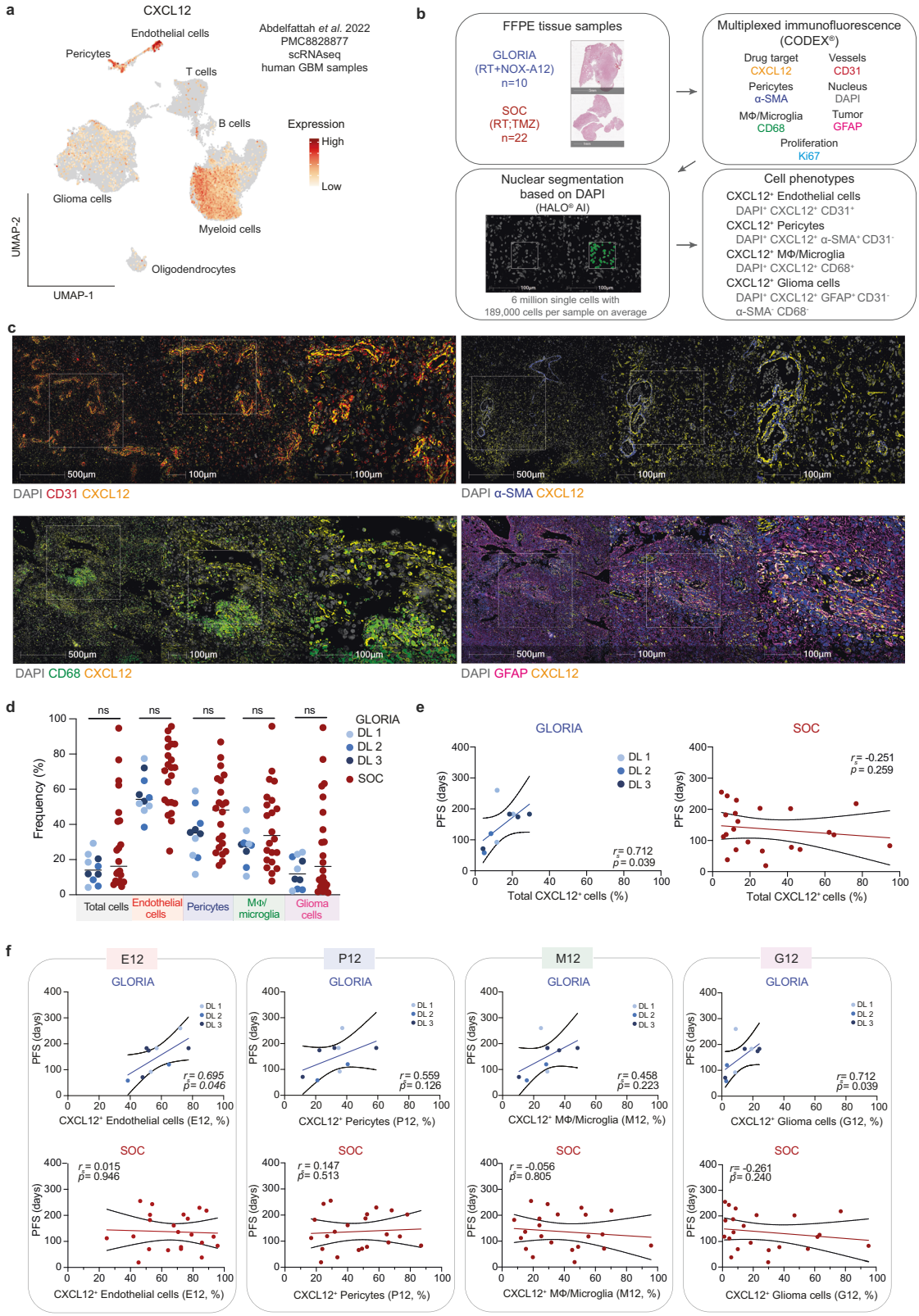

were to be treated at the same DL. The dose escalation was planned to be continued until at least two patients among a cohort of three to six patients experienced DLT (i.e., ≥33% of patients with a DLT at that DL), but the dose would not be escalated beyond 600 mg/week. The RP2D was defined as the DL just below this toxic DL, or 600 mg/week, if this DL is not toxic. DLTs, according to the common terminology criteria for adverse events (CTCAE, version 5.0), were defined as any grade 3–4 non-hematological toxicities (excluding grade 3 vomiting and/or nausea, if encountered without adequate and optimal prophylactic therapy), at any DL, assessed by the Investigator and/or the sponsor as related to NOX-A12.

Inclusion criteria of the dose-escalation arm of the trial were age ≥18 years, incompletely resected or biopsied GBM (detectable postoperative residual tumor), absence of MGMT promoter (hyper)

Fig. 3 | CXCL12 positivity in endothelial cells and glioma cells correlates with PFS in the GLORIA cohort. a UMAP projection overlayed with *CXCL12* mRNA expression in cell types from scRNAseq in human GBM samples (dataset from Abdelfattah et al.[35]). **b** Experimental setup of mIF imaging and outline of analysis pipeline. FFPE tissue samples were used for 7-plex mIF imaging; GLORIA cohort (RT + NOX-A12) ($n = 10$) and SOC cohort (RT; TMZ) ($n = 22$). All tumor areas were confirmed independently by two neuropathologists. Cell types and CXCL12 positivity were identified as indicated. **c** Representative images of GBM tissue samples from GLORIA cohort patients ($n = 10$) showing CXCL12 (yellow) expression in the cell types of interest: $CD31^+$ endothelial cells (red); α-SMA^+ pericytes (blue); $CD68^+$ MΦ/microglia (green) and $GFAP^+$ glioma cells (magenta). **d** Frequency of $CXCL12^+$ cells per cell type measured in the GLORIA cohort (in blue; different DLs as indicated; $n = 10$) and in the SOC cohort (in red; $n = 22$). Unpaired two-tailed Mann–Whitney *U* test; ns: not significant ($p > 0.05$). **e** Spearman's rank correlation (r_s) calculated between PFS (days) and total $CXCL12^+$ cells (%) measured in the GLORIA cohort (left; in blue and with DLs as indicated; $n = 10$) and in the SOC cohort (right; in red; $n = 22$). r_s- and *p* values (two-tailed) are depicted in the corresponding graphs. **f** Spearman's rank correlation (r_s) calculated between PFS (days) and $CXCL12^+$ endothelial cells (%) out of total endothelial cells (E12), $CXCL12^+$ pericytes (%) out of total pericytes (P12), $CXCL12^+$ MΦ/Microglia (%) out of total MΦ/microglia (M12) and $CXCL12^+$ glioma cells (%) out of total glioma cells (G12) measured in the GLORIA cohort (upper panels; in blue with DLs as indicated; $n = 10$) and in the SOC cohort (lower panels; in red; $n = 22$). r_s- and *p* values (two-tailed) are depicted in the corresponding graphs. Source data are provided as a Source Data file. DL dose level, FFPE formalin-fixed paraffin-embedded, GBM glioblastoma, MΦ macrophages, mIF multiplexed immunofluorescence, NOX-A12 olaptesed pegol, PFS progression-free survival, RT radiotherapy, scRNAseq single-cell RNA sequencing, SOC standard-of-care, TMZ temozolomide, UMAP uniform manifold approximation, and projection.

methylation, Eastern Cooperative Oncology Group (ECOG) performance score ≤2, estimated life expectancy ≥3 months, stable or decreasing dose of corticosteroids and adequate hepatic and renal function. Sex was determined based on self-report. All patients were neuropathologically confirmed as GBM, IDH-wildtype (CNS WHO grade 4) according to the WHO classification for CNS tumors 2021 by immunohistochemistry (IHC). If patients were ≤54 years of age, they were assessed additionally by pyrosequencing for IDH1 and IDH2. GLORIA was conducted at six academic centers in Germany, whereas the protocol was approved by ethics committees at each participating site (ethic committees of the university hospitals of Mannheim, Bonn, Leipzig, Essen, Tübingen, and Münster). The study design and conduct complied with all relevant regulations regarding the use of human study participants. The trial followed the guidelines of the Declaration of Helsinki and the International Conference on Harmonization Good Clinical Practices Guidelines. Each patient provided written informed consent in accordance with established guidelines. The trial was reviewed by an independent data safety and monitoring committee. No trial participant received financial compensation. The sponsor agreed to the separate report of the dose escalation part of the trial as provided in this manuscript after the end of follow-up of the last patient of DL 3, as all patients in the expansion arm receive differing treatment combinations, limiting comparability. This dose escalation part was the only part of the trial in the initial protocol versions before the expansion arms were added to explore additional combination treatment options of interest. A minimally redacted version of the study protocol is provided in Supplementary Note 2.

Treatment and endpoints

Following adequate cranial wound healing and implantation of a venous port catheter, treatment with NOX-A12 was initiated within six weeks post-cranial surgery. After an initial dose of 70, 160, or 230 mg per day, respectively, on day 1, patients were administered a fixed dose of 200, 400, or 600 mg NOX-A12 per week (DL 1, DL 2, DL 3) by continuous (24 h) i.v. infusion over a commercially available closed pump system (CADD®-Solis VIP Ambulatory Infusion Pump by Smiths Medical) starting on day 1. Treatment with NOX-A12 ended after 26 weeks. Patients with disease progression during the 26-week treatment period continued treatment with all assessments if deemed appropriate by the investigator. Continuation of treatment with NOX-A12 beyond 26 weeks was allowed as per each investigator's decision, if the patient had clear clinical benefit. No simultaneous systemic oncologic treatment was permitted. Baseline patient and treatment characteristics are enlisted in Supplementary Data 4. Clinical and radiographic follow-up assessments included standard and advanced magnetic resonance imaging (MRI) sequences. The primary endpoint of the trial was safety as per the incidence of AEs. Secondary endpoints included NOX-A12 plasma levels, MTD, RP2D, imaging parameters with a specific emphasis on monitoring response, vascularization, topography of recurrence, PFS, OS, and clinician/patient-reported outcomes (CRO/PRO). Topography of recurrence as well as CRO and PRO (NANO, QOL) are not reported here, as analyses are planned after overall completion of the trial. As an additional exploratory endpoint, tumor tissue obtained in surgery was post-hoc analyzed by mIF staining (CODEX®). RT was initiated on day 2 after the start of NOX-A12 and administered as intensity-modulated, image-guided RT in a normofractionated (2 Gy per fraction) or hypofractionated (2.67 Gy per fraction) fashion up to cumulative doses of 60 or 40.05 Gy, respectively. For treatment planning, pre- and post-surgery MRI scans were co-registered on planning computer tomography (CT) scans. Gross tumor volumes (GTV), clinical target volumes (CTV), and planning target volumes (PTV) were defined as per current guidelines[52].

Assessment of clinical and radiographic response

Patients visited the study site once weekly when presenting for the change of the medication cassette of the pump. Clinical routine follow-up visits included regular AE monitoring, physical and neurological assessments, vital signs, ECG, and blood tests. AEs were assessed and graded by the investigators according to the National Cancer Institute CTCAE, version 5.0. Baseline MRIs were obtained within a week prior to treatment initiation and up to 6 weeks post-surgery or post-biopsy. Follow-up MRIs were obtained every 8 weeks under treatment and at EOT. MRI imaging sequences included: 3D T1-weighted volumetric imaging (3D T1), T2-fluid-attenuated inversion recovery (FLAIR) imaging, diffusion-weighted imaging (DWI), T1-weighted dynamic contrast-enhanced perfusion imaging (DCE), T2-weighted turbo spin-echo imaging (T2 TSE), T2-weighted dynamic susceptibility contrast-enhanced perfusion imaging (DSC), and post-contrast 3D T1 imaging. The following additional advanced imaging parameters were calculated: DWI-derived ADC; diffusion susceptibility contrast (DSC)-derived leakage-corrected normalized rCBV and threshold-calculated FTB^{high} (rCBV >1.75); DCE-derived transfer constant of contrast agent (Ktrans) between the blood and the extravascular extracellular space (EES), fractional EES volume (υ_e), and fractional plasma volume (υ_p). Following acquisition, MRI images were uploaded to a secure online portal (decidemedical, Clinflows) where a central quality check was performed. All image post-processing and interpretation were performed using IB Neuro™ (Imaging Biometrics), Olea Sphere (Olea Medical), and Mint Lesion™ (Mint Medical GmbH) software and assessed by a central reader not involved in the treatment of the patients (SB). MRI response values for all patients can be found in Supplementary Data 4.

Outcome assessment

All MRI images were uploaded to an imaging database, and outcome was centrally assessed by a board-certified radiologist with expertize in the field blinded for study site and clinical status. Target lesions (TLs)

https://doi.org/10.1038/s41467-024-48416-9

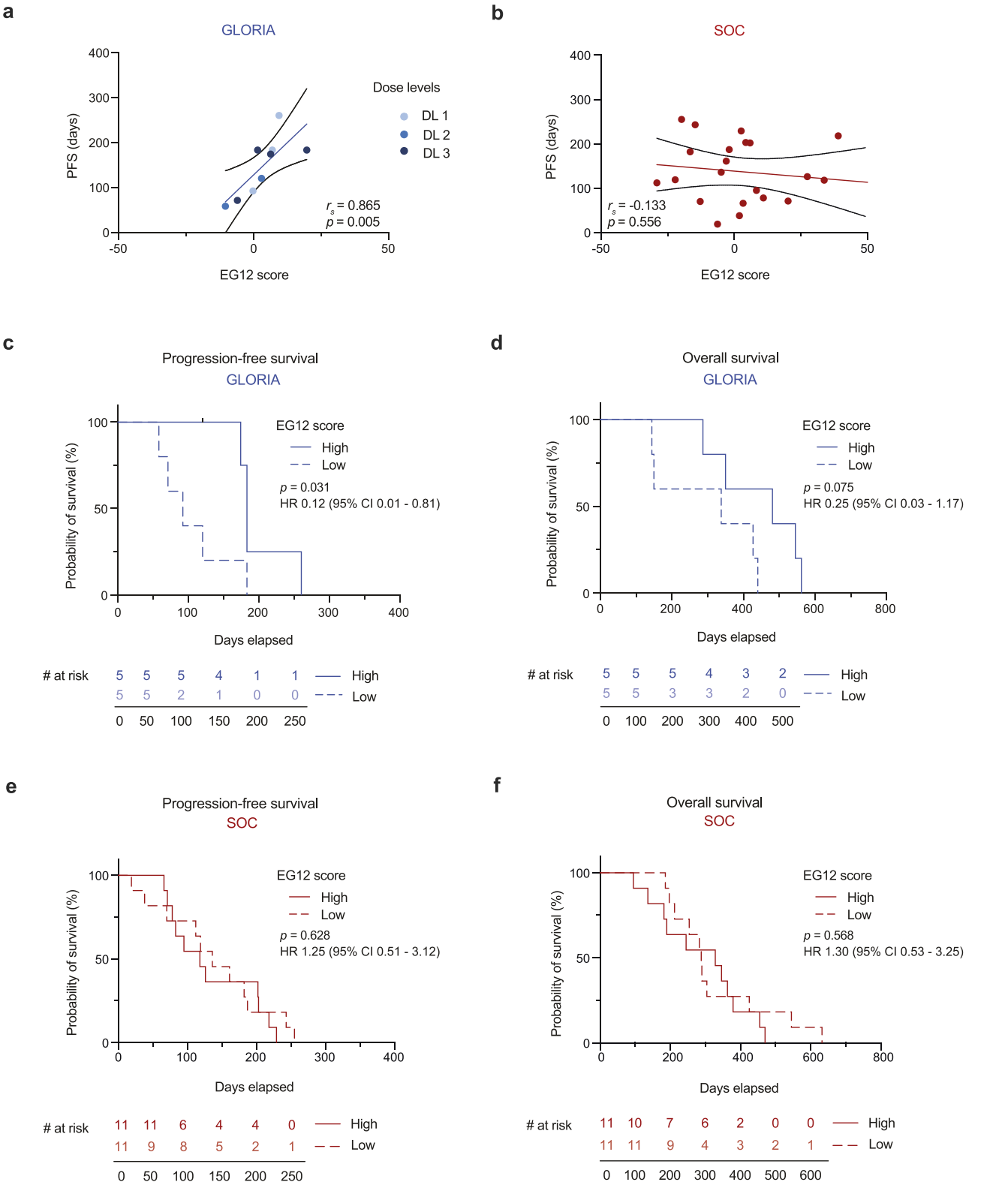

Fig. 4 | EG12 correlates with PFS and is associated with improved survival in the GLORIA, but not in a SOC cohort. a, **b** Correlation analysis of progression-free survival (days) with EG12 score in corresponding tumor tissue of the GLORIA cohort ($n = 9$; colors depict DL as indicated) (**a**) and the SOC cohort ($n = 22$) (**b**). Spearman's rank correlation (r_s); r_s- and p values (two-tailed) are depicted in the corresponding graphs. **c**, **d** Kaplan–Meier curves of progression-free (**c**) and overall survival (**d**) in days in the GLORIA cohort according to high ($n = 5$; continuous line) versus low ($n = 5$; dashed line) EG12 score. **e**, **f** Kaplan–Meier curves of progression-free (**e**) and overall survival (**f**) in days according to high ($n = 11$; continuous line) versus low ($n = 11$; dashed line) EG12 score in the SOC cohort. Log-rank test (two-tailed); p values are depicted in the corresponding graphs. Source data are provided as a Source Data file. CI confidence interval, DL dose level, HR hazard ratio, PFS progression-free survival, SOC standard-of-care.

and NTLs were identified, validated, and assessed in regard to tumor size (SPD) and corresponding timepoint tumor response according to the modified Criteria for Radiographic Response (mRANO)[53]. One patient enrolled had a singular residual tumor lesion meeting the inclusion criteria, while not qualifying for a TL (<10 mm in at least one diameter as per mRANO), thus documented as NTL. New non-measurable contrast-enhancing lesions only constituted progression in the case of complete response (CR). NTLs only impacted the response assessment in the case of a complete response of TLs. Preliminary tumor progression (PD) or regression (partial response, PR) required confirmation in a successive scan after 8 weeks. PFS was calculated as time (in days) between the first day of treatment with NOX-A12 to the day of PD. The PFS event was defined as the first date at which progression criteria had been met, i.e., (1) the date of the first sequentially confirmed MRI assessment resulting in preliminary PD or (2) the date of the radiographic assessment irrespective of its outcome in case of simultaneous investigator-assessed clinical progression attributable to no other cause apart from the tumor or; (3) the date of death by any cause if the patient died before clinical or radiographic progression. If preliminary PD was not confirmed in a sequential MRI and there was no subsequent SD, PR, or CR, the date of preliminary PD was still considered as an event for PFS if (1) the patient stopped protocol treatment due to clinical progression; (2) no further response assessments were done; or (3) the patient died due to any cause. For patients without a clinical or confirmed radiographic progression prior to a change of systemic therapy, PFS was censored at the date of initiation of a new anticancer treatment. Independent of MRI or clinical assessment, the diagnosis of PD was not established in the case of histopathologically confirmed pseudo-progression after re-surgery, which was the case in one patient where treatment with NOX-A12 was continued afterwards. OS was calculated as the time from the first day of treatment with NOX-A12 until death by any cause. The individual clinical courses, therapies, investigator decisions, and definitions of PFS and OS events for all patients are described in detailed narratives provided in Supplementary Note 1.

SOC cohort

To benchmark tissue and outcome, we established a reference cohort of GBM patients treated outside of the study with SOC RT and optional TMZ at the University Hospital Bonn between 2010 and 2023. All patients had consented to analyses of preserved tissue and imaging studies. The procedures were approved by the Ethics Committee of the University Hospital Bonn (approval number: 222/23-EP). Histological criteria for selection of reference SOC patients were: newly-diagnosed GBM, IDH-wildtype (CNS WHO grade 4) according to the valid WHO classification for CNS tumors, absence of MGMT promoter methylation as confirmed by pyrosequencing[54]. Clinical criteria were: ECOG of 0–2, status post biopsy or incomplete resection, and first-line therapy with RT (and optionally TMZ, $n = 18/22$ receiving TMZ). In addition, despite leading to a possible (positive) survivorship bias, the availability of a baseline MRI scan and at least 2 consecutive scans suitable for mRANO assessment was mandatory for all SOC patients. The patient characteristics are provided in Supplementary Table 3. Sex was determined based on self-report. The PFS event was defined as the first date at which progression criteria had been met, i.e., the date of the sequentially confirmed MRI assessment resulting in preliminary PD as per mRANO, the date of initiation of second-line therapy or the date of death by any cause if the patient died before clinical or radiographic progression. PFS was defined as the time interval from the first day of RT to the PFS event. OS was calculated as the time from the first day of RT until death by any cause.

Plasma NOX-A12 and CXCL12 concentrations

A liquid chromatography-UV assay, based on an anion-exchange chromatography analysis coupled to a UV detector, was used to detect and quantify the analyte NOX-A12 in patient plasma samples. The comparable calibration curve, generated from a standard-of-dilution series, corresponded to a linear range of NOX-A12 concentrations in human plasma from 0.5 to 200 µg/mL (0.034–13.6 µM). Quantification of CXCL12 concentrations in patient plasma samples was performed by a contractor (Swiss BioQuant AG) using HPLC-MS/MS bioanalytics. The comparable calibration curve corresponded to a linear range of CXCL12 (human SDF-1α and SDF-1β) concentrations in human plasma from 25 to 2500 nM.

Buffers and solutions for multiplexed immunofluorescence

TCEP-reducing solution: 2.5 mM TCEP (Sigma, 646547) and 2.5 mM EDTA pH 8.0 (Invitrogen, AM9261) in ddH_2O, pH 7.0. Buffer C: 150 mM NaCl (Carl Roth, 9265.2), 2 mM Tris stock solution (Carl Roth, AE15.3), pH 7.2, 1 mM EDTA, and 0.02% w/v NaN_3 (AppliChem, A14300,1000) in ddH_2O. High-salt PBS: 900 mM NaCl in 1× DPBS (Gibco, 14190-094). CODEX® antibody stabilizer solution: 0.5 M NaCl, 5 mM EDTA, and 0.02% w/v NaN_3 in PBS antibody stabilizer solution (CANDOR Biosciences GmbH, 131125). Staining solution 1 (S1): 5 mM EDTA, 0.5% w/v bovine serum albumin (BSA, Carl Roth, 8076.3) and 0.02% w/v NaN_3 in 1× DPBS, stored at 4 °C. Staining solution 2 (S2): 61 mM NaH_2PO_4 (Sigma, S0876), 39 mM $NaH_2PO_4 \cdot H2O$ (Sigma, S9638), 250 mM NaCl in a 1:0.7 v/v solution of S1 and doubly-distilled H_2O (ddH_2O); final pH 6.8–7.0, stored at 4 °C. Staining solution 4 (S4): 0.5 M NaCl in S1, stored at 4 °C. Blocking buffer: S2 buffer containing B1 (1:20), B2 (1:20), B3 (1:20), and BC4 (1:15), stored at 4 °C. Blocking reagent 1 (B1): 1 mg/ml mouse IgG (Sigma, I5381) in S2, stored at 4 °C. Blocking reagent 2 (B2): 1 mg/ml rat IgG (Sigma, I4121) in S2, stored at 4 °C. Blocking reagent 3 (B3): sheared salmon sperm DNA (Invitrogen, AM9680), 10 mg/ml in H2O, stored at 4 °C. Blocking component 4 (BC4): Mixture of 57 non-modified oligonucleotides (Biomers) at a final concentration of 0.05 mM each in TE buffer (Sigma, 93302), stored at 4 °C (Supplementary Data 5). BS3 fixative solution: 200 mg/ml BS3 (ThermoFisher, 21580) in DMSO from a freshly opened ampoule (Sigma, D2650-5x5ML), stored at 20 °C in 3 µl aliquots. H2 buffer: 150 mM NaCl, 10 mM Tris pH 7.5, 10 mM $MgCl_2 \cdot 6\ H_2O$ (Carl Roth, 2189.1), 0.1% w/v TritonTM X-100 (Sigma, X-100) and 0.02% w/v NaN_3 in ddH_2O. Plate buffer: H2 buffer containing DAPI nuclear stain (1:300, Biolegend, 422801) and 0.5 mg/ml sheared salmon sperm DNA. Fluorescent oligonucleotide stock solution (Biomers): 100 µM Fluorescent oligonucleotide dissolved in 1× TE buffer, stored in the dark at −20 °C. Fluorescent oligonucleotide working solution: Fluorescent oligonucleotide stock solution diluted 1:10 in 1× TE buffer, stored in the dark at 4 °C. Plate Buffer: H2 buffer containing DAPI nuclear stain (1:300) and 0.5 mg/ml sheared salmon sperm DNA.

Multiplexed immunofluorescence of tumor tissue

All tumor samples were obtained following informed consent as part of SOC surgical procedures. All patients had consented to in-depth analyses of tissue. FFPE tumor samples were sliced by standard procedures at 3 µm slice thickness and adhered onto poly-L-lysine-coated coverslips. Antibody conjugation, tissue staining, and mIF imaging were performed (with modifications) as described elsewhere[36,55]. In short, purified, carrier-free antibodies were conjugated to maleimide-modified oligonucleotides (Biomers), concentrated, reduced, and washed with buffer. Maleimide-modified oligonucleotides were first dissolved in 1× DPBS, then added to the reduced antibody and incubated at room temperature for two hours in a 2:1 (w/w) ratio with the antibodies. Next, the conjugated antibodies were washed in high-salt PBS three times and then eluted by centrifugation at 3000 × *g* for 2 min in the CODEX® antibody stabilizer solution. The conjugated antibodies were stored at 4 °C until usage. Prepared FFPE tissues were baked at 55 °C for 30 min, and rehydrated by immersion in fresh xylene, twice, for 5 min and in descending concentrations of ethanol, each step for 5 min (100% twice, 95% twice, 70%, ddH2O twice). Heat-induced

epitope retrieval was performed using 1× Dako target retrieval solution, pH 9 (Agilent) at high pressure, for 20 min. Tissues were then washed for 10 min in 1× TBS IHC wash buffer with Tween 20 (ThermoFisher, 28360). Tissues were blocked for 1 h at room temperature using 100 µl of blocking buffer. Conjugated antibodies were added to the blocking buffer, concentrated through a 50 kDa Amicon Ultra Filter, and resolved in the blocking buffer. Tissues were incubated with the antibody staining solution in a humidity chamber overnight at 4 °C. The following antibodies were used: Ki-67, 0.01 mg/ml, clone B56, BD Biosciences, Cat.# 556003 (RRID:AB_396287); SDF-1/CXCL12, 0.01 mg/ml, clone 79018, ThermoFisher, Cat.# MA5-23759 (RRID:AB_2608711); α-SMA, 0.01 mg/ml, clone 1A4, ThermoFisher, Cat.# 14-9760-82 (RRID:AB_2572996); CD31, 0.01 mg/ml, clone EP3095, Abcam, Cat.# ab226157; GFAP, 0.01 mg/ml, clone 2.2B10, ThermoFisher Scientific, Cat.# 13-0300 (RRID:AB_2532994); CD68, 0.005 mg/ml, clone KP-1, Biolegend, Cat.# 916104 (RRID:AB_2616797). The antibodies and their characteristics are additionally provided in a table overview in Supplementary Data 5 and the Reporting Summary. After staining, tissues were washed twice in S2 buffer and fixed with a three-step fixation process. First, tissues were fixed in S4 containing 1.6% paraformaldehyde (Electron Microscopy Science, 15710-S) for 10 min, followed by a 15 min-long incubation in 100% ice-cold methanol (Sigma, 34860-1L-R) for 5 min, and a final fixation with BS3 fixative solution dissolved in 1× PBS at room temperature for 20 min. Tissues were stored in S4 in a six-well plate at 4 °C for up to 2 weeks, or further processed for imaging. 400 nM fluorescent oligonucleotide working solution was aliquoted in Corning™ black 96-well plates (Merk, CLS3925-100EA) in 250 µl of plate buffer, according to the multi-cycle reaction panel. Image acquisition was performed on Zeiss Axio Observer 7 microscope equipped with a Colibri 7 LED Light source (Carl Zeiss), and a Prime BSI PCIe camera (Teledyne Photometrics). Imaging cycles were performed using an Akoya Phenocycler™ instrument and CODEX® instrument manager software (Akoya Biosciences). Automated images were acquired with the Plan-Apochromat 20×/0.8 M27 ($a = 0.55$ mm) objective (Carl Zeiss), and the imaging pipeline was controlled by a focus strategy with autofocus for each support point created, with a three z-stack image with a distance of 1.5 µm. DAPI (1:300 final concentration) was imaged in each cycle at an exposure time of 20 milliseconds and LED intensity of 40%. The images were processed with CODEX® Processor (Akoya Biosciences) and analyzed with HALO® Image Analysis software (Indica Labs, v.3.3). After each multi-cycle reaction, standard H&E staining was performed on the same tissue slice to confirm histopathological features. The H&E staining was analyzed independently by a neuropathologist with 5 years of experience and a board-certified neuropathologist with >30 years of experience in the field. With consensus, pathological features of GBM (CNS WHO grade 4) were again confirmed, and zonal characteristics within the tumor tissue were depicted. Adjacent regions like leptomeninges, hemorrhage, or healthy brain tissue were excluded, and only confirmed tumorous tissue parts were considered for the following analyses. Annotated H&E staining can be found in Suppl. Data 1. Analyses were performed using the Highplex FL module (v. 4.1.2) from HALO®. A nucleus/cytoplasm membrane % completeness threshold for positivity was set as follows: DAPI, Nucleus % Completeness Threshold 15%; CXCL12, Nucleus and Cytoplasm % Completeness Threshold 35%; CD68, Nucleus and Cytoplasm % Completeness Threshold 20%; CD31, Nucleus and Cytoplasm % Completeness Threshold 30%; Ki-67, Nucleus % Completeness Threshold 30%, α-SMA, Nucleus and Cytoplasm % Completeness Threshold 35%; GFAP, Nucleus and Cytoplasm % Completeness Threshold 30%. Cellular phenotypes were defined as follows: endothelial cells ($DAPI^+$, $CD31^+$), pericytes ($DAPI^+$, α-SMA^+, $CD31^-$), Mϕ/microglia ($DAPI^+$, $CD68^+$), tumor cells ($DAPI^+$, $GFAP^+$, $CD68^-$, $CD31^-$, α-SMA^-). All phenotypes were also assessed for CXCL12 expression positivity. Nuclear segmentation was based on DAPI with a custom-trained deep learning neural network algorithm, with nuclear segmentation aggressiveness of 0.5 and nuclear size for positivity set between 12 and 1000 µm^2. Details on the multi-cycle reactions and oligo sequences can be found in Supplementary Data 5.

scRNAseq analysis

Dataset GSE182109[35] was downloaded from the Broad Institute Single Cell Portal (https://singlecell.broadinstitute.org/single_cell). Data was analyzed and visualized using R version 4.2.2. *CXCL12* expression was overlayed on UMAP using scCustomize (Version 1.1.1)[56] using the FeaturePlot_scCustom() function with RColorBrewer (Version 1.1–3) and the color pallet "OrRd". Cells were called positive for *CXCL12* if they had a log-normalized count of 1 or more.

Statistics and reproducibility

No formal sample size calculations were performed for this dose-escalation trial, and thus, no statistical method was used to predetermine the sample size. The dose escalation was designed as a modified 3 + 3 rule-based design as described above and in the study protocol provided in Supplementary Note 2. No data were excluded from the analyses. The experiments were not randomized, and thus, investigators were not blinded to allocation during experiments and outcome assessment. The independent central reader was blinded to all clinical aspects of the trial. Also, mIF was performed and analyzed blinded to all clinical aspects of the trial and patient identities. mIF sample sizes are provided for cohorts and subgroups.

Graphical elements were generated using GraphPad Prism 9 (GraphPad Software) and Adobe Illustrator 2023 (Adobe Inc.). Database management (eCRF) was carried out using Viedoc version 4.66 eCRF (Viedoc Technologies) and Microsoft Excel 2019 (Microsoft Corporation). Statistical tests were performed using GraphPad Prism 10 and R (V.3.3.2, x86_64-pc-linux-gnu) as specified in the figure legends. Descriptive statistics were applied to characterize the patient collectives, treatment response, and observed toxicity. Survival rates were estimated using the Kaplan–Meier method and statistically assessed by log-rank test and Cox proportional hazards regression. Group differences for continuous variables were evaluated using the unpaired two-tailed Mann–Whitney *U* test. Spearman's rank correlation was used for correlation analysis.

Reporting summary

Further information on research design is available in the Nature Portfolio Reporting Summary linked to this article.

Data availability

The study protocol is made available as Supplementary Note 2. The data generated in this study are provided in the Supplementary Information and Source Data file. High-resolution images of Supplementary Fig. 6 are provided in the following repository: "Giordano, Layer, Leonardelli et al. Supplementary Fig. 6", Mendeley Data, V1, https://doi.org/10.17632/wfhnv7j2wh.1 (https://data.mendeley.com/datasets/wfhnv7j2wh/1). The publicly available scRNAseq dataset used for re-analysis (from Abdelfattah et al.[35]) can be accessed via the GEO archive provided under accession ID GSE182109. Identifying individual participant data is protected and is not available due to data privacy laws. Individual de-identified participant data are available upon written request from the sponsor (according to local legal requirements for at least ten years). Source data are provided with this paper.

Code availability

All code generated in this study to analyze and plot scRNAseq data has been deposited in the GitHub repository under accession code Giordano_Layer_Leonardelli_etal_CXCL12_GBM_GSE182109 (https://github.com/BaldLab).

References

1. Ostrom, Q. T. et al. CBTRUS statistical report: primary brain and other central nervous system tumors diagnosed in the United States in 2012–2016. *Neuro-Oncol.* **21**, v1–v100 (2019).
2. Stupp, R. et al. Effects of radiotherapy with concomitant and adjuvant temozolomide versus radiotherapy alone on survival in glioblastoma in a randomised phase III study: 5-year analysis of the EORTC-NCIC trial. *Lancet Oncol.* **10**, 459–466 (2009).
3. Wen, P. Y. et al. Glioblastoma in adults: a Society for Neuro-Oncology (SNO) and European Society of Neuro-Oncology (EANO) consensus review on current management and future directions. *Neuro-Oncol.* **22**, 1073–1113 (2020).
4. Hegi, M. E. et al. MGMT gene silencing and benefit from temozolomide in glioblastoma. *N. Engl. J. Med.* **352**, 997–1003 (2005).
5. Kreth, F.-W. et al. Gross total but not incomplete resection of glioblastoma prolongs survival in the era of radiochemotherapy. *Ann. Oncol.* **24**, 3117–3123 (2013).
6. Nabors, L. B. et al. Two cilengitide regimens in combination with standard treatment for patients with newly diagnosed glioblastoma and unmethylated MGMT gene promoter: results of the open-label, controlled, randomized phase II CORE study. *Neuro-Oncol.* **17**, 708–717 (2015).
7. Stupp, R. et al. Effect of tumor-treating fields plus maintenance temozolomide vs maintenance temozolomide alone on survival in patients with glioblastoma: a randomized clinical trial. *JAMA* **318**, 2306–2316 (2017).
8. Sim, H.-W. et al. A randomized phase II trial of veliparib, radiotherapy, and temozolomide in patients with unmethylated MGMT glioblastoma: the VERTU study. *Neuro Oncol.* **23**, 1736–1749 (2021).
9. Stummer, W. et al. Extent of resection and survival in glioblastoma multiforme: identification of and adjustment for bias. *Neurosurgery* **62**, 564–576 (2008).
10. Aldave, G. et al. Prognostic value of residual fluorescent tissue in glioblastoma patients after gross total resection in 5-aminolevulinic acid-guided surgery. *Neurosurgery* **72**, 915–921 (2013).
11. Karschnia, P. et al. Prognostic validation of a new classification system for extent of resection in glioblastoma: A report of the RANO *resect* group. *Neuro-Oncol.* **25**, 940–954 (2023).
12. Brown, T. J. et al. Association of the extent of resection with survival in glioblastoma: a systematic review and meta-analysis. *JAMA Oncol.* **2**, 1460 (2016).
13. Brown, J. M. Vasculogenesis: a crucial player in the resistance of solid tumours to radiotherapy. *Br. J. Radiol.* **87**, 20130686 (2014).
14. Gerhardt, H. et al. VEGF guides angiogenic sprouting utilizing endothelial tip cell filopodia. *J. Cell Biol.* **161**, 1163–1177 (2003).
15. Tammela, T. et al. Blocking VEGFR-3 suppresses angiogenic sprouting and vascular network formation. *Nature* **454**, 656–660 (2008).
16. Takahashi, T. et al. Ischemia- and cytokine-induced mobilization of bone marrow-derived endothelial progenitor cells for neovascularization. *Nat. Med.* **5**, 434–438 (1999).
17. Ceradini, D. J. et al. Progenitor cell trafficking is regulated by hypoxic gradients through HIF-1 induction of SDF-1. *Nat. Med.* **10**, 858–864 (2004).
18. Du, R. et al. HIF1α induces the recruitment of bone marrow-derived vascular modulatory cells to regulate tumor angiogenesis and invasion. *Cancer Cell* **13**, 206–220 (2008).
19. Walters, M. J. et al. Inhibition of CXCR7 extends survival following irradiation of brain tumours in mice and rats. *Br. J. Cancer* **110**, 1179–1188 (2014).
20. Giordano, F. A. et al. Targeting the post-irradiation tumor microenvironment in glioblastoma via inhibition of CXCL12. *Cancers (Basel)* **11**, 272 (2019).
21. Brown, J. M. Radiation damage to tumor vasculature initiates a program that promotes tumor recurrences. *Int. J. Radiat. Oncol.* **108**, 734–744 (2020).
22. Rempel, S. A., Dudas, S., Ge, S. & Gutiérrez, J. A. Identification and localization of the cytokine SDF1 and its receptor, CXC chemokine receptor 4, to regions of necrosis and angiogenesis in human glioblastoma. *Clin. Cancer Res.* **6**, 102–111 (2000).
23. Tabatabai, G., Frank, B., Möhle, R., Weller, M. & Wick, W. Irradiation and hypoxia promote homing of haematopoietic progenitor cells towards gliomas by TGF-beta-dependent HIF-1alpha-mediated induction of CXCL12. *Brain* **129**, 2426–2435 (2006).
24. Komatani, H., Sugita, Y., Arakawa, F., Ohshima, K. & Shigemori, M. Expression of CXCL12 on pseudopalisading cells and proliferating microvessels in glioblastomas: an accelerated growth factor in glioblastomas. *Int. J. Oncol.* **34**, 665–672 (2009).
25. Feig, C. et al. Targeting CXCL12 from FAP-expressing carcinoma-associated fibroblasts synergizes with anti-PD-L1 immunotherapy in pancreatic cancer. *Proc. Natl Acad. Sci. USA* **110**, 20212–20217 (2013).
26. Fearon, D. T. The carcinoma-associated fibroblast expressing fibroblast activation protein and escape from immune surveillance. *Cancer Immunol. Res.* **2**, 187–193 (2014).
27. Seo, Y. D. et al. Mobilization of CD8+ T cells via CXCR4 blockade facilitates PD-1 checkpoint therapy in human pancreatic cancer. *Clin. Cancer Res.* **25**, 3934–3945 (2019).
28. Maderna, E., Salmaggi, A., Calatozzolo, C., Limido, L. & Pollo, B. Nestin, PDGFRbeta, CXCL12 and VEGF in glioma patients: different profiles of (pro-angiogenic) molecule expression are related with tumor grade and may provide prognostic information. *Cancer Biol. Ther.* **6**, 1018–1024 (2007).
29. Hattermann, K. et al. The chemokine receptor CXCR7 is highly expressed in human glioma cells and mediates antiapoptotic effects. *Cancer Res.* **70**, 3299–3308 (2010).
30. Kioi, M. et al. Inhibition of vasculogenesis, but not angiogenesis, prevents the recurrence of glioblastoma after irradiation in mice. *J. Clin. Invest.* **120**, 694–705 (2010).
31. Thomas, R. P. et al. Macrophage exclusion after radiation therapy (MERT): a first in human phase I/II trial using a CXCR4 Inhibitor in glioblastoma. *Clin. Cancer Res.* **25**, 6948–6957 (2019).
32. Liu, S.-C. et al. Blockade of SDF-1 after irradiation inhibits tumor recurrences of autochthonous brain tumors in rats. *Neuro-Oncol.* **16**, 21–28 (2014).
33. Wlotzka, B. et al. In vivo properties of an anti-GnRH Spiegelmer: an example of an oligonucleotide-based therapeutic substance class. *Proc. Natl Acad. Sci. USA* **99**, 8898–8902 (2002).
34. Vater, A. et al. Hematopoietic stem and progenitor cell mobilization in mice and humans by a first-in-class mirror-image oligonucleotide inhibitor of CXCL12. *Clin. Pharm. Ther.* **94**, 150–157 (2013).
35. Abdelfattah, N. et al. Single-cell analysis of human glioma and immune cells identifies S100A4 as an immunotherapy target. *Nat. Commun.* **13**, 767 (2022).
36. Black, S. et al. CODEX multiplexed tissue imaging with DNA-conjugated antibodies. *Nat. Protoc.* **16**, 3802–3835 (2021).
37. Shekarian, T. et al. Immunotherapy of glioblastoma explants induces interferon-γ responses and spatial immune cell rearrangements in tumor center, but not periphery. *Sci. Adv.* **8**, eabn9440 (2022).
38. Greenfield, J. P., Cobb, W. S. & Lyden, D. Resisting arrest: a switch from angiogenesis to vasculogenesis in recurrent malignant gliomas. *J. Clin. Invest* **120**, 663–667 (2010).
39. Kozin, S. V. et al. Recruitment of myeloid but not endothelial precursor cells facilitates tumor regrowth after local irradiation. *Cancer Res* **70**, 5679–5685 (2010).

40. Tabouret, E. et al. Recurrence of glioblastoma after radiochemotherapy is associated with an angiogenic switch to the CXCL12-CXCR4 pathway. *Oncotarget* **6**, 11664–11675 (2015).
41. Yeo, A. T. et al. Single-cell RNA sequencing reveals evolution of immune landscape during glioblastoma progression. *Nat. Immunol.* **23**, 971–984 (2022).
42. Hoogstrate, Y. et al. Transcriptome analysis reveals tumor microenvironment changes in glioblastoma. *Cancer Cell* **41**, 678–692.e7 (2023).
43. Karimi, E. et al. Single-cell spatial immune landscapes of primary and metastatic brain tumours. *Nature* **614**, 555–563 (2023).
44. Polley, M.-Y. C. & Dignam, J. J. Statistical considerations in the evaluation of continuous biomarkers. *J. Nucl. Med.* **62**, 605–611 (2021).
45. Tsien, C. I. et al. NRG Oncology/RTOG1205: a randomized phase II trial of concurrent bevacizumab and reirradiation versus bevacizumab alone as treatment for recurrent glioblastoma. *J. Clin. Oncol.* **41**, 1285–1295 (2023).
46. Lombardi, G. et al. Regorafenib compared with lomustine in patients with relapsed glioblastoma (REGOMA): a multicentre, open-label, randomised, controlled, phase 2 trial. *Lancet Oncol.* **20**, 110–119 (2019).
47. Wu, D. et al. The blood–brain barrier: structure, regulation, and drug delivery. *Sig Transduct. Target Ther.* **8**, 217 (2023).
48. Hoellenriegel, J. et al. The Spiegelmer NOX-A12, a novel CXCL12 inhibitor, interferes with chronic lymphocytic leukemia cell motility and causes chemosensitization. *Blood* **123**, 1032–1039 (2014).
49. Chernikova, S., Ahn, G.-O., Liu, S.-C., Stafford, J. & Brown, J. M. Abstract C291: targeting SDF-1 (CXCL12) pathway to inhibit the recurrence of breast cancer brain metastases after whole-brain irradiation. *Mol. Cancer Ther.* **12**, C291–C291 (2013).
50. Deng, L. et al. SDF-1 blockade enhances anti-VEGF therapy of glioblastoma and can be monitored by MRI. *Neoplasia* **19**, 1–7 (2017).
51. Le Tourneau, C., Lee, J. J. & Siu, L. L. Dose escalation methods in phase I cancer clinical trials. *J. Natl. Cancer Inst.* **101**, 708–720 (2009).
52. Niyazi, M. et al. ESTRO-ACROP guideline 'target delineation of glioblastomas. *Radiother. Oncol.* **118**, 35–42 (2016).
53. Ellingson, B. M., Wen, P. Y. & Cloughesy, T. F. Modified criteria for radiographic response assessment in glioblastoma clinical trials. *Neurotherapeutics* **14**, 307–320 (2017).
54. Mikeska, T. et al. Optimization of quantitative MGMT promoter methylation analysis using pyrosequencing and combined bisulfite restriction analysis. *J. Mol. Diagn.* **9**, 368–381 (2007).
55. Krämer, B. et al. Single-cell RNA sequencing identifies a population of human liver-type ILC1s. *Cell Rep.* **42**, 111937 (2023).
56. Marsh, S., Salmon, M. & Hoffman, P. samuel-marsh/scCustomize: Version 1.1.1. https://doi.org/10.5281/ZENODO.5706430. (2023).

Acknowledgements

We wish to thank all patients and their families for their commitment to participate in this study. The clinical study was sponsored by TME Pharma AG (Berlin, Germany). TME Pharma AG also provided NOX-A12 clinical trial supply and partial funding for consumables related to this work. Parts of the translational research were supported by grants from the Deutsche Forschungsgemeinschaft (DFG, German Research Foundation; SFB 1389 UNITE Glioblastoma/TP-B05-404521405 to F.A.G.). J.P.L. was supported by a grant from *Novartis Stiftung für therapeutische Forschung* (foundation for therapeutic research) for personal equipment. S.L. was supported by post-doc research fellowships within the Mildred-Scheel School of Oncology Cologne-Bonn supported by the German Cancer Aid—Project ID 70113307 (Deutsche Krebshilfe) in which context expertize in mIF imaging was established for a project unrelated to this study. L.L.F. is supported by the BONFOR program of the Medical Faculty of the University of Bonn, Germany (grant ID 2022–1A-09). M.H. is a member of EXC2151 and supported by the Deutsche Forschungsgemeinschaft (DFG, German Research Foundation) under Germany's Excellence Strategy—EXC2151–390873048. We thank the study site staff for their ongoing support, particularly Christiane Landwehr, Katja Klever, Joana Kömpel, Mirco Muscheid, Monika Brüggemann, Inga Krause, Nadja Talhi, Sabrina Agkatsev, Gina Seidel. We thank Ute Heuser-Figgemeier and Alexandra Brüggemann from the Institute of Neuropathology and Sandra Bald and Simone Glees from the Department of Dermatology at the University Hospital Bonn for their help with the GBM tissue processing. The UKB histopathology research core facility is supported by the Deutsche Forschungsgemeinschaft (DFG, German Research Foundation) under Germany's Excellence Strategy—EXC2151–390873048. We would like to thank the Microscopy Core Facility of the Medical Faculty at the University of Bonn for providing instrumentation funded by the Deutsche Forschungsgemeinschaft (DFG, German Research Foundation)—project number 388168919.

Author contributions

This study and its translational analysis were conceptualized and conceived by F.A.G., J.P.L., S.L., and M.H. F.A.G., J.P.L., T.Z., C.S., E.S., L.C.S., K.S., C.O., S.K., P.H., M.P., M.G., C.S., and U.H.-treated patients. S.B. and J.P.L. assessed and reviewed the patient's imaging. Material preparation and data collection were performed by J.P.L., S.L., and M.H. Histological staining was assessed by L.L.F. and T.P. mIF was established by S.L. and performed by S.L., J.P.L., and R.T. RNA sequencing data was analyzed by D.C., S.L., J.P.L., and M.H. Computational data analysis was performed by J.P.L. and S.L. F.A.G., U.H., and M.H. provided funding and resources. The first draft of the manuscript was written by J.P.L. and S.L. Tables and figures were created by J.P.L. and S.L. F.A.G., M.P., U.H., and M.H. reviewed and edited the data and manuscript. All authors commented on previous versions of the manuscript. All authors read and approved the final manuscript.

Funding

Open Access funding enabled and organized by Projekt DEAL.

Competing interests

F.A.G. reports travel expenses, stocks and honoraria from TME Pharma AG related to this work; research grants and travel expenses from ELEKTA AB; grants, research grants, travel expenses and honoraria from Carl Zeiss Meditec AG; travel expenses and research grants from Varian Medical Systems, Inc.; travel expenses and/or honoraria from Bristol-Myers Squibb, Cureteq AG, Roche Pharma AG, MSD Sharp and Dohme GmbH, Siemens Healthineers AG, Varian Medical Systems, and AstraZeneca GmbH; non-financial support from Oncare GmbH and Opasca GmbH and patent US10857388B2 together with Carl Zeiss Meditec AG; all unrelated to this work. J.P.L. reports stocks and travel expenses from TME Pharma AG related to this work; travel expenses from Carl Zeiss Meditec AG, stocks and honoraria from Siemens Healthineers AG, and stocks from Bayer AG and BioNTech AG, all unrelated to this work. S.L. reports travel expenses from TME Pharma AG related to this work. C.S. has received speaker and/or advisory board honoraria from AbbVie, Bristol-Myers Squibb, HRA Pharma, Medac, Novocure, Roche, and Seagen not related to this work. E.S. reports travel expenses and honoraria for lectures from Carl Zeiss Meditec AG. C.O. reports travel support from Novocure; honoria by Horizon and Novocure and has received a Clinician Scientist Stipend of the University Medicine Essen Clinician Scientist Academy (UMEA) sponsored by the faculty of medicine and Deutsche Forschungsgemeinschaft (DFG). U.H. reports honoraria from Medac and Bayer AG, unrelated to this work. M.H. reports travel expenses, honoraria for webinars and research support (consumables) from TME Pharma AG related to this work. M.H. also reports honoraria from Bristol-Myers Squibb and Novartis unrelated to this work. A patent application related to biomarker identification has been filed by F.A.G., J.P.L., S.L., and M.H. (EP23000076.2; EP23000075.4). The remaining authors declare no competing interests.

Additional information

Supplementary information The online version contains supplementary material available at https://doi.org/10.1038/s41467-024-48416-9.

Correspondence and requests for materials should be addressed to Frank A. Giordano or Michael Hölzel.

Peer review information *Nature Communications* thanks the anonymous reviewers for their contribution to the peer review of this work. A peer review file is available.

Reprints and permissions information is available at http://www.nature.com/reprints

Publisher's note Springer Nature remains neutral with regard to jurisdictional claims in published maps and institutional affiliations.

Frank A. Giordano[1,2,13] ✉, Julian P. Layer[3,4,13], Sonia Leonardelli[4,13], Lea L. Friker[4,5], Roberta Turiello[4], Dillon Corvino[4], Thomas Zeyen[6], Christina Schaub[6], Wolf Müller[7], Elena Sperk[1], Leonard Christopher Schmeel[3], Katharina Sahm[2,8,9], Christoph Oster[10], Sied Kebir[10], Peter Hambsch[11], Torsten Pietsch[5], Sotirios Bisdas[12], Michael Platten[2,8,9], Martin Glas[10], Clemens Seidel[11], Ulrich Herrlinger[6,13] & Michael Hölzel[4,13] ✉

[1]Department of Radiation Oncology, University Medical Center Mannheim, Medical Faculty Mannheim, University of Heidelberg, Mannheim, Germany. [2]DKFZ-Hector Cancer Institute at the University Medical Center Mannheim, Mannheim, Germany. [3]Department of Radiation Oncology, University Hospital Bonn, University of Bonn, Bonn, Germany. [4]Institute of Experimental Oncology, Medical Faculty, University Hospital Bonn, University of Bonn, Bonn, Germany. [5]Institute of Neuropathology, University Hospital Bonn, University of Bonn, Bonn, Germany. [6]Department of Neurooncology, Center for Neurology, University Hospital Bonn, Bonn, Germany. [7]Institute of Neuropathology, University Hospital Leipzig, University of Leipzig, Leipzig, Germany. [8]Department of Neurology, Medical Faculty Mannheim, MCTN, Heidelberg University, Mannheim, Germany. [9]DKTK Clinical Cooperation Unit Neuroimmunology and Brain Tumor Immunology, German Cancer Research Center, Heidelberg, Germany. [10]Division of Clinical Neurooncology, Department of Neurology, Center for Translational Neuro- and Behavioral Sciences (C-TNBS) and West German Cancer Center, German Cancer Consortium, Partner Site Essen, University Hospital Essen, University Duisburg-Essen, Essen, Germany. [11]Department of Radiation Oncology, University Hospital Leipzig, University of Leipzig, Leipzig, Germany. [12]Lysholm Department of Neuroradiology, University College London, London, UK. [13]These authors contributed equally: Frank A. Giordano, Julian P. Layer, Sonia Leonardelli, Ulrich Herrlinger, Michael Hölzel. ✉e-mail: Frank.Giordano@umm.de; michael.hoelzel@ukbonn.de

3.2 Hamed M*, Potthoff AL*, Layer JP, Koch D, Borger V, Heimann M, Scafa D, Sarria GR, Holz JA, Schmeel FC, Radbruch A, Güresir E, Schäfer N, Schuss P, Garbe S, Giordano FA, Herrlinger U, Vatter H, Schmeel LC*, Schneider M*. Benchmarking Safety Indicators of Surgical Treatment of Brain Metastases Combined with Intraoperative Radiotherapy: Results of Prospective Observational Study with Comparative Matched-Pair Analysis. Cancers (Basel). 2022 Mar 16;14(6):1515.

Hintergrund und Zielsetzung der Arbeit: Neben dem klinischen *Outcome* ist auch das Sicherheitsprofil einer Behandlung ein entscheidender Faktor bei der Wahl der optimalen Therapieform. Die unmittelbare IORT nach Resektion einer Hirnmetastase kann prinzipiell durch die zusätzliche Intervention ein erhöhtes Risiko für perioperative Morbidität und Mortalität darstellen. In dieser Arbeit sollte daher das zusätzliche perioperative Risiko einer Resektion mit IORT gegenüber einer Resektion ohne IORT eruiert werden. Zu diesem Zweck erfolgte ein individuelles Matching retrospektiv erhobener Patientenfälle, die eine IORT erhalten hatten, mit Patientenfällen, in denen keine IORT erfolgt war.

Methoden und Ergebnisse: Für 35 konsekutive Fälle von Patienten mit Hirnmetastasen, die im Universitätsklinikum Bonn zwischen November 2020 und Oktober 2021 mit einer Resektion und anschließender IORT behandelt wurden, wurden Patientensicherheitsindikatoren, nosokomiale Erkrankungen und Hirnchirurgie-bedingte Komplikationen erhoben. Die Ergebnisse wurden mittels einer *comparative matched-pair* Analyse im Verhältnis 1:3 mit denen einer institutionellen Datenbank mit insgesamt 388 konsekutiven Patientenfällen mit Resektion ohne IORT gegenübergestellt. Es ergaben sich keine signifikanten Unterschiede für die perioperativen Komplikationen oder die 30 Tages-Mortalität.

Schlussfolgerungen: Trotz der zusätzlichen medizinischen Intervention ergaben sich keine Hinweise auf eine relevante perioperative Risikoerhöhung durch die IORT. Die Ergebnisse belegen eine gute Verträglichkeit der IORT nach Resektion von Hirnmetastasen.

cancers

MDPI

Article

Benchmarking Safety Indicators of Surgical Treatment of Brain Metastases Combined with Intraoperative Radiotherapy: Results of Prospective Observational Study with Comparative Matched-Pair Analysis

Motaz Hamed [1,†], Anna-Laura Potthoff [1,*,†], Julian P. Layer [2], David Koch [2], Valeri Borger [1], Muriel Heimann [1], Davide Scafa [2], Gustavo R. Sarria [2], Jasmin A. Holz [2], Frederic Carsten Schmeel [3], Alexander Radbruch [3], Erdem Güresir [1], Niklas Schäfer [4], Patrick Schuss [1,5], Stephan Garbe [2], Frank A. Giordano [2], Ulrich Herrlinger [4], Hartmut Vatter [1], Leonard Christopher Schmeel [2,‡] and Matthias Schneider [1,*,‡]

1 Department of Neurosurgery, University Hospital Bonn, 53127 Bonn, Germany; motaz.hamed@ukbonn.de (M.H.); valeri.borger@ukbonn.de (V.B.); muriel.heimann@ukbonn.de (M.H.); erdem.gueresir@ukbonn.de (E.G.); patrick.schuss@ukbonn.de (P.S.); hartmut.vatter@ukbonn.de (H.V.)
2 Department of Radiation Oncology, University Hospital Bonn, 53127 Bonn, Germany; julian.layer@ukbonn.de (J.P.L.); david.koch@ukbonn.de (D.K.); davide.scafa@ukbonn.de (D.S.); gustavo.sarria@ukbonn.de (G.R.S.); jasmin.holz@ukbonn.de (J.A.H.); stephan.garbe@ukbonn.de (S.G.); frank.giordano@ukbonn.de (F.A.G.); christopher.schmeel@ukbonn.de (L.C.S.)
3 Department of Neuroradiology, University Hospital Bonn, 53127 Bonn, Germany; carsten.schmeel@ukbonn.de (F.C.S.); alexander.radbruch@ukbonn.de (A.R.)
4 Division of Clinical Neuro-Oncology, Department of Neurology, University Hospital Bonn, 53127 Bonn, Germany; niklas.schaefer@ukbonn.de (N.S.); ulrich.herrlinger@ukbonn.de (U.H.)
5 Department of Neurosurgery, BG Klinikum Unfallkrankenhaus Berlin, 12683 Berlin, Germany
* Correspondence: anna-laura.potthoff@ukbonn.de (A.-L.P.); matthias.schneider@ukbonn.de (M.S.)
† These authors contributed equally to this work.
‡ These authors contributed equally to this work.

check for updates

Citation: Hamed, M.; Potthoff, A.-L.; Layer, J.P.; Koch, D.; Borger, V.; Heimann, M.; Scafa, D.; Sarria, G.R.; Holz, J.A.; Schmeel, F.C.; et al. Benchmarking Safety Indicators of Surgical Treatment of Brain Metastases Combined with Intraoperative Radiotherapy: Results of Prospective Observational Study with Comparative Matched-Pair Analysis. *Cancers* **2022**, *14*, 1515. https://doi.org/10.3390/cancers14061515

Academic Editor: Dirk Rades

Received: 25 January 2022
Accepted: 8 March 2022
Published: 16 March 2022

Publisher's Note: MDPI stays neutral with regard to jurisdictional claims in published maps and institutional affiliations.

Simple Summary: Patients with brain metastasis (BM) are at advanced stages of metastatic cancer, and surgical resection is often required in order to avoid severe neurologic deficits. After surgery, patients are usually committed to postoperative radiotherapy. In recent years, intraoperative radiotherapy (IORT) has been proposed as an alternative to conventional postsurgical radiation approaches. This possibility has several advantages, e.g., as IORT is administered only once during the surgical procedure, patients do not have to attend several radiotherapy sessions afterward. However, the application of radiation therapy directly into the open brain during surgery might be accompanied by severe perioperative complications and, therefore, might negatively impact the overall benefit. In the present study, we show that patients who underwent surgery for BM combined with IORT do not suffer from elevated levels of perioperative complications compared to patients without IORT. Therefore, IORT constitutes a safe treatment strategy for cancer patients with BM.

Abstract: Intraoperative radiotherapy (IORT) of the operative cavity for surgically treated brain metastasis (BM) has gained increasing prominence with respect to improved local tumor control. However, IORT immediately performed at the time of surgery might be associated with increased levels of perioperative adverse events (PAEs). In the present study, we performed safety metric profiling in patients who had undergone surgery for BM with and without IORT in order to comparatively analyze feasibility of IORT as an adjuvant radiation approach. Between November 2020 and October 2021, 35 patients were surgically treated for BM with IORT at our neuro-oncological center. Perioperative complication profiles were collected in a prospective observational cohort study by means of patient safety indicators (PSIs), hospital-acquired conditions (HACs), and specific cranial-surgery-related complications (CSCs) as high-standard quality metric tools and compared to those of an institutional cohort of 388 patients with BM resection without IORT in a balanced comparative matched-pair analysis. Overall, 4 out of 35 patients (11%) with IORT in the course BM

resection suffered from PAEs, accounting for 3 PSIs (9%) and 1 HAC (3%). Balanced matched-pair analysis did not reveal significant differences in the perioperative complication profiles between the cohorts of patients with and without IORT ($p = 0.44$). Thirty-day mortality rates were 6% for patients with IORT versus 8% for patients without IORT ($p = 0.73$). The present study demonstrates that IORT constitutes a safe and clinically feasible adjuvant treatment modality in patients undergoing surgical resection of BM.

Keywords: surgery for brain metastasis; intraoperative radiotherapy; perioperative complication profiling

1. Introduction

Postoperative adjuvant cranial radiotherapy constitutes the standard clinical practice following surgical resection of brain metastases (BMs) [1,2]. In recent years, low-energy X-ray intraoperative radiation therapy (IORT) has been increasingly proposed as a viable alternative to conventional postsurgical irradiation approaches, as this technique yields considerable advantages: the delay between surgery and radiation therapy is greatly reduced, the dose gradient is steep, and challenges in target volume delineation are avoided due to postoperative anatomical alterations. The combination of these beneficial factors is associated with reduced doses to healthy brain tissue and may prevent repopulation of residual microscopic disease [3–7]. The safety of IORT has been demonstrated in the setting of surgically resected glioblastoma [8] and its efficacy is currently being evaluated in a Phase III clinical trial [9]. To date, known data regarding IORT in surgically treated BM are limited to several single institutional studies indicating promising high rates of local tumor control and a low incidence of radiation necrosis [10]. These studies are mainly focused on radiotherapeutic parameters, such as dosage, size of applicator, and time span of IORT procedures [3,10,11]. From an interdisciplinary perspective, the avoidance of postoperative complications in patients with surgically resected BM is of paramount importance to prevent prolonging the initiation of further adjuvant (including systemic) therapies [12,13]. In the context of IORT in BM, it remains unknown whether the concentrated radiation exposure administered intraoperatively has adverse consequences, e.g., for wound healing or other identifiable postoperative complications for the severely affected patients.

Therefore, the present prospective observational study aimed to investigate the frequency or occurrence of established perioperative adverse events (PAEs) during and after IORT in surgically treated BM. The results obtained were compared with data from patients without IORT who underwent standard postoperative adjuvant radiotherapy in order to benchmark the value and potential safety of IORT in patients with surgically treated BM.

2. Materials and Methods

2.1. Patients

Study data of all consecutive patients who were admitted to the Neurosurgical Department of the University Hospital Bonn and underwent surgical resection of BM and IORT between November 2020 and October 2021 were prospectively collected and managed using SPSS (version 25, IBM Corp., Armonk, NY, USA). Informed consent was obtained from the patients or the patients' representatives. Information collected for each patient included sociodemographic characteristics, location of primary tumor, radiological and histopathological characteristics of both the tumor of primary origin and the intracranial metastatic lesion, and functional status at admission, among others. The comorbidity burden was objectified using the Charlson comorbidity index (CCI) [14]. The Karnofsky performance score (KPS) was used to classify the patients according to their functional status at admission. A stratification cut-off of 70 was chosen according to Péus et al. with regard to the patient's ability to carry on their normal activities and work [15].

All patients received preoperative contrast-enhanced T1-weighted MRI providing 3D image guidance for both surgery and radiation treatment. For IORT, optic nerves, chiasma,

and brain stem were identified preoperatively and intraoperatively as organs at risk (OAR), and applied doses were defined based on dose–depth profiles of the utilized spherical applicators ranging from 1.5 to 5 cm in diameter. IORT was delivered using INTRABEAM® 600 (Carl Zeiss Meditec AG, Oberkochen, Germany) nominal 50 kV photons at an optimal dose of 30 Gy prescribed to the applicator surface. A decrease in the prescribed dose toward 24 Gy was acceptable in case of OAR doses exceeding the constraints of 12 Gy to the optical nerves and chiasma or 12.5 Gy to the brain stem following the Quantitative Analyses of Normal Tissue Effects in the Clinic (QUANTEC) recommendations [16].

Perioperative complications were assessed by means of a publicly available list of events introduced by the Agency for Healthcare Research and Quality and the Center for Medicare and Medicaid Services, and referred to as patient safety indicators (PSIs) and hospital-acquired conditions (HACs) [17,18]. PSIs included the complicative occurrence of pressure ulcers, iatrogenic pneumothorax, transfusion reactions, peri- and postoperative hemorrhage, pulmonary embolism, acute postoperative respiratory failure, deep-vein thrombosis, postoperative sepsis, wound dehiscence, and accidental puncture or laceration. Within the group of HACs, screening was performed for pneumonia, catheter-associated urinary tract infections, blood incompatibility, crushing injury, manifestation of poor glycemic control (diabetic ketoacidosis, nonketotic hyperosmolar coma, and hyperglycemic coma), fall injuries, and vascular catheter-associated infections. In addition, to assess complications specific to cranial surgeries, postoperative periods were screened for iatrogenic postoperative infarction, cerebrospinal fluid (CSF) leakage, postoperative meningitis and ventriculitis, brain edema, cerebrovascular venous thrombosis, postoperative seizures, and postoperative new or worsened neurological deficits; they were classified as cranial-surgery-related complications (CSCs) as previously described [19,20]. Perioperative complications were defined as any intra- and/or postoperative adverse event with or without further surgical interventions occurring within 30 days of the initial BM resection.

This study was conducted in accordance with the Declaration of Helsinki and approved by the Ethics Committee of the University Hospital Bonn (approval number 018/21).

2.2. Matching Procedure

Matching was used to control for measured pretreatment variables that were prognostic of the outcome. For the matched-pair analysis, the statistical computing program R (version 4.1.2 (The R Foundation, Boston, MA, USA); The R Foundation for Statistical Computing, https://www.r-studio.com (accessed on 25 January 2022)) was used. Propensity score matching was performed at a ratio of 1:3 between the cohort of 35 prospectively collected patients with IORT and a retrospectively collected cohort of 388 patients with surgically treated BM without IORT. The matching cohort of patients without IORT consisted of all patients aged $\geq$18 years who had undergone surgery for BM at our neuro-oncological center between 2013 and 2018. Within this time span, no patient received IORT at our neuro-oncological center. The study protocol for retrospective data collection was approved by the local ethics committee (approval number 250/19). Informed consent was not sought as a retrospective study design was chosen. Patients with leptomeningeal disease were excluded. To produce a covariate balance in the two groups and therefore increase the robustness of the data, the following known prognostic parameters were selected for matching: age [21], KPS and CCI at admission [19,21,22], tumor entity, and status of solitary versus multiple BM [19]. The balance was measured by the standardized mean differences, variance ratios, and empirical cumulative density function statistics, and visualized using a love plot. To display the distribution of propensity scores, we chose a jitter plot.

2.3. Statistics

Data analyses were performed using the computer software package SPSS (version 25, IBM Corp., Armonk, NY, USA) and GraphPad PRISM (GraphPad Software, San Diego, CA, USA). Categorical variables were analyzed in contingency tables using Fisher's exact test. The Mann–Whitney U test was chosen to compare continuous variables as

the data were mostly not normally distributed. Results with $p < 0.05$ were considered statistically significant.

3. Results

3.1. Patient Baseline Characteristics

Between November 2020 and October 2021, 35 patients underwent surgical therapy for BM combined with IORT at our neuro-oncological center. The median age was 63 years (IQR 54–71 years) including 18 women (51%) and 17 men (49%) (Table 1). The most common tumor entity of the intracranial metastatic lesion was NSCLC (60%), followed by melanoma (11%), and breast cancer (6%). Fifteen patients (43%) suffered from multiple BMs at the date of the operation. The median dose of IORT was 30 Gy (16–30 Gy). The median duration of IORT was 20 min (IQR 17–21 min). Overall, perioperative unfavorable events following resection of BM combined with IORT were present in 4 of 35 patients (11%). Two patients (6%) died within 30 days of surgery. The reasons for death were fulminant pulmonary embolism on day 15 following neurosurgical resection and sepsis from postoperative catheter-associated urinary tract infection. For further details on patient characteristics, see Table 1.

Table 1. Baseline characteristics of patients with IORT.

Baseline Characteristics	*n*
Female sex	18 (51%)
Median age (IQR) (in years)	63 (54–71)
Primary site of cancer	
Lung	21 (60%)
Melanoma	4 (11%)
Breast	2 (6%)
Others	8 (23%)
Multiple BMs	15 (43%)
Preoperative KPS $\geq$ 70	25 (71%)
Median CCI (IQR)	10 (8–11)
ASA $\geq$ 3	24 (69%)
Median duration of surgery (IQR)	272 (187–250)
Median dose of IORT (in Gy)	30 (16–30)
Median duration of IORT (IQR) (in min)	20 (17–21)
Perioperative complications	4 (11%)
30-day mortality	2 (6%)

Values represent the absolute number of patients unless indicated otherwise. ASA, American Society of Anesthesiology physical status classification system; BM, brain metastasis; CCI, Charlson comorbidity index; Gy, gray; IORT, intraoperative radiotherapy; IQR, interquartile range; KPS, Karnofsky performance status.

The functional status at discharge objectified by the KPS did not significantly differ for the groups with and without IORT (70 (60–90) vs. 80 (70–90), $p = 0.52$).

3.2. Perioperative Complications

Subclassification of intraoperative and early postoperative unfavorable events revealed three PSIs and one HAC (Table 2).

PSIs consisted of postoperative hemorrhage with the need for revision surgery, postoperative pulmonary embolism, and postoperative sepsis from urinary tract infection in 1 out of 35 patients (3%). HACs accounted for postoperative pneumonia in one subject (3%). No specific CSC was found.

3.3. Safety-Metric Profiling for IORT in a Comparative Matched-Pair Analysis

In order to compare the complication risk profiles of patients with surgically treated BM dependent on the presence of IORT, we decided to perform multivariate and propensity score matching with additional balance optimization. For this purpose, patients with BM and IORT were individually matched at a ratio of 1:3 to a cohort of 388 patients that had

undergone resection of BM without IORT between 2013 and 2018 at our neuro-oncological center (Figure 1).

Table 2. Overview of perioperative complications of patients with IORT.

No. of Patients with IORT	*n* = 35
No. of complications	4 (11)
PSIs	
Postoperative hemorrhage	1 (3)
Postoperative pulmonary embolism	1 (3)
Postoperative sepsis (urinary tract infection)	1 (3)
HACs	
Pneumonia	1 (3)
Specific CSCs	0 (0)

Values represent the number of patients unless indicated otherwise (%). CSCs, cranial surgery-related complications; HAC, hospital-acquired conditions; IORT, intraoperative radiotherapy; No., number; PSIs, patient safety indicators.

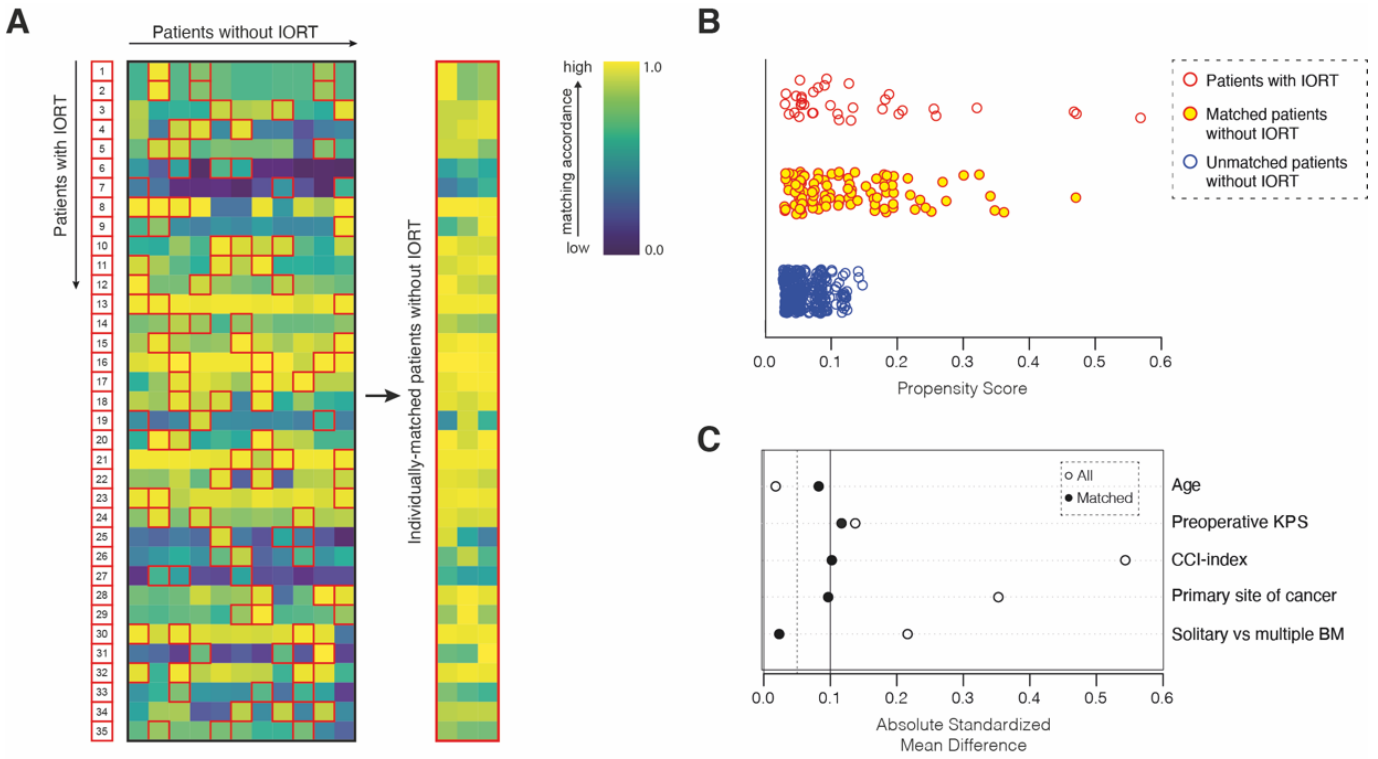

Figure 1. Illustration of the matching procedure for patients with surgically treated BM dependent on the presence of IORT. (**A**) Comparative matched-pair analysis at a ratio of 1:3 identified 105 out of 388 patients with surgically treated BM without IORT that individually corresponded to the present series of 35 patients with surgically treated BM combined with IORT. Heat map is a color-coded illustration of the matching strategy of patients without IORT to individually matched IORT cases by means of age at admission, KPS at admission, CCI at admission, and tumor entity and solitary versus multiple BM as matching parameters. Red frames depict individually matched patients without IORT. (**B**) Visualization of obtained propensity scores for matched and unmatched patients with BM. (**C**) Love plot depicting the balance of the matching analysis for each matching parameter determined by the standardized mean differences. BM, brain metastasis; CCI, Charlson comorbidity index; IORT, intraoperative radiotherapy; KPS, Karnofsky performance score.

Patient age, CCI and KPS at admission, primary site of cancer, as well as solitary versus multiple intracranial metastatic status as known prognostic parameters for survival in patients with an advanced metastatic stage of cancer disease were chosen as matching

variables. Hence, the matched-pair analysis yielded two individually matched cohorts of 35 patients with IORT and 105 patients without IORT that did not significantly differ with regard to the above-mentioned prognostic survival parameters (Table 3). Safety-metric profiling by means of PSIs, HACs, and specific CSCs as highly standardized quality rating tools did not reveal significant differences between the two groups of matched patients with resected BM dependent on the presence of IORT ($p = 0.44$). Similarly, 30-day mortality did not significantly differ between patients with and without IORT ($p = 0.73$) (Table 3).

Table 3. Comparative matched-pair analysis on perioperative complication profiles for patients with versus without IORT.

Variables	Surgery with IORT *n* = 35	Surgery without IORT *n* = 105	*p*-Value
Matching variables			
Age (years)	63 (54–71) †	65 (56–73) †	0.69
Preoperative KPS	80 (60–90) †	80 (70–90) †	0.73
CCI	10 (8–11) †	9 (8–11) †	0.74
Primary site of cancer			0.70
Lung cancer	21 (60)	58 (55)	
Others	14 (40)	47 (45)	
Solitary versus multiple BM			1.0
Multiple BM	15 (43)	46 (44)	
Solitary BM	20 (57)	59 (56)	
Perioperative complications	4 (11)	19 (18)	0.44
PSIs	3 (9)	12 (11)	n.s.
HACs	1 (3)	3 (3)	n.s.
Specific CSCs	0 (0)	4 (4)	0.04
30-day mortality	2 (6)	8 (8%)	0.73

Values represent the number of patients unless indicated otherwise (%). BM, brain metastasis; CCI, Charlson comorbidity index; CSCs, cranial surgery-related complications; HAC, hospital-acquired conditions; IORT, intraoperative radiotherapy; IQR, interquartile range; KPS, Karnofsky performance status; PSIs, patient safety indicators. † Median (IQR).

4. Discussion

IORT has gained growing attention with regard to its high rates of local tumor control as well as low incidences of radiation necrosis [10]. In addition, IORT should allow for the reduction of a patient's socio-economic burden compared to standard surgery followed by multiple adjuvant radiation sessions [23], thereby also enabling faster initiation of systemic treatment. However, such additional intraoperative procedures accompanied by an extended time of surgery might result in elevated levels of early postoperative unfavorable events, which in turn may impair the initially supposed overall benefit of a combined surgery–radiation approach. In the present study, we aimed to analyze the prevalence of perioperative complications in patients who had undergone surgical removal of BM. The data indicate that the addition of IORT delivered immediately within the resection cavity following resection of BM is not associated with higher levels of perioperative unfavorable events within 30 days of surgery compared to a resection policy without IORT.

In contrast to the above-mentioned concerns of increased complication rates in the IORT cohort, these results might partly be attributed to radiation-induced activation of cell survival pathways and stimulation of the innate immune system. Both direct and indirect effects trigger inflammatory cytokine signaling and local immune cell recruitment [24], which may promote healing responses of the surgical-induced intracranial wound surface, leading to a superior antimicrobial milieu and reduced risk of intracavitary side infections. Compared to a postoperative stereotactic radiosurgical regime, the steep dose fall-off to the surgical wound surface in the setting of IORT results in lower dose exposure of the whole brain and in eloquent areas at risk, such as the optic apparatus and the brainstem [3]. Furthermore, by direct apposition of the applicator surface to the cavity wall, treatment dose delivery is highly accurate, and changes in cavity size due to tissue rearrangement

during the delay between resection and radiation in case of SRS do not occur [10]. These advantages of IORT may have provided a rationale for the preservation of safety metric profiles of a conventional postoperative radiation regime observed in the present study.

In order to comprehensively assess the overall complication profiles, we used PSIs and HACs as publicly available and highly standardized classification tools [20]. Overall, the complication rate for the IORT group was found to reach about 11%. This level of PAE is within the range of reported data on the prevalence of perioperative complications in the course of BM surgery [25]. Moreover, a PSA- and HAC-based assessment of PAEs will also cover transient events, such as catheter-associated urinary tract infections and pneumonia and, therefore, quantitatively surpass previously reported complication levels of several studies that concentrated exclusively on adverse events that entailed further surgical interventions [26].

Thus, for the first time, the results of this study provide a benchmark insight into the expectable postoperative complication rate after BM surgery with simultaneous IORT and might thereby assist the consideration of potential benefits of such an approach for the individual patient. Beyond these insights into the feasibility of IORT as a modality of adjuvant radiotherapy, future analysis will have to comprehensively evaluate the issue of local tumor control rates and OS compared to conventional postsurgical irradiation approaches. The first available data indicate a 1-year local control rate of 88% in a cohort of 54 patients with BM and IORT with a median dose of 30 Gy [10]. In another study, where a median marginal dose of 20 Gy was used, a 1-year control rate of 84% was reported [11] indicating a dose dependency on the tumor control rate [27]. With regard to the advantages of a single intraoperative delivery compared to repeated postsurgical sessions of radiation, currently available data on tumor control indicate a promising overall benefit of IORT in the setting of surgically treated BM.

5. Limitations

Despite the prospective observational design of the present study, several limitations have to be considered in its interpretation. Primarily, the prospective sample size of 35 patients is considered quite small. Nevertheless, employing a matched-pair approach might have outweighed some confounding factors when comparing the safety profiles to those of BM patients without IORT. Furthermore, the present feasibility analysis of IORT in surgery for BM does not take into account neurocognitive assessment, which is known to significantly add to valuable outcome analysis in the field of neuro-oncology. Despite these limitations in sample size, the findings of the present study may suffice to conceive further large-scale, cross-regional databases to accurately evaluate the safety, feasibility, and efficacy of IORT in the setting of surgery for BM.

6. Conclusions

The present study findings indicate that IORT is a safe and clinically feasible adjuvant treatment modality in patients undergoing surgical resection of BM. The preservation of perioperative standard safety-metric profiles known for surgical BM resection without IORT presented herein might constitute another aspect to establish immediate intraoperatively delivered adjuvant radiation as a promising treatment approach. Further studies are needed to comprehensively evaluate the efficacy and overall value of IORT in the long-term follow-up.

Author Contributions: Conceptualization, M.H. (Motaz Hamed), A.-L.P., P.S., L.C.S. and M.S.; methodology, M.H. (Motaz Hamed), A.-L.P., J.P.L., D.K., L.C.S. and M.S.; software, A.-L.P., L.C.S.; validation, A.-L.P. and M.S.; formal analysis, M.H. (Motaz Hamed), A.-L.P., L.C.S. and M.S.; data curation, M.H. (Motaz Hamed), A.-L.P., P.S. and M.S.; writing—original draft preparation, M.H. (Motaz Hamed), A.-L.P., P.S., L.C.S. and M.S.; writing—review and editing, M.H. (Motaz Hamed), A.-L.P., J.P.L., D.K., V.B., M.H. (Muriel Heimann), D.S., G.R.S., J.A.H., F.C.S., A.R., E.G., N.S., P.S., S.G., F.A.G., U.H., H.V., L.C.S. and M.S.; visualization, A.-L.P. and M.S.; supervision, P.S., H.V., L.C.S. and M.S. All authors have read and agreed to the published version of the manuscript.

Funding: This research did not receive any external funding.

Institutional Review Board Statement: The study was conducted in accordance with the Declaration of Helsinki and approved by the Ethics Committee of the University of Bonn (approval number 018/21, date of approval 25 January 2022).

Informed Consent Statement: Informed consent was received from every patient of the prospectively collected cohort of patients with IORT. For the retrospectively collected cohort of patients without IORT informed consent was not required.

Data Availability Statement: No new data were created or analyzed in this study. Data sharing is not applicable to this article.

Conflicts of Interest: The authors declare that the article content was composed in the absence of any commercial or financial relationship that could be construed as a potential conflict of interest. J.P.L. reports stocks and travel expenses from NOXXON Pharma A.G. F.A.G. reports research grants and travel expenses from ELEKTA AB; grants, stocks, travel expenses, and honoraria from NOXXON Pharma A.G.; research grants, travel expenses, and honoraria from Carl Zeiss Meditec A.G.; travel expenses and honoraria from Bristol-Myers Squibb, Roche Pharma AG, MSD Sharp and Dohme GmbH, and AstraZeneca GmbH; no-financial support from Oncare GmbH and Opasca GmbH. G.R.S., personal fees and travel expenses from Carl Zeiss Meditec A.G., personal fees from Roche Pharma A.G., personal fees from MedWave Clinical Trials, and travel expenses from Guerbet SA are not related to this work.

References

1. Nahed, B.V.; Alvarez-Breckenridge, C.; Brastianos, P.K.; Shih, H.; Sloan, A.; Ammirati, M.; Kuo, J.S.; Ryken, T.C.; Kalkanis, S.N.; Olson, J.J. Congress of Neurological Surgeons Systematic Review and Evidence-Based Guidelines on the Role of Surgery in the Management of Adults With Metastatic Brain Tumors. *Neurosurgery* **2019**, *84*, E152–E155. [CrossRef] [PubMed]
2. Kocher, M.; Soffietti, R.; Abacioglu, U.; Villa, S.; Fauchon, F.; Baumert, B.G.; Fariselli, L.; Tzuk-Shina, T.; Kortmann, R.D.; Carrie, C.; et al. Adjuvant whole-brain radiotherapy versus observation after radiosurgery or surgical resection of one to three cerebral metastases: Results of the EORTC 22952-26001 study. *J. Clin. Oncol. Off. J. Am. Soc. Clin. Oncol.* **2011**, *29*, 134–141. [CrossRef] [PubMed]
3. Vargo, J.A.; Sparks, K.M.; Singh, R.; Jacobson, G.M.; Hack, J.D.; Cifarelli, C.P. Feasibility of dose escalation using intraoperative radiotherapy following resection of large brain metastases compared to post-operative stereotactic radiosurgery. *J. Neuro-Oncol.* **2018**, *140*, 413–420. [CrossRef] [PubMed]
4. Weil, R.J.; Mavinkurve, G.G.; Chao, S.T.; Vogelbaum, M.A.; Suh, J.H.; Kolar, M.; Toms, S.A. Intraoperative radiotherapy to treat newly diagnosed solitary brain metastasis: Initial experience and long-term outcomes. *J. Neurosurg.* **2015**, *122*, 825–832. [CrossRef] [PubMed]
5. Raleigh, D.R.; Seymour, Z.A.; Tomlin, B.; Theodosopoulos, P.V.; Berger, M.S.; Aghi, M.K.; Geneser, S.E.; Krishnamurthy, D.; Fogh, S.E.; Sneed, P.K.; et al. Resection and brain brachytherapy with permanent iodine-125 sources for brain metastasis. *J. Neurosurg.* **2017**, *126*, 1749–1755. [CrossRef]
6. Kalapurakal, J.A.; Goldman, S.; Stellpflug, W.; Curran, J.; Sathiaseelan, V.; Marymont, M.H.; Tomita, T. Phase I study of intraoperative radiotherapy with photon radiosurgery system in children with recurrent brain tumors: Preliminary report of first dose level (10 Gy). *Int. J. Radiat. Oncol. Biol. Phys.* **2006**, *65*, 800–808. [CrossRef] [PubMed]
7. Sarria, G.R.; Smalec, Z.; Muedder, T.; Holz, J.A.; Scafa, D.; Koch, D.; Garbe, S.; Schneider, M.; Hamed, M.; Vatter, H.; et al. Dosimetric Comparison of Upfront Boosting With Stereotactic Radiosurgery Versus Intraoperative Radiotherapy for Glioblastoma. *Front. Oncol.* **2021**, *11*, 759873. [CrossRef] [PubMed]
8. Sarria, G.R.; Sperk, E.; Han, X.; Sarria, G.J.; Wenz, F.; Brehmer, S.; Fu, B.; Min, S.; Zhang, H.; Qin, S.; et al. Intraoperative radiotherapy for glioblastoma: An international pooled analysis. *Radiother. Oncol. J. Eur. Soc. Ther. Radiol. Oncol.* **2020**, *142*, 162–167. [CrossRef] [PubMed]
9. Giordano, F.A.; Brehmer, S.; Murle, B.; Welzel, G.; Sperk, E.; Keller, A.; Abo-Madyan, Y.; Scherzinger, E.; Clausen, S.; Schneider, F.; et al. Intraoperative Radiotherapy in Newly Diagnosed Glioblastoma (INTRAGO): An Open-Label, Dose-Escalation Phase I/II Trial. *Neurosurgery* **2019**, *84*, 41–49. [CrossRef]
10. Cifarelli, C.P.; Brehmer, S.; Vargo, J.A.; Hack, J.D.; Kahl, K.H.; Sarria-Vargas, G.; Giordano, F.A. Intraoperative radiotherapy (IORT) for surgically resected brain metastases: Outcome analysis of an international cooperative study. *J. Neuro-Oncol.* **2019**, *145*, 391–397. [CrossRef]
11. Kahl, K.H.; Balagiannis, N.; Hock, M.; Schill, S.; Roushan, Z.; Shiban, E.; Muller, H.; Grossert, U.; Konietzko, I.; Sommer, B.; et al. Intraoperative radiotherapy with low-energy x-rays after neurosurgical resection of brain metastases-an Augsburg University Medical Center experience. *Strahlenther. Onkol.* **2021**, *197*, 1124–1130. [CrossRef] [PubMed]

12. Schuss, P.; Lehmann, F.; Schäfer, N.; Bode, C.; Scharnböck, E.; Schaub, C.; Heimann, M.; Potthoff, A.L.; Weller, J.; Güresir, E.; et al. Postoperative Prolonged Mechanical Ventilation in Patients With Newly Diagnosed Glioblastoma-An Unrecognized Prognostic Factor. *Front. Oncol.* **2020**, *10*, 607557. [CrossRef] [PubMed]
13. Schuss, P.; Schäfer, N.; Bode, C.; Borger, V.; Eichhorn, L.; Giordano, F.A.; Güresir, E.; Heimann, M.; Ko, Y.D.; Landsberg, J.; et al. The Impact of Prolonged Mechanical Ventilation on Overall Survival in Patients With Surgically Treated Brain Metastases. *Front. Oncol.* **2021**, *11*, 658949. [CrossRef]
14. Sundararajan, V.; Henderson, T.; Perry, C.; Muggivan, A.; Quan, H.; Ghali, W.A. New ICD-10 version of the Charlson comorbidity index predicted in-hospital mortality. *J. Clin. Epidemiol.* **2004**, *57*, 1288–1294. [CrossRef]
15. Peus, D.; Newcomb, N.; Hofer, S. Appraisal of the Karnofsky Performance Status and proposal of a simple algorithmic system for its evaluation. *BMC Med. Inf. Decis. Mak.* **2013**, *13*, 72. [CrossRef]
16. Marks, L.B.; Yorke, E.D.; Jackson, A.; Ten Haken, R.K.; Constine, L.S.; Eisbruch, A.; Bentzen, S.M.; Nam, J.; Deasy, J.O. Use of normal tissue complication probability models in the clinic. *Int. J. Radiat. Oncol. Biol. Phys.* **2010**, *76*, S10–S19. [CrossRef]
17. Agency for Healthcare Research and Quality. *Patient Safety Indicators*; Agency for Healthcare Research and Quality: Rockville, MD, USA, 2015.
18. U.S. Centers for Medicare & Medicaid Services. *Hospital-Acquired Conditions*; U.S. Centers for Medicare & Medicaid Services: Baltimore, MD, USA, 2020.
19. Schneider, M.; Heimann, M.; Schaub, C.; Eichhorn, L.; Potthoff, A.L.; Giordano, F.A.; Güresir, E.; Ko, Y.D.; Landsberg, J.; Lehmann, F.; et al. Comorbidity Burden and Presence of Multiple Intracranial Lesions Are Associated with Adverse Events after Surgical Treatment of Patients with Brain Metastases. *Cancers* **2020**, *12*, 3209. [CrossRef] [PubMed]
20. Schneider, M.; Ilic, I.; Potthoff, A.L.; Hamed, M.; Schäfer, N.; Velten, M.; Güresir, E.; Herrlinger, U.; Borger, V.; Vatter, H.; et al. Safety metric profiling in surgery for temporal glioblastoma: Lobectomy as a supra-total resection regime preserves perioperative standard quality rates. *J. Neuro-Oncol.* **2020**, *149*, 455–461. [CrossRef]
21. Heimann, M.; Schäfer, N.; Bode, C.; Borger, V.; Eichhorn, L.; Giordano, F.A.; Güresir, E.; Jacobs, A.H.; Ko, Y.D.; Landsberg, J.; et al. Outcome of Elderly Patients With Surgically Treated Brain Metastases. *Front. Oncol.* **2021**, *11*, 713965. [CrossRef]
22. Ilic, I.; Faron, A.; Heimann, M.; Potthoff, A.L.; Schäfer, N.; Bode, C.; Borger, V.; Eichhorn, L.; Giordano, F.A.; Güresir, E.; et al. Combined Assessment of Preoperative Frailty and Sarcopenia Allows the Prediction of Overall Survival in Patients with Lung Cancer (NSCLC) and Surgically Treated Brain Metastasis. *Cancers* **2021**, *13*, 3353. [CrossRef]
23. Pilar, A.; Gupta, M.; Ghosh Laskar, S.; Laskar, S. Intraoperative radiotherapy: Review of techniques and results. *Ecancermedicalscience* **2017**, *11*, 750. [CrossRef] [PubMed]
24. Barker, H.E.; Paget, J.T.; Khan, A.A.; Harrington, K.J. The tumour microenvironment after radiotherapy: Mechanisms of resistance and recurrence. *Nat. Rev. Cancer* **2015**, *15*, 409–425. [CrossRef] [PubMed]
25. Gupta, S.; Dawood, H.; Giantini Larsen, A.; Fandino, L.; Knelson, E.H.; Smith, T.R.; Lee, E.Q.; Aizer, A.; Dunn, I.F.; Bi, W.L. Surgical and Peri-Operative Considerations for Brain Metastases. *Front. Oncol.* **2021**, *11*, 662943. [CrossRef] [PubMed]
26. Schneider, M.; Borger, V.; Grigutsch, D.; Güresir, Á.; Potthoff, A.L.; Velten, M.; Vatter, H.; Güresir, E.; Schuss, P. Elevated body mass index facilitates early postoperative complications after surgery for intracranial meningioma. *Neurosurg. Rev.* **2021**, *44*, 1023–1029. [CrossRef] [PubMed]
27. Cifarelli, C.P.; Jacobson, G.M. Intraoperative Radiotherapy in Brain Malignancies: Indications and Outcomes in Primary and Metastatic Brain Tumors. *Front. Oncol.* **2021**, *11*, 768168. [CrossRef]

3.3 Layer JP*, Hamed M*, Potthoff AL, Dejonckheere CS, Layer K, Sarria GR, Scafa D, Koch D, Köksal M, Kugel F, Grimmer M, Holz JA, Zeyen T, Friker LL, Borger V, Schmeel FC, Weller J, Hölzel M, Schäfer N, Garbe S, Forstbauer H, Giordano FA, Herrlinger U, Vatter H, Schneider M*, Schmeel LC*. Outcome assessment of intraoperative radiotherapy for brain metastases: results of a prospective observational study with comparative matched-pair analysis. J Neurooncol. 2023 Aug;164(1):107-116.

Hintergrund und Zielsetzung der Arbeit: Bislang lagen nur sehr eingeschränkt Daten zum klinischen *Outcome* einer IORT von resezierten Hirnmetastasen vor. Insbesondere in Bezug auf primäre klinische Endpunkte ist letztlich ein direkter Vergleich mit dem Goldstandard der adjuvanten FSRT notwendig, allerdings gibt es bislang keinerlei prospektiv-randomisierte Daten und auch noch zu wenig Vordaten, die eine solche Studie hinreichend begründen würden. Ziel dieser Arbeit war daher, durch individuelles *Matching* retrospektiv erhobener FSRT-Fälle mit IORT-Patienten einen möglichst realistischen Vergleich der beiden Modalitäten in Bezug auf das klinische *Outcome* vorzunehmen.

Methoden und Ergebnisse: Insgesamt 35 konsekutive Patienten mit Hirnmetastasen, die im Universitätsklinikum Bonn zwischen November 2020 und Oktober 2021 mit einer IORT behandelt wurden, wurden in Bezug auf die RN-Rate, die lokale Kontrolle, die distante intrazerebrale Kontrolle und das Gesamtüberleben ausgewertet. Die Einjahres-Überlebensrate und das Gesamtüberleben wurden mittels einer *comparative matched-pair* Analyse einer Datenbank mit insgesamt 388 konsekutiven Patientenfällen mit Resektion und adjuvanter EBRT gegenübergestellt, wobei ein individuelles *Matching* der FSRT- auf die IORT-Fälle im Verhältnis 2:1 erfolgte. Bei einer sehr geringen RN-Rate von nur 2,9% ergab sich nach einem Jahr eine lokale Kontrollrate von 97,1% und eine distante intrazerebrale Kontrollrate von 73,5%. Bei einem medianen Gesamtüberleben von 17,5 Monaten ergaben sich keine signifikanten Unterschiede zu der gematchten FSRT-Vergleichskohorte.

Schlussfolgerungen: Die IORT weist in den zentrumseigenen Daten insbesondere eine sehr gute Lokalkontrolle bei beachtenswert niedriger RN-Inzidenz auf. Im Vergleich zu gematchten FSRT-Fällen ist das Gesamtüberleben der IORT-Patienten trotz nachteilig kürzerem *Follow-up* nicht unterlegen. Letztlich können diese Beobachtungen die

Grundlage einer prospektiv-randomisierten Phase 2/3-Studie sein, um endgültige Wirksamkeitsaussagen im direkten Vergleich zur FSRT treffen zu können.

Journal of Neuro-Oncology (2023) 164:107–116
https://doi.org/10.1007/s11060-023-04380-w

RESEARCH

Outcome assessment of intraoperative radiotherapy for brain metastases: results of a prospective observational study with comparative matched-pair analysis

Julian P. Layer[1,2] · Motaz Hamed[3] · Anna-Laura Potthoff[3] · Cas S. Dejonckheere[1] · Katharina Layer[1] · Gustavo R. Sarria[1] · Davide Scafa[1] · David Koch[1] · Mümtaz Köksal[1] · Fabian Kugel[1] · Molina Grimmer[1] · Jasmin A. Holz[1] · Thomas Zeyen[4] · Lea L. Friker[2,5] · Valeri Borger[3] · F. Carsten Schmeel[6] · Johannes Weller[4] · Michael Hölzel[2] · Niklas Schäfer[4] · Stephan Garbe[1] · Helmut Forstbauer[7] · Frank A. Giordano[8,9,10] · Ulrich Herrlinger[4] · Hartmut Vatter[3] · Matthias Schneider[3] · L. Christopher Schmeel[1]

Received: 6 April 2023 / Accepted: 20 June 2023 / Published online: 21 July 2023

Abstract

Purpose Intraoperative radiation therapy (IORT) is an emerging alternative to adjuvant stereotactic external beam radiation therapy (EBRT) following resection of brain metastases (BM). Advantages of IORT include an instant prevention of tumor regrowth, optimized dose-sparing of adjacent healthy brain tissue and immediate completion of BM treatment, allowing an earlier admission to subsequent systemic treatments. However, prospective outcome data are limited. We sought to assess long-term outcome of IORT in comparison to EBRT.

Methods A total of 35 consecutive patients, prospectively recruited within a study registry, who received IORT following BM resection at a single neuro-oncological center were evaluated for radiation necrosis (RN) incidence rates, local control rates (LCR), distant brain progression (DBP) and overall survival (OS) as long-term outcome parameters. The 1 year-estimated OS and survival rates were compared in a balanced comparative matched-pair analysis to those of our institutional database, encompassing 388 consecutive patients who underwent adjuvant EBRT after BM resection.

Results The median IORT dose was 30 Gy prescribed to the applicator surface. A 2.9% RN rate was observed. The estimated 1 year-LCR was 97.1% and the 1 year-DBP-free survival 73.5%. Median time to DBP was 6.4 (range 1.7–24) months in the subgroup of patients experiencing intracerebral progression. The median OS was 17.5 (0.5-not reached) months with a 1 year-survival rate of 61.3%, which did not not significantly differ from the comparative cohort ($p=0.55$ and $p=0.82$, respectively).

Conclusion IORT is a safe and effective fast-track approach following BM resection, with comparable long-term outcomes as adjuvant EBRT.

Keywords Surgery for brain metastases · Intraoperative radiotherapy · IORT · Local tumor control · Survival · Adjuvant radiotherapy

Introduction

Over the course of their disease, up to 40% of cancer patients develop brain metastases (BM) [1]. With novel therapeutic options prolonging their overall survival (OS) [2–5], the diagnostic incidence of BM and risk of local recurrence are increasing [6, 7]. Although BMs do nowadays not necessarily impact overall survival [8, 9], local treatment is critical to prevent or stabilize neurological deterioration and impairment of quality of life (QOL) [10, 11]. If feasible, large or symptomatic lesions require surgical intervention. Adjuvant radiation therapy (RT) of both potential tumor remnants and the resection cavity improves local control rates (LCR) [12–14]. Considering the tumor localization, histology and volumes, common RT regimens apply stereotactic external-beam RT (EBRT) of one (stereotactic radiosurgery, SRS) to seven fractions (fractionated stereotactic radiotherapy,

Julian P. Layer and Motaz Hamed are shared first authorship.

Matthias Schneider and Leonard Christopher Schmeel are shared last authorship.

Extended author information available on the last page of the article

FSRT) either before resection or afterwards, following adequate wound healing and recovery from surgery [14–18]. As an alternative, low-energy intraoperative RT (IORT) has increasingly gained attention in the past years. Initial reports suggest promising LCR [19, 20] and a favorable safety profile [21] with a comparatively lower radiation necrosis (RN) incidence [22]. Available data are solely based on retrospective single institution experiences, with a radiation oncology focus on dosage and technical aspects of the IORT approach [23, 24]. Nonetheless, its safety profile has been previously explored in brain tissue for treating glioblastoma [25, 26] and its efficacy is currently evaluated in a phase III trial (NCT02685605). Several advantages of IORT include a steep dose gradient, improved healthy brain tissue sparing [27] and avoiding RT target-volume delineation challenges caused by post-surgery tissue alterations. The instant application of local high dose RT to the tumor bed may prevent early repopulation of residual microscopic tumor. Furthermore, an accelerated completion of the interdisciplinary BM treatment eases a faster recovery, shorter in hospital-times and earlier initiation of subsequent systemic treatments.

We previously reported on a favorable perioperative safety profile of patients receiving IORT for BM in a matched-pair fashion with 388 BM patients who underwent conventional post-surgical RT [28]. Here, we report on their clinical long-term outcome and assess their survival in comparison to the same matched institutional cohort.

Methods

Patients

The study collected data from consecutively recruited patients admitted to the Neurosurgical Department of the University Hospital Bonn between November 2020 and October 2021, who had undergone surgical resection of BM combined with IORT. In all cases, BM were histopathologically confirmed. At a weekly tumor board meeting, interdisciplinary consensus was used to determine the treatment strategies for each patient individually [29]. Treatment plans were also coordinated with the referring physicians and considered the patient's past oncological therapies. Besides receiving a histopathological diagnosis in case of cancer of unknown primary, criteria for surgical resection were presence or severe risk of acute neurological impairment or clinically significant mass effects as abnormal intracranial pressure or hemispheric shift. In case of multiple BMs, only the clinically manifest lesion was considered for surgical removal to prevent mass effects and tumor-related hydrocephalus [28, 30]. Clinical inclusion criteria for IORT were gross total resection, intraoperative confirmation of BM on frozen tumor sections, no previous intracerebral irradiation and fulfillment of dose constraints as described below. The data were prospectively collected and managed using SPSS (version 25, IBM Corp., Armonk, NY). Informed consent was obtained from all patients. The collected information included, among others, sociodemographic characteristics, primary tumor location, radiological and histopathological characteristics of the intracranial metastatic lesions, baseline functional status. The Karnofsky performance score (KPS) was used to classify the patients according to their functional status at admission. A stratification cut-off of 70 was chosen according to Péus et al. with regard to the patient's ability to carry on their normal activity and work [31]. Diagnostic-Specific Graded Prognostic Assessment (DS-GPA) [32] scores were calculated by standard procedures. The study was conducted in accordance with the principles of the Declaration of Helsinki and approved by the Ethics Committee of the University Hospital Bonn (approval number: 018/21 and 057/22).

IORT

Preoperative contrast-enhanced T1-weighted MRI imaging was used to provide 3D image guidance for both surgery and radiation treatments. Optic nerves, chiasm, and brain stem were identified preoperatively and intraoperatively as organs at risk (OARs) for IORT and delivered doses were defined based on dose-depth template profiles corresponding to each applicator diameter. The INTRABEAM® 600 (Carl Zeiss Meditec AG, Oberkochen, Germany) was used to deliver IORT with a spherical applicator ranging from 1.5 to 5.0 cm diameter by application of nominal 50 kV photons at a standard dose of 30 Gy prescribed to the applicator surface. Decreasing the prescribed dose down to 16 Gy was acceptable in case of OAR doses exceeding the constraints of 12 Gy to the optical system or 12.5 Gy to the brain stem following the QUANTEC (Quantitative Analyses of Normal Tissue Effects in the Clinic) recommendations [33] considering the specific (1.3–1.5 times higher) RBE of low energy photons. In individual cases, an anatomical positioning of the applicator required consideration of further OAR that were not regularly assessed, e.g., cochlea or thalamus, with equal consideration of the QUANTEC recommendations.

Follow-up

All patients had regular follow-up (FU) visits including physical examination and magnetic resonance imaging (MRI). MRI assessments were performed according to the RANO criteria by board-certified radiologists. In case of uncertain clinical or radiographic response, the interdisciplinary neuro-oncological tumor board was consulted and a combined decision was taken upon findings. The following conditions qualified for diagnosis of RN: (1) after initial

suspected progressive disease (PD), a minimum of two FU MRI time points showed no sign of ongoing PD; (2) advanced MRI incorporating dynamic susceptibility contrast (DSC) or diffusion weighted imaging (DWI) was concordantly suggestive of RN; (3) RN was confirmed histopathologically after surgery.

Study endpoints

The primary endpoints of the study were RN rates and cumulative 1 year-LCR. The secondary endpoints were DBP, 1 year-OS rates and estimated OS. Local control was defined as the absence of MRI-radiographic PD in or surrounding the previously irradiated BM resection cavity and calculated from the day of surgery until the date of PD. Patients lost to FU or deceased prior to radiographic progression were censored at the last FU time point. OS was defined as the time interval between the date of surgery and the date of either the last FU (censored) or death.

Matching procedure

The study performed a propensity score matching, which involved matching a cohort of 35 patients who received IORT with a cohort of 388 patients who underwent surgery for BM followed by EBRT (patient characteristics provided in Suppl. Table 1). The matching was performed at a ratio of 1:2, and the statistical computing program R (version 4.1.2; The R Foundation for Statistical Computing, https://www.r-project.org/) was used for the analysis as previously described [28]. The group of EBRT patients included all patients aged 18 years or older who underwent surgery for BM at the University Hospital Bonn neuro-oncological center between 2013 and 2018, and who did not receive IORT but EBRT (SRS, FSRT or whole brain radiotherapy (WBRT)) during that period. The study aimed to increase the robustness of the data by selecting known prognostic parameters, such as age [34], KPS and Charlson comorbidity index (CCI) at admission [34–36], tumor entity, and the status of solitary versus multiple BM [35], for matching. The balance of these parameters was measured and visualized to ensure that the two groups were comparable. A jitter plot was used to display the distribution of propensity scores. The study protocol for retrospective data collection was approved by the local Ethics committee (approval number: 250/19 and 057/22).

Statistics

The computer software packages used for the data analyses were SPSS and GraphPad Prism (version 9, GraphPad Software, Boston, MA). Fisher's exact test was used to analyze categorical variables, which were presented in contingency tables. The Mann–Whitney U test was used to compare continuous variables, as the data were not normally distributed. Statistical significance was defined as a p-value of less than 0.05.

Results

Patient and tumor characteristics

Between November 2020 and October 2021, 35 consecutive BM patients receiving IORT to the resection cavity were enrolled. Their median age was 63 (range 43–80) years and the median KPS was 80 (50–100). Of note, 29% of patients had a KPS < 70. The median DS-GPA score was 2 (0–4). The most frequent BM localization was the frontal lobe (37.1%) followed by the occipital lobe (25.7%). Most histopathology results corresponded to non-small cell lung cancer (NSCLC, 54%), followed by melanoma (11%) and breast cancer (6%). With a range of 2 to 10 intracranial lesions, 15 patients (43%) suffered from multiple BM at the time of surgery. Further details on patient characteristics can be found in Table 1.

Treatment and dosimetry

No dose constraints were exceeded and all patients completed treatment. The median IORT duration was 18:12 (6:56–49:00) min and the median prescription dose was 30

Table 1 Patient and tumor characteristics*

	n = 35
Median age (IQR) (in yrs)	63 (54–71)
Female sex	19 (54.3)
Primary site of cancer	
Lung	21 (60)
Melanoma	4 (11)
Kidney	4 (11)
Breast	2 (6)
Others	4 (11)
Multiple BMs	15 (43)
Preoperative KPS < = 70	14 (40)
Median DS-GPA score	2 (0–4)
Concomitant systemic treatment	3 (9)
Median dose of IORT (in Gy)	30 (16–30)
Median duration of IORT (in min)	18.2 (6.9–49)

BM brain metastasis, *CCI* Charlson comorbidity index, *DS-GPA* diagnosis-specific graded prognostic assessment, *Gy* gray, *IQR* interquartile range, *KPS* Karnofsky performance score, *mOS* median overall survival, *n* number of patients, *yrs* years

*Values represent the number of patients unless indicated otherwise (%)

(16–30) Gy. The median applicator size was 2.5 (1.5–5.0) cm. The brainstem and the optic tracts (optic nerves and chiasm) were regularly assessed as OARs. Doses to other structures were negligible and therefore not considered relevant for this report. The median distance from the applicator surface was 35.5 (10–65) mm to the brainstem and 60 (13–70) mm to the optic tracts, with a median estimated OAR dose exposure of 0.7 (0.0–6.0) Gy and 0.0 (0.0–4.4) Gy, respectively.

Radiation necrosis rate, local tumor control and distant brain progression

In all patients, a gross total resection was achieved. After a median FU of 10.4 (0.5–24.5) months and a median imaging FU of 7.9 (0.1–24.4) months incorporating a median of 6 (1–13) MRI assessments, only one RN event was noted at 18.7 months. Hence, an overall RN rate of 2.9% was observed (Fig. 1a). As this patient's RN was a grade 2 event, only mild conservative management was initiated and subsequently led to clinical remission. Of note, the patient did not experience distant intracranial progression and is still alive and systemically stable after 23.2 months of FU.

A second patient showed local recurrence after 2.9 months, in addition to previous distant intracranial progression. The latter led to clinical deterioration and subsequent exitus. The overall IORT 1-year LCR was 97.1% (Fig. 1b). With an overall distant brain progression rate of 29.4%, the median DBP-free survival (DBPS) was 24 (0.5-not reached) months and the 1 year-DBPS 73.5% (Fig. 1c). The median time to DBP was 6.4 (range 1.7–24) months in the subgroup of patients experiencing distant intracranial progression. Leptomeningeal spread occurred in 5.7% of cases (2 cases), after 18.2 and 21.9 months, respectively.

Survival and comparison to matched EBRT cohort

For the IORT cohort, the median OS was 17.5 (0.5-not reached) months and the 1 year-survival rate 61.3% (Fig. 1d). 70 patients from the institutional database of patients, who underwent surgery with subsequent EBRT (Suppl. Table 1) and individually corresponded to the present series were matched at a ratio of 1:2 to those receiving

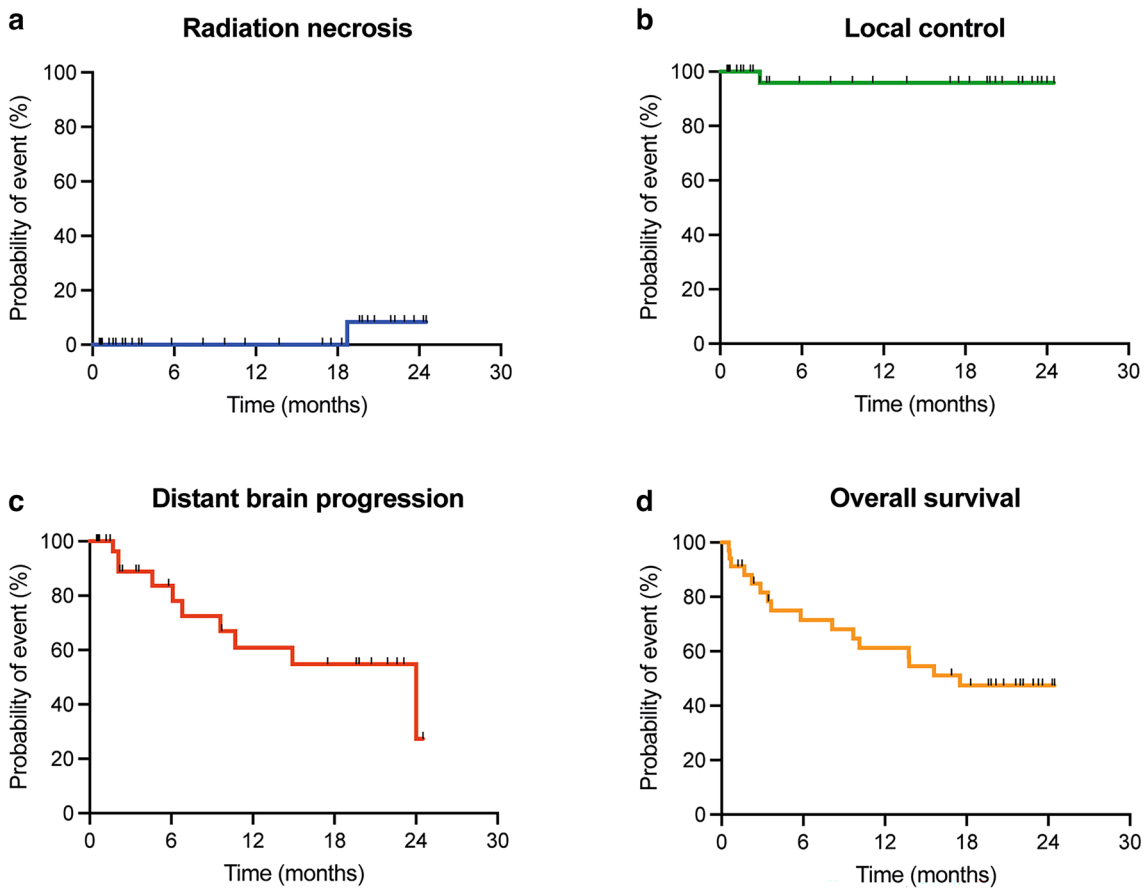

Fig. 1 Outcome of IORT patients. Kaplan–Meier curves for **a** radiation necrosis, **b** local control, **c** distant brain progression and **d** overall survival

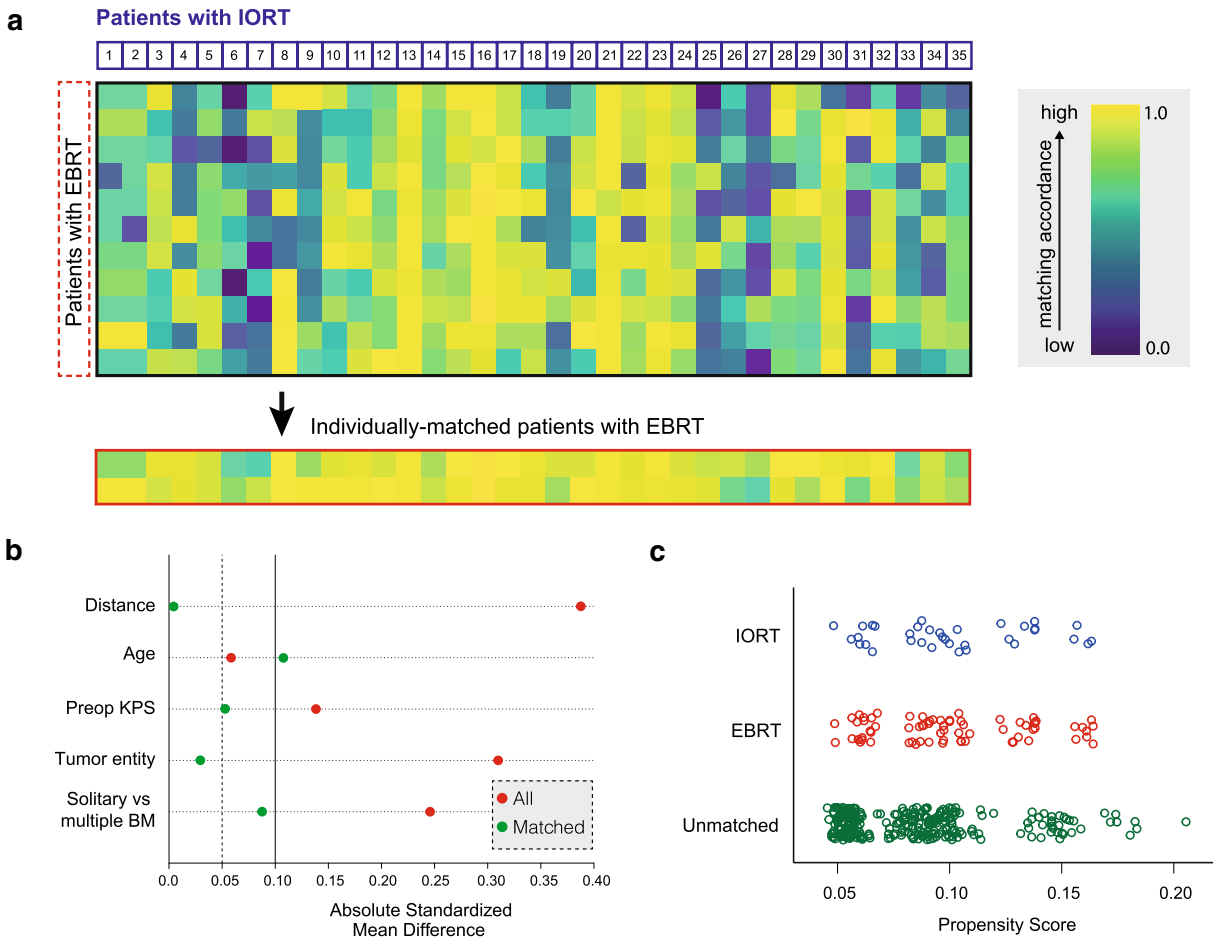

Fig. 2 Graphical visualization of the applied matching procedure. **a** Comparative matched pair analysis at a ratio of 1:2 identifies 70 out of 388 patients with resected BM not receiving IORT who individually correspond to the present series of 35 patients with resected BM undergoing IORT. Heat map as color-coded illustration of the matching strategy of patients not receiving IORT to IORT cases stratified by age, KPS at admission, tumor entity and solitary versus multiple BM as matching parameters. The red box illustrates individually-matched patients without IORT. **b** Love plot demonstrating the balance of the matching analysis for each matching parameter determined by the standardized mean differences. **c** Illustration of propensity scores obtained as described in **a** for matched (blue: IORT; red: EBRT) and unmatched BM patients (green). *BM* brain metastasis, *EBRT* external beam radiation therapy; *IORT* intraoperative radiotherapy, *KPS* Karnofsky performance score.

IORT (Fig. 2). The two patient populations did not differ significantly by the matching variables age (p = 0.74), KPS (p = 0.88), primary site of cancer (p = 1.00) and frequency of multiple BM (p = 0.68). Concomitant systemic treatment was equally distributed (p = 0.99). With 61.3% versus 68.2%, the 1 year-survival was not significantly different between IORT and EBRT, respectively (p = 0.82; Table 2). Furthermore, the median OS was comparable with 17.5 months and 26 months, in each respective cohort (p = 0.55; Fig. 3).

Discussion

IORT following BM resection is an emerging alternative to adjuvant EBRT, but long-term experience and efficiency are yet to be established. Taken together with our previous study [28], this is the first report on IORT for BM that covers both short and long-term clinical FU of a consecutive patient cohort and matches and compares their survival outcomes to those of EBRT.

There is consensus on the beneficial effect of adjuvant RT on local control after BM resection [14, 16, 37]. However, depending on the individual clinical context, it remains controversial which RT sequencing and technique achieves best long-term outcomes at lowest toxicity levels. Despite providing convincing BDFS [38, 39], WBRT was abandoned

Table 2 Comparative matched pair analysis on survival outcome in patients with surgically-treated BM stratified for IORT versus EBRT*

	Surgery with IORT n = 35	Surgery with EBRT n = 70	p-value
Matching variables			
Age (years)	63 (54–71)	63 (57–70)	0.74
Preoperative KPS	80 (60–90)	80 (70–90)	0.88
Primary site of cancer			1.0
Lung Cancer	21 (60)	41 (59)	
Others	14 (40)	29 (41)	
Solitary vs. multiple			0.68
Multiple	15 (43)	27 (39)	
Solitary	20 (57)	43 (61)	
Outcome parameters			
1 year-survival	19/35** (61.3)	33/70*** (68.2)	0.82
mOS (months)	17.5	26	0.55

BM brain metastasis, *CCI* Charlson comorbidity index, *EBRT* external beam radiation therapy, *Gy* gray, *IQR* interquartile range, *KPS* Karnofsky performance score, *mOS* median overall survival, *n* number of patients

*Values represent the number of patients unless indicated otherwise (%)

**2 of 35 patients censored with lost to follow-up < 12 months (33 patients with event at any time)

***17 of 70 patients censored with lost to follow-up < 12 months (53 patients with event at any time)

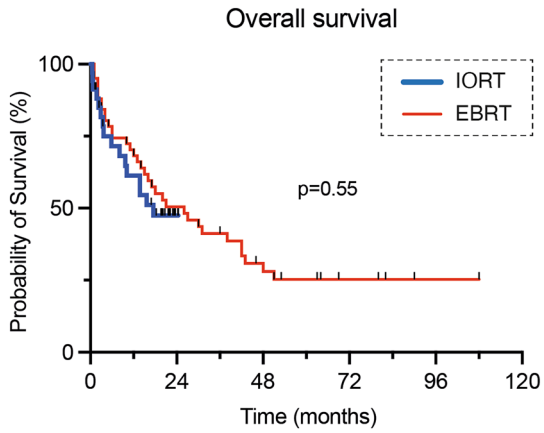

Fig. 3 Kaplan Meier survival curves for patients with surgically-treated BM stratified for IORT versus EBRT. *EBRT* external beam radiation therapy, *IORT* intraoperative radiotherapy

due to an inferior toxicity profile [15, 40–42] in comparison to modern stereotactic RT approaches. Accordingly, previous intracavitary treatment modalities, such as permanent intracerebral radio-isotopic seed implantation, yielded very good LCRs, [43–45] yet are prone to induce RN [46, 47]. Moreover, arterial occlusion [48], seed detachment and necessity of subsequent re-surgery could arise. For stereotactic RT, reports on LCR and toxicity differ significantly depending on entities, BM volume and number, but also the fractionation scheme [14, 15, 17, 18, 49]. Besides classical outcome parameters, patient-centered factors such as reduction of hospitalization times, timely treatment access and quality of life have become increasingly important both from patient-centered and socioeconomic view points. This applies in particular to BM patients in a palliative care setting that may suffer from neurological impairment along with a limited life expectancy. Additionally, most patients from our collective were first diagnosed with BM during staging of an extracranial primary tumor. For these patients, swiftness is particularly important, since at time of brain surgery they often still require completion of staging examinations and the initiation of systemic treatment [50]. IORT can expedite these urgent subsequent steps by approximately two to 3 weeks. Furthermore, patients at first diagnosis of metastatic cancer [51], especially with favorable prognostic factors like solitary BM [52], are likely to experience DBP requiring reirradiation to potentially closely located brain structures. The specific physical features of 50 kV IORT provide an increased linear energy transfer and a higher relative biological effectiveness [53] with steep dose gradients allowing both optimized tumoricidal effect and OAR sparing. Thus, patients may benefit from preservation of neurological functions and improved subsequent reirradiation options. The main disadvantage of IORT is a lack of dose modulation options that render certain anatomic conditions challenging. Therefore, it is not surprising that, in line with previous reports [20], most of the BM treated in this cohort were located either craniofrontal or occipital.

Consistent with our previously reported perioperative safety profile [28], we here report a favorable overall RN rate of just 2.9% after IORT. This is an improvement in comparison to adjuvant SRS or FSRT where RN rates typically range between 8% [14] to more than 20% [49], but also to some previous series of IORT patients. While Kahl et al. reported

2.5% [22], Cifarelli et al. noted a RN rate of 7% [19] and Diehl et al. of 11.1% [20]. Of note, the latter also included few patients receiving additional post-surgery stereotactic radiosurgery. In line with previous reports, we found only a comparably low incidence of leptomeningeal spread after IORT [19, 22]. This may be an additional clinical advantage of IORT over other RT techniques that requires further scientific attention. Our observed 1-year LCR of 97.1% compares well with the 94% observed by Cifarelli et al. [19] and outperforms most studies on both adjuvant and definitive SRS or FSRT with rates roughly between 80 to 90% [14, 17, 18, 49, 54–56]. Definitive SRS of BM is the primary alternative option to resection when systemic treatment delays are to be avoided. Both effectiveness and safety of single fraction EBRT mainly depend on lesion volume [55]. Compared to SRS only [56], our data indicate a superior LCR and RN rate for IORT of BM > 2 cm, while equally avoiding additional treatment times following surgery.

By matched pair analysis, we demonstrated comparable long-term survival outcomes of EBRT and IORT. The 1 year-survival rate of 57% reported here is also within the range of previous reports for IORT [20, 22]. Meanwhile, despite being marginally different, the matched cohort exhibited outstanding long-term survival. Many of the patients from this cohort surpassed a FU that timewise cannot be achieved yet for the IORT group and, thus, long-term survivors are censored at an earlier time point in the latter. In addition, there are remaining risk factors that could not be adjusted between the groups. While age, CCI, KPS and singularity of BM were considered as matching factors, DS-GPA scores were not. Depending on the tumor entity, this score covers further disease-specific risk factors. However, DS-GPA scores do not qualify for matching analyses as they are not applicable to all tumor entities, nor are they prognostically comparable between different entities [32]. The IORT cohort had a relatively low median DS-GPA score of only 2 and included a total of 25.7% of patients with at least 3 BM. Regardless of these unfavorable prognostic factors, the IORT cohort achieved outstanding local control as well as convincing RN rates in comparison to previous reports, while demonstrating equal long-term outcomes compared to matched EBRT cases.

Limitations

Although the present study had a prospective observational design, its interpretation should take into account several limitations. The most significant limitation is the relatively small sample size of 35 patients, which may impact the generalizability of the findings. Of note, IORT remains a novel treatment option for BM with only very limited data available from comparably sized patient collectives. As an additional methodological measure, using a matched-pair approach could have helped to mitigate some confounding factors when comparing the long-term outcome of patients undergoing EBRT and IORT to BM. However, certain confounding factors, such as different prognostic profiles according to each histology or variable systemic treatment effects, were not regarded. Moreover, since FU MRIs were frequently carried out in local centers using minimized imaging protocols lacking DSC and/or DWI, no reliable data on local control and RN rates were available for the comparative cohort, hence it could not be included in the analysis. Despite these limitations in sample size, the present study may suffice to conceive further large-scale, cross-regional databases to accurately evaluate the safety, feasibility, and efficacy of IORT in the setting of BM surgery. This is the most comprehensive investigation on an IORT patient cohort thus far, incorporating dosimetric aspects, perioperative mortality and RN rate, as well as survival and local control outcomes.

Conclusions

IORT is a timely feasible fast-track approach for complementing surgical BM treatment, with long-term safety and control outcomes comparable to those of adjuvant stereotactic RT. On-going phase II and III studies will soon elucidate the actual role of IORT in this setting.

Supplementary Information The online version contains supplementary material available at https://doi.org/10.1007/s11060-023-04380-w.

Acknowledgements We thank Katja Klever and Monika Brüggemann for their support in patient follow-up and the medical team of Helmut Forstbauer for aiding in data acquisition.

Author contributions This study was conceptualized by JPL, MS and LCS. Surgery was performed by MH, ALP, VB, HV and MS. IORT was planned and performed by JPL, CSD, KL, DS, DK, MK, FK, MG, JAH, SG, FAG and LCS. Patient follow-up was conducted by JPL, MH, APL, CSD, KL, DS, DK, MK, TZ, LLF, VB, FCS, JW, NS, HF, FAG, UH, HV, MS, LCS. Material preparation and data collection were performed by JPL, ALP and MS. Analysis was performed by JPL and ALP. MH, FAG, HV, MS and LCS provided funding and resources. The first draft of the manuscript was written by JPL. GRS, MS and LCS reviewed and edited the data and manuscript. All authors commented on previous versions and approved the final manuscript.

Funding Open Access funding enabled and organized by Projekt DEAL. The authors declare that the article content was composed in the absence of any commercial or financial relationship that could be construed as a potential conflict of interest. JPL was supported by a grant from Novartis Stiftung für therapeutische Forschung.

Data availability The data presented in this study are available in this article. Further datasets generated during and/or analysed during the current study are available from the corresponding author on reasonable request.

Declarations

Conflict of interests J.P.L reports stocks and travel expenses from TME/NOXXON Pharma AG; stocks and honoraria from Siemens Healthineers and stocks from Bayer AG and BioNTech AG. F.A.G. reports research grants and travel expenses from ELEKTA AB and Varian Medical Systems Inc.; grants, stocks, travel expenses and honoraria from TME/NOXXON Pharma AG; research grants, travel expenses and honoraria from Carl Zeiss Meditec AG; travel expenses and honoraria from Bristol-Myers Squibb, Cureteq AG, Guerbet SA, Roche Pharma AG, MSD Sharp and Dohme GmbH and AstraZeneca GmbH; non-financial support from Oncare GmbH and Opasca GmbH. G.R.S. reports personal fees and travel expenses from Carl Zeiss Meditec AG, personal fees from Roche Pharma AG, personal fees from MedWave Clinical Trials and travel expenses from Guerbet SA, not related to this work. U. H. reports advisory Board and/or lecture honoraria from Bayer AG and Medac GmbH.

Ethics approval The study was conducted in accordance with the principles of the Declaration of Helsinki and approved by the Ethics Committee of the University Hospital Bonn (Approval Number: 018/21 and 057/22). Informed consent was obtained from all patients.

References

1. Cagney DN, Martin AM, Catalano PJ et al (2017) Incidence and prognosis of patients with brain metastases at diagnosis of systemic malignancy: a population-based study. Neuro Oncol 19:1511–1521. https://doi.org/10.1093/neuonc/nox077
2. Antonia SJ, Villegas A, Daniel D et al (2018) Overall survival with durvalumab after chemoradiotherapy in stage III NSCLC. N Engl J Med 379:2342–2350. https://doi.org/10.1056/NEJMoa1809697
3. Motzer RJ, Tannir NM, McDermott DF et al (2018) Nivolumab plus Ipilimumab versus Sunitinib in advanced renal-cell carcinoma. N Engl J Med 378:1277–1290. https://doi.org/10.1056/NEJMoa1712126
4. Larkin J, Chiarion-Sileni V, Gonzalez R et al (2019) Five-year survival with combined nivolumab and ipilimumab in advanced melanoma. N Engl J Med 381:1535–1546. https://doi.org/10.1056/NEJMoa1910836
5. Modi S, Jacot W, Yamashita T et al (2022) Trastuzumab deruxtecan in previously treated HER2-low advanced breast cancer. N Engl J Med 387:9–20. https://doi.org/10.1056/NEJMoa2203690
6. Nayak L, Lee EQ, Wen PY (2012) Epidemiology of brain metastases. Curr Oncol Rep 14:48–54. https://doi.org/10.1007/s11912-011-0203-y
7. Davis FG, Dolecek TA, McCarthy BJ, Villano JL (2012) Toward determining the lifetime occurrence of metastatic brain tumors estimated from 2007 United States cancer incidence data. Neuro Oncol 14:1171–1177. https://doi.org/10.1093/neuonc/nos152
8. Yamamoto M, Sato Y, Serizawa T et al (2012) Subclassification of recursive partitioning analysis class ii patients with brain metastases treated radiosurgically. Int J Radiation Oncol Biol Phys 83:1399–1405. https://doi.org/10.1016/j.ijrobp.2011.10.018
9. Nieder C, Stanisavljevic L, Aanes SG et al (2022) 30-day mortality in patients treated for brain metastases: extracranial causes dominate. Radiat Oncol 17:92. https://doi.org/10.1186/s13014-022-02062-x
10. Schödel P, Schebesch K-M, Brawanski A, Proescholdt M (2013) Surgical resection of brain metastases—impact on neurological outcome. IJMS 14:8708–8718. https://doi.org/10.3390/ijms14058708
11. Verhaak E, Gehring K, Hanssens PEJ, Sitskoorn MM (2019) Health-related quality of life of patients with brain metastases selected for stereotactic radiosurgery. J Neurooncol 143:537–546. https://doi.org/10.1007/s11060-019-03186-z
12. Kocher M, Soffietti R, Abacioglu U et al (2011) Adjuvant whole-brain radiotherapy versus observation after radiosurgery or surgical resection of one to three cerebral metastases: results of the EORTC 22952–26001 study. JCO 29:134–141. https://doi.org/10.1200/JCO.2010.30.1655
13. Lehrer EJ, Peterson JL, Zaorsky NG et al (2019) Single versus multifraction stereotactic radiosurgery for large brain metastases: an international meta-analysis of 24 trials. Int J Radiation Oncol Biol Phys 103:618–630. https://doi.org/10.1016/j.ijrobp.2018.10.038
14. Eitz KA, Lo SS, Soliman H et al (2020) Multi-institutional analysis of prognostic factors and outcomes after hypofractionated stereotactic radiotherapy to the resection cavity in patients with brain metastases. JAMA Oncol 6:1901. https://doi.org/10.1001/jamaoncol.2020.4630
15. Brown PD, Ballman KV, Cerhan JH et al (2017) Postoperative stereotactic radiosurgery compared with whole brain radiotherapy for resected metastatic brain disease (NCCTG N107C/CEC·3): a multicentre, randomised, controlled, phase 3 trial. Lancet Oncol 18:1049–1060. https://doi.org/10.1016/S1470-2045(17)30441-2
16. Mahajan A, Ahmed S, McAleer MF et al (2017) Post-operative stereotactic radiosurgery versus observation for completely resected brain metastases: a single-centre, randomised, controlled, phase 3 trial. Lancet Oncol 18:1040–1048. https://doi.org/10.1016/S1470-2045(17)30414-X
17. Jhaveri J, Chowdhary M, Zhang X et al (2019) Does size matter? Investigating the optimal planning target volume margin for post-operative stereotactic radiosurgery to resected brain metastases. J Neurosurg 130:797–803. https://doi.org/10.3171/2017.9.JNS171735
18. Layer JP, Layer K, Sarria GR et al (2023) Five-Fraction stereotactic radiotherapy for brain metastases—a retrospective analysis. Curr Oncol 30:1300–1313. https://doi.org/10.3390/curroncol30020101
19. Cifarelli CP, Brehmer S, Vargo JA et al (2019) Intraoperative radiotherapy (IORT) for surgically resected brain metastases: outcome analysis of an international cooperative study. J Neurooncol 145:391–397. https://doi.org/10.1007/s11060-019-03309-6
20. Diehl CD, Pigorsch SU, Gempt J et al (2022) Low-energy X-Ray Intraoperative radiation therapy (Lex-IORT) for resected brain metastases: a single-institution experience. Cancers 15:14. https://doi.org/10.3390/cancers15010014
21. Krauss P, Steininger K, Motov S et al (2022) Resection of supratentorial brain metastases with intraoperative radiotherapy Is it safe? Analysis and experiences of a single center cohort. Front Surg 9:1071804. https://doi.org/10.3389/fsurg.2022.1071804

22. Kahl K-H, Balagiannis N, Höck M et al (2021) Intraoperative radiotherapy with low-energy x-rays after neurosurgical resection of brain metastases-an Augsburg University Medical center experience. Strahlenther Onkol 197:1124–1130. https://doi.org/10.1007/s00066-021-01831-z
23. Sarria GR, Smalec Z, Muedder T et al (2021) Dosimetric comparison of upfront boosting with stereotactic radiosurgery versus intraoperative radiotherapy for glioblastoma. Front Oncol 11:759873. https://doi.org/10.3389/fonc.2021.759873
24. Dahshan BA, Weir JS, Bice RP et al (2021) Dose homogeneity analysis of adjuvant radiation treatment in surgically resected brain metastases: comparison of IORT, SRS, and IMRT indices. Brachytherapy 20:426–432. https://doi.org/10.1016/j.brachy.2020.11.004
25. Giordano FA, Brehmer S, Mürle B et al (2019) Intraoperative radiotherapy in newly diagnosed glioblastoma (INTRAGO): an open-label, dose-escalation phase I/II trial. Neurosurgery 84:41–49. https://doi.org/10.1093/neuros/nyy018
26. Sarria GR, Sperk E, Han X et al (2020) Intraoperative radiotherapy for glioblastoma: an international pooled analysis. Radiother Oncol 142:162–167. https://doi.org/10.1016/j.radonc.2019.09.023
27. Herskind C, Ma L, Liu Q et al (2017) Biology of high single doses of IORT: RBE, 5 R's, and other biological aspects. Radiat Oncol 12:24. https://doi.org/10.1186/s13014-016-0750-3
28. Hamed M, Potthoff A-L, Layer JP et al (2022) Benchmarking safety indicators of surgical treatment of brain metastases combined with intraoperative radiotherapy: results of prospective observational study with comparative matched-pair analysis. Cancers 14:1515. https://doi.org/10.3390/cancers14061515
29. Schäfer N, Bumes E, Eberle F et al (2021) Implementation, relevance, and virtual adaptation of neuro-oncological tumor boards during the COVID-19 pandemic: a nationwide provider survey. J Neurooncol 153:479–485. https://doi.org/10.1007/s11060-021-03784-w
30. Hamed M, Potthoff A-L, Heimann M et al (2023) Survival in patients with surgically treated brain metastases: does infratentorial location matter? Neurosurg Rev 46:80. https://doi.org/10.1007/s10143-023-01986-6
31. Péus D, Newcomb N, Hofer S (2013) Appraisal of the karnofsky performance status and proposal of a simple algorithmic system for its evaluation. BMC Med Inform Decis Mak 13:72. https://doi.org/10.1186/1472-6947-13-72
32. Sperduto PW, Kased N, Roberge D et al (2012) Summary report on the graded prognostic assessment: an accurate and facile diagnosis-specific tool to estimate survival for patients with brain metastases. JCO 30:419–425. https://doi.org/10.1200/JCO.2011.38.0527
33. Marks LB, Yorke ED, Jackson A et al (2010) Use of normal tissue complication probability models in the clinic. Int J Radiation Oncol Biol Phys 76:S10–S19. https://doi.org/10.1016/j.ijrobp.2009.07.1754
34. Heimann M, Schäfer N, Bode C et al (2021) Outcome of elderly patients with surgically treated brain metastases. Front Oncol 11:713965. https://doi.org/10.3389/fonc.2021.713965
35. Schneider M, Heimann M, Schaub C et al (2020) Comorbidity burden and presence of multiple intracranial lesions are associated with adverse events after surgical treatment of patients with brain metastases. Cancers 12:3209. https://doi.org/10.3390/cancers12113209
36. Ilic I, Potthoff A-L, Borger V et al (2022) Bone Mineral density as an individual prognostic biomarker in patients with surgically-treated brain metastasis from lung cancer (NSCLC). Cancers 14:4633. https://doi.org/10.3390/cancers14194633
37. Patchell RA, Tibbs PA, Regine WF et al (1998) Postoperative radiotherapy in the treatment of single metastases to the brain: a randomized trial. JAMA 280:1485–1489. https://doi.org/10.1001/jama.280.17.1485
38. Sahgal A, Aoyama H, Kocher M et al (2015) Phase 3 trials of stereotactic radiosurgery with or without whole-brain radiation therapy for 1 to 4 brain metastases: individual patient data meta-analysis. Int J Radiation Oncol Biol Phys 91:710–717. https://doi.org/10.1016/j.ijrobp.2014.10.024
39. Brown PD, Jaeckle K, Ballman KV et al (2016) Effect of radiosurgery alone vs radiosurgery with whole brain radiation therapy on cognitive function in patients with 1 to 3 brain metastases: a randomized clinical trial. JAMA 316:401. https://doi.org/10.1001/jama.2016.9839
40. Soffietti R, Kocher M, Abacioglu UM et al (2013) A European organisation for research and treatment of cancer phase III trial of adjuvant whole-brain radiotherapy versus observation in patients with one to three brain metastases from solid tumors after surgical resection or radiosurgery: quality-of-life results. J Clin Oncol 31:65–72. https://doi.org/10.1200/JCO.2011.41.0639
41. Mulvenna P, Nankivell M, Barton R et al (2016) Dexamethasone and supportive care with or without whole brain radiotherapy in treating patients with non-small cell lung cancer with brain metastases unsuitable for resection or stereotactic radiotherapy (QUARTZ): results from a phase 3, non-inferiority, randomised trial. Lancet 388:2004–2014. https://doi.org/10.1016/S0140-6736(16)30825-X
42. Hong AM, Fogarty GB, Dolven-Jacobsen K et al (2019) Adjuvant whole-brain radiation therapy compared with observation after local treatment of melanoma brain metastases: a multicenter, randomized phase III trial. J Clin Oncol 37:3132–3141. https://doi.org/10.1200/JCO.19.01414
43. Wernicke AG, Hirschfeld CB, Smith AW et al (2017) Clinical outcomes of large brain metastases treated with neurosurgical resection and intraoperative cesium-131 brachytherapy: results of a prospective trial. Int J Radiat Oncol Biol Phys 98:1059–1068. https://doi.org/10.1016/j.ijrobp.2017.03.044
44. Raleigh DR, Seymour ZA, Tomlin B et al (2017) Resection and brain brachytherapy with permanent iodine-125 sources for brain metastasis. J Neurosurg 126:1749–1755. https://doi.org/10.3171/2016.4.JNS152530
45. Yang L, Wang C, Zhang W et al (2022) Iodine-125 brachytherapy treatment for newly diagnosed brain metastasis in non-small cell lung cancer: a biocentric analysis. Front Oncol 12:1005876. https://doi.org/10.3389/fonc.2022.1005876
46. Wowra B, Schmitt HP, Sturm V (1989) Incidence of late radiation necrosis with transient mass effect after interstitial low dose rate radiotherapy for cerebral gliomas. Acta Neurochir (Wien) 99:104–108. https://doi.org/10.1007/BF01402316
47. Huang K, Sneed PK, Kunwar S et al (2009) Surgical resection and permanent iodine-125 brachytherapy for brain metastases. J Neurooncol 91:83–93. https://doi.org/10.1007/s11060-008-9686-2
48. Bernstein M, Lumley M, Davidson G et al (1993) Intracranial arterial occlusion associated with high-activity iodine-125 brachytherapy for glioblastoma. J Neuro-Oncol 17:253–260. https://doi.org/10.1007/BF01049980
49. Doré M, Martin S, Delpon G et al (2017) Stereotactic radiotherapy following surgery for brain metastasis: predictive factors for local control and radionecrosis. Cancer/Radiothérapie 21:4–9. https://doi.org/10.1016/j.canrad.2016.06.010
50. Potthoff A-L, Heimann M, Lehmann F et al (2023) Survival after resection of brain metastasis: impact of synchronous versus metachronous metastatic disease. J Neurooncol. https://doi.org/10.1007/s11060-023-04242-5
51. Lutterbach J, Cyron D, Henne K, Ostertag CB (2008) Radiosurgery followed by planned observation in patients with one

to three brain metastases. Neurosurgery 62(Suppl 2):776–784. https://doi.org/10.1227/01.neu.0000316281.07124.ea
52. Sawrie SM, Guthrie BL, Spencer SA et al (2008) Predictors of distant brain recurrence for patients with newly diagnosed brain metastases treated with stereotactic radiosurgery alone. Int J Radiat Oncol Biol Phys 70:181–186. https://doi.org/10.1016/j.ijrobp.2007.05.084
53. Liu Q, Schneider F, Ma L et al (2013) Relative biologic effectiveness (RBE) of 50 kV X-rays measured in a phantom for intraoperative tumor-bed irradiation. Int J Radiat Oncol Biol Phys 85:1127–1133. https://doi.org/10.1016/j.ijrobp.2012.08.005
54. Lehrer EJ, Ahluwalia MS, Gurewitz J et al (2022) Imaging-defined necrosis after treatment with single-fraction stereotactic radiosurgery and immune checkpoint inhibitors and its potential association with improved outcomes in patients with brain metastases: an international multicenter study of 697 patients. J Neurosurg. https://doi.org/10.3171/2022.7.JNS22752
55. Minniti G, Clarke E, Lanzetta G et al (2011) Stereotactic radiosurgery for brain metastases: analysis of outcome and risk of brain radionecrosis. Radiat Oncol 6:48. https://doi.org/10.1186/1748-717X-6-48
56. Minniti G, Scaringi C, Paolini S et al (2016) Single-fraction versus multifraction (3 × 9 Gy) stereotactic radiosurgery for large (>2 cm) brain metastases: a comparative analysis of local control and risk of radiation-induced brain necrosis. Int J Radiat Oncol Biol Phys 95:1142–1148. https://doi.org/10.1016/j.ijrobp.2016.03.013

Authors and Affiliations

Julian P. Layer[1,2] · Motaz Hamed[3] · Anna-Laura Potthoff[3] · Cas S. Dejonckheere[1] · Katharina Layer[1] · Gustavo R. Sarria[1] · Davide Scafa[1] · David Koch[1] · Mümtaz Köksal[1] · Fabian Kugel[1] · Molina Grimmer[1] · Jasmin A. Holz[1] · Thomas Zeyen[4] · Lea L. Friker[2,5] · Valeri Borger[3] · F. Carsten Schmeel[6] · Johannes Weller[4] · Michael Hölzel[2] · Niklas Schäfer[4] · Stephan Garbe[1] · Helmut Forstbauer[7] · Frank A. Giordano[8,9,10] · Ulrich Herrlinger[4] · Hartmut Vatter[3] · Matthias Schneider[3] · L. Christopher Schmeel[1]

✉ Julian P. Layer
julian.layer@ukbonn.de

[1] Department of Radiation Oncology, University Hospital Bonn, Venusberg-Campus 1, 53127 Bonn, Germany

[2] Institute of Experimental Oncology, University Hospital Bonn, Bonn, Germany

[3] Department of Neurosurgery, University Hospital Bonn, Bonn, Germany

[4] Division of Clinical Neuro-Oncology, Department of Neurology, University Hospital Bonn, Bonn, Germany

[5] Institute of Neuropathology, University Hospital Bonn, Bonn, Germany

[6] Department of Neuroradiology, University Hospital Bonn, Bonn, Germany

[7] Oncology Practice Network Troisdorf, Troisdorf, Germany

[8] Department of Radiation Oncology, University Medical Center Mannheim, Mannheim, Germany

[9] DKFZ-Hector Cancer Institute of the University Medical Center Mannheim, Mannheim, Germany

[10] Mannheim Institute of Intelligent Systems in Medicine (MIISM), Medical Faculty Mannheim, University of Heidelberg, Mannheim, Germany

3.4 Layer JP, Shiban E, Brehmer S, Diehl CD, de Castro DG, Hamed M, Dejonckheere CS, Cifarelli DT, Friker LL, Herrlinger U, Hölzel M, Vatter H, Schneider M, Combs SE, Schmeel LC, Cifarelli CP, Giordano FA, Sarria GR*, Kahl KH*. Multicentric assessment of safety and efficacy of combinatorial adjuvant brain metastasis treatment by intraoperative radiotherapy and immunotherapy. Int J Radiat Oncol Biol Phys. 2024 Apr 1;118(5):1552-1562.

Hintergrund und Zielsetzung der Arbeit: Eine wachsende Zahl von Tumorpatienten erhält bereits in frühen Therapielinien neue, zielgerichtete systemische Therapeutika mit nur eingeschränkter Datenlage zu Synergismen und unerwünschten Interaktionen bei paralleler Durchführung einer interventionellen Therapie. Hierzu zählen insbesondere auch immuntherapeutische Ansätze wie die Checkpoint-Inhibition. Häufig wird daher bei der Indikationsstellung zur Resektion und Bestrahlung einer Hirnmetastase auf die Einleitung der Systemtherapie aus Sicherheitsgründen zunächst verzichtet oder deren Fortführung unterbrochen. Dies gilt im Besonderen für die IORT, für die bislang keine Verträglichkeitsdaten in Kombination mit einer zielgerichteten Therapie bestehen. Auch für das klinische *Outcome* dieser Kombination liegen bislang keine Daten vor. Ziel dieser Arbeit war die systematische Auswertung der Sicherheit und Effektivität einer Kombination der IORT von Hirnmetastasen mit ICIs und TTs.

Methoden und Ergebnisse: In einer multizentrischen Erhebung weltweit führender Zentren für IORT von Hirnmetastasen wurden sämtliche IORT-Fälle mit simultaner bzw. zeitnah durchgeführter Systemtherapie mit einem ICI oder einer TT retrospektiv ausgewertet. Die Patientenverläufe wurden in Bezug auf Toxizität, RN-Rate, leptomeningeale Tumoraussaat, lokale Kontrolle, distanten intrazerebralen Progress und Gesamtüberleben untersucht. In den sechs teilnehmenden Zentren wurden insgesamt 103 Läsionen mit einem medianen Durchmesser von 34 mm in die Studie eingeschlossen. Es wurde ein einziges mit der IORT in Zusammenhang stehendes Grad 3 Event registriert (2,2% aller Events). Wunddehiszenzen traten in keinem Fall auf. Ferner wurde eine kumulative RN-Rate von 4,9% beobachtet. Schwergradige Toxizität trat signifikant häufiger bei Patienten auf, deren Systemtherapie in den ersten zwei Monaten nach der IORT eingeleitet wurde. Nach einem Jahr betrug die lokale Kontrollrate 98,0% und die intrazerebrale Kontrollrate 60,0%. Kumulativ kam es bei 4,9% der Patienten zu einer

leptomeningealen Tumoraussaat. Der frühzeitige Beginn der Systemtherapie (binnen zwei Monaten nach IORT) war in einer uni- und multivariaten Analyse mit einem nicht-signifikanten Trend zur Verbesserung der distanten intrazerebralen Kontrolle und des Gesamtüberlebens verbunden. Eine Dosisverschreibung von unter 25 Gy war im Trend mit einem geringeren RN-Risiko bei jedoch gleichbleibender Lokalkontrolle assoziiert.

Schlussfolgerungen: Die Kombination von Resektion, IORT und systemischer Therapie mit ICIs und TTs ist sicher und führt nicht zu erhöhter Toxizität, insbesondere nicht in Bezug auf Wundinfektionen und RNs. Zugleich zeigten sich in dieser Arbeit vielversprechende Kontrollraten trotz der erheblichen Größe der behandelten Hirnmetastasen. Eine systemische Therapie kann möglicherweise bereits vor der Operation und sollte zeitnah nach der IORT eingeleitet werden, um die Gesamtprognose des Patienten nicht zu gefährden.

INTERNATIONAL JOURNAL OF
RADIATION ONCOLOGY • BIOLOGY • PHYSICS
www.redjournal.org

CLINICAL INVESTIGATION

Multicentric Assessment of Safety and Efficacy of Combinatorial Adjuvant Brain Metastasis Treatment by Intraoperative Radiation Therapy and Immunotherapy

Julian P. Layer, MD,[*,†] Ehab Shiban, MD,[‡] Stefanie Brehmer, MD,[§] Christian D. Diehl, MD,[‖] Douglas Guedes de Castro, MD,[¶] Motaz Hamed, MD,[#] Cas S. Dejonckheere, MD,[*] Daniel T. Cifarelli, MD,[**] Lea L. Friker, MD,[†,††] Ulrich Herrlinger, MD,[‡‡] Michael Hölzel, MD,[†] Hartmut Vatter, MD,[#] Matthias Schneider, MD,[#] Stephanie E. Combs, MD,[‖] Leonard Christopher Schmeel, MD,[*] Christopher P. Cifarelli, MD, PhD,[**] Frank A. Giordano, MD,[§§,‖‖,¶¶] Gustavo R. Sarria, MD,[*] and Klaus-Henning Kahl, MD[##]

[*]*Department of Radiation Oncology, University Hospital Bonn, Bonn, Germany;* [†]*Institute of Experimental Oncology, University Hospital Bonn, Bonn, Germany;* [‡]*Department of Neurosurgery, University Hospital Augsburg, Augsburg, Germany;* [§]*Department of Neurosurgery, University Medical Center Mannheim, Mannheim, Germany;* [‖]*Department of Radiation Oncology, Klinikum Rechts der Isar, Technical University of Munich, Munich, Germany;* [¶]*Department of Radiation Oncology, A. C. Camargo Cancer Center, São Paulo, Brazil;* [#]*Department of Neurosurgery, University Hospital Bonn, Bonn, Germany;* [**]*Department of Neurosurgery, West Virginia University, Morgantown, West Virginia;* [††]*Institute of Neuropathology, University Hospital Bonn, Bonn, Germany;* [‡‡]*Division of Clinical Neuro-Oncology, Department of Neurology, University Hospital Bonn, Bonn, Germany;* [§§]*Department of Radiation Oncology, University Medical Center Mannheim, Mannheim, Germany;* [‖‖]*DKFZ-Hector Cancer Institute of the University Medical Center Mannheim, Mannheim, Germany;* [¶¶]*Mannheim Institute of Intelligent Systems in Medicine (MIISM), Medical Faculty Mannheim, University of Heidelberg, Mannheim, Germany; and* [##]*Department of Radiooncology, University Hospital Augsburg, Augsburg, Germany*

Received Aug 11, 2023; Accepted for publication Jan 3, 2024

Corresponding author: Gustavo R. Sarria, MD; E-mail: gustavo.sarria@ukbonn.de

Gustavo R. Sarria and Klaus-Henning Kahl made equal contributions to this study.

Disclosures: J.P.L. reports stocks and travel expenses from TME Pharma AG, travel expenses from Carl Zeiss Meditec AG, stocks and honoraria from Siemens Healthineers, and stocks from Bayer AG and BioNTech AG. S.B. reports travel expenses and honoraria from Carl Zeiss Meditec AG. C.D.D. reports travel expenses from Carl Zeiss Meditec AG. M.H. reports travel expenses from Carl Zeiss Meditec AG. H.V. reports travel expenses from Carl Zeiss Meditec AG. M.S. reports travel expenses from Carl Zeiss Meditec AG. S. E.C. reports travel expenses and honoraria from Carl Zeiss Meditech AG. L.C. S. reports travel expenses from Carl Zeiss Meditec AG. C.P.C. reports travel expenses and speaking honoraria from Carl Zeiss Meditech AG. F.A.G. reports research grants and travel expenses from Elekta AB and Varian Medical Systems, Inc; grants, stocks, travel expenses, and honoraria from TME Pharma AG; research grants, travel expenses, and honoraria from Carl Zeiss Meditec AG; travel expenses and honoraria from Bristol-Myers Squibb, Cureteq AG, Guerbet SA, Roche Pharma AG, MSD Sharp & Dohme GmbH, and AstraZeneca GmbH; and nonfinancial support from Oncare GmbH and Opasca GmbH. G.R.S. reports personal fees and travel expenses from Carl Zeiss Meditec AG, personal fees from MedWave Clinical Trials, and travel expenses from Guerbet SA. K.-H.K. reports honoraria and travel expenses from Varian, Elekta AB, Carl Zeiss Meditec AG, AstraZeneca, Roche, Icotec AG, Bristol-Myers Squibb, MSD Sharp & Dohme, Merck, and Sanofi-Aventis and advisory board membership for Bristol-Myers Squibb, MSD Sharp & Dohme, Merck, and Sanofi-Aventis.

Data Sharing Statement: The data presented in this study are available in the article. Further data sets generated and/or analyzed during the current study are available from the corresponding author on reasonable request.

Acknowledgments—We thank Katja Klever and Monika Brüggemann for their support in patient follow-up and the medical team of Helmut Forstbauer for aiding in data acquisition.

Supplementary material associated with this article can be found in the online version at doi:10.1016/j.ijrobp.2024.01.009.

Int J Radiation Oncol Biol Phys, Vol. 118, No. 5, pp. 1552–1562, 2024
0360-3016/$ - see front matter
https://doi.org/10.1016/j.ijrobp.2024.01.009

Purpose: After surgical resection of brain metastases (BMs), intraoperative radiation therapy (IORT) provides a promising alternative to adjuvant external beam radiation therapy by enabling superior organ-at-risk preservation, reduction of in-hospital times, and timely admission to subsequent systemic treatments, which increasingly comprise novel targeted immunotherapeutic approaches. We sought to assess the safety and efficacy of IORT in combination with immune checkpoint inhibitors (ICIs) and other targeted therapies (TTs).

Methods and Materials: In a multicentric approach incorporating individual patient data from 6 international IORT centers, all patients with BMs undergoing IORT were retrospectively assessed for combinatorial treatment with ICIs/TTs and evaluated for toxicity and cumulative rates, including wound dehiscence, radiation necrosis, leptomeningeal spread, local control, distant brain progression (DBP), and estimated overall survival.

Results: In total, 103 lesions with a median diameter of 34 mm receiving IORT combined with immunomodulatory systemic treatment or other TTs were included. The median follow-up was 13.2 (range, 1.2-102.4) months, and the median IORT dose was 25 (range, 18-30) Gy prescribed to the applicator surface. There was 1 grade 3 adverse event related to IORT recorded (2.2%). A 4.9% cumulative radiation necrosis rate was observed. The 1-year local control rate was 98.0%, and the 1-year DBP-free survival rate was 60.0%. Median time to DBP was 5.5 (range, 1.0-18.5) months in the subgroup of patients experiencing DBP, and the cumulative leptomeningeal spread rate was 4.9%. The median estimated overall survival was 26 (range, 1.2 to not reached) months with a 1-year survival rate of 74.0%. Early initiation of immunotherapy/TTs was associated with a nonsignificant trend toward improved DBP rate and overall survival.

Conclusions: The combination of ICIs/TTs with IORT for resected BMs does not seem to increase toxicity and yields encouraging local control outcomes in the difficult-to-treat subgroup of larger BMs. Time gaps between surgery and systemic treatment could be shortened or avoided. The definitive role of IORT in local control after BM resection will be defined in a prospective trial.

Introduction

The rise of novel immunotherapeutic agents has redrawn the treatment patterns for many tumor entities in recent years.[1,2] As a consequence of improved local control and prolonged survival, the diagnostic incidence of brain metastases (BMs) has increased significantly,[3,4] with nearly every second patient developing BMs over the course of the disease.[5,6] This is also attributed to the fact that many novel immunotherapeutic drugs cannot penetrate the blood-brain barrier (BBB) sufficiently to induce stable tumor control within the brain.[7,8] Although overall survival (OS) is largely dictated by extracranial disease progression,[9] BMs usually require medical intervention to prevent or stabilize neurologic deterioration and impairment of quality of life.[10,11] Local treatment options include surgery, radiosurgery, fractionated stereotactic radiation therapy (RT), and surgery followed by adjuvant RT of the resection cavity. Surgery and adjuvant RT are usually indicated for larger BMs to improve local control rates, as smaller-volume BMs do not need surgery.[12-14] Although the most common form of RT application is stereotactic external beam RT (EBRT) with 1 to 7 fractions,[12-15] intraoperative RT (IORT) provides an excellent alternative, yielding equal clinical outcomes[16-19] with superior organ-at-risk (OAR) preservation[20] and a favorable toxicity profile.[21,22] However, data are very limited regarding potential desirable and undesirable effects[23,24] of concomitant or sequential treatment with increasingly available immunostimulating systemic therapy.[25] We thus sought to assess the safety and efficacy of combination treatment with IORT to BMs and immunotherapy (IT) in this multicentric retrospective series.

Methods and Materials

Patients

In a multicentric approach, patient databases of 4 European, 1 North American, and 1 South American university hospitals were retrospectively screened for patients with BMs receiving IORT with concomitant or sequential IT or targeted therapy (TT) between 2014 and 2023. IT was defined as authority-approved administration of an ICI (ie, anti-PD-L1, anti-PD-1, and anti-CTLA4). TT was defined as authority-approved administration of a drug using a tumor-specific nonimmunogenic or immunogenic target other than immune checkpoint blockade (ie, BRAF/MEK inhibition, [multi-]tyrosine kinase inhibition, or antibodies against essential tumor signaling pathways). For inclusion, at least 1 available imaging follow-up (FU) and information on received systemic treatment were mandatory. All patients underwent surgical resection and IORT following interdisciplinary evaluation in a neuro-oncological tumor board. BMs were pathologically confirmed in all cases. The criteria for surgical resection were presence or severe risk of acute neurologic impairment, clinically significant mass effects as abnormal intracranial pressure or hemispheric shift, and histopathologic confirmation of diagnosis in case of cancer of unknown primary. Only the clinically relevant lesion receiving IORT was considered for surgical removal in case of multiple BMs. Requirements for IORT were gross total resection, intraoperative confirmation of BM on frozen tumor sections, and fulfillment of dose constraints. The data collected from eligible patients included sociodemographic characteristics, functional status with Karnofsky performance score, tumor location, histology, baseline

and FU radiologic features of the lesion, and systemic therapy status. Diagnostic-Specific Graded Prognostic Assessment (DS-GPA)[26] scores were calculated by standard procedures.

IORT

Three-dimensional image guidance for both surgery and IORT was provided by preoperative contrast-enhanced T1-weighted magnetic resonance imaging (MRI). The optic nerve, optic chiasm, and brain stem were identified preoperatively and intraoperatively as OARs for IORT, and delivered doses were defined based on dose-depth template profiles corresponding to each applicator diameter. Following macroscopic complete resection of the lesion, a frozen section was assessed intraoperatively by a board-certified neuropathologist, confirming the presence of malignant cells with an extracranial solid tumor origin. Neurosurgical MRI navigation was used to intraoperatively assess the minimum distance of the resection cavity to OARs and cavity extends, followed by selection of the optimal fitting for spherical applicators ranging from 1.5 to 5.0 cm in diameter. The selected applicator was placed in the resection cavity without applying pressure to the adjacent healthy brain tissue but with the aim of ubiquitous direct tissue contact avoiding air entrapment for optimal dose distribution. The IORT was only performed when a safe and orderly execution was ensured. The INTRABEAM 600 (Carl Zeiss Meditec AG) was used to deliver IORT by application of nominal 50-kV photons at a standard dose of 20 to 30 Gy prescribed to the applicator surface. The dose profile in depth was obtained before each procedure according to preperformed Monte Carlo calculations with radiance (GMV). Decreasing the prescribed dose down to 16 Gy was acceptable in case of OAR doses exceeding the constraints of 8 Gy to the optical system or the brain stem following QUANTEC (Quantitative Analyses of Normal Tissue Effects in the Clinic) recommendations[27] with consideration of the specific (1.3-1.5 times higher) relative biologic effectiveness of low-energy photons. In individual cases, anatomic positioning of the applicator required consideration of a further, not regularly assessed, OAR (eg, cochlea or thalamus) with equal consideration of the QUANTEC recommendations. The irradiation time ranged from 7 to 49 minutes depending on the applicator size and the prescribed dose. Following removal of the applicator, the surgery was continued as per standard procedures with wound sealing.

Follow-up

All patients had regular FU visits, including physical examination and MRI, as per guideline recommendations. Adverse events (AEs) were assessed and graded by clinicians according to the National Cancer Institute Common Terminology Criteria for Adverse Events, version 5.0. Acute toxicities were considered AEs occurring within the first 8 weeks of FU, whereas late toxicities were defined as all AEs recorded at a later time point. MRI assessments were performed according to the RANO criteria[28] by board-certified radiologists. In case of uncertain clinical/radiographic response, the interdisciplinary neuro-oncological tumor board was consulted for shared decision-making. The following conditions qualified for diagnosis of radiation necrosis (RN): (1) after initial suspected progressive disease (PD), a minimum of 2 FU MRIs showed no sign of ongoing PD; (2) advanced MRI incorporating dynamic susceptibility contrast perfusion imaging or diffusion-weighted imaging was concordantly suggestive of RN; (3) positron emission tomography imaging, such as ^{18}F-fluoroethyl-tyrosine positron emission tomography, with findings consistent with RN; and (4) RN was confirmed histopathologically following resection.

Study endpoints

The primary endpoints were toxicity, namely cumulative RN rates, and 1-year local control rate (LCR). The secondary endpoints were cumulative distant brain progression (DBP) rates, leptomeningeal spread (LMS) rates, 1-year OS rates, and estimated OS. For toxicity assessment, simultaneous IORT and IT/TT was defined as an initiation of treatment within the first 2 months after date of surgery. Local control was defined as the absence of MRI radiographic PD, as per RANO-BM criteria,[28] within 1 cm surrounding the previously irradiated BM resection cavity and absence of clinical deterioration attributable to the treated lesion. Local control was calculated from the day of surgery until the local PD date. Patients lost to FU or deceased before radiographic progression were censored at the last FU time point. DBP was defined as an MRI radiographic emergence/progression of intracranial lesions, as per RANO-BM criteria, in at least 1-cm distance to the resection cavity receiving IORT or clinical deterioration not attributed to the IORT but a distant brain lesion. DBP rates were calculated from the day of surgery to the PD date. Patients lost to FU or deceased before the event were censored at the last FU time point. LMS was defined as either MRI radiographic suspicion or cytologic confirmation of pachymeningeal or leptomeningeal tumor cell spread. OS was defined as the time interval between the date of surgery and the date of either the last FU (censored) or death.

Ethics

This study was conducted in accordance with the principles of the Declaration of Helsinki and was approved by the Ethics Committee of the University Hospital Bonn (approval number: 057/22).

Statistics

The software package used for the data analyses was GraphPad Prism (version 9, GraphPad Software). Figures and

graphs were created using GraphPad Prism and Adobe Illustrator 2023 (Adobe, Inc). Descriptive statistics incorporated the calculation of percentages and median values with minimum to maximum range. For survival analysis, the Kaplan-Meier method was used and curves with 95% confidence intervals were generated. Hazard ratios and their 95% confidence intervals were calculated using the Mantel-Haenszel method. The Fisher exact test was used to analyze categorical variables. The Mann-Whitney test was used to compare continuous variables, as the data were not normally distributed. Statistical significance was defined as $P < .05$. The particular statistical methods applied are specified in the corresponding figures.

Results

Patient and tumor characteristics

A total sample size (n) of 114 consecutive patients with BMs receiving IORT to the resection cavity combined with immune checkpoint inhibitors (ICIs) or other TTs were screened. Of these, sufficient FU information (at least 1 imaging FU and systemic therapy information) was available for 99 patients with 105 treated lesions. Two cases were removed from the outcome analyses because the IORT lesion received additional immediate stereotactic body RT, leaving a total of 103 lesions analyzed. The median patient age was 63 years (range, 35-85; n = 99), and the median Karnofsky performance score was 80 (range, 40-100). The median DS-GPA score was 2 (range, 0-4; n = 99). The most frequent BM localization was the frontal lobe (35.0%), whereas most histopathology results corresponded to lung cancer (54.4%). With a range of 1 to 16 intracranial lesions, 48 cases (46.6%) suffered from multiple BMs at the time of surgery. Further details on patient characteristics are provided in Table 1.

Table 1 Patient characteristics for the evaluated BMs (n = 103)

Variable	No. (%)	Median (range)
Gender		
Male	56 (54.4)	
Female	47 (45.6)	
Age (y)		63 (35-85)
Tumor entity		
NSCLC	53 (51.5)	
Melanoma	25 (24.3)	
RCC	13 (12.6)	
Breast	4 (3.9)	
SCLC	3 (2.9)	
Others	5 (4.9)	
Localization		
Frontal lobe	36 (35.0)	
Parietal lobe	28 (27.2)	
Occipital lobe	18 (17.5)	
Temporal lobe	13 (12.6)	
Cerebellum	8 (7.8)	
Maximum presurgical diameter (mm)		34 (8-70)
Presurgical tumor volume (cm^3)		22.9 (1.2-701.7)
Multiple BMs	48 (46.6)	
Number of BMs		1 (1-16)
RT to other BMs	50 (48.5)	
Relevant overlap (≥10% isodose)	14 (13.6)	
Extracranial metastases	66 (64.1)	
KPS		80 (40-100)
DS-GPA		2 (0-4)

Abbreviations: BM = brain metastasis; DS-GPA = Diagnostic-Specific Graded Prognostic Assessment; KPS = Karnofsky performance score; NSCLC = non-small cell lung cancer; RCC = renal cell carcinoma; RT = radiation therapy; SCLC = small cell lung cancer.

Treatment

The median FU was 13.2 (range, 1.2-102.4; n = 99) months. The brain stem and optic tracts (optic nerve and chiasma) were regularly assessed as OARs, and no dose constraints were exceeded. All patients completed treatment. The median IORT prescription dose was 25 Gy (range, 16-30; n = 103) to the surface, which corresponds to a dose delivery of approximately 60% in 3 mm, 45% in 5 mm, and 22% in 10 mm tissue depth, slightly varying depending on applicator diameter. The median applicator size was 2 cm (range, 1.5-4.0; n = 103). Whereas 90 patients (87.4%) received IORT plus ICIs, another 25 patients (24.3%) received other TTs. Of note, some patients received both ICI and TT in parallel or combinations of either substance group. The median time to ICI initiation after IORT was 1.1 (range, −22.3 to 34; n = 90) months. TT was initiated after a median time of 1.2 months (range, −38.9 to 22.9; n = 25). Table 2 depicts further treatment characteristics and lists the specific administered substances.

Toxicity

Under combinatory treatment, mild and anticipated toxicity was reported. A summary of the observed AEs is provided in Table 3. No grade 4 or 5 events were deemed related to IORT. Figure 1a and b show the maximum toxicity observed for individual patients. A cumulative RN rate of 4.9% (n = 5) was observed with a median time to RN of 12.8 (range, 7.8-

Table 2 Treatment characteristics (n = 103)

Variable	No. (%)	Median (range)
IORT dose (Gy)		25 (16-30)
18	5 (4.9)	
20	40 (38.8)	
24	4 (3.9)	
25	3 (2.9)	
26	1 (1.0)	
30	50 (48.5)	
Applicator diameter (mm)		20 (15-40)
Time from first diagnosis to IORT (mo)		1 (0-297)
Immune checkpoint inhibitor	90 (87.4)*	
Pembrolizumab	36 (40.0)	
Ipilimumab + nivolumab	20 (22.2)	
Atezolizumab	16 (15.5)	
Nivolumab	13 (14.4)	
Durvalumab	4 (4.4)	
Ipilimumab	1 (1.1)	
Time from IORT to IT (mo)		1.1 (−22.3 to 34)
Number of IT cycles		6 (1-93)
TT drug	25 (24.3)*	
BRAF/MEK inhibitor	6 (24.0)	
TKI	5 (20.0)	
MKI	6 (24.0)	
VEGF targeting*	6 (24.0)	
Androgen deprivation	3 (12.0)	
Anti-HER2neu	3 (12.0)	
Anti-TNFα	1 (4.0)	
Time from IORT to TT (mo)		1.2 (−38.9 to 22.9)
Duration of TT treatment (mo)		7 (2-68)

Abbreviations: IT = immunotherapy; IORT = intraoperative radiation therapy; MKI = multikinase inhibitor; TKI = tyrosine kinase inhibitor; TT = targeted therapy.
* Some patients received both IT and TT in parallel or combinations of either substance group.

18.9) months (Fig. 1c). Of these RN events, 4 were grade 1, and 1 was grade 3. The latter occurred in a patient with renal cell carcinoma receiving IORT with 30 Gy to a frontal 34-mm BM after 7.8 months. This patient had received systemic treatment with cabozantinib initiated 5 weeks after surgery for a total of 7 months before it was terminated due to an unfavorable overall toxicity profile. The RN was treated successfully with bevacizumab after previous failure of dexamethasone treatment. No wound dehiscences of any grade were noted. There were significantly more severe AEs (P = .049; Fig. 1d) in total but also treatment-related AEs (P = .025; Fig. 1e; RN and autoimmune infection) recorded for patients who commenced systemic treatment in parallel to resection and IORT, defined as initiation of treatment within the first 2 months following surgery. The full list of acute and long-term AEs is provided in Table E1.

Outcome

The overall 1-year and 2-year LCRs were 98.0% (Fig. 2a) and 93.7%, respectively. With an overall DBP rate of 36.9%, the median DBP-free rate was not reached, while the 1-year DBP-free survival rate was 60.0% (Fig. 2b). The median time to DBP was 5.5 (range, 1.0-18.5; n = 38) months in the subgroup of patients experiencing distant intracranial progression. The cumulative LMS rate was 4.9% with a median time to LMS of 6.2 (range, 4.2-18.2) months (Fig. 2c). The

Table 3 Summary of adverse events (n = 147)

	Acute events	Late events	All events
Grade	No. (%)	No. (%)	No. (%)
1	22 (44.9)	43 (43.9)	65 (44.2)
2	20 (40.8)	18 (18.4)	38 (25.9)
3	6 (12.2)	33 (33.7)	39 (26.5)
4	1 (2.0)*	2 (2.0)†	3 (2.0)
5	0 (0.0)	2 (2.0)‡	2 (1.4)
Any grade	49 (33.3)	98 (66.7)	147 (100.0)

* Fulminant autoimmune hepatitis unrelated to intraoperative radiation therapy but likely related to pembrolizumab.
† One patient experienced immune checkpoint inhibitor–related autoimmune vasculitis of grade 4 under pembrolizumab, and another patient experienced an unrelated cardiac infarction causing pulmonary vein congestion and ultimately an atypical pneumonia.
‡ An 81-year-old patient with lung cancer experienced reactivation of a pre-existing chronic lymphocytic leukemia, ultimately causing his demise following septicemia. Another patient died due to distant brain progression-related intracranial bleeding 4 months after intraoperative radiation therapy.

median OS after IORT was 26 months (range, 1.2 to not reached), and the 1-year OS rate was 74.0% (Fig. 2d). The initiation of IT/TT within 2 months following IORT was associated with a nonsignificant trend toward prolongation of both distant brain control and OS (Fig. 2e). There were no variables significantly associated with local recurrence or RN in uni- or multivariate analysis, whereas DS-GPA provided the best prognostic separation (hazard ratio, 0.05; $P = .173$) for local recurrence. However, median-based classification of the dose prescription (≤24 Gy vs ≥25 Gy) showed a trend for increased RN risk ($P = .158$; Fig. E1), but not local recurrence ($P > 0.999$), DBP-free survival ($P = .782$), or OS ($P = .318$). Age ($P = .022$) and DS-GPA ($P = .049$) were significantly associated with OS in multivariate analysis.

Discussion

In contrast to the preceding era of uniform chemotherapy, ITs have recently reshaped the landscape of oncology dramatically toward precision-tailored treatments. This success is due to promising efficacy in a growing number of tumor entities and good patient tolerability with a relatively favorable toxicity profile, also in combination with other local or systemic therapies. Here, we provide evidence that IORT is an overall well-tolerated combination partner for ICI and other novel TTs.

In particular, in highly immunogenic entities, such as melanoma, there are several reports of synergistic systemic effects of combined focal RT and systemic IT, often referred to as the *abscopal effect*.[29,30] However, the brain was long considered a privileged organ where the underlying mechanisms do not apply due to the filtering properties of the BBB, thus preventing sufficient penetration of the tumor tissue and limiting the bioavailability of drugs[8] in an a priori immune-cold, secluded microenvironment.[31] Nevertheless, there are numerous clinical case reports of abscopal systemic tumor responses following high-dose RT of BMs, particularly with concomitant IT.[32,33] Recent advances in research have shed more light on the characteristics of the immunologic tumor microenvironment of BMs, claiming a very distinct, yet nonnegligible, role of the immune system for brain compartments.[34-36] RT generates neoantigens,[37] activates nonredundant immune pathways in the tumor,[38] and increases permeability of the BBB, thus improving brain penetration of ITs/TTs.[39] These mechanisms make RT a specifically interesting combination partner for targeted approaches in entities and individual patients considered nonresponsive to treatment.[40]

Independent of prognostic factors, BM resection necessitates additional RT to improve local tumor control. Nonetheless, depending on individual tumor features and clinical context, it remains controversial which RT sequencing and technique achieves the best long-term outcomes at the lowest toxicity levels. Our observed 1-year LCR of 97.1% is in line with previous reports on IORT[16,19] and furthermore strengthens the notion that this RT technique might be superior to both definitive and adjuvant EBRT regimens where LCRs of 85% to 90% can be expected at most.[12,14,15,41-43] Yet, prospective trials are required to confirm this hypothesis. A large pooled analysis with 179 patients assessed very recently outcomes for the combination of stereotactic body RT and IT,[44] reporting a LCR of 94.2% and a cumulative grade ≥2 RN rate of 6.9% after a median FU of 14.8 months. Notably, the median diameter of the investigated lesions was only 7 mm. With a median lesion diameter of 34 mm, we provide with IORT plus IT/TT a treatment rationale with particularly good outcome and tolerability for large lesions. Of note, the tumor lesions reported here are measured presurgically for obvious technical reasons, but adjuvant EBRT faces the dilemma of about 30% target volume increase.[45] This additionally strengthens the data provided here for these already presurgically large lesions with a median volume of 22.9 cm^3. Furthermore, larger lesion size was not associated with inferior outcome in this collective. Besides good local tumor control, we also demonstrated convincing intracranial control with a 1-year DBP-free survival of 60.0% and a cumulative LMS rate of only 4.8%. Although the exact underlying mechanisms remain unknown and require further scientific attention, a positive effect of the instant dose application thus preventing intracranial spread or LMS of tumor cells from around the resection cavity appears reasonable. Besides this timely eradication of remaining tumor cells, IORT may synergistically prevent the re-establishment of a protumorigenic tumor microenvironment. IT and TT may benefit from the high-dose local RT effects facilitating antigen presentation and subsequent immune-stimulatory properties, thereby enabling more effective killing of distantly circulating tumor cells.[24] Proteomic profiles of wound fluids from patients

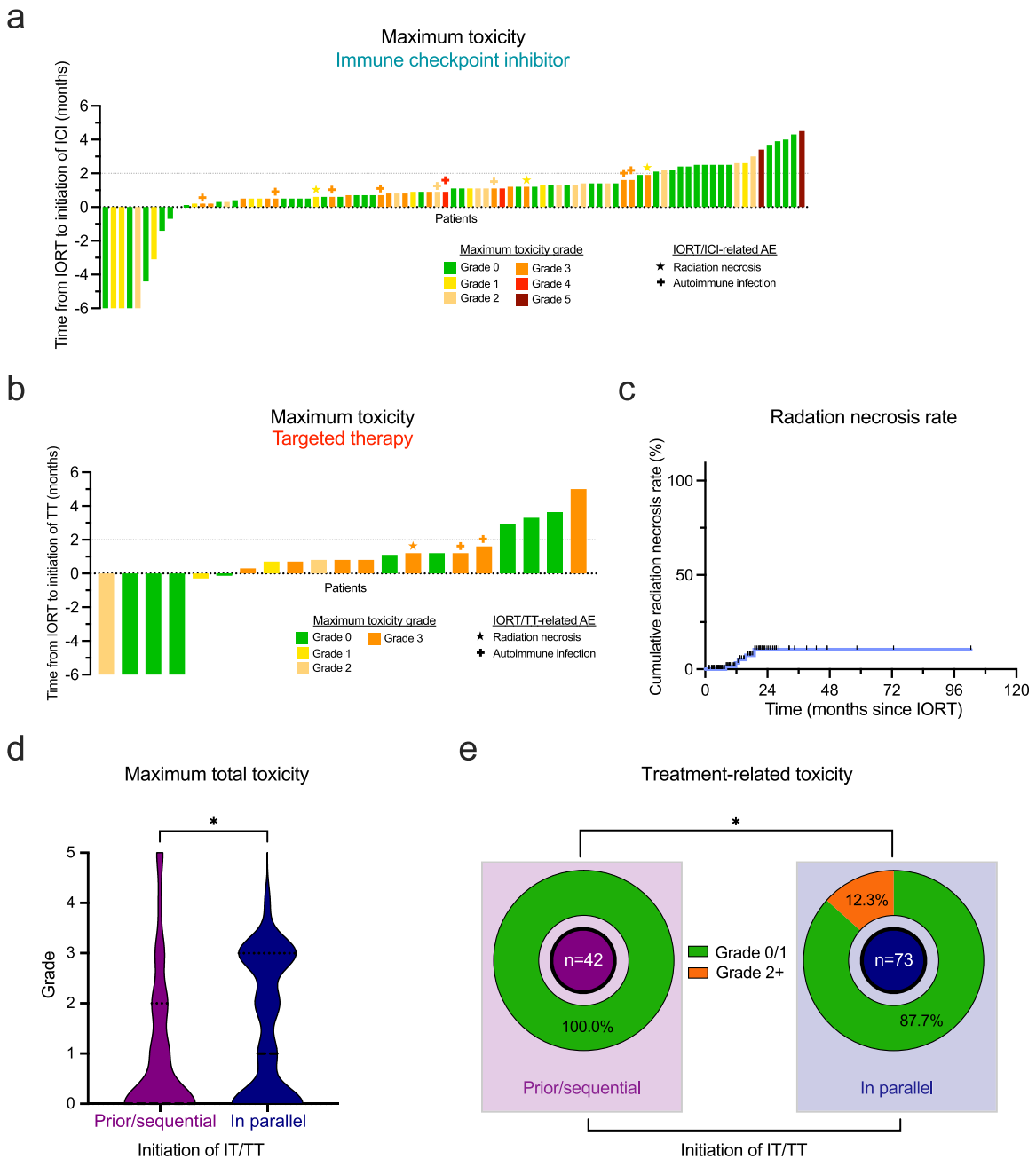

Fig. 1. Toxicity profile of IORT with immune checkpoint inhibition or other targeted therapies. (a, b) Waterfall plot illustrating time from IORT to initiation of ICI therapy (a) and TT (b) for each individual patient with treatment initiation between 6 months before and after IORT. Color labeling represents the maximum overall toxicity observed as per CTCAE grading (independent of the relation to treatment), and icons symbolize occurrence of therapy-associated AEs (IORT/ IT/TT-related AEs). (c) Cumulative radiation necrosis rate (%) over time in months since IORT. (d) Violin plots demonstrating the distribution of the maximum reported toxicity as per CTCAE grading for patients receiving IT/TT before or after (later than 2 months following surgery) IORT compared with treatment initiation in parallel with IORT (within 2 months following surgery). Dashed lines indicate the median; $^*P < .05$, Mann-Whitney test. (e) Donut chart depicting maximum grade IORT/IT/TT-related toxicity (grade ≤1 vs grade ≥2) depending on time point of IT/TT initiation as defined in (d). $^*P > .05$, Fisher exact test. *Abbreviations*: AE = adverse event; CTCAE = Common Terminology Criteria for Adverse Events; ICI = immune checkpoint inhibitor; IORT = intraoperative radiation therapy; IT = immunotherapy; TT = targeted therapy.

with breast cancer exhibited an abrogation of pathways promoting migration and invasiveness following IORT, which may explain the LCRs and DBP-free survival observed in particular.[46] Furthermore, the kV energy of photon-IORT delivers 1.3 to 1.5 times higher relative biological effectiveness,[47] possibly overcoming typical limitations of common

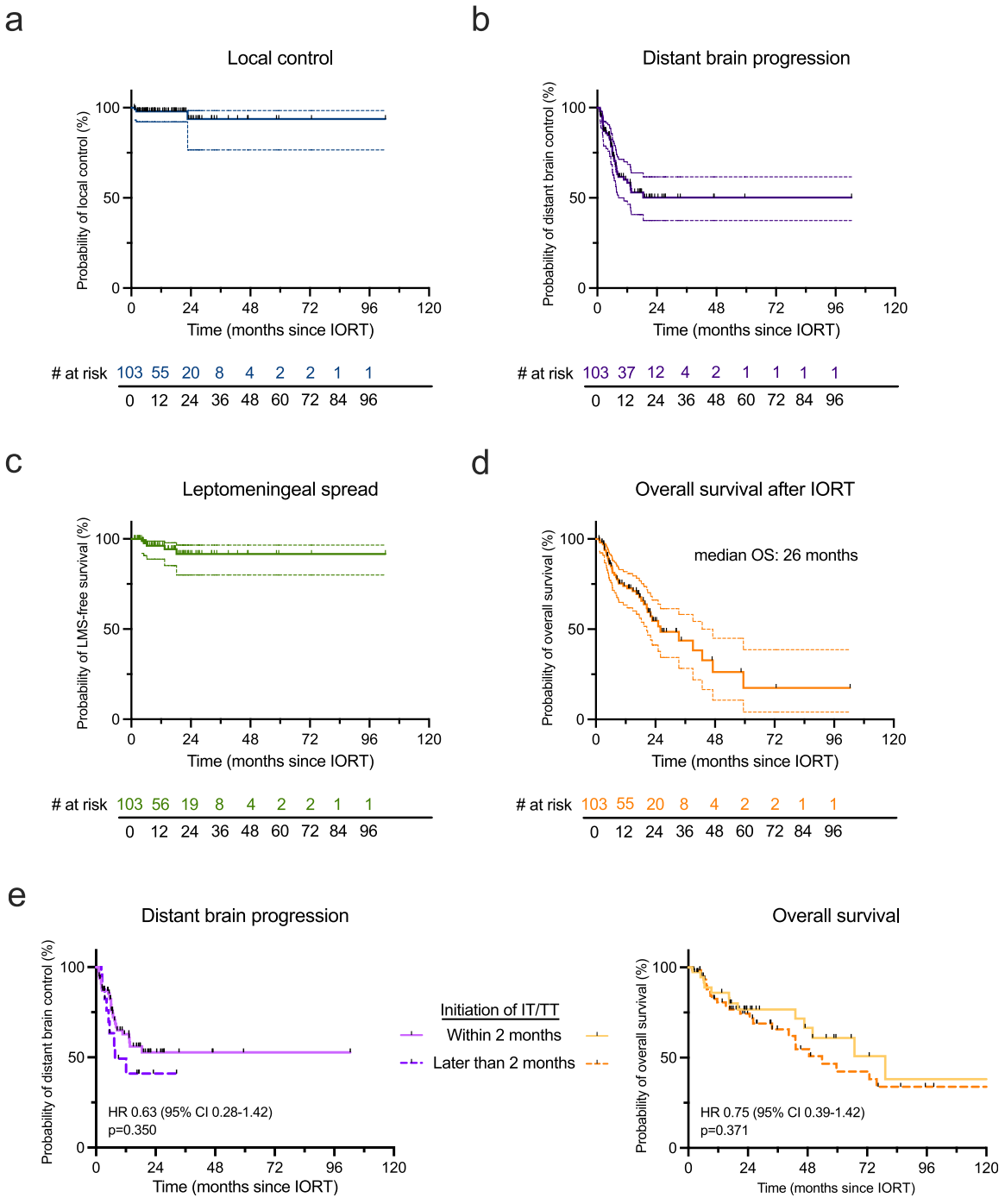

Fig. 2. Outcome parameters of IORT with immune checkpoint inhibition and other targeted therapies. (a-d) Kaplan-Meier plots depicting percent local control rate (a), distant brain progression-free survival (b), leptomeningeal spread-free survival (c), and overall survival (d) over time in months since IORT. Dashed lines indicate 95% CIs. (e, f) Kaplan-Meier plots for distant brain progression-free survival (e) and overall survival (f) dependent on time point of IT/TT initiation (within vs later than 2 months after IORT). HRs with CIs and *P* values are indicated in the lower left corner and were calculated for initiation of IT/TT within 2 months versus later than 2 months. Data were analyzed by log-rank test. *Abbreviations:* HR = hazard ratio; IT = immunotherapy; LMS = leptomeningeal spread; OS = overall survival; TT = targeted therapy.

RT dosing like tumor hypoxia, repair, and reduced radiosensitivity of surviving tumor cells.[48] Nevertheless, the sharp fall-off dose profile of IORT[20] might prevent a farther in-depth tumoricidal effect, which is the principle of EBRT delivery modalities.[15] Yet, the healthy brain-sparing properties of IORT prevent both neurologic and cognitive impairment of patients and allow for targeted reirradiation in case of distant recurrence.

The "one-stop-shop" characteristic of IORT enables timely admission to subsequent systemic treatments while reducing in-hospital times[49] and might furthermore allow for earlier reduction of often necessary systemic corticosteroids than EBRT, which is a known risk factor for TT efficacy predominantly in the early initiation phase.[50] Although the OS reported in this series needs to be interpreted cautiously due to its retrospective nature and potential selection bias, we additionally provide first evidence of encouraging survival outcomes following combinatorial treatment, at least noninferior to previous reports on IORT[18] but also a matched retrospective comparison of IORT and EBRT cases.[19] As mentioned, this is hypothesis generating and should be evaluated within a prospective clinical trial.

Overall, our data indicate good tolerability and a favorable safety profile of this combinatorial approach. While predominantly confirming a lack of sufficient data for most drugs, a systematic meta-analysis previously reported generally acceptable toxicity of cranial stereotactic EBRT with IT.[51] Yet, TTs and, in particular, BRAF inhibitors were associated with a high risk of severe toxicity,[51] which we cannot confirm for our IORT cohort. The toxicity reported here is rather mild and in line with previous reports on IORT, which did not specifically address IT/TT cases.[21,22] Of note, only a minority of IORT patients of previous series received concomitant systemic therapy at all. Patel et al observed a nonsignificant trend toward higher RN incidence for RT and ipilimumab versus RT only.[52] Regardless of this, the reported RN rate of 30% significantly exceeds the cumulative RN rate of 5.7% presented here, despite the numerous patients in this collective receiving duplet immune checkpoint blockade, which is associated with increased toxicity,[2] let alone a less favorable toxicity profile in combination with stereotactic radiotherapy (SRT).[53] Similar to previous retrospective single-center reports,[16-19] IORT patients seem to have a very low RN risk, which is not altered by concomitant IT/TT.

Timing of IT matters, but the optimal sequence of and time intervals between RT and IT remain controversial. Patient- and tumor-centered factors cannot be excluded to additionally influence this question. The PACIFIC trial showed strong evidence for sequential durvalumab treatment in locally advanced lung cancer with a time gap of at least 1 day but up to 6 weeks.[1] In the RTOG 3505 trial, IT with nivolumab was initiated 4 to 12 weeks after RT.[54] However, a large retrospective analysis noted improved clinical outcome when ICIs were started at least 1 month before RT.[55] This divergence prompted us to assess the IORT + IT effects in a wide time range of treatment initiation and to investigate possible timing effects. Within the low-toxicity collective reported here, we notably observed increased toxicity for the subgroup of patients commencing their systemic treatment not before but in the first 2 months following resection and IORT. Additionally, we noted a trend toward improved clinical outcome in both of these groups compared with even later initiation of IT. While requiring confirmation in prospective data, this would contradict the common concept of preventing increased perioperative risks by decidedly long postsurgery treatment gaps but suggest a benefit regarding both outcome and tolerability for even earlier, preinterventional initiation of the systemic treatment.

Wound dehiscence is a common complication following BM resection,[56,57] with reported increased incidence for synchronous IT in head and neck cancer.[58] In this series, we observed not a single case of wound dehiscence, rendering IORT safe for patients with BMs receiving IT/TT. Notably, there is a well-known risk for wound infections with concomitant bevacizumab,[59] which was underrepresented in our collective with just 2 patients receiving this VEGF pathway TT. Our data are thus in accordance with previous reports that claim fewer toxicities for cranial RT with bevacizumab than for extracranial RT.[51] It is worth highlighting that 2 patients were a priori removed from the analyses due to receiving an additional sequential SRT boost after IORT. One of these patients with renal cell carcinoma receiving the VEGF-targeting multikinase inhibitor axitinib and avelumab later experienced both a wound dehiscence requiring surgical intervention and grade 3 RN. Our observations raise suspicion over the safety of this treatment combination and suggest that RT prescription requires reconsideration, as IORT with a sequential SRT boost was previously reported to be related to higher toxicity.[18] Although IORT to BMs without sequential SRT boosting appears safe independent of the dose prescription, the results of the multivariate analyses suggest to limit the dose to 25 Gy to the surface. This limits the IORT duration and thus the window of risk for anesthesia side effects but may also be protective for RN while noninferior regarding clinical outcome. Again, this will have to be confirmed in larger prospective trials.

Our study has several limitations. The retrospective nature of the assessment may cause an incomplete portrait of toxicity compared with controlled prospective clinical trials as well as patient selection bias. This is particularly important because the multicenter aspect additionally attributes to heterogeneity in this regard. Notably, most of our patients presented with lung primary histology. Other histologies, such as breast cancer, were underrepresented. Furthermore, the IORT dose prescription and FU protocols of the contributing centers were not derived from a single trial and not homogenized, which may impact the generalizability of the findings. Given the current small number of IORT patients in this setting, randomized prospective data are required. Our efforts thus mark a first step toward a multicentric, prospective study of IORT cases in centers around the world to ease the interpretation of its therapeutic value. This is the largest investigation on an IORT patient cohort to date, incorporating patient data from over 100 BM treatments in 6 international tertiary referral centers, and it is the first assessment of IORT as a potential combination partner for IT and TT approaches, paving the way to a more patient-centered, fast, safe and individual care for patients with BMs.

Conclusion

The combination of IT/TT with IORT for resected BMs does not seem to increase toxicity, while yielding encouraging local control and LMS rates, particularly for large BMs. Times between surgery and systemic treatment should be shortened with this approach, as timely admission to systemic therapy was associated with a trend toward improved clinical outcome. A prospective clinical trial will elucidate the actual role of IORT in this setting.

References

1. Antonia SJ, Villegas A, Daniel D, et al. Overall survival with durvalumab after chemoradiotherapy in stage III NSCLC. *N Engl J Med* 2018;379:2342-2350.
2. Larkin J, Chiarion-Sileni V, Gonzalez R, et al. Combined nivolumab and ipilimumab or monotherapy in untreated melanoma. *N Engl J Med* 2015;373:23-34.
3. Davis FG, Dolecek TA, McCarthy BJ, et al. Toward determining the lifetime occurrence of metastatic brain tumors estimated from 2007 United States cancer incidence data. *Neuro Oncol* 2012;14:1171-1177.
4. Lamba N, Wen PY, Aizer AA. Epidemiology of brain metastases and leptomeningeal disease. *Neuro Oncol* 2021;23:1447-1456.
5. Cagney DN, Martin AM, Catalano PJ, et al. Incidence and prognosis of patients with brain metastases at diagnosis of systemic malignancy: A population-based study. *Neuro Oncol* 2017;19:1511-1521.
6. Chamberlain MC, Baik CS, Gadi VK, et al. Systemic therapy of brain metastases: Non-small cell lung cancer, breast cancer, and melanoma. *Neuro Oncol* 2017;19:i1-i24.
7. Ishiyama H, Teh BS, Ren H, et al. Spontaneous regression of thoracic metastases while progression of brain metastases after stereotactic radiosurgery and stereotactic body radiotherapy for metastatic renal cell carcinoma: Abscopal effect prevented by the blood-brain barrier? *Clin Genitourin Cancer* 2012;10:196-198.
8. Di Giacomo AM, Valente M, Cerase A, et al. Immunotherapy of brain metastases: Breaking a "dogma. *J Exp Clin Cancer Res* 2019;38:419.
9. Yamamoto M, Sato Y, Serizawa T, et al. Subclassification of recursive partitioning analysis class II patients with brain metastases treated radiosurgically. *Int J Radiat Oncol Biol Phys* 2012;83:1399-1405.
10. Schödel P, Schebesch K-M, Brawanski A, et al. Surgical resection of brain metastases—impact on neurological outcome. *Int J Mol Sci* 2013;14:8708-8718.
11. Verhaak E, Gehring K, Hanssens PEJ, et al. Health-related quality of life of patients with brain metastases selected for stereotactic radiosurgery. *J Neurooncol* 2019;143:537-546.
12. Mahajan A, Ahmed S, McAleer MF, et al. Post-operative stereotactic radiosurgery versus observation for completely resected brain metastases: A single-centre, randomised, controlled, phase 3 trial. *Lancet Oncol* 2017;18:1040-1048.
13. Lehrer EJ, Peterson JL, Zaorsky NG, et al. Single versus multifraction stereotactic radiosurgery for large brain metastases: An international meta-analysis of 24 trials. *Int J Radiat Oncol Biol Phys* 2019;103:618-630.
14. Eitz KA, Lo SS, Soliman H, et al. Multi-institutional analysis of prognostic factors and outcomes after hypofractionated stereotactic radiotherapy to the resection cavity in patients with brain metastases. *JAMA Oncol* 2020;6:1901-1909.
15. Brown PD, Ballman KV, Cerhan JH, et al. Postoperative stereotactic radiosurgery compared with whole brain radiotherapy for resected metastatic brain disease (NCCTG N107C/CEC·3): A multicentre, randomised, controlled, phase 3 trial. *Lancet Oncol* 2017;18:1049-1060.
16. Cifarelli CP, Brehmer S, Vargo JA, et al. Intraoperative radiotherapy (IORT) for surgically resected brain metastases: Outcome analysis of an international cooperative study. *J Neurooncol* 2019;145:391-397.
17. Kahl K-H, Balagiannis N, Höck M, et al. Intraoperative radiotherapy with low-energy x-rays after neurosurgical resection of brain metastases-an Augsburg University Medical Center experience. *Strahlenther Onkol* 2021;197:1124-1130.
18. Diehl CD, Pigorsch SU, Gempt J, et al. Low-Energy X-Ray Intraoperative Radiation Therapy (Lex-IORT) for resected brain metastases: A single-institution experience. *Cancers* 2022;15:14. (Basel).
19. Layer JP, Hamed M, Potthoff A-L, et al. Outcome assessment of intraoperative radiotherapy for brain metastases: Results of a prospective observational study with comparative matched-pair analysis. *J Neurooncol* 2023;164:107-116.
20. Sarria GR, Smalec Z, Muedder T, et al. Dosimetric comparison of upfront boosting with stereotactic radiosurgery versus intraoperative radiotherapy for glioblastoma. *Front Oncol* 2021;11 759873.
21. Hamed M, Potthoff A-L, Layer JP, et al. Benchmarking safety indicators of surgical treatment of brain metastases combined with intraoperative radiotherapy: Results of prospective observational study with comparative matched-pair analysis. *Cancers* 2022;14:1515.
22. Krauss P, Steininger K, Motov S, et al. Resection of supratentorial brain metastases with intraoperative radiotherapy. Is it safe? Analysis and experiences of a single center cohort. *Front Surg.* 2022;9 1071804.
23. Demaria S, Bhardwaj N, McBride WH, et al. Combining radiotherapy and immunotherapy: A revived partnership. *Int J Radiat Oncol Biol Phys* 2005;63:655-666.
24. Weichselbaum RR, Liang H, Deng L, et al. Radiotherapy and immunotherapy: A beneficial liaison? *Nat Rev Clin Oncol* 2017;14:365-379.
25. Haslam A, Prasad V. Estimation of the percentage of US patients with cancer who are eligible for and respond to checkpoint inhibitor immunotherapy drugs. *JAMA Netw Open* 2019;2 e192535.
26. Sperduto PW, Kased N, Roberge D, et al. Summary report on the graded prognostic assessment: An accurate and facile diagnosis-specific tool to estimate survival for patients with brain metastases. *J Clin Oncol* 2012;30:419-425.
27. Marks LB, Yorke ED, Jackson A, et al. Use of normal tissue complication probability models in the clinic. *Int J Radiat Oncol Biol Phys* 2010;76:S10-S19.
28. Lin NU, Lee EQ, Aoyama H, et al. Response assessment criteria for brain metastases: Proposal from the RANO group. *Lancet Oncol* 2015;16:e270-e278.
29. Grimaldi AM, Simeone E, Giannarelli D, et al. Abscopal effects of radiotherapy on advanced melanoma patients who progressed after ipilimumab immunotherapy. *Oncoimmunology* 2014;3:e28780.
30. Koller KM, Mackley HB, Liu J, et al. Improved survival and complete response rates in patients with advanced melanoma treated with concurrent ipilimumab and radiotherapy versus ipilimumab alone. *Cancer Biol Ther* 2017;18:36-42.
31. Engelhardt B, Vajkoczy P, Weller RO. The movers and shapers in immune privilege of the CNS. *Nat Immunol* 2017;18:123-131.
32. Lin X, Lu T, Xie Z, et al. Extracranial abscopal effect induced by combining immunotherapy with brain radiotherapy in a patient with lung adenocarcinoma: A case report and literature review. *Thorac Cancer* 2019;10:1272-1275.
33. Suwinski R. Combination of immunotherapy and radiotherapy in the treatment of brain metastases from non-small cell lung cancer. *J Thorac Dis* 2021;13:3315-3322.
34. Louveau A, Smirnov I, Keyes TJ, et al. Structural and functional features of central nervous system lymphatic vessels. *Nature* 2015;523:337-341.
35. Quail DF, Joyce JA. The microenvironmental landscape of brain tumors. *Cancer Cell* 2017;31:326-341.
36. Strickland MR, Alvarez-Breckenridge C, Gainor JF, et al. Tumor immune microenvironment of brain metastases: Toward unlocking antitumor immunity. *Cancer Discov* 2022;12:1199-1216.
37. Lhuillier C, Rudqvist N-P, Yamazaki T, et al. Radiotherapy-exposed $CD8^+$ and $CD4^+$ neoantigens enhance tumor control. *J Clin Invest* 2021;131 e138740.

38. Twyman-Saint Victor C, Rech AJ, Maity A, et al. Radiation and dual checkpoint blockade activate non-redundant immune mechanisms in cancer. *Nature* 2015;520:373-377.
39. Sprowls SA, Arsiwala TA, Bumgarner JR, et al. Improving CNS delivery to brain metastases by blood-tumor barrier disruption. *Trends Cancer* 2019;5:495-505.
40. Lussier DM, Alspach E, Ward JP, et al. Radiation-induced neoantigens broaden the immunotherapeutic window of cancers with low mutational loads. *Proc Natl Acad Sci U S A* 2021;118 e2102611118.
41. Minniti G, Scaringi C, Paolini S, et al. Single-fraction versus multifraction (3 × 9 Gy) stereotactic radiosurgery for large (>2 cm) brain metastases: A comparative analysis of local control and risk of radiation-induced brain necrosis. *Int J Radiat Oncol Biol Phys* 2016;95:1142-1148.
42. Lehrer EJ, Ahluwalia MS, Gurewitz J, et al. Imaging-defined necrosis after treatment with single-fraction stereotactic radiosurgery and immune checkpoint inhibitors and its potential association with improved outcomes in patients with brain metastases: An international multicenter study of 697 patients. *J Neurosurg* 2022;138:1178-1187.
43. Layer JP, Layer K, Sarria GR, et al. Five-fraction stereotactic radiotherapy for brain metastases - a retrospective analysis. *Curr Oncol* 2023;30:1300-1313.
44. Hall J, Lui K, Tan X, et al. Factors associated with radiation necrosis and intracranial control in patients treated with immune checkpoint inhibitors and stereotactic radiotherapy. *Radiother Oncol* 2023;189 109920.
45. Jarvis LA, Simmons NE, Bellerive M, et al. Tumor bed dynamics after surgical resection of brain metastases: Implications for postoperative radiosurgery. *Int J Radiat Oncol Biol Phys* 2012;84:943-948.
46. Belletti B, Vaidya JS, D'Andrea S, et al. Targeted intraoperative radiotherapy impairs the stimulation of breast cancer cell proliferation and invasion caused by surgical wounding. *Clin Cancer Res* 2008;14:1325-1332.
47. Liu Q, Schneider F, Ma L, et al. Relative biologic effectiveness (RBE) of 50 kV x-rays measured in a phantom for intraoperative tumor-bed irradiation. *Int J Radiat Oncol Biol Phys* 2013;85:1127-1133.
48. Herskind C, Ma L, Liu Q, et al. Biology of high single doses of IORT: RBE, 5 R's, and other biological aspects. *Radiat Oncol* 2017;12:24.
49. Dejonckheere CS, Layer JP, Hamed M, et al. Intraoperative or postoperative stereotactic radiotherapy for brain metastases: Time to systemic treatment onset and other patient-relevant outcomes. *J Neurooncol* 2023;164:683-691.
50. Maslov DV, Tawagi K, Kc M, et al. Timing of steroid initiation and response rates to immune checkpoint inhibitors in metastatic cancer. *J Immunother Cancer* 2021;9 e002261.
51. Kroeze SGC, Fritz C, Hoyer M, et al. Toxicity of concurrent stereotactic radiotherapy and targeted therapy or immunotherapy: A systematic review. *Cancer Treat Rev* 2017;53:25-37.
52. Patel KR, Shoukat S, Oliver DE, et al. Ipilimumab and stereotactic radiosurgery versus stereotactic radiosurgery alone for newly diagnosed melanoma brain metastases. *Am J Clin Oncol* 2017;40:444-450.
53. Bodensohn R, Werner S, Reis J, et al. Stereotactic radiosurgery and combined immune checkpoint therapy with ipilimumab and nivolumab in patients with melanoma brain metastases: A retrospective monocentric toxicity analysis. *Clin Transl Radiat Oncol* 2023;39 100573.
54. Gerber DE, Urbanic JJ, Langer C, et al. Treatment design and rationale for a randomized trial of cisplatin and etoposide plus thoracic radiotherapy followed by nivolumab or placebo for locally advanced non−small-cell lung cancer (RTOG 3505). *Clin Lung Cancer* 2017;18:333-339.
55. Samstein R, Rimner A, Barker CA, et al. Combined immune checkpoint blockade and radiation therapy: Timing and dose fractionation associated with greatest survival duration among over 750 treated patients. *Int J Radiat Oncol Biol Phys* 2017;99:S129-S130.
56. Barami K, Fernandes R. Incidence, risk factors and management of delayed wound dehiscence after craniotomy for tumor resection. *J Clin Neurosci* 2012;19:854-857.
57. Gupta S, Dawood H, Giantini Larsen A, et al. Surgical and peri-operative considerations for brain metastases. *Front Oncol* 2021;11 662943.
58. Mays AC, Yarlagadda B, Achim V, et al. Examining the relationship of immunotherapy and wound complications following flap reconstruction in patients with head and neck cancer. *Head Neck* 2021;43:1509-1520.
59. Sharma K, Marcus JR. Bevacizumab and wound-healing complications: Mechanisms of action, clinical evidence, and management recommendations for the plastic surgeon. *Ann Plast Surg* 2013;71:434-440.

3.5 Layer JP, Layer K, Sarria GR, Röhner F, Dejonckheere CS, Friker LL, Zeyen T, Koch D, Scafa D, Leitzen C, Köksal M, Schmeel FC, Schäfer N, Landsberg J, Hölzel M, Herrlinger U, Schneider M, Giordano FA, Schmeel LC. Five-Fraction Stereotactic Radiotherapy for Brain Metastases—A Retrospective Analysis. Curr Oncol. 2023; 30(2):1300-1313

Hintergrund und Zielsetzung der Arbeit: Zur Verbesserung der lokalen Tumorkontrolle besteht unabhängig vom Resektionsstatus eine Indikation zur definitiven oder adjuvanten Bestrahlung einer Hirnmetastase. Bislang existiert jedoch kein standardisiertes Vorgehen bezüglich der strahlentherapeutischen Fraktionierungs- und Dosisverordnung, die primär von Faktoren wie der Tumorlokalisation, -histologie und -größe abhängt. Insbesondere für palliative Patienten ist eine möglichst kurze Bestrahlungszeit erstrebenswert, um Belastungen zu reduzieren und Lebensqualität zu erhalten, ohne jedoch die klinischen Behandlungsergebnisse zu gefährden. Ziel dieser Arbeit war es, die Toxizität sowie Effektivität einer verkürzten adjuvanten FSRT mit 7 Gy statt der zumeist verwendeten 5 Gy-Einzeldosis zu untersuchen.

Methoden und Ergebnisse: In einer retrospektiven Auswertung der entsprechenden Behandlungsfälle am Universitätsklinikum Bonn aus den Jahren 2016 bis 2018 wurden insgesamt 36 Patienten mit insgesamt 49 behandelten Hirnmetastasen bzw. Resektionshöhlen inkludiert. Es ergaben sich keine höhergradigen Toxizitäten (≥ Grad 3 nach CTCAE) im posttherapeutischen Verlauf. Die RN-Rate lag bei kumulativ 14,3% bei einem medianen Intervall bis zum Auftreten dieser von 12,9 Monaten. Die kumulative lokale Kontrollrate lag bei 83,1% nach einem, und 50,0% nach zwei Jahren. Das Auftreten einer RN war mit der Verabreichung einer Immuntherapie, jungem Alter (≤ 45 Jahre) sowie einem großen PTV und einem hohen $V_{100\%}$ des Gehirns assoziiert. Bezüglich der Prognose ergab sich eine signifikant bessere Lokalkontrolle und ein besseres PFS für Patienten, bei denen eine RN diagnostiziert wurde.

Schlussfolgerungen: Eine hypofraktionierte FSRT mit 7 Gy-Einzeldosis ist sowohl im definitiven als auch im adjuvanten Setting sicher und birgt bei reduzierter Behandlungszeit mit anderen FSRT-Dosiskonzepten vergleichbare Ergebnisse. Insbesondere junge Patienten mit großen Zielvolumen und paralleler Immuntherapie erleiden eine RN, wobei

diese in keinem der untersuchten Fälle interventionell behandlungsbedürftig und überdies mit einem verbesserten lokalen klinischen Ansprechen assoziiert war.

Current Oncology

MDPI

Article

Five-Fraction Stereotactic Radiotherapy for Brain Metastases—A Retrospective Analysis

Julian P. Layer [1,2], Katharina Layer [1], Gustavo R. Sarria [1], Fred Röhner [1], Cas S. Dejonckheere [1], Lea L. Friker [2,3], Thomas Zeyen [4], David Koch [1], Davide Scafa [1], Christina Leitzen [1], Mümtaz Köksal [1], Frederic Carsten Schmeel [5], Niklas Schäfer [4], Jennifer Landsberg [6], Michael Hölzel [2], Ulrich Herrlinger [4], Matthias Schneider [7], Frank A. Giordano [1,8] and Leonard Christopher Schmeel [1,*]

1 Department of Radiation Oncology, University Hospital Bonn, University of Bonn, 53127 Bonn, Germany
2 Institute of Experimental Oncology, University Hospital Bonn, University of Bonn, 53127 Bonn, Germany
3 Institute of Neuropathology, University Hospital Bonn, University of Bonn, 53127 Bonn, Germany
4 Division of Clinical Neuro-Oncology, Department of Neurology, University Hospital Bonn, 53127 Bonn, Germany
5 Department of Neuroradiology, University Hospital Bonn, 53127 Bonn, Germany
6 Department of Dermatology, University Hospital Bonn, 53127 Bonn, Germany
7 Department of Neurosurgery, University Hospital Bonn, University of Bonn, 53127 Bonn, Germany
8 Department of Radiation Oncology, University Medical Center Mannheim, University of Heidelberg, 68167 Mannheim, Germany
* Correspondence: christopher.schmeel@ukbonn.de

Abstract: Purpose: To determine the safety and outcome profile of five-fraction stereotactic radiotherapy (FSRT) for brain metastases (BM), either as a definitive or adjuvant treatment. Methods: We assessed clinical data of patients receiving five fractions of 7 Gy each (cumulative physical dose of 35 Gy) to BM or surgical cavities. The primary endpoints were toxicity and radiation necrosis (RN) rates. Secondary endpoints were 1-year cumulative local control rate (LCR) and estimated overall survival (OS). Results: A total of 36 eligible patients receiving FSRT to a total of 49 targets were identified and included. The median follow up was 9 (1.1–56.2) months. The median age was 64.5 (34–92) years, the median ECOG score was 1, and the median Diagnostic-Specific Graded Prognostic Assessment (DS-GPA) score was 2. Treatment was well tolerated and there were no grade 3 adverse events or higher. The overall RN rate was 14.3% and the median time to RN was 12.9 (1.8–23.8) months. RN occurrence was associated with immunotherapy, young age (≤45 years), and large PTV. The cumulative 1-year local control rate was 83.1% and the estimated median local progression free-survival was 18.8 months. The estimated median overall survival was 11 (1.1–56.2) months and significantly superior in those patients presenting with RN. Conclusions: FSRT with 5 × 7 Gy represents a feasible, safe, and efficient fast track approach of intensified FSRT with acceptable LC and comparable RN rates for both the adjuvant and definitive RT settings.

Keywords: FSRT; stereotactic radiotherapy; hypofractionation; brain metastases; radiation necrosis; toxicity

Citation: Layer, J.P.; Layer, K.; Sarria, G.R.; Röhner, F.; Dejonckheere, C.S.; Friker, L.L.; Zeyen, T.; Koch, D.; Scafa, D.; Leitzen, C.; et al. Five-Fraction Stereotactic Radiotherapy for Brain Metastases—A Retrospective Analysis. *Curr. Oncol.* **2023**, *30*, 1300–1313. https://doi.org/10.3390/curroncol30020101

Received: 15 December 2022
Revised: 10 January 2023
Accepted: 15 January 2023
Published: 17 January 2023

1. Introduction

Brain metastases (BM) occur syn- or metachronously in up to 40% of patients with solid tumors [1,2]. Due to improved diagnostic imaging and prompt detection, but also novel systemic therapies and thus extended survival, prevalence is continuously increasing [2–6]. Even though overall survival (OS) does not only depend on BM [7,8], local treatment is indicated to prevent neurological impairment. Ablative options include surgery and radiotherapy (RT). While larger symptomatic lesions commonly require a priori resection and adjuvant radiotherapy [9], solitary stereotactic radiotherapy (SRT) is sufficient for multiple smaller and/or asymptomatic BM [10–13]. However, no standardized radiotherapy

fractionation schema exists. Choosing an appropriate regimen depends on factors such as tumor localization, histology, and size [14,15]. Furthermore, dose prescription requires meticulous balance between desired local control and toxicity, such as radiation necrosis (RN) [16]. Due to its inferior toxicity profile, whole brain RT (WBRT) has been abandoned as a first-line strategy by most practitioners [11]. Standard SRT concepts either apply single-fraction stereotactic radiosurgery (SRS) or fractionated SRT (FSRT) with three [17] to twelve [18,19] fractions. Recent reports suggest the superior local control and reduced RN risk of FSRT [17,20] compared to SRS. Nonetheless, particularly in palliative situations, dose fractionation requires discretion to balance local control and side effects while avoiding potential overtreatment. Therefore, short-term treatment is generally preferred to improve quality of life (QOL) and limit patient visits and in-hospital time [21,22]. Among common FSRT concepts, five fractions of 5-6 Gy have been reported. The effectiveness and toxicity of 7 Gy single doses, comprising a slightly higher biologically effective dose and shortened treatment time, have not been well studied [23].

Even though initial prospective data suggest acceptable toxicity and comparable outcomes [24], this particular fractionation scheme appears somewhat outdated due to rather more protracted fractionation schemata. However, current RT techniques allow for both highly conformal planning and dose delivery, thereby possibly limiting toxicity [25]. Intensified hypofractionation strategies have subsequently gained reappraisal in the setting of oligometastatic solid tumors and are trending as the current treatment of choice for visceral and lymphatic metastases [26–28]. They are equally regarded as a minimal life disrupting approach in the principally curative setting [29].

The objective of this study was to report the safety and efficiency profile of using 5×7 Gy to treat BM in either an adjuvant or definitive setting.

2. Materials and Methods

2.1. Patient Selection

For this monocentric retrospective study, all consecutive patients with histologically confirmed solid tumors receiving either adjuvant or definitive FSRT with 5×7 Gy (cumulative physical dose 35 Gy, EQD2Gy = 49.6 Gy, BED = 59.5 Gy [α/β = 10 Gy]) to treat BM at University Hospital Bonn between 2016 and 2018 were assessed for eligibility. The inclusion criteria included age over 18 years, a pathology-confirmed malignant primary tumor, an ECOG score ≤ 2, and a total number of BM ≤ 10. The exclusion criteria were previous SRT of the same volume and simultaneous primary intracranial tumors.

2.2. Data Accrual

Clinical data were extracted from the clinical database and corresponding patient reports using SQL queries. The parameters of the treatments performed were extracted directly from the Eclipse planning system used for irradiation planning (Varian Eclipse 15.6, Varian Medical Systems, Palo Alto, CA, USA). Diagnostic-Specific Graded Prognostic Assessment (DS-GPA) [30] scores were calculated by standard procedures.

2.3. Fractionated Stereotactic Radiotherapy (FSRT)

Following interdisciplinary evaluation, linear accelerator-based FSRT was administered with intensity-modulated image-guided techniques, employing a 6 to 10 MV energy of 7-Gy single doses to a cumulative 35-Gy dose. The baseline magnetic resonance imaging (MRI) T1-Gd scan with 1 mm slice thickness was co-registered to planning computer tomography (CT) in all cases. The latter was acquired in a neutral supine position with patient fixation ensured by a thermoformed framed mask system. Gross tumor volume (GTV) was defined either as any T1-Gd contrast enhancing lesion or the resection cavity including any possible residual contrast enhancement. A 2 mm margin was added for the planning target volume (PTV) in both scenarios, as per institutional standards. Eclipse software was used for treatment planning and ExacTrac (Brainlab, München, Germany) was used for positioning matching. PTV coverage parameters included a D_{min} of 95% and

a $D_{100\%}$ < 99% of the prescription dose. Organ at risk D_{max} constraints were defined as 22.5 Gy for optic nerves, 22.5 Gy for the optic chiasm, and 31.0 Gy for the brain stem.

2.4. Follow-Up

Follow-up (FU) visits included a physical examination and MRI imaging. Adverse events (AE) were assessed and graded by clinicians according to the National Cancer Institute Common Terminology Criteria for Adverse Events (CTCAE), Version 5.0 [31]. Acute toxicities were considered AEs occurring within the first three months of FU, whereas late toxicities were defined as all AEs recorded at a later timepoint. MRI reporting was performed according to the RANO criteria [32] by board-certified neuroradiologists. In case of doubt, in regard to either clinical or radiological response assessment, the interdisciplinary neuro-oncology tumor board was consulted. Uncertain cases received additional advanced imaging, including dynamic susceptibility contrast (DSC) MRI and MR spectroscopy. RN was diagnosed when any of the following conditions applied: (1) after initial suspected progressive disease (PD), at least two follow-up MR imaging time points showed no sign of PD; (2) advanced MRI incorporating DSC and diffusion weighted imaging (DWI) was suggestive of RN; (3) RN was confirmed pathologically after surgery.

2.5. Study Endpoints

The primary endpoints were RN and neurological adverse event rates according to the CTCAE criteria. Secondary endpoints included estimated OS and cumulative 1-year local control rates (LCRs). OS was defined as the time interval between the first day of SRT and the date of either the last FU (censoring) or death. LC was defined as an absence of MRI-radiographic progression in the previously irradiated metastatic volume. In case of re-resection and a pathologic confirmation of RN, this event was not considered a progression. Patients that were lost to FU or deceased prior to radiographic progression were censored at the last FU time point.

2.6. Statistical Analyses

Data analysis was performed with GraphPad Prism 9 (GraphPad Software, San Diego, CA, USA). If not stated otherwise, the Mann–Whitney test was employed to determine significance. The Chi-square test was used to assess the significance of contingency tables. For statistical comparison of high and low variable values, the collective was divided into the respective groups by its median. The Log-rank test was used for statistical assessment of survival and control rates and is presented according to the Kaplan–Meier method. Results with $p < 0.05$ were considered statistically significant. Specifically, statistical tests and analyses were performed as indicated in the respective figure legends. Figures were generated using GraphPad Prism 9 and Adobe Illustrator 2021 (Adobe Inc., Mountain View, CA, USA).

3. Results

3.1. Patient Characteristics

A total of 36 patients receiving FSRT to a total of 49 BM or resection cavities were screened and included. The median age was 64.5 (34–92) years, the median ECOG score was 1 (0–2), and the median DS-GPA score was 2 (0–4). The most frequent histology was non-small cell lung cancer (NSCLC; 33.3%), followed by melanoma (22.2%) and breast cancer (11.1%). Additionally, 9 of 36 (25%) patients had been treated with immunotherapy before RT and 24.5% had previously received RT, with five of these cases being WBRT. A total of six patients (16.7%) had received sequential SRS to distant lesions, three patients (8.3%) had received sequential FSRT, and five patients (13.9%) had received sequential WBRT. Further patient characteristics are depicted in Table 1. The most common BM location was the frontal lobe (28.6%). Regarding treatment setting, 30.6% received adjuvant and 69.4% definitive treatment. Median FU was 9 months (range 1.1 to 56.2 months). More detailed results can be found in Table 2.

Table 1. Patient characteristics.

Patient Characteristic	*n* (%)	Median (Range)/Mean (±SD)
Total number	36 (100)	
Male	20 (55.6)	
Female	16 (44.4)	
Age (years)		64.5 (34–92)
Total number of brain lesions		3 (1–10)
ECOG performance score		1 (0–2)
0	16 (44.4)	
1	11 (30.6)	
2	9 (25)	
DS-GPA		2 (0–4)/2.1 (±0.98)
Histology		
NSCLC	12 (33.3)	
Melanoma	8 (22.2)	
Breast	4 (11.1)	
SCLC	3 (8.3)	
CRC	2 (5.6)	
Esophageal	1 (2.8)	
Pancreatic	1 (2.8)	
Thyroid	1 (2.8)	
Ovarian	1 (2.8)	
SCC	1 (2.8)	
RCC	1 (2.8)	
Sarcoma	1 (2.8)	
Immunotherapy		
Yes	9 (25)	
No	27 (75)	
Previous RT		
Yes	7 (19.4)	
No	29 (80.6)	
Sequential RT to distant lesions		
SRS	6 (16.7)	
FSRT	3 (8.3)	
WBRT	5 (13.9	

CRC: colorectal cancer; FSRT: fractionated stereotactic radiotherapy; NSCLC: non-small cell lung cancer; RCC: renal cell carcinoma; RT: radiotherapy; SCC: squamous cell carcinoma; SCLC: small cell lung cancer; SD: standard deviation, SRS: stereotactic radiosurgery; WBRT: whole brain radiotherapy.

Table 2. Lesion characteristics.

Lesion Characteristic	*n* (%)	Median (Range)/Mean (±SD)
Total number	49 (100)	
Location		
Frontal	14 (28.6)	
Occipital	9 (18.4)	
Cerebellum	9 (18.4)	
Temporal	7 (14.3)	
Parietal	7 (14.3)	
Central	3 (6.1)	
Treatment setting		
Definitive	34 (69.4)	
Adjuvant	15 (30.6)	
Immunotherapy		
Yes	12 (24.5)	
No	37 (75.5)	

Table 2. *Cont.*

Lesion Characteristic	*n* (%)	Median (Range)/Mean (±SD)
Previous RT		
Yes	12 (24.5)	
No	37 (75.5)	
Radiation necrosis		
Yes	7 (14.3)	
No	42 (85.3)	
PTV (cc)		13 (0.7–74.4)/15.8 (±14.4)
Conformity index		1.06 (0.21–3.5)/1.14 (±0.43)

PTV: planning target volume; RT: radiotherapy.

3.2. Treatment and Dosimetry

All patients completed treatment. The median treatment time was 5 (5–8) days. The mean PTV_{median} dose was 35.8 (±1.28) Gy. The median PTV was 13.0 cc (0.7–74.4), with 8.2 cc (0.7–28.8) for definitive FSRT and 25.4 cc (5.6–74.4) for adjuvant treatment ($p < 0.001$). The PTV was significantly larger in the adjuvant RT subgroup than in the definitive RT subgroup (Figure 1; $p < 0.001$). A median of 2 (1–5) planning fields was used for RT planning. The median conformity index was 1.1 (0.2–3.5) and did not differ significantly between definitive and adjuvant SRT ($p = 0.31$). The median $D_{0.1cc}$ was 37.4 Gy (36.0–42.1) and median brain $V_{50\%}$ was 40.9 cc (8.2–229.1). Further dosimetric features are described in Table 2 and Supplementary Figure S1.

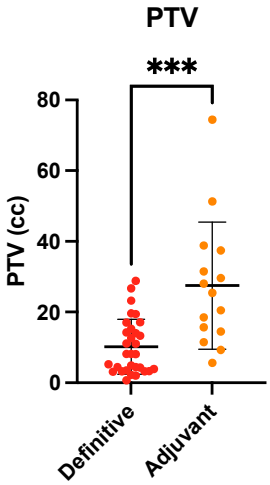

Figure 1. PTV of brain metastases undergoing definitive (red) vs. adjuvant (orange) SRT. *** $p < 0.001$, Mann–Whitney test. PTV: planning target volume; SRT: stereotactic radiotherapy.

3.3. Toxicity

A total of 54 events were recorded (Table 3). Of these, 44 were acute and 10 late adverse effects. In terms of grade, 75.9% were grade 1 and 24.1% grade 2 events. There were no grade 3 or higher adverse events (AE). The most common event was fatigue (30.6%), followed by cephalgia, nausea and vertigo (13.9%). The full list of AEs can be found in Table 4.

Table 3. Adverse events overview.

Grade	Acute Toxicity	Late Toxicity	Total
Grade 1	33 (61.1%)	7 (13%)	40 (74.1%)
Grade 2	11 (20.3%)	3 (5.6%)	14 (25.9%)
Grade 3+	0	0	0
Total	44 (81.4%)	10 (18.6%)	54 (100%)

Table 4. Full list of adverse events by grade.

Adverse Event	Grade 1	Grade 2	Grade 3+	Total
Fatigue	5	6	0	11 (30.6%)
Cephalgia	7	2	0	5 (13.9%)
Vertigo	4	1	0	5 (13.9%)
Nausea	5	0	0	5 (13.9%)
Alopecia	3	1	0	4 (11.1%)
Neuropathies	1	1	0	2 (5.6%)
Cognitive deterioration	2	0	0	2 (5.6%)
Fever	2	0	0	2 (5.6%)
Gait deterioration	2	0	0	2 (5.6%)
Skin reactions	2	0	0	2 (5.6%)
Mucositis	0	1	0	1 (2.8%)
Dysphagia	0	1	0	1 (2.8%)
Seizures	0	1	0	1 (2.8%)
Anemia	1	0	0	1 (2.8%)
Ataxia	1	0	0	1 (2.8%)
Cramps	1	0	0	1 (2.8%)
Gastrointestinal	1	0	0	1 (2.8%)
Tremor	1	0	0	1 (2.8%)
Viscerocranial pain	1	0	0	1 (2.8%)
Visional impairment	1	0	0	1 (2.8%)
	40	14	0	54 (100%)

RN was observed in seven targets (14.3%). Of these, one was pathologically confirmed. No patient had symptomatic RN $\geq$ grade 3. Four RN cases were located in the parietal lobe. Thus, 57.1% of patients with parietal metastatic localization developed RN during FU. The other RN cases occurred in the frontal, temporal, and occipital lobes. The tumor histology of RN patients was melanoma in three patients (RN incidence 37.5%), lung cancer (16.7%) in two patients, and breast and renal cancer in one patient. Median time to RN was 387 (53–726) days. Additionally, 57.1% of patients with RN had received immunotherapy (IT) prior to RT, and 71.4% of the patients had received SRT as an adjuvant treatment. A total of 75% of the RN patients receiving IT suffered from severe associated immunologic side effects (such as pancreatitis or hypophysitis) that eventually caused treatment interruption. Further characteristics of the RN patients can be found in Supplementary Table S1. At 53 (34–79) years, the median age of patients with RN was lower compared to the non-RN cohort (p = 0.05; Figure 2a). Patients $\leq$ 45 years of age harbored a significantly higher RN risk (p = 0.0003). The PTV significantly correlated with RN (25.4 vs. 11.1 cc; p = 0.04, Figure 2b). PTV $D_{0.1cc}$ was significantly lower in patients developing RN (p = 0.03), while conformity index, V_{10Gy}, and V_{20Gy} were not significantly different ($p > 0.05$). $V_{100\%}$ of the brain was significantly larger in RN developing lesions (p = 0.04; Figure 2c).

3.4. Survival and Control Outcomes

The cumulative 1-year local control rate (LCR) was 83.1%, while the 2-year LCR was 50%. After 3 years, the LCR was 41.7%. The median PFS was 18.8 months. The 1-year LCR was 100% for adjuvant RT vs. 70.8% for definitive RT. However, this control benefit for adjuvant RT was not significant (Figure 3a; p = 0.86), as it was restricted to the first 18 months of FU. The 2-year LCR was 43.8% in the adjuvant RT subgroup vs. 59% for the definitive RT subgroup. While local control was superior in the subgroup of FSRT with smaller PTV, this difference was not significant. There was no significant difference for LC in brain $V_{100\%}$ and $V_{50\%}$, but patients with lower PTV $D_{0.1cc}$ had a significantly higher LCR (Figure 3b; p = 0.037). RN was significantly associated with better local control (p = 0.04;

Figure 3c). Median local PFS for the subgroup of patients developing RN was 45.5 months, compared to 18.5 months for patients that did not develop RN.

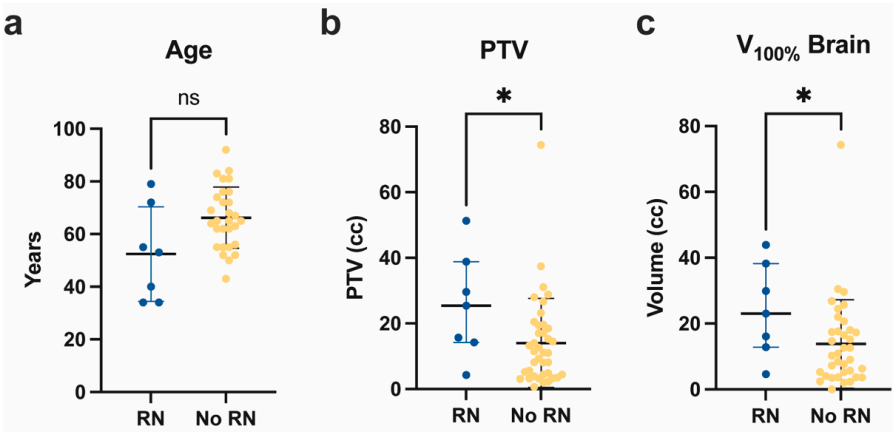

Figure 2. Characteristics of patients developing RN. Age (**a**), PTV of brain metastases (**b**), and brain $V_{100\%}$ (**c**) of patients developing (blue) vs. not developing (yellow) RN after SRT with 5 × 7 Gy. * $p < 0.05$; ns: not significant ($p \geq 0.05$); Mann–Whitney test. PTV: planning target volume; RN: radiation necrosis; SRT: stereotactic radiotherapy.

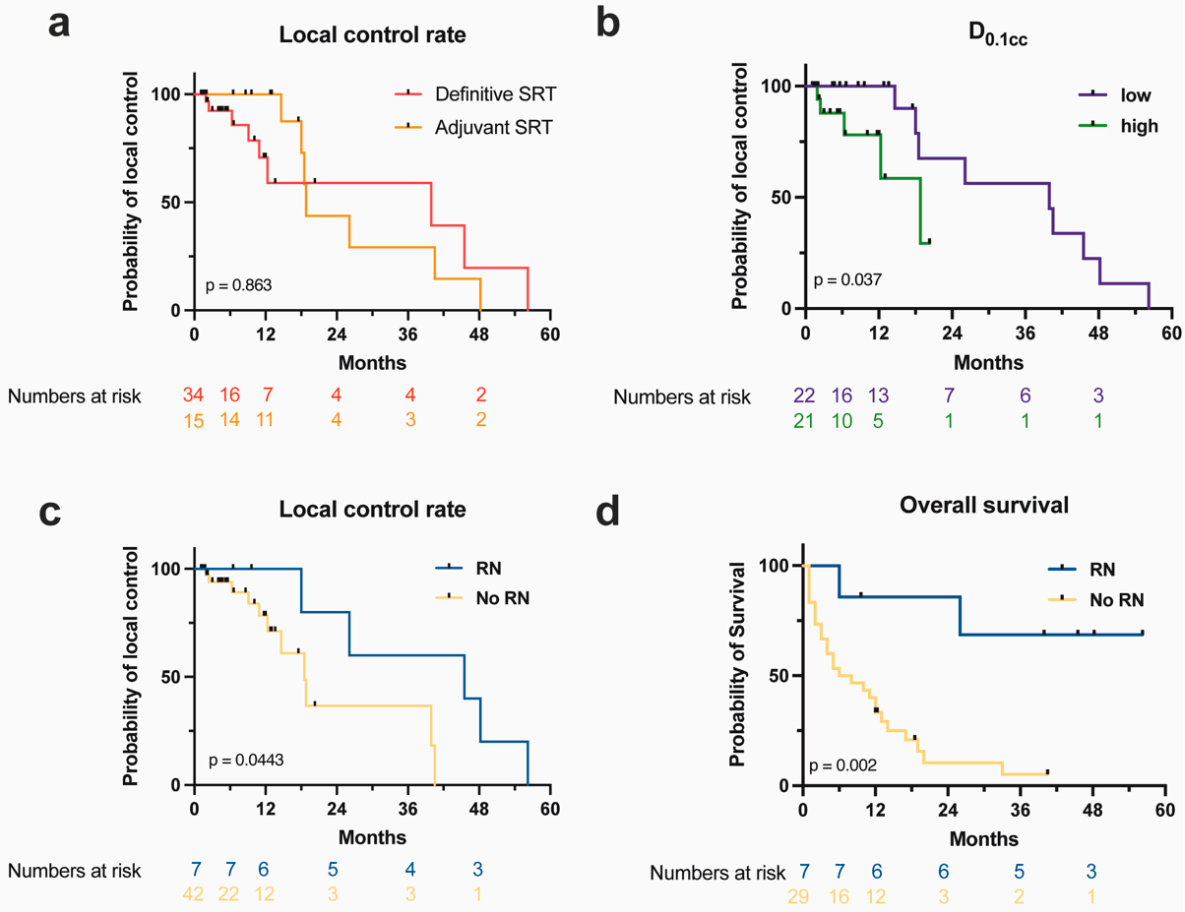

Figure 3. Local control and survival depending on patient characteristics. (**a**) Local control rate over time in months for definitive (red) and adjuvant (orange) SRT with 5 × 7 Gy (Log-rank test). (**b**) Local control rate over time in months for low (purple) vs. high (green) PTV $D_{0.1cc}$ in FSRT with 5 × 7 Gy (Log-rank test). (**c**,**d**) Local control rate (**c**) and overall survival (**d**) over time in months of patients developing (blue) vs. not developing (yellow) RN after SRT with 5 × 7 Gy (Log-rank test). PTV: planning target volume; RN: radiation necrosis; SRT: stereotactic radiotherapy.

Only one patient (2.8%) died due to radiology-confirmed local intracerebral progression, whereas 19.4% died of systemic progression. In addition, 53.1% of patients developed distant cerebral metastases and 63.3% progressed systemically, as confirmed by radiologic FU imaging. Median OS was 11 months, and OS was significantly superior in the RN subgroup (39.9 months) compared to the non-RN subgroup (7.0 months) (Figure 3d; $p = 0.023$).

4. Discussion

Interdisciplinary treatment of BM remains challenging and requires individualized shared decision making by the patients and their involved specialists. Given a continuously aging population with longer life expectancy, improved diagnostic tools, technical progress, and the rise of targeted therapies, the incidence of BM is likely to continue to increase [2,6]. However, similar to patients in our series, patient mortality is mostly due to systemic progression rather than local intracerebral progression [7]. Therefore, achieving and maintaining local control of brain metastases through RT is of utmost importance for symptom control and improved quality of life [33], despite the fact that it may not relevantly prolong OS [34]. Achieving sufficient local control and avoiding excessive toxicity requires careful therapeutic balancing. While single-fraction SRS has been widely adopted and likely has the highest biological effective dose (BED), either the location or volume of BM may necessitate fractionated alternatives [17,20]. Larger brain metastases were shown to benefit from FSRT with a relative reduction in RN rate, yielding a similar or even better LCR than SRS [35].

A systematic meta-analysis of eleven studies reporting a 6-month 80% LCR after SRT for BM recommended, in referral to a single fraction of 20 Gy, a minimum EQD2 dose of 40 Gy using an α/β of 12 Gy [36]. However, among the various available options, optimal SRT dosing and fractionation for BM remains controversial with no general consensus. Emerging evidence suggests that FSRT for BM improves patients' QOL [11] and leads to both treatment and in-patient times being as short as possible [21,22]. This is of particular importance in BM patients with dismal prognosis and neurological deficits impairing individual mobility. For the same reasons, WBRT in BM patients ineligible for SRT has been questioned by the results of the QUARTZ trial [37]. Besides patient-centered beneficial aspects, intensified hypofractionation may also translate into socioeconomic cost reductions [38–40] while potentially allowing increased patient numbers and timely treatment access. The ongoing COVID-19 pandemic, with dynamically shifting and hardly predictable short-term patient numbers [41], has revealed the necessity of optimizing resources and time with the aim of reducing unnecessary harmful patient exposure to healthcare facilities [42]. This is the first detailed report on a fast track five-fraction SRT approach covering toxicity and, particularly, RN rate while also including dosimetry and outcome parameters.

Our data provide preliminary evidence on five-fraction SRT as a safe and feasible approach with both optimal adjuvant and definitive outcomes. Previously reported LCRs vary significantly and merely a handful of series have reported on this (Table 5) [24,43–46]. Our results resemble those cited above. Nevertheless, in comparison to other fractionation schemes (Table 6) [12,16–18,47–56] and intraoperative RT (IORT) [57], the LCR appears slightly weaker in our series, although it yields reasonable overall local control. This may be due to the specific composition of the patient cohort included. While melanoma was relatively overrepresented in our collective (22.2%), levels of NSCLC (33.3%) and breast cancer (11.1%) were below the average. The median age of 64.5 years was relatively high compared to other studies and the median GPA of 2 was relatively low. This rather unfavorable prognostic setting might have led to lower OS and a relevant number of lost-to-FU cases, which partially explains the pronounced drop in the 2-year LCR. The crossover in the LCR between definitive and adjuvant RT in the second year of FU may be explained by the significantly larger PTVs treated in the adjuvant setting, which might also explain the improved LCR with lower $D_{0.1cc}$ as larger PTVs require higher central doses.

Table 5. Studies on the FSRT of brain metastases with 5 × 7 Gy.

Authors	Year	Dose (Gy)	RT Setting	BM Size (Median)	RT Technique	Lesions	Histology	1y-LCR (%)	2y-LCR (%)	RN Rate (%)	Median Time to RN (Months)	Toxicity
Current series	2022	7/35	both	13 cc	Conventional FSRT	49	mixed	83.1	50	14.3	12.7	0% G3+
Di Perri et. al. [43]	2020	7/35	both	11 cc	Cyberknife FSRT	89	mixed	62.5	n. a.	>40	n. a.	n. a.
Ernst-Stecken et al. [24]	2006	7/35	definitive	13 cc	Conventional FSRT	72	mixed	76	n. a.	n. a.	n. a.	2% G3+
Jeong et al. [44]	2015	7/35	definitive	17.6 cc	Cyberknife FSRT	38	mixed	87	65.2	15.8	10.5	n. a.
Koide et al. [45]	2019	7/35	definitive	7.2 cc	Conventional FSRT	58	mixed	64.7	n. a.	3.5	n. a.	0% G3+
Mengue et al. [46]	2020	7/35	both	2.3 cm	Cyberknife FSRT	158	mixed	<80	<60	NA	n. a.	n. a.

BM: brain metastases; FSRT: fractionated stereotactic radiotherapy; LCR: local control rate; NA: not available; n. a.: not assessed; RN: radiation necrosis; RT: radiotherapy.

Table 6. Studies on the FSRT of brain metastases with other fractionation schemes.

Authors	Year	Dose (Gy)	RT Setting	BM Size (Median)	RT Technique	Lesions	Histology	1y-LCR (%)	2y-LCR (%)	RN Rate (%)	Median Time to RN (Months)	Toxicity
Brown et al. [47]	2017	12–20	adjuvant	<3 cm	Conventional SRS	93	mixed	61.8	n. a.	n. a.	n. a.	39% G3+
Choi et al. [48]	2021	Median 20	definitive	0.5 cc	Conventional SRS	311	melanoma	n. a.	n. a.	6.1	10.2	n. a.
Doré et al. [49]	2017	7.7/23.3	adjuvant	11.4 cc	Conventional FSRT	95	mixed	84	n. a.	20.6	15	n. a.
Eitz et al. [50]	2020	Median 6/30	adjuvant	23.9 cc	Conventional FSRT	581	mixed	84	75	8.6	13.1	6.9% G3
Fokas et al. [18]	2012	5/35	both	2 cc	Conventional FSRT	61	mixed	75	n. a.	1.6	n. a.	2% G3+
Jhaveri et al. [51]	2019	5–7/21–35	adjuvant	15/20 cc	Conventional FSRT	139	mixed	84.8	n. a.	21.1	n. a.	n. a.
Kohutek et al. [16]	2015	15–22	definitive	1.1 cm	Conventional SRS	271	mixed	n. a.	n. a.	25.8	10.7	n. a.
Lehrer et al. [52]	2022	Median 20	definitive	1.6 cc	Conventional SRS	4,536	mixed	90.5	n. a.	9.8	n. a.	n. a.
Lischalk et al. [53]	2015	6–8/30–40	definitive	5.6 cc	Cyberknife FSRT	13	NSCLC	90	90	15.4	11	15% G3+
Minniti et al. [12]	2011	15–20	definitive	1.9 cc	Conventional SRS	310	mixed	92	84	24	11	5.8% G3+
Minniti et al. [54]	2014	9–12/27–36	definitive	16.4 cc	Conventional FSRT	171	mixed	88	72	18	12	4% G3+
Minniti et al. [17]	2016	9/27	definitive	17.9 cc	Conventional FSRT	138	mixed	91	n. a.	8	12	n. a.
	2016	15–18	definitive	12.2 cc	Conventional SRS	151	mixed	77	n. a.	20	10	n. a.
Piras et al. [55]	2022	6–8/30–40	definitive	1.8 cc	Conventional FSRT	57	mixed	n. a.	n. a.	2.4	9	7% G2 0% G3
Wegner et al. [56]	2015	8/24	definitive	15.6 cc	Conventional FSRT	36	mixed	63	n. a.	0	n. d.	0% G3

BM: brain metastases; FSRT: fractionated stereotactic radiotherapy; LCR: local control rate; NA: not available; n. a.: not assessed; NSCLC: non-small cell lung cancer; RN: radiation necrosis; RT: radiotherapy; SRS: stereotactic radiosurgery.

Notably, no grade 3 AEs occurred under or after FSRT. Compacted treatment time and dose escalation were not associated with a higher risk of AEs compared to more commonly applied schemes. This holds not only true for acute toxicity and late toxicity, but also for the anticipated RN risk. Even though SRS was associated with a higher risk of RN in previous series [16], we did not observe an increased RN rate or any grade 3 or higher clinical appearance in this patient collective with intensified hypofractionation. While the heterogeneity of our collective in terms of tumor entities and treatment parameters may contribute to RN development, the RN rate reported is in line with several other studies on other fractionation schemes that reported rates of up to 18% [54] in the definitive setting and up to 21.1% [51] in the adjuvant setting (Table 6). Similar five-fraction studies by Jeong et al. and Lischalk et al. previously reported RN rates of 15.8% [44] and 20% [53], respectively. Of note, 50% of these latter patients had received a prescribed total dose of 40 Gy and both RN patients requiring surgery had also received a maximum dose of more than 41 Gy, whereas in this collective only three lesions (6.1%) reached this dose level. Comparable with our results, an increased risk of RN with increasing tumor volumes has been reported in previous studies [16,49,51,54]. Additionally, the time to occurrence of RN is in line with the literature [50], though there is inconsistent data regarding the anatomic brain regions at particular risk of RN. Accordingly, despite there being reports of high RN incidence in the parietal lobe [12], others have conflictingly reported on increased RN rates in different brain sections [48,58]. Increased RN rates among melanoma BM are most likely due to more frequently applied IT, which was previously identified as an independent risk factor for RN [44]. As patients receiving targeted and pro-immunogenic therapies were underrepresented in earlier preceding studies, the comparable RN rate described here is even more compelling. Notably, 75% of the RN patients receiving IT in this study discontinued treatment due to intolerable immunologic side effects. Larger PTV size and lower $D_{0.1cc}$ were associated with RN, while other dosimetric parameters were not related to either RN or LCR. This implies that immune therapy and lesion volume are relatively more relevant than other dosimetric factors for RN. While the longer OS of younger patients may contribute to the higher incidence of RN observed in this series, the contribution of immunological factors cannot be ruled out. Even though the exact mechanisms remain unknown, the link between irradiation and vascular or glial damage promoting a proinflammatory tumor microenvironment (TME) with subsequent activation of microglia, macrophages, and CD3+ T-cells has been established [59,60]. FSRT was shown to induce tumor immunogenicity [61,62]; furthermore, RN after SRS seems to be associated with improved OS [52]. Favoring an immunologically 'hot' TME may induce both favorable and unfavorable side effects, such as tumoricidal immune cell activity and RN. Therefore, despite an overall good clinical outcome, careful patient selection and close FU is suggested in order to avoid increased toxicity.

Although this study is the most comprehensive manuscript to date reporting on 5 × 7 Gy FSRT, it carries several limitations. Data were collected retrospectively from a rather heterogeneous patient collective undergoing adjuvant and definitive RT for several different entities. The fractionation regimen was at the physicians' discretion, and for most patients the decision between FSRT and SRS was based on lesion volumes. Other reasons for FSRT included glucocorticoid intolerance of any kind (i.e., allergic reactions, gastric or duodenal ulcers, glaucoma, uncontrolled diabetes, sleep disturbances), which were routinely administered preceding SRS in our clinic during the study period. Low average performance and prognostic scores caused detriments in FU and PFS, and thus rather poor OS outcomes. Taken together, patient selection bias might have led to discordant outcomes when compared to the available literature. However, this collective represents an average patient population at a German university hospital and reflects a real-world situation instead of a carefully selected study population. Prospective randomized trials are needed to bring further insight into the optimal fractionation scheme for BM. The first randomized controlled phase III trial investigating SRS vs. FSRT for BM with a diameter of 2 cm to 4 cm was recently initiated [19]. Further studies that incorporate accelerated,

intensified hypofractionated fractionation schemes are warranted. Additionally, the best treatment sequencing has not been defined yet. Recently, an NRG study protocol initiated recruiting, seeking to determine the best sequencing between pre- or post-operative SRS for BM (NCT05438212). The impact of short-term interventions on QOL will be the main focus of future developments in FSRT.

5. Conclusions

Five fractions of 7 Gy each appears to be a safe and effective alternative to more protracted fractionation schemes. Intensified FSRT might yield acceptable local control and toxicity rates in both the adjuvant and definitive RT settings while also maintaining short treatment times. These hypothesis-generating findings should be further studied within a clinical trial.

Supplementary Materials: The following supporting information can be downloaded at: https://www.mdpi.com/article/10.3390/curroncol30020101/s1, Figure S1: Dosimetric specifications of patients; Table S1: Characteristics of patients with radiation necrosis.

Author Contributions: This study was conceptualized by J.P.L. and L.C.S. All authors contributed to the study design. Material preparation and data collection were performed by J.P.L., K.L. and L.C.S. Analysis was performed by J.P.L. M.H. and F.A.G. provided funding and resources. The first draft of the manuscript was written by J.P.L. G.R.S. and L.C.S. reviewed and edited the data and manuscript. All authors commented on previous versions of the manuscript. All authors have read and agreed to the published version of the manuscript.

Funding: J.P.L. was supported by a grant from Novartis Stiftung für therapeutische Forschung (foundation for therapeutic research).

Institutional Review Board Statement: This study was conducted in accordance with the Declaration of Helsinki and the proceedings were approved by the Institutional Review Board of the University Hospital Bonn on 8 February 2022 (057/22).

Informed Consent Statement: Not applicable due to the retrospective character of this study.

Data Availability Statement: The data presented in this study are available in this article (and Supplementary Materials).

Conflicts of Interest: The authors declare that the article content was composed in the absence of any personal, commercial, or financial relationship that could be construed as a potential conflict of interest.

References

1. Nayak, L.; Lee, E.Q.; Wen, P.Y. Epidemiology of Brain Metastases. *Curr. Oncol. Rep.* **2012**, *14*, 48–54. [CrossRef] [PubMed]
2. Cagney, D.N.; Martin, A.M.; Catalano, P.J.; Redig, A.J.; Lin, N.U.; Lee, E.Q.; Wen, P.Y.; Dunn, I.F.; Bi, W.L.; Weiss, S.E.; et al. Incidence and Prognosis of Patients with Brain Metastases at Diagnosis of Systemic Malignancy: A Population-Based Study. *Neuro Oncol.* **2017**, *19*, 1511–1521. [CrossRef] [PubMed]
3. Johnson, J.D.; Young, B. Demographics of Brain Metastasis. *Neurosurg. Clin. N. Am.* **1996**, *7*, 337–344. [CrossRef] [PubMed]
4. Sundermeyer, M.L.; Meropol, N.J.; Rogatko, A.; Wang, H.; Cohen, S.J. Changing Patterns of Bone and Brain Metastases in Patients with Colorectal Cancer. *Clin. Color. Cancer* **2005**, *5*, 108–113. [CrossRef] [PubMed]
5. Kuksis, M.; Gao, Y.; Tran, W.; Hoey, C.; Kiss, A.; Komorowski, A.S.; Dhaliwal, A.J.; Sahgal, A.; Das, S.; Chan, K.K.; et al. The Incidence of Brain Metastases among Patients with Metastatic Breast Cancer: A Systematic Review and Meta-Analysis. *Neuro Oncol.* **2021**, *23*, 894–904. [CrossRef]
6. Lamba, N.; Wen, P.Y.; Aizer, A.A. Epidemiology of Brain Metastases and Leptomeningeal Disease. *Neuro Oncol.* **2021**, *23*, 1447–1456. [CrossRef]
7. Yamamoto, M.; Sato, Y.; Serizawa, T.; Kawabe, T.; Higuchi, Y.; Nagano, O.; Barfod, B.E.; Ono, J.; Kasuya, H.; Urakawa, Y. Subclassification of Recursive Partitioning Analysis Class II Patients With Brain Metastases Treated Radiosurgically. *Int. J. Radiat. Oncol. Biol. Phys.* **2012**, *83*, 1399–1405. [CrossRef]
8. Nieder, C.; Stanisavljevic, L.; Aanes, S.G.; Mannsåker, B.; Haukland, E.C. 30-Day Mortality in Patients Treated for Brain Metastases: Extracranial Causes Dominate. *Radiat. Oncol.* **2022**, *17*, 92. [CrossRef]

9. Mahajan, A.; Ahmed, S.; McAleer, M.F.; Weinberg, J.S.; Li, J.; Brown, P.; Settle, S.; Prabhu, S.S.; Lang, F.F.; Levine, N.; et al. Post-Operative Stereotactic Radiosurgery versus Observation for Completely Resected Brain Metastases: A Single-Centre, Randomised, Controlled, Phase 3 Trial. *Lancet Oncol.* **2017**, *18*, 1040–1048. [CrossRef]
10. Chang, E.L.; Wefel, J.S.; Hess, K.R.; Allen, P.K.; Lang, F.F.; Kornguth, D.G.; Arbuckle, R.B.; Swint, J.M.; Shiu, A.S.; Maor, M.H.; et al. Neurocognition in Patients with Brain Metastases Treated with Radiosurgery or Radiosurgery plus Whole-Brain Irradiation: A Randomised Controlled Trial. *Lancet Oncol.* **2009**, *10*, 1037–1044. [CrossRef]
11. Kocher, M.; Soffietti, R.; Abacioglu, U.; Villà, S.; Fauchon, F.; Baumert, B.G.; Fariselli, L.; Tzuk-Shina, T.; Kortmann, R.-D.; Carrie, C.; et al. Adjuvant Whole-Brain Radiotherapy Versus Observation After Radiosurgery or Surgical Resection of One to Three Cerebral Metastases: Results of the EORTC 22952-26001 Study. *JCO J. Clin. Oncol.* **2011**, *29*, 134–141. [CrossRef] [PubMed]
12. Minniti, G.; Clarke, E.; Lanzetta, G.; Osti, M.F.; Trasimeni, G.; Bozzao, A.; Romano, A.; Enrici, R.M. Stereotactic Radiosurgery for Brain Metastases: Analysis of Outcome and Risk of Brain Radionecrosis. *Radiat. Oncol.* **2011**, *6*, 48. [CrossRef]
13. Yamamoto, M.; Serizawa, T.; Shuto, T.; Akabane, A.; Higuchi, Y.; Kawagishi, J.; Yamanaka, K.; Sato, Y.; Jokura, H.; Yomo, S.; et al. Stereotactic Radiosurgery for Patients with Multiple Brain Metastases (JLGK0901): A Multi-Institutional Prospective Observational Study. *Lancet Oncol.* **2014**, *15*, 387–395. [CrossRef] [PubMed]
14. Kim, Y.-J.; Cho, K.H.; Kim, J.-Y.; Lim, Y.K.; Min, H.S.; Lee, S.H.; Kim, H.J.; Gwak, H.S.; Yoo, H.; Lee, S.H. Single-Dose Versus Fractionated Stereotactic Radiotherapy for Brain Metastases. *Int. J. Radiat. Oncol. Biol. Phys.* **2011**, *81*, 483–489. [CrossRef]
15. Baliga, S.; Garg, M.K.; Fox, J.; Kalnicki, S.; Lasala, P.A.; Welch, M.R.; Tomé, W.A.; Ohri, N. Fractionated Stereotactic Radiation Therapy for Brain Metastases: A Systematic Review with Tumour Control Probability Modelling. *Br. J. Radiol.* **2017**, *90*, 20160666. [CrossRef]
16. Kohutek, Z.A.; Yamada, Y.; Chan, T.A.; Brennan, C.W.; Tabar, V.; Gutin, P.H.; Jonathan Yang, T.; Rosenblum, M.K.; Ballangrud, Å.; Young, R.J.; et al. Long-Term Risk of Radionecrosis and Imaging Changes after Stereotactic Radiosurgery for Brain Metastases. *J. Neurooncol.* **2015**, *125*, 149–156. [CrossRef]
17. Minniti, G.; Scaringi, C.; Paolini, S.; Lanzetta, G.; Romano, A.; Cicone, F.; Osti, M.; Enrici, R.M.; Esposito, V. Single-Fraction Versus Multifraction (3 × 9 Gy) Stereotactic Radiosurgery for Large (>2 Cm) Brain Metastases: A Comparative Analysis of Local Control and Risk of Radiation-Induced Brain Necrosis. *Int. J. Radiat. Oncol. Biol. Phys.* **2016**, *95*, 1142–1148. [CrossRef] [PubMed]
18. Fokas, E.; Henzel, M.; Surber, G.; Kleinert, G.; Hamm, K.; Engenhart-Cabillic, R. Stereotactic Radiosurgery and Fractionated Stereotactic Radiotherapy: Comparison of Efficacy and Toxicity in 260 Patients with Brain Metastases. *J. Neurooncol.* **2012**, *109*, 91–98. [CrossRef]
19. Putz, F.; Pirschel, W.; Fietkau, R. FSRT-Trial: Erste Phase-III-Studie zum Vergleich fraktionierte stereotaktische Radiotherapie (FSRT) versus Einzeitradiochirurgie (SRS) bei Hirnmetastasen. *Forum* **2022**, *37*, 241–245. [CrossRef]
20. Putz, F.; Weissmann, T.; Oft, D.; Schmidt, M.A.; Roesch, J.; Siavooshhaghighi, H.; Filimonova, I.; Schmitter, C.; Mengling, V.; Bert, C.; et al. FSRT vs. SRS in Brain Metastases-Differences in Local Control and Radiation Necrosis-A Volumetric Study. *Front. Oncol.* **2020**, *10*, 559193. [CrossRef]
21. Lutz, S.T.; Chow, E.L.; Hartsell, W.F.; Konski, A.A. A Review of Hypofractionated Palliative Radiotherapy. *Cancer* **2007**, *109*, 1462–1470. [CrossRef] [PubMed]
22. Gripp, S.; Mjartan, S.; Boelke, E.; Willers, R. Palliative Radiotherapy Tailored to Life Expectancy in End-Stage Cancer Patients: Reality or Myth? *Cancer* **2010**, *116*, 3251–3256. [CrossRef] [PubMed]
23. Gondi, V.; Bauman, G.; Bradfield, L.; Burri, S.H.; Cabrera, A.R.; Cunningham, D.A.; Eaton, B.R.; Hattangadi-Gluth, J.A.; Kim, M.M.; Kotecha, R.; et al. Radiation Therapy for Brain Metastases: An ASTRO Clinical Practice Guideline. *Pract. Radiat. Oncol.* **2022**, *12*, 265–282. [CrossRef]
24. Ernst-Stecken, A.; Ganslandt, O.; Lambrecht, U.; Sauer, R.; Grabenbauer, G. Phase II Trial of Hypofractionated Stereotactic Radiotherapy for Brain Metastases: Results and Toxicity. *Radiother. Oncol.* **2006**, *81*, 18–24. [CrossRef] [PubMed]
25. Vergalasova, I.; Liu, H.; Alonso-Basanta, M.; Dong, L.; Li, J.; Nie, K.; Shi, W.; Teo, B.-K.K.; Yu, Y.; Yue, N.J.; et al. Multi-Institutional Dosimetric Evaluation of Modern Day Stereotactic Radiosurgery (SRS) Treatment Options for Multiple Brain Metastases. *Front. Oncol.* **2019**, *9*, 483. [CrossRef] [PubMed]
26. Iyengar, P.; Wardak, Z.; Gerber, D.E.; Tumati, V.; Ahn, C.; Hughes, R.S.; Dowell, J.E.; Cheedella, N.; Nedzi, L.; Westover, K.D.; et al. Consolidative Radiotherapy for Limited Metastatic Non–Small-Cell Lung Cancer: A Phase 2 Randomized Clinical Trial. *JAMA Oncol.* **2018**, *4*, e173501. [CrossRef]
27. Palma, D.A.; Olson, R.; Harrow, S.; Gaede, S.; Louie, A.V.; Haasbeek, C.; Mulroy, L.; Lock, M.; Rodrigues, G.B.; Yaremko, B.P.; et al. Stereotactic Ablative Radiotherapy versus Standard of Care Palliative Treatment in Patients with Oligometastatic Cancers (SABR-COMET): A Randomised, Phase 2, Open-Label Trial. *Lancet* **2019**, *393*, 2051–2058. [CrossRef]
28. Palma, D.A.; Olson, R.; Harrow, S.; Gaede, S.; Louie, A.V.; Haasbeek, C.; Mulroy, L.; Lock, M.; Rodrigues, G.B.; Yaremko, B.P.; et al. Stereotactic Ablative Radiotherapy for the Comprehensive Treatment of Oligometastatic Cancers: Long-Term Results of the SABR-COMET Phase II Randomized Trial. *J. Clin. Oncol.* **2020**, *38*, 2830–2838. [CrossRef]
29. Musunuru, H.B.; Quon, H.; Davidson, M.; Cheung, P.; Zhang, L.; D'Alimonte, L.; Deabreu, A.; Mamedov, A.; Loblaw, A. Dose-Escalation of Five-Fraction SABR in Prostate Cancer: Toxicity Comparison of Two Prospective Trials. *Radiother. Oncol.* **2016**, *118*, 112–117. [CrossRef]

30. Sperduto, P.W.; Kased, N.; Roberge, D.; Xu, Z.; Shanley, R.; Luo, X.; Sneed, P.K.; Chao, S.T.; Weil, R.J.; Suh, J.; et al. Summary Report on the Graded Prognostic Assessment: An Accurate and Facile Diagnosis-Specific Tool to Estimate Survival for Patients With Brain Metastases. *JCO J. Clin. Oncol.* **2012**, *30*, 419–425. [CrossRef]
31. Common Terminology Criteria for Adverse Events (CTCAE) Version 5.0 n.d. Available online: https://ctep.cancer.gov/protocoldevelopment/electronic_applications/docs/ctcae_v5_quick_reference_5x7.pdf (accessed on 10 December 2021).
32. Lin, N.U.; Lee, E.Q.; Aoyama, H.; Barani, I.J.; Barboriak, D.P.; Baumert, B.G.; Bendszus, M.; Brown, P.D.; Camidge, D.R.; Chang, S.M.; et al. Response Assessment Criteria for Brain Metastases: Proposal from the RANO Group. *Lancet Oncol.* **2015**, *16*, e270–e278. [CrossRef]
33. Steinmann, D.; Vordermark, D.; Gerstenberg, W.; Aschoff, R.; Gharbi, N.; Müller, A.; Schäfer, C.; Theodorou, M.; Wypior, H.-J.; Geinitz, H.; et al. Quality of Life in Patients with Limited (1–3) Brain Metastases Undergoing Stereotactic or Whole Brain Radiotherapy: A Prospective Study of the DEGRO QoL Working Group. *Strahlenther. Onkol.* **2020**, *196*, 48–57. [CrossRef]
34. Park, K.; Bae, G.H.; Kim, W.K.; Yoo, C.-J.; Park, C.W.; Kim, S.-K.; Cha, J.; Kim, J.W.; Jung, J. Radiotherapy for Brain Metastasis and Long-Term Survival. *Sci. Rep.* **2021**, *11*, 8046. [CrossRef]
35. Lehrer, E.J.; Peterson, J.L.; Zaorsky, N.G.; Brown, P.D.; Sahgal, A.; Chiang, V.L.; Chao, S.T.; Sheehan, J.P.; Trifiletti, D.M. Single versus Multifraction Stereotactic Radiosurgery for Large Brain Metastases: An International Meta-Analysis of 24 Trials. *Int. J. Radiat. Oncol. Biol. Phys.* **2019**, *103*, 618–630. [CrossRef] [PubMed]
36. Wiggenraad, R.; Kanter, A.V.; Kal, H.B.; Taphoorn, M.; Vissers, T.; Struikmans, H. Dose–Effect Relation in Stereotactic Radiotherapy for Brain Metastases. A Systematic Review. *Radiother. Oncol.* **2011**, *98*, 292–297. [CrossRef]
37. Mulvenna, P.; Nankivell, M.; Barton, R.; Faivre-Finn, C.; Wilson, P.; McColl, E.; Moore, B.; Brisbane, I.; Ardron, D.; Holt, T.; et al. Dexamethasone and Supportive Care with or without Whole Brain Radiotherapy in Treating Patients with Non-Small Cell Lung Cancer with Brain Metastases Unsuitable for Resection or Stereotactic Radiotherapy (QUARTZ): Results from a Phase 3, Non-Inferiority, Randomised Trial. *Lancet* **2016**, *388*, 2004–2014. [CrossRef] [PubMed]
38. Manning, M.A.; Cardinale, R.M.; Benedict, S.H.; Kavanagh, B.D.; Zwicker, R.D.; Amir, C.; Broaddus, W.C. Hypofractionated Stereotactic Radiotherapy as an Alternative to Radiosurgery for the Treatment of Patients with Brain Metastases. *Int. J. Radiat. Oncol. Biol. Phys.* **2000**, *47*, 603–608. [CrossRef] [PubMed]
39. Hunter, D.; Mauldon, E.; Anderson, N. Cost-Containment in Hypofractionated Radiation Therapy: A Literature Review. *J. Med. Radiat. Sci.* **2018**, *65*, 148–157. [CrossRef]
40. Scarpelli, D.B.; Fatheree, S.; Jaboin, J.J. Cost-Effectiveness of Stereotactic Radiosurgery and Stereotactic Body Radiation Therapy in Treating Brain Metastases. *Pract. Radiat. Oncol.* **2021**, *11*, 488–490. [CrossRef]
41. Medenwald, D.; Brunner, T.; Christiansen, H.; Kisser, U.; Mansoorian, S.; Vordermark, D.; Prokosch, H.-U.; Seuchter, S.A.; Kapsner, L.A.; Our MII research group. Shift of Radiotherapy Use during the First Wave of the COVID-19 Pandemic? An Analysis of German Inpatient Data. *Strahlenther. Onkol.* **2022**, *198*, 334–345. [CrossRef] [PubMed]
42. Akuamoa-Boateng, D.; Wegen, S.; Ferdinandus, J.; Marksteder, R.; Baues, C.; Marnitz, S. Managing Patient Flows in Radiation Oncology during the COVID-19 Pandemic: Reworking Existing Treatment Designs to Prevent Infections at a German Hot Spot Area University Hospital. *Strahlenther. Onkol.* **2020**, *196*, 1080–1085. [CrossRef] [PubMed]
43. Di Perri, D.; Tanguy, R.; Malet, C.; Robert, A.; Sunyach, M.-P. Risk of Radiation Necrosis after Hypofractionated Stereotactic Radiotherapy (HFSRT) for Brain Metastases: A Single Center Retrospective Study. *J. Neurooncol.* **2020**, *149*, 447–453. [CrossRef] [PubMed]
44. Jeong, W.J.; Park, J.H.; Lee, E.J.; Kim, J.H.; Kim, C.J.; Cho, Y.H. Efficacy and Safety of Fractionated Stereotactic Radiosurgery for Large Brain Metastases. *J. Korean Neurosurg. Soc.* **2015**, *58*, 217–224. [CrossRef] [PubMed]
45. Koide, Y.; Tomita, N.; Adachi, S.; Tanaka, H.; Tachibana, H.; Kodaira, T. Retrospective Analysis of Hypofractionated Stereotactic Radiotherapy for Tumors Larger than 2 Cm. *Nagoya J. Med. Sci.* **2019**, *81*, 397–406. [CrossRef]
46. Mengue, L.; Bertaut, A.; Ngo Mbus, L.; Doré, M.; Ayadi, M.; Clément-Colmou, K.; Claude, L.; Carrie, C.; Laude, C.; Tanguy, R.; et al. Brain Metastases Treated with Hypofractionated Stereotactic Radiotherapy: 8 Years Experience after Cyberknife Installation. *Radiat. Oncol.* **2020**, *15*, 82. [CrossRef]
47. Brown, P.D.; Ballman, K.V.; Cerhan, J.H.; Anderson, S.K.; Carrero, X.W.; Whitton, A.C.; Greenspoon, J.; Parney, I.F.; Laack, N.N.I.; Ashman, J.B.; et al. Postoperative Stereotactic Radiosurgery Compared with Whole Brain Radiotherapy for Resected Metastatic Brain Disease (NCCTG N107C/CEC·3): A Multicentre, Randomised, Controlled, Phase 3 Trial. *Lancet Oncol.* **2017**, *18*, 1049–1060. [CrossRef] [PubMed]
48. Choi, S.; Hong, A.; Wang, T.; Lo, S.; Chen, B.; Silva, I.; Kapoor, R.; Hsiao, E.; Fogarty, G.B.; Carlino, M.S.; et al. Risk of Radiation Necrosis after Stereotactic Radiosurgery for Melanoma Brain Metastasis by Anatomical Location. *Strahlenther. Onkol.* **2021**, *197*, 1104–1112. [CrossRef]
49. Doré, M.; Martin, S.; Delpon, G.; Clément, K.; Campion, L.; Thillays, F. Stereotactic Radiotherapy Following Surgery for Brain Metastasis: Predictive Factors for Local Control and Radionecrosis. *Cancer/Radiothérapie* **2017**, *21*, 4–9. [CrossRef]
50. Eitz, K.A.; Lo, S.S.; Soliman, H.; Sahgal, A.; Theriault, A.; Pinkham, M.B.; Foote, M.C.; Song, A.J.; Shi, W.; Redmond, K.J.; et al. Multi-Institutional Analysis of Prognostic Factors and Outcomes After Hypofractionated Stereotactic Radiotherapy to the Resection Cavity in Patients With Brain Metastases. *JAMA Oncol.* **2020**, *6*, 1901. [CrossRef]

51. Jhaveri, J.; Chowdhary, M.; Zhang, X.; Press, R.H.; Switchenko, J.M.; Ferris, M.J.; Morgan, T.M.; Roper, J.; Dhabaan, A.; Elder, E.; et al. Does Size Matter? Investigating the Optimal Planning Target Volume Margin for Postoperative Stereotactic Radiosurgery to Resected Brain Metastases. *J. Neurosurg.* **2019**, *130*, 797–803. [CrossRef]
52. Lehrer, E.J.; Ahluwalia, M.S.; Gurewitz, J.; Bernstein, K.; Kondziolka, D.; Niranjan, A.; Wei, Z.; Lunsford, L.D.; Fakhoury, K.R.; Rusthoven, C.G.; et al. Imaging-Defined Necrosis after Treatment with Single-Fraction Stereotactic Radiosurgery and Immune Checkpoint Inhibitors and Its Potential Association with Improved Outcomes in Patients with Brain Metastases: An International Multicenter Study of 697 Patients. *J. Neurosurg.* **2022**. *publish before print*. [CrossRef]
53. Lischalk, J.W.; Oermann, E.; Collins, S.P.; Nair, M.N.; Nayar, V.V.; Bhasin, R.; Voyadzis, J.-M.; Rudra, S.; Unger, K.; Collins, B.T. Five-Fraction Stereotactic Radiosurgery (SRS) for Single Inoperable High-Risk Non-Small Cell Lung Cancer (NSCLC) Brain Metastases. *Radiat. Oncol.* **2015**, *10*, 216. [CrossRef] [PubMed]
54. Minniti, G.; D'Angelillo, R.M.; Scaringi, C.; Trodella, L.E.; Clarke, E.; Matteucci, P.; Osti, M.F.; Ramella, S.; Enrici, R.M.; Trodella, L. Fractionated Stereotactic Radiosurgery for Patients with Brain Metastases. *J. Neurooncol.* **2014**, *117*, 295–301. [CrossRef]
55. Piras, A.; Boldrini, L.; Menna, S.; Sanfratello, A.; D'Aviero, A.; Cusumano, D.; Di Cristina, L.; Messina, M.; Spada, M.; Angileri, T.; et al. Five-Fraction Stereotactic Radiotherapy for Brain Metastases: A Single-Institution Experience on Different Dose Schedules. *Oncol. Res. Treat.* **2022**, *45*, 408–414. [CrossRef]
56. Wegner, R.E.; Leeman, J.E.; Kabolizadeh, P.; Rwigema, J.-C.; Mintz, A.H.; Burton, S.A.; Heron, D.E. Fractionated Stereotactic Radiosurgery for Large Brain Metastases. *Am. J. Clin. Oncol.* **2015**, *38*, 135–139. [CrossRef] [PubMed]
57. Kahl, K.-H.; Shiban, E.; Gutser, S.; Maurer, C.J.; Sommer, B.; Müller, H.; Konietzko, I.; Grossert, U.; Berlis, A.; Janzen, T.; et al. Focal Cavity Radiotherapy after Neurosurgical Resection of Brain Metastases: Sparing Neurotoxicity without Compromising Locoregional Control. *Strahlenther. Onkol.* **2022**, *198*, 1105–1111. [CrossRef]
58. Korytko, T.; Radivoyevitch, T.; Colussi, V.; Wessels, B.W.; Pillai, K.; Maciunas, R.J.; Einstein, D.B. 12 Gy Gamma Knife Radiosurgical Volume Is a Predictor for Radiation Necrosis in Non-AVM Intracranial Tumors. *Int. J. Radiat. Oncol. Biol. Phys.* **2006**, *64*, 419–424. [CrossRef]
59. McLaughlin, M.; Patin, E.C.; Pedersen, M.; Wilkins, A.; Dillon, M.T.; Melcher, A.A.; Harrington, K.J. Inflammatory Microenvironment Remodelling by Tumour Cells after Radiotherapy. *Nat. Rev. Cancer* **2020**, *20*, 203–217. [CrossRef]
60. Constanzo, J.; Midavaine, É.; Fouquet, J.; Lepage, M.; Descoteaux, M.; Kirby, K.; Tremblay, L.; Masson-Côté, L.; Geha, S.; Longpré, J.-M.; et al. Brain Irradiation Leads to Persistent Neuroinflammation and Long-Term Neurocognitive Dysfunction in a Region-Specific Manner. *Prog. Neuropsychopharmacol. Biol. Psychiatry* **2020**, *102*, 109954. [CrossRef]
61. Dewan, M.Z.; Galloway, A.E.; Kawashima, N.; Dewyngaert, J.K.; Babb, J.S.; Formenti, S.C.; Demaria, S. Fractionated but Not Single-Dose Radiotherapy Induces an Immune-Mediated Abscopal Effect When Combined with Anti-CTLA-4 Antibody. *Clin. Cancer Res.* **2009**, *15*, 5379–5388. [CrossRef]
62. Vanpouille-Box, C.; Alard, A.; Aryankalayil, M.J.; Sarfraz, Y.; Diamond, J.M.; Schneider, R.J.; Inghirami, G.; Coleman, C.N.; Formenti, S.C.; Demaria, S. DNA Exonuclease Trex1 Regulates Radiotherapy-Induced Tumour Immunogenicity. *Nat. Commun.* **2017**, *8*, 15618. [CrossRef] [PubMed]

3.6 Dejonckheere CS*, Layer JP*, Hamed M, Layer K, Glasmacher A, Friker LL, Potthoff AL, Zeyen T, Scafa D, Koch D, Garbe S, Holz JA, Kugel F, Grimmer M, Schmeel FC, Gielen GH, Forstbauer H, Vatter H, Herrlinger U, Giordano FA, Schneider M, Schmeel LC, Sarria GR. Intraoperative or postoperative stereotactic radiotherapy for brain metastases: time to systemic treatment onset and other patient-relevant outcomes. J Neurooncol. 2023 Sep;164(3):683-691.

Hintergrund und Zielsetzung der Arbeit: Die IORT bietet den Vorteil, dass die reine Behandlungszeit auch gegenüber der in 3.5 beschriebenen hypofraktionierten SBRT nochmals drastisch reduziert werden kann. Neben diesen beschriebenen Vorteilen im direkten Vergleich zur FSRT stellt sich die Frage nach weiteren patientenzentrierten sekundären Endpunkten wie der kumulativen Hospitalisierungszeit, der Zeit bis zur Einleitung der nächsten Therapie oder der notwendigen postoperativen Steroiddosen, die in der vorliegenden Arbeit untersucht wurden.

Methoden und Ergebnisse: Alle konsekutiven Patientenfälle mit gesicherter Diagnose einer Hirnmetastase, die am Universitätsklinikum Bonn zwischen November 2020 und Juni 2023 eine IORT erhielten, wurden eingeschlossen. 95 Patienten wurden gescreent, bei 84 war die IORT durchführbar (88%) und bei 64 wurde schlussendlich eine IORT durchgeführt (67%). Zum Vergleich wurden im gleichen Zeitraum retrospektiv 53 konsekutive Fälle, bei denen eine Hirnmetastase mit einer adjuvanten FSRT behandelt wurde und die sich in den klinischen Charakteristika nicht signifikant unterschieden, eingeschlossen. Es bestanden keine signifikanten Unterschiede in der Dauer der postoperativen Steroidtherapie sowie der postoperativen Hospitalisierungsdauer durch die IORT. Die kumulative Hospitalisierungszeit (sämtliche Tage mit Krankenhausbesuch bis zum Abschluss der Bestrahlung) war mit 11 versus 19 Tagen bei der IORT ebenso wie die Zeit bis zur Einleitung der nächsten Therapie signifikant kürzer als bei der FSRT.

Schlussfolgerungen: Die IORT verursacht trotz der zusätzlichen intraoperativen Intervention keine verlängerten Krankenhausaufenthalte oder erhöhten Kortisonbedarf. Ferner ist sie mit einer hohen Umsetzbarkeitsrate zuverlässig anwendbar. Im Vergleich zur adjuvanten FSRT erspart sie den Patienten nicht nur potenziell belastende Behandlungstage, sondern sie ermöglicht auch eine prognostisch begünstigende, deutlich raschere Einleitung dringlicher Folgetherapien.

Journal of Neuro-Oncology (2023) 164:683–691
https://doi.org/10.1007/s11060-023-04464-7

RESEARCH

Intraoperative or postoperative stereotactic radiotherapy for brain metastases: time to systemic treatment onset and other patient-relevant outcomes

Cas S. Dejonckheere[1] · Julian P. Layer[1,2] · Motaz Hamed[3] · Katharina Layer[1] · Andrea Glasmacher[1] · Lea L. Friker[2,4] · Anna-Laura Potthoff[3] · Thomas Zeyen[5] · Davide Scafa[1] · David Koch[1] · Stephan Garbe[1] · Jasmin A. Holz[1] · Fabian Kugel[1] · Molina Grimmer[1] · Frederic Carsten Schmeel[6] · Gerrit H. Gielen[4] · Helmut Forstbauer[7] · Hartmut Vatter[3] · Ulrich Herrlinger[5] · Frank A. Giordano[8] · Matthias Schneider[3] · Leonard Christopher Schmeel[1] · Gustavo R. Sarria[1]

Received: 4 August 2023 / Accepted: 23 September 2023 / Published online: 9 October 2023

Abstract

Purpose Intraoperative radiotherapy (IORT) has become a viable treatment option for resectable brain metastases (BMs). As data on local control and radiation necrosis rates are maturing, we focus on meaningful secondary endpoints such as time to next treatment (TTNT), duration of postoperative corticosteroid treatment, and in-hospital time.

Methods Patients prospectively recruited within an IORT study registry between November 2020 and June 2023 were compared with consecutive patients receiving adjuvant stereotactic radiotherapy (SRT) of the resection cavity within the same time frame. TTNT was defined as the number of days between BM resection and start of the next extracranial oncological therapy (systemic treatment, surgery, or radiotherapy) for each of the groups.

Results Of 95 BM patients screened, IORT was feasible in 84 cases (88%) and ultimately performed in 64 (67%). The control collective consisted of 53 SRT patients. There were no relevant differences in clinical baseline features. Mean TTNT (range) was 36 (9 – 94) days for IORT patients versus 52 (11 – 126) days for SRT patients ($p = 0.01$). Mean duration of postoperative corticosteroid treatment was similar (8 days; $p = 0.83$), as was mean postoperative in-hospital time (11 versus 12 days; $p = 0.97$). Mean total in-hospital time for BM treatment (in- and out-patient days) was 11 days for IORT versus 19 days for SRT patients ($p < 0.001$).

Conclusion IORT for BMs results in faster completion of interdisciplinary treatment when compared to adjuvant SRT, without increasing corticosteroid intake or prolonging in-hospital times. A randomised phase III trial will determine the clinical effects of shorter TTNT.

Keywords Intraoperative radiotherapy · Brain metastasis · Stereotactic radiotherapy · Time to next treatment

Cas S. Dejonckheere and Julian P. Layer contributed equally.

✉ Cas S. Dejonckheere
cas.dejonckheere@ukbonn.de

[1] Department of Radiation Oncology, University Hospital Bonn, Venusberg-Campus 1, 53127 Bonn, Germany

[2] Institute of Experimental Oncology, University Hospital Bonn, 53127 Bonn, Germany

[3] Department of Neurosurgery, University Hospital Bonn, 53127 Bonn, Germany

[4] Institute of Neuropathology, University Hospital Bonn, 53127 Bonn, Germany

[5] Division of Clinical Neuro-Oncology, Department of Neurology, University Hospital Bonn, 53127 Bonn, Germany

[6] Department of Neuroradiology, University Hospital Bonn, 53127 Bonn, Germany

[7] Oncology Practice Network Troisdorf, 53840 Troisdorf, Germany

[8] Department of Radiation Oncology, University Medical Center Mannheim, 68167 Mannheim, Germany

Introduction

Following recent advances in systemic treatment options and subsequent improved overall survival, the relative diagnostic incidence of brain metastases (BMs) is on the rise [1–3]. A cornerstone in their managment is postoperative local control, as this remains the primary treatment objective to prevent neurological decline and avoid additional interventions [4]. For large or symptomatic lesions, the standard of care includes maximal surgical resection followed by one to several fractions of adjuvant stereotactic radiotherapy (SRT), in order to improve local control. The latter yields superior outcomes over whole-brain radiotherapy in terms of neurocognition and quality of life [5–7]. To allow for postoperative patient stabilisation and sufficient surgical wound healing, adjuvant radiation treatment is only initiated after a postoperative interval of several weeks, which increases the overall BM treatment time and delays the onset of systemic treatments [8].

In recent years, intraoperative radiotherapy (IORT) is emerging as a viable alternative treatment option for resectable BMs [9–11]. Low-level X-rays applied directly to the resection cavity result in high rates of local tumour control, while simultaneously omitting the need for adjuvant SRT in the case of solitary BMs or reducing the total number of treatment days in the case of multiple BMs [12–15]. A swift completion of interventional BM treatments might shorten the time to systemic therapy initiation, which could potentially improve survival outcomes, especially in treatment-naive patients or those with high tumour burden at the time of BM surgery. Furthermore, the instant application of a single high local radiation dose might prevent early repopulation of residual microscopic tumour. Other advantages of IORT include a steep dose gradient with improved sparing of healthy brain tissue and omitting challenging target volume delineation caused by postoperative tissue alterations [16]. Despite all the above-mentioned, patient-centered outcomes are currently scarce in this setting. Herein, we report meaningful secondary endpoints of IORT patients compared to an institutional SRT cohort, including time to next extracranial oncological treatment (TTNT), duration of postoperative corticosteroid treatment and in-hospital times.

Materials and methods

IORT patients

Consecutive patients who underwent BM exeresis combined with IORT at our university center within a prospective registry between November 2020 and June 2023 were screened. Criteria for surgery included presence or severe risk of acute neurological impairment and clinically significant mass effect, i.e. signs of raised intracranial pressure or hemispheric shift. In patients with multiple BMs, only the clinically manifest lesion was considered for surgical removal in order to prevent mass effects or tumour-related hydrocephalus. IORT was considered in the case of planned gross total resection and intraoperative neuropathological confirmation of BM by frozen section.

Preoperative contrast-enhanced T1-weighted magnetic resonance imaging (MRI) provided three-dimensional guidance for both surgery and IORT. Optic nerves, optic chiasm, and brainstem were identified pre- and intraoperatively as organs at risk (OARs). A spherical applicator ranging from 1.5 to 5 cm diameter was placed into the surgical cavity according to the best-fit rule, covering the entire surface. A standard recommended dose of 30 Gy was prescribed to the applicator surface (nominal 50 kV photons) [16]. Delivered OAR doses were calculated based on dose-depth template profiles corresponding to the applicator diameter. In the case of OAR doses exceeding Quantitative Analyses of Normal Tissue Effects in the Clinic (QUANTEC) constraints (i.e. 12 Gy for the optical system or 12.5 Gy for the brainstem), a decrease in the prescribed dose to 16 Gy (minimum) was acceptable. IORT was delivered with the INTRABEAM 600 (Carl Zeiss Meditec AG, Oberkochen, Germany).

Patient demographics and clinical characteristics were collected from the electronic health records. The Karnofsky Performance Score (KPS) classified patients according to their functional status at the time of admission, with a stratification cut-off of 70, depending on a patient's ability to carry out normal activity and work [17]. Diagnosis-Specific Graded Prognostic Assessment (DS-GPA) scores were calculated by standard procedures [18].

This study was conducted in accordance with the Declaration of Helsinki and approved by the Institutional Review Board of the University Hospital Bonn (018/21 and 057/22).

Controls

The control collective consisted of two patient groups: patients screened for IORT but not receiving it for one of several reasons (Table 1), thus subsequently requiring adjuvant SRT of the resection cavity and patients planned for adjuvant SRT of the resection cavity within the same time frame. Inclusion criteria for both groups were surgically resected histologically confirmed solid tumour BM receiving one to seven fractions of adjuvant SRT of the resection cavity and a total BM number ≤ 10 at the time of surgery.

All patients received a planning computer tomography (CT) in supine position with an individual thermoplastic stereotactic fixation mask. A postoperative contrast-enhanced T1-weighted planning MRI with 1 mm slice thickness was

Table 1 Reasons for not receiving IORT for resectable brain metastasis. IORT = intraoperative radiotherapy; OAR = organ at risk

IORT not possible or feasible (*n* = 11)
logistics (*n* = 6)
expected violation of OAR constraint (*n* = 3)
patient declining surgery (*n* = 2)
IORT possible and feasible, but not performed (*n* = 20)
frozen section unclear (*n* = 7)
resection cavity not spherical (*n* = 5)
technical reasons (*n* = 4)
logistics (*n* = 2)
measured violation of OAR constraint (*n* = 1)
patient declining surgery (*n* = 1)

coregistered with this planning CT and the gross tumour volume (GTV) was defined as the resection cavity including any possible residual contrast (Gd) enhancement. A 2 mm isotropic margin was added for the planning target volume (PTV), as per institutional standards. SRT was administered with intensity-modulated image-guided techniques, employing 6 – 10 MV photon energies and ensuring a target volume coverage of 99 – 120%. All patients were treated on a TrueBeam STx (Varian Medical Systems, Palo Alto, CA, USA) linear accelerator, using ExacTrac (Brainlab, München, Germany) for position matching.

Literature search

To put the data into perspective, international literature (MEDLINE) and study registries (National Clinical Trials) were screened for similar retrospective and prospective IORT collectives, using the search terms *intraoperative radiotherapy* and *brain metastasis*. Where available, data on TTNT were extracted and summarised.

Statistical analysis

The primary endpoint of this trial was TTNT, defined as the number of days between BM resection and start of the next oncological intervention (systemic treatment, extracranial surgery or radiation) for each of the groups. Patients were included in the analysis if they received such treatment and the exact date of treatment start was known. Reasons for exclusion were initial patient decline of the proposed subsequent treatment and logistic reasons for delay in case of extracranial surgery.

Mean, median, standard deviation (SD), and range were calculated for all applicable clinical data. Differences in baseline patient characteristics between groups were assessed using Fisher's exact test, Pearson's χ^2, or Student's unpaired *t*-test, as appropriate. For the comparison of TTNT between groups, the Mann-Whitney-*U*-test was used. The log-rank test was used for the statistical assessment of event rates, presented according to the Kaplan-Meier method. The statistical significance level was defined as $p < 0.05$. Microsoft Excel version 16 (Microsoft, Redmond, WA, USA), SPSS Statistics version 27 (IBM, Armonk, NY, USA), and GraphPad Prism version 9 (GraphPad Software, San Diego, CA, USA) were used to perform the analyses and Adobe Illustrator 2023 (Adobe Inc., Mountain View, CA, USA) to generate graphical images.

Results

Of 95 BM patients screened, IORT was deemed feasible in 84 cases (88%) and ultimately performed in 64 (67%). Sufficient data were available for 62 patients undergoing IORT and 52 receiving adjuvant SRT of the resection cavity. A flowchart of patient selection is provided in Fig. 1. Patient and treatment characteristics are summarised in Table 2. There were no relevant differences in baseline characteristics between both groups. Data on local control, distant brain failure, radiation necrosis incidence, and overall survival for a subset of 35 IORT patients with mature follow-up are reported elsewhere [15].

Thirty-nine patients (63%) in the IORT group versus 31 patients (60%) in the adjuvant SRT group received postoperative extracranial treatment, with systemic therapies being the most common (84% and 97%, respectively). There was no difference in the types of additional treatment ($p = 0.11$). The location (i.e. same or different center), a potential confounder which can cause logistic delay due to outpatient referral systems, was not significantly different between both groups ($p = 0.08$). Neither duration of postoperative corticosteroid treatment nor postoperative in-hospital time was significantly different between both groups: $p = 0.83$ (Fig. 2a) and $p = 0.97$ (Fig. 2b), respectively. Mean total in-hospital time for BM treatment (in- and out-patient) was 11 days for IORT versus 19 days for SRT patients ($p < 0.001$; Fig. 2c). Mean TTNT (range) was 36 (9 – 94) days for IORT patients versus 52 (11 – 126) days for adjuvant SRT patients ($p = 0.01$; Fig. 2d – *e*). Results are summarised in Table 3.

Discussion

IORT for resectable BM yields comparable outcome to adjuvant SRT of the resection cavity in terms of local control and radiation necrosis rates [12–15, 19]. As long-term follow-up results from the first prospective IORT collectives are maturing, we here focus on meaningful secondary endpoints that have a major impact on treatment decisions, both from the patients' but also from an economical and logistical perspective. The high incidence of BMs along with

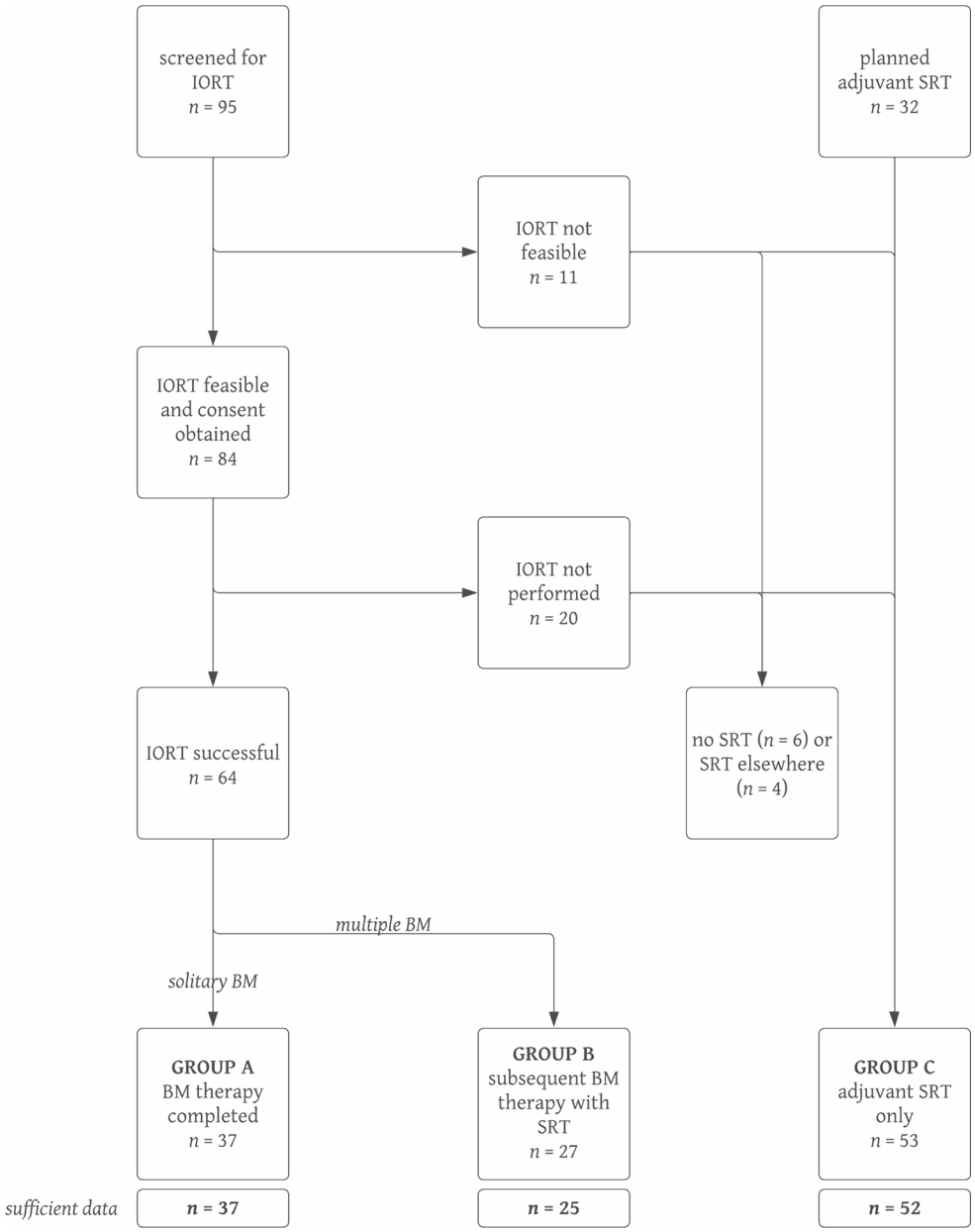

Fig. 1 Flowchart of patient selection. IORT = intraoperative radiotherapy; SRT = stereotactic radiotherapy; BM = brain metastasis

their generally poor prognosis indicate that every treatment step should be optimised. Asymptomatic patients might be diagnosed during staging of an extracranial primary tumour, meaning that in such treatment-naive patients, rapid completion of interdisciplinary BM treatment is of particularly high interest, as it might shorten the time to subsequent salvage therapy, which could potentially impact survival chances.

This is the first assessment of IORT feasibility in daily practice of a specialised university center with high turnover, demonstrating a feasibility rate of 88%, which proves the general applicability of IORT as a standard procedure for BM treatment. In the comparative analysis, extracranial oncological therapy could be started on average 16 days earlier following IORT, regardless of potential confounders such as type of treatment or location. If IORT is not available or possible, standard SRT of the resection cavity should be performed to improve local control [5, 6]. In order to prevent impaired surgical wound healing, adjuvant SRT is initiated after a postoperative interval of several weeks, which increases overall BM treatment time and delays onset of salvage systemic therapy. Yaghi et al. ($n = 176$) found that a postoperative delay of > 22 days had a decreased risk of all-cause mortality [8]. However, those waiting > 40 days after BM resection doubled their risk of local tumour progression. The median postoperative time to SRT onset was 25 days in the current SRT collective, well within this time frame.

Table 2 Patient and treatment characteristics. IORT = intraoperative radiotherapy; SRT = stereotactic radiotherapy; KPS = Karnofsky Performance Score; DS-GPA = Diagnosis-Specific Graded Prognostic Assessment; Gy = Gray; GI = gastrointestinal; GU = genitourinary; BM = brain metastasis

	IORT	SRT	*p*
n	62	52	
female sex, *n* (%)	31 (50)	25 (48)	0.85
median age at surgery (range) in years	63 (35 – 91)	64 (34 – 87)	0.86
KPS at surgery, *n* (%)	49 (79)	43 (83)	0.77
≥ 70	13 (21)	9 (17)	
< 70			
median DS-GPA at surgery (range)	2 (0 – 4)	2 (0 – 4)	0.39
extracranial metastases at surgery, *n* (%)	52 (84)	27 (68)	0.09
median radiation dose (range) in Gy *	30 (16 – 30)	35 (20 – 45)	
primary lobe, *n* (%)			
frontal	24 (39)	17 (33)	0.07
parietal	2 (3)	10 (19)	
occipital	16 (26)	8 (15)	
temporal	8 (13)	8 (15)	
cerebellum	12 (19)	9 (17)	
primary tumour, *n* (%)			
lung	37 (60)	25 (48)	0.26
melanoma	10 (16)	9 (17)	
GI	5 (8)	7 (13)	
GU	6 (10)	3 (6)	
breast	3 (5)	3 (6)	
gynaecological	1 (2)	1 (2)	
other	0 (0)	4 (8)	
number of BMs at surgery, *n* (%)			
solitary	36 (58)	31 (60)	0.49
multiple	26 (42)	21 (40)	
(range of multiple BMs)	(2 – 10)	(2 – 10)	
median time (range) to			
SRT onset in days		25 (11 – 173)	
SRT completion in days		34 (11 – 187)	

* Due to radiobiological differences between IORT and SRT, the difference between the administered doses is not deemed relevant and thus not calculated

Reasons for longer TTNT in SRT patients are many fold and include incomplete staging, which might be postponed until after SRT (e.g. due to conflicting appointments), side effects, undesirable combination with planned systemic therapy (e.g. BRAF and MEK inhibitors in melanoma patients), patient refusal to undergo parallel treatments [20]. In line with our previous report on posteroperative morbidity, we demonstrate that IORT is not associated with prolonged hospitalisation or corticosteroid intake [21]. Moreover, patients who underwent IORT had a faster completion of interdisciplinary BM treatment, when compared to those undergoing adjuvant SRT. Even though postoperative in-hospital times were similar, total in-hospital times (in- and out-patient) for BM treatment were significantly shorter for IORT patients (8 days on average), which might save limited treatment resources, reduce BM treatment costs, and positively impact quality of life.

Apart from shorter TTNT and faster recovery after BM treatment, IORT has several other theoretical advantages. The instant application of a single high local radiation dose might prevent early repopulation of residual microscopic tumour and the steep dose gradient improves sparing of healthy brain tissue, potentially preserving neurological functions and possibly improving subsequent re-irradiation options if ever needed. In patients with solitary BM, a repeat MRI for treatment planning is not required, which further reduces costs and in-hospital time. With IORT, challenging target volume delineation caused by postoperative tissue alterations can be omitted. Furthermore, completing radiation treatment while the patient is asleep promotes comfort and reduces patient burden. There is, however, a general lack of evidence on these theoretical advantages of IORT, which is why they should be assessed in ongoing and future prospective trials.

SRT does have the advantage that dose distribution and OAR constraints can be reproduced more accurately, for example in patients requiring SRT for other BMs at a later point in time. An ongoing trial of image-guided IORT will enable real-time planning.

Other published IORT collectives were identified, the results of which are summarised in Table 4. Only Brehmer et al. directly compared TTNT between their prospectively recruited IORT patients ($n = 10$) and a control collective of patients undergoing adjuvant SRT of the resection cavity within the same time frame ($n = 19$) [22]. On average, IORT patients started systemic treatment 15 days earlier when compared to those receiving adjuvant SRT, in accordance with our results. Mean postoperative time to SRT onset

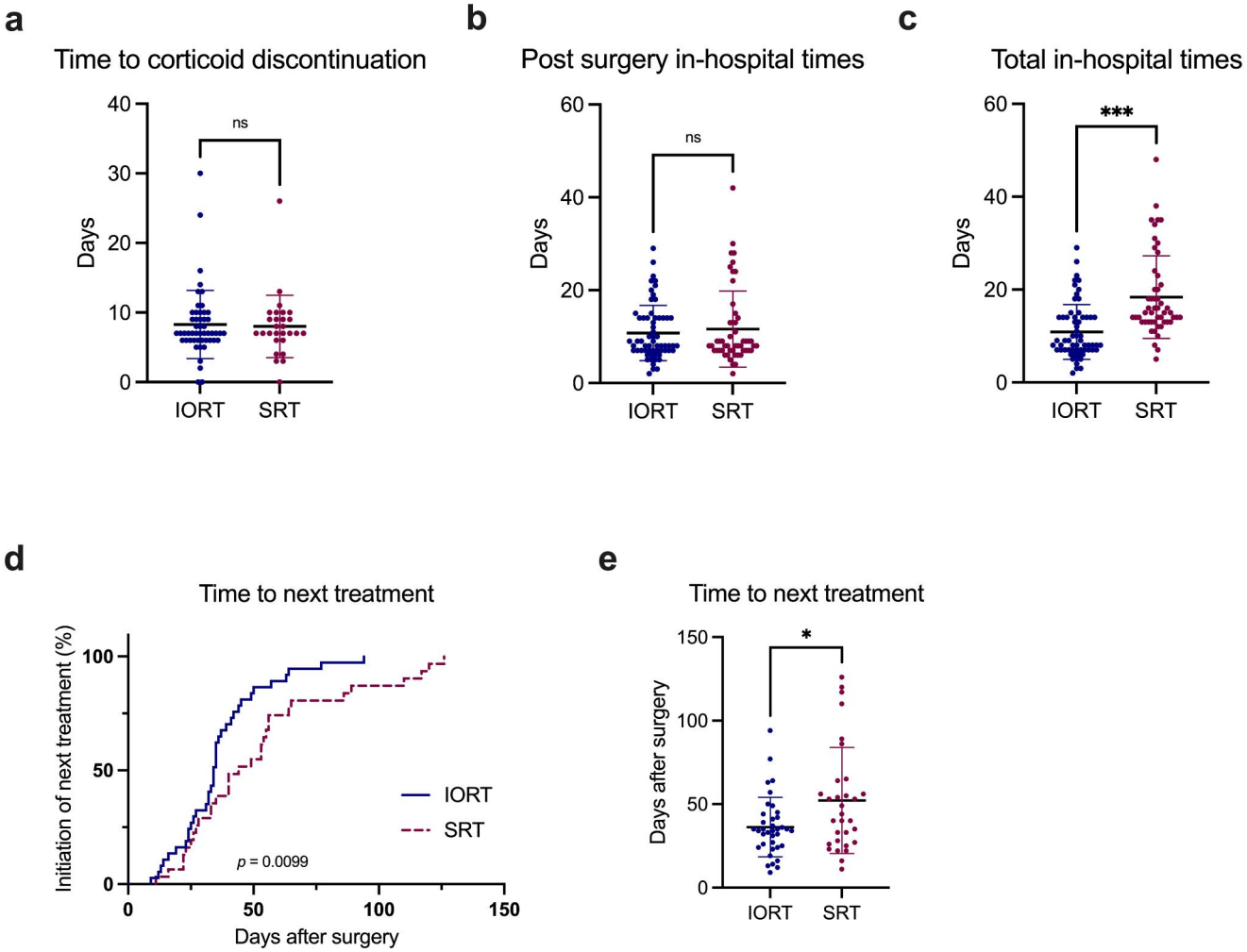

Fig. 2 Comparison of meaningful patient-centered secondary endpoints between IORT and adjuvant SRT patients. Scatter plots showing (**a**) time in days to corticoid discontinuation, (**b**) postoperative in-patient time, and (**c**) total (in- and out-patient) in-hospital time, Mann-Whitney-*U*-test. (**d**) Kaplan-Meier curve for patients reaching initiation of their next extracranial oncological treatment (log-rank test). (**e**) Scatter plot for time to next extracranial oncological treatment (Mann-Whitney-*U*-test). * $p < 0.05$, *** $p < 0.001$, ns = not significant. IORT = intraoperative radiotherapy; SRT = stereotactic radiotherapy

was 27 days, consistent with the recommendation of Yaghi et al. As this was a planned safety interim analysis, it was underpowered for this secondary endpoint, but the preliminary data confirm that TTNT tends to be reduced in IORT patients. The prospective phase II trial is designed to recruit 50 patients, will evaluate local efficacy of IORT for BM, and will assess TTNT as a preplanned secondary endpoint (INTRAMET; NCT03226483) [19]. Kahl et al. reported a median TTNT (range) of 18 (0–130) days after IORT in 24 patients requiring subsequent systemic treatment [13]. Diehl et al. observed that in 5 IORT patients, TTNT was ≤15 days, which is shorter than wound healing and adjuvant SRT would have required [14]. Both retrospective cohorts did, however, not include a control collective receiving adjuvant SRT of the resection cavity.

This trial carries certain limitations. First, a relatively small sample size, which might be subject to selection bias. Due to the recent implementation of IORT in clinical BM workflows, there are still limited available data on this topic. To our best knowledge, we present the largest collective to date investigating TTNT in this context. Secondly, BM patients represent a heterogeneous collective, with a multitude of systemic treatment options and required diagnostic investigations. The latter could have led to differences in TTNT between IORT and SRT patients. The similarity of baseline patient and treatment characteristics does, however, partly compensate for this. Lastly, it cannot be yet concluded if shorter TTNT and faster completion of BM treatment translate into improved survival or quality of life. As data of prospective IORT trials are maturing, the clinical relevance of these parameters will be elucidated.

Table 3 Time to next treatment, duration of postoperative corticosteroid treatment, and in-hospital time. IORT = intraoperative radiotherapy; SRT = stereotactic radiotherapy; SD = standard deviation

	IORT	SRT	*p*
received postoperative extracranial treatment, *n* (%)			
yes	39 (63) *	31 (60)	0.99
no	18 (29) **	15 (29)	
unknown	5 (8)	6 (11)	
type of additional treatment, *n* (%)			
chemotherapy	6 (16)	12 (39)	0.11
immunotherapy	20 (54)	12 (39)	
chemoimmunotherapy	4 (11)	6 (19)	
antihormone therapy	1 (3)	0 (0)	
extracranial surgery	3 (8)	1 (3)	
extracranial radiotherapy	3 (8)	0 (0)	
location of postoperative extracranial treatment, *n* (%)			
same center	21 (54)	23 (74)	0.08
different center	18 (46)	8 (26)	
time to next treatment			
median (range) in days	34 (9 – 94)	44 (11 – 126)	**0.01**
mean ± SD in days	36 ± 18	52 ± 32	
postoperative corticosteroid treatment			
median (range) in days	7 (0 – 30)	7 (0 – 14)	0.83
mean ± SD in days	8 ± 5	8 ± 3	
postoperative in-hospital time (in-patient)			
median (range) in days	8 (2 – 29)	8 (2 – 42)	0.97
mean ± SD in days	11 ± 6	12 ± 8	
total in-hospital time (in- and out-patient)			
median (range) in days	8 (2 – 29)	15 (7 – 48)	**< 0.001**
mean ± SD in days	11 ± 6	19 ± 9	

* Extracranial surgery had to be postponed in one patient suffering COVID pneumonia and another patient initially declined immunotherapy. Both patients were excluded from the analysis

** Two patients had already started systemic therapy prior to surgery and were also excluded from the analysis

Table 4 Other published IORT collectives. IORT = intraoperative radiotherapy; TTNT = time to next treatment; 1yLCR = 1-year local control rate; 1yDBC = 1-year distant brain control; RN = radiation necrosis; 1yOS = 1-year overall survival; SRT = stereotactic radiotherapy: CI = confidence interval; n.r. = not reported

author (year)	type	IORT outcome of published trials				*n*		TTNT (days)
		1yLCR (%)	1yDBC (%)	RN (%)	1yOS (%)	IORT	SRT	
current (2023)	prospective study registry	97 *	74 *	3 *	58 *	62	52	*mean (range)* IORT: 36 (9 – 94) SRT: 52 (11 – 126)
Brehmer et al. (2023) [19]	prospective phase II (preliminary)					35	/	*mean (95% CI)* 45 (35–55)
Guedes de Castro et al. (2023) [23]	prospective phase II	88	13	10	80	10	/	n.r.
Diehl et al. (2022) [14]	retrospective	93	71	11	58	18	/	in 5 IORT patients ≤ 15 (shorter than wound healing and adjuvant SRT would have required)
Kahl et al. (2021) [13]	retrospective	84	34	3	62	40	/	*median (range)* 18 (0–130)
Cifarelli et al. (2019) [12]	retrospective	88	58	7	73	54	/	n.r.
Brehmer et al. (2018) [22]	prospective phase II (preliminary)					10	19	*mean (range)* IORT: 46 (27–83) SRT: 61 (16–229)
Weil et al. (2015) [24]	prospective	n.r.	n.r.	13	n.r.	23	/	n.r.

* Results of a subset of 35 IORT patients with mature follow-up [15]

Conclusion

IORT for BMs results in faster completion of interdisciplinary treatment when compared to adjuvant SRT, without increasing corticosteroid intake or prolonging hospital stay. Apart from emerging evidence regarding excellent local control and comparable radiation necrosis rates, these data add to the favourable therapy profile of IORT in this setting. A randomised phase III trial will determine the clinical effects of shorter TTNT.

Acknowledgements The authors would like to thank Katja Klever and Monika Brüggemann for their assistance with obtaining the follow-up data.

Authors' contributions C.S.D., J.P.L., and G.R.S. designed the study. Formal analysis was done by C.S.D. and J.P.L. Statistical analysis was performed by J.P.L. The first draft of the manuscript was written by C.S.D. and both J.P.L. and G.R.S. reviewed and edited. All remaining authors commented, read, and approved the final manuscript.

Funding and conflict of interest The authors declare that no funds, grants, or other support were received during the preparation of this manuscript. J.P.L reports stocks and travel expenses from TME Pharma AG, travel expenses from Carl Zeiss Meditec AG, stocks and honoraria from Siemens Healthineers, and stocks from Bayer AG and BioNTech AG. U. H. reports advisory board and lecture honoraria from Bayer AG and Medac GmbH. F.A.G. reports research grants, personal fees, and travel expenses from Carl Zeiss Meditec AG, personal fees from Roche Pharma AG and Medac GmbH, grants and personal fees from AstraZeneca, Bristol-Myers Squibb, Cureteq AG, Elekta AB, FoMF GmbH, Guerbet SA, MSD Sharp, Dohme GmbH, and Opasca GmbH, stocks, grants, and personal fees from TME Pharma AG, compensation for advisory boards from the Federal Joint Committee (G-BA) of the Federal Republic of Germany and of the German Cancer Aid, and non-financial support from Oncare GmbH and Opasca GmbH. G.R.S. reports personal fees and travel expenses from Carl Zeiss Meditec AG, personal fees from Roche Pharma AG, personal fees from MedWave Clinical Trials, and travel expenses from Guerbet SA, not related to this work.
Open Access funding enabled and organized by Projekt DEAL.

Data Availability Data will be made available upon reasonable request to the corresponding author.

Declarations

Competing interests The authors declare no competing interests.

References

1. Cagney DN, Martin AM, Catalano PJ, Redig AJ, Lin NU, Lee EQ et al (2017) Incidence and prognosis of patients with brain metastases at diagnosis of systemic malignancy: a population-based study. Neuro Oncol 19:1511–1521. https://doi.org/10.1093/neuonc/nox077
2. Nayak L, Lee EQ, Wen PY (2012) Epidemiology of brain metastases. Curr Oncol Rep 14:48–54. https://doi.org/10.1007/s11912-011-0203-y
3. Davis FG, Dolecek TA, McCarthy BJ, Villano JL (2012) Toward determining the lifetime occurrence of metastatic brain tumors estimated from 2007 United States cancer incidence data. Neuro Oncol 14:1171–1177. https://doi.org/10.1093/neuonc/nos152
4. Nieder C, Stanisavljevic L, Aanes SG, Mannsåker B, Haukland EC (2022) 30-day mortality in patients treated for brain metastases: extracranial causes dominate. Radiat Oncol 17:92. https://doi.org/10.1186/s13014-022-02062-x
5. Patchell RA, Tibbs PA, Regine WF, Dempsey RJ, Mohiuddin M, Kryscio RJ et al (1998) Postoperative Radiotherapy in the treatment of single metastases to the BrainA Randomized Trial. JAMA 280:1485–1489. https://doi.org/10.1001/jama.280.17.1485
6. Redmond KJ, De Salles AAF, Fariselli L, Levivier M, Ma L, Paddick I et al (2021) Stereotactic Radiosurgery for Postoperative Metastatic Surgical Cavities: a critical review and International Stereotactic Radiosurgery Society (ISRS) Practice Guidelines. Int J Radiat Oncol Biol Phys 111:68–80. https://doi.org/10.1016/j.ijrobp.2021.04.016
7. Layer JP, Layer K, Sarria GR, Röhner F, Dejonckheere CS, Friker LL et al (2023) Five-fraction stereotactic radiotherapy for Brain Metastases-A retrospective analysis. Curr Oncol 30:1300–1313. https://doi.org/10.3390/curroncol30020101
8. Yaghi NK, Radu S, Nugent JG, Mazur-Hart DJ, Pang BW, Bowden SG et al (2022) Optimal timing of radiotherapy following brain metastases surgery. Neuro-Oncology Pract 9:133–141. https://doi.org/10.1093/nop/npac007
9. Diehl CD, Giordano FA, Grosu A-L, Ille S, Kahl K-H, Onken J et al (2023) Opportunities and Alternatives of Modern Radiation Oncology and surgery for the management of Resectable Brain Metastases. Cancers (Basel) 15. https://doi.org/10.3390/cancers15143670
10. Krauss P, Steininger K, Motov S, Sommer B, Bonk MN, Cortes A et al (2022) Resection of supratentorial brain metastases with intraoperative radiotherapy. Is it safe? Analysis and experiences of a single center cohort. Front Surg 9:1071804. https://doi.org/10.3389/fsurg.2022.1071804
11. Cifarelli CP, Jacobson GM (2021) Intraoperative Radiotherapy in Brain Malignancies: indications and outcomes in primary and metastatic brain tumors. Front Oncol 11:768168. https://doi.org/10.3389/fonc.2021.768168
12. Cifarelli CP, Brehmer S, Vargo JA, Hack JD, Kahl KH, Sarria-Vargas G et al (2019) Intraoperative radiotherapy (IORT) for surgically resected brain metastases: outcome analysis of an international cooperative study. J Neurooncol 145:391–397. https://doi.org/10.1007/s11060-019-03309-6
13. Kahl K-H, Balagiannis N, Höck M, Schill S, Roushan Z, Shiban E et al (2021) Intraoperative radiotherapy with low-energy x-rays after neurosurgical resection of brain metastases-an Augsburg University Medical Center experience. Strahlentherapie Und Onkol 197:1124–1130. https://doi.org/10.1007/s00066-021-01831-z

14. Diehl CD, Pigorsch SU, Gempt J, Krieg SM, Reitz S, Waltenberger M et al (2022) Low-energy X-Ray Intraoperative Radiation Therapy (Lex-IORT) for resected brain metastases: a Single-Institution experience. Cancers (Basel) 15. https://doi.org/10.3390/cancers15010014
15. Layer JP, Hamed M, Potthoff A-L, Dejonckheere CS, Layer K, Sarria GR et al (2023) Outcome assessment of intraoperative radiotherapy for brain metastases: results of a prospective observational study with comparative matched-pair analysis. J Neurooncol. https://doi.org/10.1007/s11060-023-04380-w
16. Vargo JA, Sparks KM, Singh R, Jacobson GM, Hack JD, Cifarelli CP (2018) Feasibility of dose escalation using intraoperative radiotherapy following resection of large brain metastases compared to post-operative stereotactic radiosurgery. J Neurooncol 140:413–420. https://doi.org/10.1007/s11060-018-2968-4
17. Péus D, Newcomb N, Hofer S (2013) Appraisal of the Karnofsky Performance Status and proposal of a simple algorithmic system for its evaluation. BMC Med Inform Decis Mak 13:72. https://doi.org/10.1186/1472-6947-13-72
18. Sperduto PW, Kased N, Roberge D, Xu Z, Shanley R, Luo X et al (2012) Summary report on the graded prognostic assessment: an accurate and facile diagnosis-specific tool to estimate survival for patients with brain metastases. J Clin Oncol 30:419–425. https://doi.org/10.1200/JCO.2011.38.0527
19. Brehmer S, Sarria GR, Würfel S, Sulejmani A, Schneider F, Clausen S et al (2023) Results of a prospective, single-arm, open-label phase II trial of intraoperative radiotherapy after resection of brain metastases. J Clin Oncol 41:2031. https://doi.org/10.1200/JCO.2023.41.16_suppl.2031
20. Anker CJ, Grossmann KF, Atkins MB, Suneja G, Tarhini AA, Kirkwood JM (2016) Avoiding severe toxicity from combined BRAF inhibitor and Radiation Treatment: Consensus Guidelines from the Eastern Cooperative Oncology Group (ECOG). Int J Radiat Oncol Biol Phys 95:632–646. https://doi.org/10.1016/j.ijrobp.2016.01.038
21. Hamed M, Potthoff A-L, Layer JP, Koch D, Borger V, Heimann M et al (2022) Benchmarking Safety Indicators of Surgical Treatment of Brain Metastases combined with intraoperative Radiotherapy: results of prospective observational study with comparative matched-pair analysis. Cancers (Basel) 14. https://doi.org/10.3390/cancers14061515
22. Brehmer S, Welsch M, Karakoyun A, Förster A, Seiz-Rosenhagen M, Clausen S et al (2018) P05.35 intraoperative radiotherapy after resection of brain metastases (INTRAMET) - initial safety/efficacy analysis of a prospective phase II study. Neuro Oncol 20:iii310–iii311. https://doi.org/10.1093/neuonc/noy139.361
23. de Castro DG, Sanematsu PI, Pellizzon ACA, Suzuki SH, Fogaroli RC, Dias JES et al (2023) Intraoperative radiotherapy for brain metastases: first-stage results of a single-arm, open-label, phase 2 trial. J Neurooncol 162:211–215. https://doi.org/10.1007/s11060-023-04266-x
24. Zikou A, Sioka C, Alexiou GA, Fotopoulos A, Voulgaris S, Argyropoulou MI Radiation Necrosis, Pseudoprogression, Pseudoresponse, and Tumor recurrence: Imaging Challenges for the evaluation of treated gliomas. Contrast Media Mol Imaging 2018;2018:6828396. https://doi.org/10.1155/2018/6828396

4. Diskussion

Das GBM geht trotz der seit vielen Jahren andauernden intensiven Forschungsbemühungen weiterhin mit einer sehr schlechten Prognose einher. Gerade für MGMT-Promotor-unmethylierte Patienten steht weiterhin keine zielführende systemische Therapieoption zur Verfügung. Hingegen erwies sich die Strahlentherapie über sämtliche Studien der vergangenen Jahre hinweg neben der chirurgischen Resektion als konstante, verträgliche und verlässlich wirksame Komponente des multimodalen Behandlungskonzepts. Jedoch ist die Tumorkontrolle durch die *Radiatio* von auffallend kurzer Dauer. Gerade beim GBM gehen die ersten Rezidive bereits häufig mit einer erheblichen klinischen Verschlechterung der Patienten einher (Chinot *et al.*, 2014), was die geringe verbliebene Lebenserwartung auch qualitativ weitergehend beeinträchtigt. Ziel innovativer Therapieansätze muss es daher sein, Mechanismen der initialen Therapieresistenz im postradiogenen TME frühzeitig zu erkennen sowie verantwortliche Faktoren, die eine Tumorrekurrenz begünstigen, zu identifizieren und medizinisch nutzbar zu machen.

Das Chemokin CXCL12 mit seinen Rezeptoren CXCR4 und CXCR7 gilt als wichtiger Vermittler der Vaskulogenese und damit als ein potenzielles Target einer gegen das postradiogenene TME gerichteten Therapie. Wir wiesen in der hier vorgestellten Zwischenauswertung der GLORIA-Studie erstmalig nach, dass eine CXCL12-Inhibition durch das L-Ribonukleinsäure (RNA)-Aptamer NOX-A12 in Kombination mit einer Bestrahlung zu einer Ablösung des Chemokins von Endothelzellen, seiner Bindung sowie konsekutiv zu seiner Akkumulation im Plasma führte. Letztlich resultierte hieraus eine nachweislich reduzierte Perfusion des Tumorgewebes. Gemäß den Ergebnissen unserer Untersuchungen beeinflusst das jeweilige Expressionsprofil des *Drug targets* CXCL12 in bestimmten Zellkompartimenten die klinische Wirksamkeit von NOX-A12. Dieser detailliert beschriebene, definierte EG12-*Score* ist für Patienten, die mit einer Strahlentherapie und NOX-A12 behandelt werden, möglicherweise prädiktiv für ein Therapieansprechen. In einer SOC-Kohorte ergaben sich hingegen eher entgegengesetzte klinische Trends, die jedoch bei Weitem nicht ausreichen, um eine zusätzliche allgemein-prognostische Rolle für den EG12-*Score* zu proklamieren. Unabhängig von der grundsätzlichen Logik des Zusammenhangs zwischen einer lokalen

CXCL12-Expression und dem Therapieansprechen auf eine CXCL12-Inhibition, drängt sich dennoch die Frage nach den Gründen für das schlechte Ansprechen der $EG12^{low}$-Patienten auf. Besonders interessant ist diesbezüglich, dass mit den Endothel- und Gliomzellen zwei ganz unterschiedliche Tumorkompartimente für ein Therapieansprechen entscheidend zu sein scheinen. Endotheliale Zellen wiesen die höchste Frequenz einer CXCL12-Positivität auf, wohingegen die Positivität der glialen Zellen die beste Korrelation mit dem PFS bot. Möglicherweise begründet sich diese duale Abhängigkeit des GBM-TME von CXCL12 zusätzlich durch komplementäre Mechanismen der CXCL12-Produktion. Die CXCL12-Expression wird gemeinhin als *Downstream*-Bestandteil einer Signalkaskade beschrieben, die primär durch die Hypoxie-bedingte Aktivierung von HIF1α aktiviert wird (Tabatabai *et al.*, 2006). Auch die Daten vorhergehender Studien mit dem CXCR4-Rezeptorantagonist Plerixafor legen dies nahe (Kioi *et al.*, 2010). CXCL12 ist deshalb ein so wichtiges Ziel einer adjuvanten GBM-Therapie, da gerade die Bestrahlung durch ihre gefäßzerstörende und koagulierende Wirkung die vaskuläre Architektur des TME zerstört und somit eine massive lokale Hypoxie bewirkt. CXCR4-positive knochenmarkstämmige Zellen wanderten daraufhin in *in vivo*-Modellen entlang eines CXCL12-Gradienten in das TME ein und initiierten dort die Vaskulogenese (Du *et al.*, 2008). Dies konnte durch CXCR4-Inhibition effektiv unterbunden werden (Kioi *et al.*, 2010). Bei klinischer Anwendung in einer Phase 2-Studie kam es, anders als im Mausmodell, im erwartbaren Zeitrahmen durchaus zu Rezidiven (Thomas *et al.*, 2019). Auffällig war jedoch, dass diese Rezidive sich unerwartet häufig außerhalb des Strahlenfeldes darstellten und Plerixafor zudem auch keinen hemmenden Einfluss auf die Perfusion in diesen *Out of field*-Bereichen hatte. Da hier lokal keine Bestrahlung erfolgt war, kann bei Postulation einer Abhängigkeit der CXCL12-Wirkung von postradiogenen Veränderungen nicht von einer distanten Wirksamkeit ausgegangen werden.

Die Darstellung von CXCL12 als hypoxisches Chemokin macht für die Gliomzellareale des GBM durchaus Sinn, denn hier herrscht durch das extreme Wachstumsverhalten des Tumors und auch die entstehenden Nekrosen eine ständige Hypoxie vor. Es erscheint jedoch weniger wahrscheinlich, demgegenüber im Bereich der Endothelzellen von einer Hypoxie-induzierten CXCL12-Expression auszugehen, da es gerade diese Zellen sind, die durch ihre Lokalisation an der Übergangsstelle zu den Sauerstoff-transportierenden

Erythrozyten am längsten ein normoxisches Mikromilieu aufrechterhalten können. Hypoxiemarker wie CA9 finden sich zudem häufig im Bereich von Nekrosearealen und weisen eine starke Korrelation mit dem alternativen Angiogenese-induzierenden VEGF-Signalweg auf. Eigene Auswertungen öffentlich zugänglicher Datenbanken für *single cell RNA*-Sequenzierung legen eine zonale Heterogenität des TME nahe, wobei die Gliomzellen und die nekrotischen Tumorareale eine hohe Abhängigkeit von VEGF aufweisen. Die Tumorrandbereiche, Infiltrations- und Gefäßzonen hingegen scheinen primär unter dem Einfluss von CXCL12 zu stehen (Giordano *et al.*, SNO 2022). Es erscheint daher begründet, dass eine duale Hemmung sowohl der Angiogenese als auch der Vaskulogenese notwendig ist, um eine Revaskularisation über diesen alternativen Signalweg aus spezifischen Tumorkompartimenten heraus zu unterbinden. Möglicherweise ist eine Aktivierung des VEGF-Signalwegs der zugrundeliegende Fluchtmechanismus bei der Tumorprogression der GLORIA-Patienten. Entsprechend erfolgte für den Expansionsarm A der Studie eine wesentliche Anpassung des Behandlungskonzepts durch Hinzunahme von Bevacizumab ergänzend zu der Bestrahlung und NOX-A12. Zwischenergebnisse dieser Triple-Therapie belegen ein deutlich verbessertes klinisches Therapieansprechen mit einer *Overall response rate* von 83,3% und mit einem medianen OS von 19,9 Monaten auch ein verbessertes Gesamtüberleben im Vergleich sowohl zu SOC-Patienten als auch dem Dosiseskalationsarm der Studie (Giordano *et al.*, SNO 2023). Die Publikation der endgültigen Studienergebnisse steht gegenwärtig noch aus.

Weitergehende translationale Forschungsanstrengungen sind notwendig, um das Verständnis für die Wirkweise von NOX-A12 und Bevacizumab im postradiogenen TME sowie, darauf aufbauend, sekundären Therapieresistenzmechanismen zu verbessern. Nur eine umfassende Charakterisierung des GBM-TME kann bei diesem besonders heterogenen Tumor neue Wege für Therapieinnovationen bahnen. Dies schließt auch das immunologische TME mit ein, obwohl das GBM prinzipiell als immunologisch kalter Tumor gilt und sämtliche größeren immuntherapeutischen Studien bislang gescheitert sind (Reardon *et al.*, 2020; Lim *et al.*, 2022; Omuro *et al.*, 2023). Einzelfälle belegen allerdings eine theoretische Effektivität immunologischer Therapien auch intrazerebral (Brown *et al.*, 2016; Platten *et al.*, 2021; Grassl *et al.*, 2023). CXCL12 ist in verschiedenen Tumorentitäten als immunsupprimierendes und protumorigenes Chemokin beschrieben

worden (Fearon *et al.*, 2014). Erste eigene weitergehende Analysen von Gewebeproben aus Rezidivoperationen in der GLORIA-Studie sowie SOC-Vergleichskollektiven zeigten eine ungewöhnliche Aktivierung und Clusterbildung von $CD8^+$ T-Zellen im Tumorgewebe (Giordano *et al.*, 2022) und eine Abkapselung dieser durch M2-like polarisierte Makrophagen (Leonardelli *et al.*, 2023) ausschließlich bei Patienten mit vorhergehender Bestrahlung und CXCL-12-Inhibitortherapie. Weitergehende Analysen und die Wiederholung dieser an größeren Patientenkollektiven werden zeigen, ob es sich hierbei um Einzelfälle oder eine allgemein geltende Veränderung handelt.

Der EG12-*Score* wird im Rahmen zusätzlicher Patienteneinschlüsse in die Studie ebenso weitergehend validiert werden müssen. Die Durchführung der diesen Ausführungen zugrundeliegenden Arme der Phase 1/2-Studie erfolgte nur in MGMT-Promotor-unmethylierten Patienten, die epidemiologisch etwa die Hälfte aller GBM-Fälle ausmachen. Es gibt jedoch keine biologischen Gründe, eine Effektivität der Therapie in MGMT-Promotor-methylierten Tumoren anzuzweifeln, weshalb sie auch einer deutlich größeren Patientengruppe offenstehen könnte. Vielmehr stellt die Arbeit einen Ansatz der personalisierten Medizin in den Vordergrund, bei dem EG12 als Biomarker für eine individuelle Therapieentscheidung fungieren könnte. Die Rekrutierung weiterer Studienpatienten wird zeigen, ob die positiven ersten Ergebnisse der GLORIA-Studie sich auch in größeren Kollektiven bestätigen werden und welche weiteren medikamentösen Kombinationen möglicherweise synergistische Wirksamkeit entfalten könnten.

Generell zeigt sich in den vergangenen Jahren eine zusehende Abkehr von dem üblichen Konzept, dass eine Bestrahlung nicht simultan mit einer systemischen Tumortherapie durchgeführt werden sollte. War dies in einigen Fällen für intensive klassische Chemotherapieschemata gut mit Daten beleg- und begründbar, so gilt dies nicht mehr für die neuen Medikamentenklassen, die auf den pharmakoonkologischen Markt drängen. Einerseits weisen diese durch ihren zielgerichteteren Therapieansatz teils ein durchaus akzeptableres Toxizitätsprofil auf (Kroeze *et al.*, 2017). Andererseits erkennt man auch das Potenzial möglicher überadditiver Effekte durch systemische Ergänzung der Radiatio an und ist bereit, dafür zu einem gewissen Grad Toxizitätsrisiken in Kauf zu nehmen (Zhang *et al.*, 2022). Es gibt jedoch unter den bereits etablierten zielgerichteten Therapien auch Kombinationspartner wie die BRAF- und MEK-Inhibitoren, die sich in klinischen

Studien als schlecht verträglich mit einer Strahlentherapie erwiesen und daher nicht simultan eingenommen werden sollten (Anker *et al.*, 2016). Wichtig ist daher die frühe und sorgfältige klinische Prüfung potenzieller Kombinationen, sowohl um die Patienten zu schützen, als auch um bestehende Behandlungspfade allein durch Neukombination verfügbarer therapeutischer Substanzen verbessern zu können.

Neben den klinischen Unterschieden strahlentherapeutischer Behandlungskonzepte, die in den physikalischen Grundlagen, technischen Abläufen und insbesondere dem medizinischen Ergebnis zum Ausdruck kommen, sind im Sinne einer ganzheitlichen Betrachtung auch patientenzentrierte Faktoren und die ökonomischen Dimensionen der Behandlung zu berücksichtigen. Für das Glioblastom gibt es bislang keine ausreichenden Daten, die eine generelle Verkürzung der Behandlung erlauben würden. Lediglich bestimmte Patientengruppen mit reduziertem Allgemeinzustand und höherem Alter profitieren von einer moderaten (Perry *et al.*, 2017) bis intensivierten (Malmström et al, 2012) Hypofraktionierung. Die Strahlentherapie bleibt die unbestrittene konsolidierende Säule der GBM-Therapie und es bedarf statt einer Therapieverkürzung primär sinnvoll ergänzbarer systemischer Kombinationspartner und wirksamer Optionen der Therapieeskalation zu dieser bei einer weiterhin unzureichend kontrollierten, hochaggressiven Erkrankung.

Hingegen sind Hirnmetastasen durch alle geläufigen strahlentherapeutischen Konzepte einer hinreichenden lokalen Tumor- und Symptomkontrolle zuzuführen, während eine relevante extrazerebrale Tumorkontrolle ohnehin durch diese Therapie, abseits von Einzelfällen, bislang nicht erzielbar ist. Hier sollte daher eine sorgsame Abwägung der therapeutischen Konzepte mit Berücksichtigung individueller Patientenfaktoren und -wünsche erfolgen. Durch eine hypofraktionierte Bestrahlung ergeben sich volkswirtschaftlich betrachtet und bezogen auf den Einzelfall Einsparungspotenziale im Rahmen der fraktionsbasierten ambulanten Abrechnung der Strahlentherapie. Darüber hinaus jedoch führt diese, insbesondere in Zeiten des Fachkräftemangels, zu relevant reduzierten Belegungszeiten für die Geräte, wodurch diese somit zudem früher weiteren Patienten zur Verfügung gestellt werden können. Der Patient profitiert von einer reduzierten Fraktionszahl durch geringeren Aufwand und ersparter Zeit, die im Krankenhaus oder einem Transportmittel dorthin verbracht werden muss, was gerade für

fortgeschrittene Krebsleiden eine erhebliche Verbesserung der verbleibenden Lebensqualität darstellen kann (Jocham *et al.*, 2009; Erceg *et al.*, 2013). Die geringfügig verlängerte Bestrahlungszeit der einzelnen Sitzung fällt demgegenüber wenig ins Gewicht. Nicht vernachlässigt werden darf, dass bei einer höheren Einzeldosis die Anforderungen an die technische Präzision und die Verantwortung des beteiligten medizinischen Personals nochmals steigen. Entsprechende Therapien sollten daher nur in geeigneten und erfahrenen Zentren angeboten werden. Ein rascher Abschluss der Strahlentherapie ist jedoch auch im Sinne des therapeutischen Gesamtkonzepts, da der Patient zügiger einer weiteren notwendigen medizinischen Behandlung, vor allem einer etwaigen Einleitung einer systemischen Therapie, zugeführt werden kann.

Die IORT von Hirntumoren stellt eine innovative und, unabhängig vom zumindest nicht-unterlegenen klinischen *Outcome*, im Hinblick auf vielerlei weiche, sekundäre Faktoren gegenüber der klassischen EBRT überlegene Technik dar. So profitieren die Patienten neben einer unmittelbaren Tumorzelleradikation mit effizienter Schonung umgehender gesunder Gewebestrukturen insbesondere von einem rascheren Abschluss der strahlentherapeutischen Behandlung und einer potenziell früheren Einleitung weitergehender onkologischer Behandlungsmaßnahmen. Aktuell versucht die INTRAGO II-Studie zu beantworten, ob eine Dosiseskalation der Bestrahlung des GBM mittels IORT das *Outcome* der Patienten verbessern kann (Giordano *et al.*, 2019). Bei der IORT von Hirnmetastasen handelt es sich hingegen bereits um eine leitliniengerechte lokale Behandlungsoption. Gerade die dieser Arbeit zugrundeliegenden Studien belegen im Einklang mit teils zeitgleich entstandenen Daten anderer Zentren (Bremer *et al.*, 2018; Cifarelli *et al.*, 2019; Kahl *et al.*, 2021; Diehl *et al.*, 2022) eine gute klinische Wirksamkeit insbesondere mit einer beachtlichen lokalen Tumorkontrolle unter besonderer Berücksichtigung der hier untersuchten, prognostisch erheblich ungünstigen Subpopulation von Patienten mit großen Metastasenvolumina.

Unsere Arbeiten liefern ferner ebenso wie die anderer Forschergruppen (Cifarelli *et al.*, 2019; Kahl *et al.*, 2021; Diehl *et al.*, 2022) keine Hinweise auf eine, initial aufgrund der erheblich höheren lokaleren Dosen befürchtete, erhöhte Rate an RNs. Im Gegenteil scheint durch den steilen Dosisgradienten im gesunden Hirngewebe möglicherweise eher ein protektiver Faktor vorzuliegen. Insbesondere der Kombination einer stereotaktischen

zerebralen Bestrahlung mit einer Immuntherapie wohnt aufgrund der immunologisch stimulierenden Systemtherapie ein erhebliches Risiko für ein progredientes Hirnödem und RNs inne (Martin *et al.*, 2018). Bislang hatte niemand untersucht, wie sich eine parallele Immuntherapie auf das Wirkungs- und Nebenwirkungsprofil einer IORT von zerebralen Metastasen auswirken würde. Dies ist besonders relevant, da ein Großteil der mit einer IORT behandelten Patienten entweder an einer großen solitären Metastase erkrankt ist oder eine bislang unbekannte Raumforderung erstdiagnostiziert wurde, die zunächst histologisch gesichert werden muss. In beiden Szenarien finden sich in erheblichem Maße Patienten, deren Tumorerkrankung erstdiagnostiziert wird oder zuletzt nicht behandelt wurde. Erstdiagnostizierte Patienten sind systemisch in aller Regel noch therapienaiv und müssen dringlich einer wirksamen Systemtherapie zugeführt werden, um eine Progression während der Durchführung der Lokaltherapie zu verhindern. Dies gilt im Besonderem für solitär zerebral metastasierte Lungenkarzinome, die prinzipiell noch kurativ behandelbar sind. Insbesondere stellt sich neben den Optionen zur Verkürzung der strahlentherapeutischen Behandlungskonzepte die Frage, wie lange nach der Resektion und Bestrahlung mit der Einleitung einer Systemtherapie gewartet werden muss und ob diese möglicherweise bereits vor der Lokaltherapie initiiert werden kann. Unsere Ergebnisse deuten auf eine relative Unbedenklichkeit der Kombination von Immuntherapien, aber auch vieler anderer zielgerichteter molekularer Therapien in Kombination mit einer Resektion und IORT hin. Ferner sollten zukünftige prospektive Studien explizit die vorzeitige, präoperative Einleitung der Systemtherapie prüfen. Dies erwies sich in unserem multizentrischen, retrospektiv untersuchten Patientenkollektiv als prognostisch günstig und besser verträglich als eine Einleitung unmittelbar nach der Lokaltherapie.

Im Einklang mit Daten anderer Autoren (Patel *et al.*, 2011), ergaben sich auch in unseren Untersuchungen zu Hirnmetastasen Überlebensvorteile für Patienten mit einer Pseudoprogression. Möglicherweise sind postradiogene immunologische Vorgänge für die Größenzunahme und das Ödem der bestrahlten Läsionen verantwortlich, die sich im weiteren Verlauf positiv auf die Tumorkontrolle auswirken. Auf die GLORIA-Studie lässt sich dies aufgrund der geringen Fallzahl nicht übertragen. Jedoch zeigte sich auch hier in erhöhtem Maße eine Pseudoprogression. Dies könnte in der Tat an einer Umgehung der CXCL12-Blockade durch eine verstärkte VEGF-vermittelte Neoangiogenese liegen, die

wiederum mit einer verstärkten Ödembildung charakterisiert ist. Wiederholt wurden daher den RANO-Auswertungen folgend Therapien möglicherweise zu früh abgebrochen.

Ein weiterer Baustein eines patientenzentrierten, aber auch ökonomisch maßvollen multimodalen Therapieansatzes ist die Vermeidung unnötiger Krankenhausaufenthalte, Transportwege und Therapieverzögerungen für den Patienten. Das Ziel einer Behandlung sollte abhängig von den prognostischen Möglichkeiten eine möglichst unmittelbare Rückkehr des Patienten in sein häusliches Umfeld bei maximal geringer Belastung seiner körperlichen wie mentalen Ressourcen darstellen. Dieser Maxime folgend konnten wir in den hier dargestellten Arbeiten zeigen, dass auch abseits der gängigsten gegenwärtigen strahlentherapeutischen FSRT-Therapiekonzepte Möglichkeiten der akzelerierten Radiatio bestehen, ohne dadurch die Prognose der Patienten zwangsweise zu kompromittieren. Strahlentherapeutische Behandlungskonzepte bedürfen einer intensiven und detaillierten Aufklärung mit sorgfältiger Abwägung aller Für und Wider, gerade auch unter Berücksichtigung der weichen Faktoren, die den Patienten aufgrund ihrer Unkenntnis über die medizinischen Abläufe mindestens genauso unbekannt und dennoch wichtig sind, wie die klassischen Erfolgsfaktoren einer onkologischen Therapie (Yahanda *et al.*, 2016).

Die Strahlentherapie steht wie auch die Onkologie erst am Anfang einer umfassenden Umwälzung in Theorie und Praxis, die mit dem Einzug der ICIs begann und sich aus längst nicht erschöpften neuen therapeutischen Optionen noch ergeben wird. Es gilt, diese Potenziale insbesondere auch in der Neuroonkologie zu nutzen und auf ihre Verwendbarkeit für die Optimierung einer strahlentherapeutischen Behandlung zu prüfen. Neben der evidenzbasierten Suche nach möglichst zielgerichteten systemischen Kombinationspartnern im Sinne einer multimodalen, interdisziplinären und individuellen neuroonkologischen Behandlung liegt der Fokus für die strahlentherapeutische Fachgesellschaft hierbei in einer Patientenbetreuung auf Augenhöhe, die die individuellen Patientenbedürfnisse aktiv in die gemeinsam erarbeiteten Konzepte integriert.

5. Zusammenfassung

Maligne Hirntumoren gehen weiterhin mit einer schlechten Prognose einher. Die Strahlentherapie ist eine zentrale Säule der Behandlung sowohl des GBM als auch von Hirnmetastasen. Insbesondere für das GBM mangelt es jedoch weiterhin an dringend benötigten sinnvollen systemtherapeutischen Kombinationspartnern. Die erste Arbeit dieser Kumulation untersuchte im Rahmen einer multizentrischen Phase 1/2-Studie die Verträglichkeit und Wirksamkeit einer CXCL12-Inhibition in Kombination mit einer Bestrahlung im GBM. Hier konnten wir demonstrieren, dass diese neuartige Therapieform sicher sowie gut verträglich ist und überdies 90% der Patienten ein klinisches Ansprechen zeigten. Weitergehende translationale Analysen des TME ermöglichten eine Stratifizierung der Patienten anhand ihrer relativen CXCL12-Expression in den endothelialen und glialen Zellen (EG12-*Score*), wobei Patienten mit hohem EG12-*Score* von einem signifikant längeren PFS profitierten. Unsere Ergebnisse unterstreichen die Notwendigkeit einer tiefgreifenden Charakterisierung des TME, um dringend benötigte therapeutisch adressierbare Phänotypen zu identifizieren, und bilden die Grundlage zur weitergehenden Untersuchung des EG12-*Scores* als möglichen Biomarker zur zielgerichtet-personalisierten Therapie des GBM mit Bestrahlung und CXCL12-Inhibition.

Demgegenüber stehen für die Behandlung von Hirnmetastasen viele zielgerichtete Systemtherapien zur Verfügung, während es jedoch häufig noch an Daten zur Verträglichkeit dieser mit einer parallelen Bestrahlung mangelt. Zudem ergibt sich gerade aus der Vielfalt der Optionen in vielen Fällen ein zeitlicher Behandlungsdruck und Patienten profitieren vom raschen Abschluss einer lokalen Therapiemaßnahme, um für weitere lokale Interventionen oder Systemtherapien zur Sicherstellung des Gesamtbehandlungserfolgs zur Verfügung zu stehen. Mit der IORT von Hirnmetastasen präsentieren unsere hier dargestellten Arbeiten eine sicher durchführbare Alternative zur EBRT, die bei zumindest vergleichbarer klinischer Effektivität und Verträglichkeit trotz der erheblichen Größe der behandelten Volumina in Bezug auf zahlreiche weiche Faktoren Vorteile aufweist. So profitierten die ausgewerteten Patienten von einer kürzeren Hospitalisierungszeit bei unveränderter Kortikosteroidgabedauer, reduziertem persönlichem Aufwand und einer rascheren Zuführung zu konsekutiven Therapien. Zudem konnten wir zeigen, dass auch unüblichere verkürzte FSRT-Konzepte für

Hirnmetastasen mit nur fünf Fraktionen gut verträglich und klinisch wirksam sind. Die Kombination der IORT mit TTs und insbesondere ICIs erwies sich in unserer multizentrischen retrospektiven Auswertung der größten IORT-Fallsammlung überhaupt als insgesamt sicher und führte insbesondere in Bezug auf Wundinfektionen und RNs nicht zu erhöhter Toxizität. Eine systemische TT kann gemäß den vorgestellten Daten möglicherweise bereits vor und sollte spätestens zeitnah nach der IORT eingeleitet werden, um die Gesamtprognose des Patienten nicht zu gefährden. Die Wichtigkeit interdisziplinär abgestimmter, multimodal verzahnter und möglichst zielgerichteter Behandlungskonzepte sowie die Ergründung ihres Einflusses auf das TME wird in der Neuroonkologie in Zukunft weiterhin an Bedeutung gewinnen, um therapeutische Fortschritte für die sehr aggressiven und unverändert ungenügend kontrollierten Erkrankungsverläufe zu erzielen. Hierbei dürfen die Patientenbedürfnisse und die Therapiesicherheit nicht aus dem Blick geraten.

6. Darstellung der Überlappung durch geteilte Autorenschaften

Die vorliegende Habilitationsschrift hat sechs publizierte Originalarbeiten zur Grundlage. Fünf dieser Arbeiten habe ich als Erstautor und eine der Arbeiten als Koautor veröffentlicht. Von den Erstautorenschaften wiederum sind drei geteilt.

Bei der Veröffentlichung der GLORIA-Daten (Giordano *et al.*, Nat Comm 2024) handelt es sich um eine geteilte Erstautorenschaft mit Herrn Prof. Dr. Frank Giordano und Frau Dr. Sonia Leonardelli. Herr Giordano hat als Hauptprüfer und Begründer der GLORIA-Studie die klinische Gesamtverantwortung für die multizentrische Studie und damit auch die erste Veröffentlichung. Die präsentierten klinischen und präklinischen Daten wurden primär durch mich ausgewertet, in Kontext gesetzt und arrangiert. Bei der komplexen Auswertung der experimentellen Daten erhielt ich Unterstützung von zahlreichen Koautoren, wobei Frau Leonardelli aufgrund ihres vorrangigen Anteils an dieser Unterstützung mit einer geteilten Erstautorenschaft berücksichtigt wurde. Das initiale Manuskript wurde von mir geschrieben und von allen Autoren kommentiert sowie bearbeitet. Für unsere Veröffentlichung “Outcome assessment of intraoperative radiotherapy for brain metastases: results of a prospective observational study with comparative matched-pair analysis.” (Layer *et al.*, J Neurooncol 2023) habe ich unter anderem die primäre Datenakquise, -analyse sowie das Schreiben des Manuskripts übernommen. Herr Dr. Motaz Hamed hat den Großteil der chirurgischen Resektionen durchgeführt und erhielt hierfür im Rahmen dieses interdisziplinären Forschungsprojekts als neurochirurgischer Part die geteilte Erstautorenschaft.

In der Publikation „Intraoperative or postoperative stereotactic radiotherapy for brain metastases: time to systemic treatment onset and other patient-relevant outcomes” (Dejonckheere *et al.*, J Neurooncol 2023) habe ich die Datenakquise mit meinem geschätzten Kollegen Herrn Dr. Cas Dejonckheere geteilt. In meinen primären Aufgabenbereich fielen unter anderem die Datenanalyse, Erstellung der Abbildungen sowie Überarbeitung des initial von ihm geschriebenen Manuskripts.

Für weitere Details bitte ich um Konsultation der jeweilig in den Publikationen enthaltenen „*Author contributions*“.

7. Literaturverzeichnis

Aizer AA, Lamba N, Ahluwalia MS, Aldape K, Boire A, Brastianos PK, *et al.* Brain metastases: A Society for Neuro-Oncology (SNO) consensus review on current management and future directions. Neuro Oncol. 2022 Oct 3;24(10):1613–46.

Aldape K, Zadeh G, Mansouri S, Reifenberger G, Von Deimling A. Glioblastoma: pathology, molecular mechanisms and markers. Acta Neuropathol. 2015 Jun;129(6):829–48.

Alexander BM, Ba S, Berger MS, Berry DA, Cavenee WK, Chang SM, *et al.* Adaptive Global Innovative Learning Environment for Glioblastoma: GBM AGILE. Clin Cancer Res. 2018 Feb 15;24(4):737–43.

Anker CJ, Grossmann KF, Atkins MB, Suneja G, Tarhini AA, Kirkwood JM. Avoiding Severe Toxicity From Combined BRAF Inhibitor and Radiation Treatment: Consensus Guidelines from the Eastern Cooperative Oncology Group (ECOG). Int J Radiat Oncol Biol Phys. 2016 Jun 1;95(2):632–46.

Antonia SJ, Villegas A, Daniel D, Vicente D, Murakami S, Hui R, *et al.* Overall Survival with Durvalumab after Chemoradiotherapy in Stage III NSCLC. N Engl J Med. 2018 Dec 13;379(24):2342–50.

Baumgart L, Aftahy AK, Anetsberger A, Thunstedt D, Wiestler B, Bernhardt D, *et al.* Brain metastases in the elderly - Impact of residual tumor volume on overall survival. Front Oncol. 2023;13:1149628.

Becker SJ, Lipson EJ, Jozsef G, Molitoris JK, Silverman JS, Presser J, *et al.* How many brain metastases can be treated with stereotactic radiosurgery before the radiation dose delivered to normal brain tissue rivals that associated with standard whole brain radiotherapy? J Appl Clin Med Phys. 2023 Mar;24(3):e13856.

Bernstein M, Lumley M, Davidson G, Laperriere N, Leung P. Intracranial arterial occlusion associated with high-activity iodine-125 brachytherapy for glioblastoma. J Neurooncol. 1993 Sep;17(3):253–60.

Bernstock JD, Gary SE, Klinger N, Valdes PA, Ibn Essayed W, Olsen HE, *et al.* Standard clinical approaches and emerging modalities for glioblastoma imaging. Neuro-Oncology Advances. 2022 Jan 1;4(1):vdac080.

Blonigen BJ, Steinmetz RD, Levin L, Lamba MA, Warnick RE, Breneman JC. Irradiated volume as a predictor of brain radionecrosis after linear accelerator stereotactic radiosurgery. Int J Radiat Oncol Biol Phys. 2010 Jul 15;77(4):996–1001.

Brandsma D, Stalpers L, Taal W, Sminia P, van den Bent MJ. Clinical features, mechanisms, and management of pseudoprogression in malignant gliomas. Lancet Oncol. 2008 May;9(5):453–61.

Brastianos HC, Cahill DP, Brastianos PK. Systemic Therapy of Brain Metastases. Curr Neurol Neurosci Rep. 2015 Feb;15(2):518.

Brastianos PK, Carter SL, Santagata S, Cahill DP, Taylor-Weiner A, Jones RT, *et al.* Genomic Characterization of Brain Metastases Reveals Branched Evolution and Potential Therapeutic Targets. Cancer Discov. 2015 Nov;5(11):1164–77.

Brehmer S, Welsch M, Karakoyun A, Förster A, Seiz-Rosenhagen M, Clausen S, *et al.* P05.35 Intraoperative radiotherapy after resection of brain metastases (INTRAMET) - initial safety/efficacy analysis of a prospective phase II study, Neuro-Oncology, Volume 20, Issue suppl_3, September 2018, Pages iii310–iii311.

Brown CE, Alizadeh D, Starr R, Weng L, Wagner JR, Naranjo A, *et al.* Regression of Glioblastoma after Chimeric Antigen Receptor T-Cell Therapy. N Engl J Med. 2016 Dec 29;375(26):2561–9.

Brown PD, Ballman KV, Cerhan JH, Anderson SK, Carrero XW, Whitton AC, *et al.* Postoperative stereotactic radiosurgery compared with whole brain radiotherapy for resected metastatic brain disease (NCCTG N107C/CEC·3): a multicentre, randomised, controlled, phase 3 trial. Lancet Oncol. 2017 Aug;18(8):1049–60.

Brown PD, Jaeckle K, Ballman KV, Farace E, Cerhan JH, Anderson SK, *et al.* Effect of Radiosurgery Alone vs Radiosurgery With Whole Brain Radiation Therapy on Cognitive Function in Patients With 1 to 3 Brain Metastases: A Randomized Clinical Trial. JAMA. 2016 Jul 26;316(4):401–9.

Cagney DN, Martin AM, Catalano PJ, Redig AJ, Lin NU, Lee EQ, *et al.* Incidence and prognosis of patients with brain metastases at diagnosis of systemic malignancy: a population-based study. Neuro Oncol. 2017 Oct 19;19(11):1511–21.

Chang EL, Wefel JS, Hess KR, Allen PK, Lang FF, Kornguth DG, *et al.* Neurocognition in patients with brain metastases treated with radiosurgery or radiosurgery plus whole-brain irradiation: a randomised controlled trial. Lancet Oncol. 2009 Nov;10(11):1037–44.

Chinot OL, Wick W, Mason W, Henriksson R, Saran F, Nishikawa R, *et al.* Bevacizumab plus Radiotherapy–Temozolomide for Newly Diagnosed Glioblastoma. N Engl J Med. 2014 Feb 20;370(8):709–22.

Chitti B, Goyal S, Sherman JH, Caputy A, Sarfaraz M, Cifter G, *et al.* The role of brachytherapy in the management of brain metastases: a systematic review. J Contemp Brachytherapy. 2020 Feb;12(1):67–83.

Churilla TM, Chowdhury IH, Handorf E, Collette L, Collette S, Dong Y, *et al.* Comparison of Local Control of Brain Metastases With Stereotactic Radiosurgery vs Surgical Resection: A Secondary Analysis of a Randomized Clinical Trial. JAMA Oncol. 2019 Feb 1;5(2):243–7.

Cifarelli CP, Brehmer S, Vargo JA, Hack JD, Kahl KH, Sarria-Vargas G, *et al.* Intraoperative radiotherapy (IORT) for surgically resected brain metastases: outcome analysis of an international cooperative study. J Neurooncol. 2019 Nov;145(2):391–7.

Davis FG, Dolecek TA, McCarthy BJ, Villano JL. Toward determining the lifetime occurrence of metastatic brain tumors estimated from 2007 United States cancer incidence data. Neuro-Oncology. 2012 Sep;14(9):1171–7.

De Ruysscher D, Niedermann G, Burnet NG, Siva S, Lee AWM, Hegi-Johnson F. Radiotherapy toxicity. Nat Rev Dis Primers. 2019 Feb 21;5(1):13.

Detsky JS, Keith J, Conklin J, Symons S, Myrehaug S, Sahgal A, *et al.* Differentiating radiation necrosis from tumor progression in brain metastases treated with stereotactic radiotherapy: utility of intravoxel incoherent motion perfusion MRI and correlation with histopathology. J Neurooncol. 2017 Sep;134(2):433–41.

Di Giacomo AM, Valente M, Cerase A, Lofiego MF, Piazzini F, Calabrò L, *et al.* Immunotherapy of brain metastases: breaking a “dogma.” J Exp Clin Cancer Res. 2019 Oct 17;38(1):419.

Diehl CD, Pigorsch SU, Gempt J, Krieg SM, Reitz S, Waltenberger M, *et al.* Low-Energy X-Ray Intraoperative Radiation Therapy (Lex-IORT) for Resected Brain Metastases: A Single-Institution Experience. Cancers (Basel). 2022 Dec 20;15(1):14.

Doré M, Martin S, Delpon G, Clément K, Campion L, Thillays F. Stereotactic radiotherapy following surgery for brain metastasis: Predictive factors for local control and radionecrosis. Cancer Radiother. 2017 Feb;21(1):4–9.

Du R, Lu KV, Petritsch C, Liu P, Ganss R, Passegué E, *et al.* HIF1α Induces the Recruitment of Bone Marrow-Derived Vascular Modulatory Cells to Regulate Tumor Angiogenesis and Invasion. Cancer Cell. 2008 Mar;13(3):206–20.

Eichler AF, Chung E, Kodack DP, Loeffler JS, Fukumura D, Jain RK. The biology of brain metastases-translation to new therapies. Nat Rev Clin Oncol. 2011 Jun;8(6):344–56.

Eisenbarth D, Wang YA. Glioblastoma heterogeneity at single cell resolution. Oncogene. 2023 Jun 30;42(27):2155–65.

Eitz KA, Lo SS, Soliman H, Sahgal A, Theriault A, Pinkham MB, *et al.* Multi-institutional Analysis of Prognostic Factors and Outcomes After Hypofractionated Stereotactic Radiotherapy to the Resection Cavity in Patients With Brain Metastases. JAMA Oncol. 2020 Dec 1;6(12):1901–9.

Ellingson BM, Chung C, Pope WB, Boxerman JL, Kaufmann TJ. Pseudoprogression, radionecrosis, inflammation or true tumor progression? challenges associated with glioblastoma response assessment in an evolving therapeutic landscape. J Neurooncol. 2017 Sep;134(3):495–504.

Erceg P, Despotovic N, Milosevic DP, Soldatovic I, Zdravkovic S, Tomic S, *et al.* Health-related quality of life in elderly patients hospitalized with chronic heart failure. Clin Interv Aging. 2013;8:1539–46.

Fearon DT. The carcinoma-associated fibroblast expressing fibroblast activation protein and escape from immune surveillance. Cancer Immunol Res. 2014 Mar;2(3):187–93.

Ferreri AJM, Calimeri T, Cwynarski K, Dietrich J, Grommes C, Hoang-Xuan K, *et al.* Primary central nervous system lymphoma. Nat Rev Dis Primers. 2023 Jun 15;9(1):29.

Giordano FA, Brehmer S, Mürle B, Welzel G, Sperk E, Keller A, *et al.* Intraoperative Radiotherapy in Newly Diagnosed Glioblastoma (INTRAGO): An Open-Label, Dose-Escalation Phase I/II Trial. Neurosurgery. 2019 Jan 1;84(1):41–9.

Giordano FA, Layer JP, Leonardelli S, Friker LL, Seidel C, Schaub C, *et al.* Radiotherapy and olaptesed pegol (NOX-A12) in partially resected or biopsy-only MGMT-unmethylated

glioblastoma: Interim data from the German multicenter phase 1/2 GLORIA trial. JCO. 2022 Jun 1;40(16_suppl):2050–2050.

Giordano FA, Layer JP, Leonardelli S, Friker L, Schaub C, Turiello R, *et al.* CTNI-67. Dual inhibition of past-radiogenic angio-vasculogenesis by olaptesed pegol (NOX-A12) and bevacizumab in glioblastoma – Interim data from the first expansion arm of the German phase 1/2 GLORIA trial. Neuro-Oncology. 2022 Nov 14;24(Supplement_7):vii88–vii88.

Giordano FA, Layer JP, Leonardelli S, Friker L, Schaub C, Zeyen T, *et al.* CTNI-62. Interim data on dual inhibition of post-radiogenic angio-vasculogenesis by olaptesed pegol (NOX-A12) and bevacizumab in glioblastoma from the first expansion arm of the phase 1/2 GLORIA trial. Neuro-Oncology. 2023 Nov 10;25(Supplement_5):v90–1.

Grassl N, Poschke I, Lindner K, Bunse L, Mildenberger I, Boschert T, *et al.* A H3K27M-targeted vaccine in adults with diffuse midline glioma. Nat Med. 2023 Oct;29(10):2586–92.

Grimmer M, Sarria GR, Hamed M, Banat M, Kugel F, Lorenzana H, *et al.* Image-guided intraoperative radiotherapy after surgical resection of brain metastases: a first in-human feasibility report. Advances in Radiation Oncology. 2024 Feb;101466.

Han JH, Kim DG, Chung HT, Paek SH, Park CK, Jung HW. Radiosurgery for large brain metastases. Int J Radiat Oncol Biol Phys. 2012 May 1;83(1):113–20.

Haslam A, Prasad V. Estimation of the Percentage of US Patients With Cancer Who Are Eligible for and Respond to Checkpoint Inhibitor Immunotherapy Drugs. JAMA Netw Open. 2019 May 3;2(5):e192535.

Hegi ME, Diserens AC, Gorlia T, Hamou MF, de Tribolet N, Weller M, *et al.* MGMT gene silencing and benefit from temozolomide in glioblastoma. N Engl J Med. 2005 Mar 10;352(10):997–1003.

Herrlinger U, Tzaridis T, Mack F, Steinbach JP, Schlegel U, Sabel M, *et al.* Lomustine-temozolomide combination therapy versus standard temozolomide therapy in patients with newly diagnosed glioblastoma with methylated MGMT promoter (CeTeG/NOA-09): a randomised, open-label, phase 3 trial. Lancet. 2019 Feb 16;393(10172):678–88.

Herskind C, Ma L, Liu Q, Zhang B, Schneider F, Veldwijk MR, *et al.* Biology of high single doses of IORT: RBE, 5 R's, and other biological aspects. Radiat Oncol. 2017 Jan 19;12(1):24.

Huang K, Sneed PK, Kunwar S, Kragten A, Larson DA, Berger MS, *et al.* Surgical resection and permanent iodine-125 brachytherapy for brain metastases. J Neurooncol. 2009 Jan;91(1):83–93.

Jocham HR, Dassen T, Widdershoven G, Middel B, Halfens R. The Effect of Palliative Care in Home Care and Hospital on Quality of Life: Journal of Hospice & Palliative Nursing. 2009 Mar;11(2):119–26.

Jung E, Alfonso J, Osswald M, Monyer H, Wick W, Winkler F. Emerging intersections between neuroscience and glioma biology. Nat Neurosci. 2019 Dec;22(12):1951–60.

Jünger ST, Pennig L, Schödel P, Goldbrunner R, Friker L, Kocher M, *et al.* The Debatable Benefit of Gross-Total Resection of Brain Metastases in a Comprehensive Treatment Setting. Cancers (Basel). 2021 Mar 21;13(6):1435.

Kahl KH, Balagiannis N, Höck M, Schill S, Roushan Z, Shiban E, *et al.* Intraoperative radiotherapy with low-energy x-rays after neurosurgical resection of brain metastases-an Augsburg University Medical Center experience. Strahlenther Onkol. 2021 Dec;197(12):1124–30.

Kargiotis O, Geka A, Rao JS, Kyritsis AP. Effects of irradiation on tumor cell survival, invasion and angiogenesis. J Neurooncol. 2010 Dec;100(3):323–38.

Karschnia P, Young JS, Dono A, Häni L, Sciortino T, Bruno F, *et al.* Prognostic validation of a new classification system for extent of resection in glioblastoma: A report of the RANO resect group. Neuro-Oncology. 2023 May 4;25(5):940–54.

Keime-Guibert F, Chinot O, Taillandier L, Cartalat-Carel S, Frenay M, Kantor G, *et al.* Radiotherapy for glioblastoma in the elderly. N Engl J Med. 2007 Apr 12;356(15):1527–35.

Kim PH, Suh CH, Kim HS, Kim KW, Kim DY, Aizer AA, *et al.* Immune checkpoint inhibitor therapy may increase the incidence of treatment-related necrosis after stereotactic radiosurgery for brain metastases: a systematic review and meta-analysis. Eur Radiol. 2021 Jun;31(6):4114–29.

Kocher M, Soffietti R, Abacioglu U, Villà S, Fauchon F, Baumert BG, *et al.* Adjuvant whole-brain radiotherapy versus observation after radiosurgery or surgical resection of one to three cerebral metastases: results of the EORTC 22952-26001 study. J Clin Oncol. 2011 Jan 10;29(2):134–41.

Kohutek ZA, Yamada Y, Chan TA, Brennan CW, Tabar V, Gutin PH, *et al.* Long-term risk of radionecrosis and imaging changes after stereotactic radiosurgery for brain metastases. J Neurooncol. 2015 Oct;125(1):149–56.

Kroeze SGC, Fritz C, Hoyer M, Lo SS, Ricardi U, Sahgal A, *et al.* Toxicity of concurrent stereotactic radiotherapy and targeted therapy or immunotherapy: A systematic review. Cancer Treatment Reviews. 2017 Feb;53:25–37.

Lamba N, Cagney DN, Brigell RH, Martin AM, Besse LA, Catalano PJ, *et al.* Neurosurgical Resection and Stereotactic Radiation Versus Stereotactic Radiation Alone in Patients with a Single or Solitary Brain Metastasis. World Neurosurg. 2019 Feb;122:e1557–61.

Lamba N, Kearney RB, Catalano PJ, Hassett MJ, Wen PY, Haas-Kogan DA, *et al.* Population-based estimates of survival among elderly patients with brain metastases. Neuro Oncol. 2021 Apr 12;23(4):661–76.

Lamba N, Wen PY, Aizer AA. Epidemiology of brain metastases and leptomeningeal disease. Neuro Oncol. 2021 Sep 1;23(9):1447–56.

Le Rhun E, Preusser M, Roth P, Reardon DA, van den Bent M, Wen P, *et al.* Molecular targeted therapy of glioblastoma. Cancer Treat Rev. 2019 Nov;80:101896.

Lee JH, Lee JE, Kahng JY, Kim SH, Park JS, Yoon SJ, *et al.* Human glioblastoma arises from subventricular zone cells with low-level driver mutations. Nature. 2018 Aug;560(7717):243–7.

Lehrer EJ, Peterson JL, Zaorsky NG, Brown PD, Sahgal A, Chiang VL, *et al.* Single versus Multifraction Stereotactic Radiosurgery for Large Brain Metastases: An International Meta-analysis of 24 Trials. Int J Radiat Oncol Biol Phys. 2019 Mar 1;103(3):618–30.

Leonardelli S, Layer JP, Friker LL, Turiello R, Van Der Voort G, Corvino D, *et al.* 508MO Spatial remodeling of the immune tumor microenvironment after radiotherapy and CXCL12 inhibition in glioblastoma in the phase I/II GLORIA trial. Annals of Oncology. 2023 Oct;34:S395.

Lim M, Weller M, Idbaih A, Steinbach J, Finocchiaro G, Raval RR, *et al.* Phase III trial of chemoradiotherapy with temozolomide plus nivolumab or placebo for newly diagnosed glioblastoma with methylated MGMT promoter. Neuro Oncol. 2022 Nov 2;24(11):1935–49.

Liu Q, Schneider F, Ma L, Wenz F, Herskind C. Relative Biologic Effectiveness (RBE) of 50 kV X-rays measured in a phantom for intraoperative tumor-bed irradiation. Int J Radiat Oncol Biol Phys. 2013 Mar 15;85(4):1127–33.

Louis DN, Perry A, Wesseling P, Brat DJ, Cree IA, Figarella-Branger D, *et al.* The 2021 WHO Classification of Tumors of the Central Nervous System: a summary. Neuro Oncol. 2021 Aug 2;23(8):1231–51.

Ma Y, Wang Q, Dong Q, Zhan L, Zhang J. How to differentiate pseudoprogression from true progression in cancer patients treated with immunotherapy. Am J Cancer Res. 2019;9(8):1546–53.

Mahajan A, Ahmed S, McAleer MF, Weinberg JS, Li J, Brown P, *et al.* Post-operative stereotactic radiosurgery versus observation for completely resected brain metastases: a single-centre, randomised, controlled, phase 3 trial. Lancet Oncol. 2017 Aug;18(8):1040–8.

Malmström A, Grønberg BH, Marosi C, Stupp R, Frappaz D, Schultz H, *et al.* Temozolomide versus standard 6-week radiotherapy versus hypofractionated radiotherapy in patients older than 60 years with glioblastoma: the Nordic randomised, phase 3 trial. Lancet Oncol. 2012 Sep;13(9):916–26.

Martin AM, Cagney DN, Catalano PJ, Alexander BM, Redig AJ, Schoenfeld JD, *et al.* Immunotherapy and Symptomatic Radiation Necrosis in Patients With Brain Metastases Treated With Stereotactic Radiation. JAMA Oncol. 2018 Aug 1;4(8):1123–4.

Mehta MP, Paleologos NA, Mikkelsen T, Robinson PD, Ammirati M, Andrews DW, *et al.* The role of chemotherapy in the management of newly diagnosed brain metastases: a systematic review and evidence-based clinical practice guideline. J Neurooncol. 2010 Jan;96(1):71–83.

Mellinghoff IK, Van Den Bent MJ, Blumenthal DT, Touat M, Peters KB, Clarke J, *et al.* Vorasidenib in IDH1- or IDH2-Mutant Low-Grade Glioma. N Engl J Med. 2023 Aug 17;389(7):589–601.

Minniti G, Clarke E, Lanzetta G, Osti MF, Trasimeni G, Bozzao A, *et al.* Stereotactic radiosurgery for brain metastases: analysis of outcome and risk of brain radionecrosis. Radiat Oncol. 2011 May 15;6:48.

Minniti G, Niyazi M, Alongi F, Navarria P, Belka C. Current status and recent advances in reirradiation of glioblastoma. Radiat Oncol. 2021 Feb 18;16(1):36.

Minniti G, Scaringi C, Paolini S, Lanzetta G, Romano A, Cicone F, *et al.* Single-Fraction Versus Multifraction (3 × 9 Gy) Stereotactic Radiosurgery for Large (>2 cm) Brain Metastases: A Comparative Analysis of Local Control and Risk of Radiation-Induced Brain Necrosis. Int J Radiat Oncol Biol Phys. 2016 Jul 15;95(4):1142–8.

Morabito R, Alafaci C, Pergolizzi S, Pontoriero A, Iati' G, Bonanno L, *et al.* DCE and DSC perfusion MRI diagnostic accuracy in the follow-up of primary and metastatic intra-axial brain tumors treated by radiosurgery with cyberknife. Radiat Oncol. 2019 Apr 15;14(1):65.

Mulvenna P, Nankivell M, Barton R, Faivre-Finn C, Wilson P, McColl E, *et al.* Dexamethasone and supportive care with or without whole brain radiotherapy in treating patients with non-small cell lung cancer with brain metastases unsuitable for resection or stereotactic radiotherapy (QUARTZ): results from a phase 3, non-inferiority, randomised trial. Lancet. 2016 Oct 22;388(10055):2004–14.

Nayak L, Lee EQ, Wen PY. Epidemiology of brain metastases. Curr Oncol Rep. 2012 Feb;14(1):48–54.

Nieder C, Stanisavljevic L, Aanes SG, Mannsåker B, Haukland EC. 30-day mortality in patients treated for brain metastases: extracranial causes dominate. Radiat Oncol. 2022 Dec;17(1):92.

Niyazi M, Andratschke N, Bendszus M, Chalmers AJ, Erridge SC, Galldiks N, *et al.* ESTRO-EANO guideline on target delineation and radiotherapy details for glioblastoma. Radiotherapy and Oncology. 2023 Jul;184:109663.

Nordal RA, Nagy A, Pintilie M, Wong CS. Hypoxia and hypoxia-inducible factor-1 target genes in central nervous system radiation injury: a role for vascular endothelial growth factor. Clin Cancer Res. 2004 May 15;10(10):3342–53.

Ogasawara C, Philbrick BD, Adamson DC. Meningioma: A Review of Epidemiology, Pathology, Diagnosis, Treatment, and Future Directions. Biomedicines. 2021 Mar 21;9(3):319.

Omuro A, Brandes AA, Carpentier AF, Idbaih A, Reardon DA, Cloughesy T, *et al.* Radiotherapy combined with nivolumab or temozolomide for newly diagnosed glioblastoma with unmethylated MGMT promoter: An international randomized phase III trial. Neuro Oncol. 2023 Jan 5;25(1):123–34.

Ostrom QT, Adel Fahmideh M, Cote DJ, Muskens IS, Schraw JM, Scheurer ME, *et al.* Risk factors for childhood and adult primary brain tumors. Neuro Oncol. 2019 Nov 4;21(11):1357–75.

Ostrom QT, Cioffi G, Gittleman H, Patil N, Waite K, Kruchko C, *et al.* CBTRUS Statistical Report: Primary Brain and Other Central Nervous System Tumors Diagnosed in the United States in 2012-2016. Neuro Oncol. 2019 Nov 1;21(Suppl 5):v1–100.

Pan D, Rong X, Chen D, Jiang J, Ng WT, Mai H, *et al.* Mortality of early treatment for radiation-induced brain necrosis in head and neck cancer survivors: A multicentre, retrospective, registry-based cohort study. eClinicalMedicine. 2022 Oct;52:101618.

Panagiotakos G, Alshamy G, Chan B, Abrams R, Greenberg E, Saxena A, *et al.* Long-term impact of radiation on the stem cell and oligodendrocyte precursors in the brain. PLoS One. 2007 Jul 11;2(7):e588.

Parvez K, Parvez A, Zadeh G. The diagnosis and treatment of pseudoprogression, radiation necrosis and brain tumor recurrence. Int J Mol Sci. 2014 Jul 3;15(7):11832–46.

Patel TR, McHugh BJ, Bi WL, Minja FJ, Knisely JPS, Chiang VL. A comprehensive review of MR imaging changes following radiosurgery to 500 brain metastases. AJNR Am J Neuroradiol. 2011;32(10):1885–92.

Perry JR, Laperriere N, O'Callaghan CJ, Brandes AA, Menten J, Phillips C, *et al.* Short-Course Radiation plus Temozolomide in Elderly Patients with Glioblastoma. N Engl J Med. 2017 Mar 16;376(11):1027–37.

Platten M, Bunse L, Wick A, Bunse T, Le Cornet L, Harting I, *et al.* A vaccine targeting mutant IDH1 in newly diagnosed glioma. Nature. 2021 Apr 15;592(7854):463–8.

Putz F, Pirschel W, Fietkau R. FSRT-Trial: erste Phase-III-Studie zum Vergleich fraktionierte stereotaktische Radiotherapie (FSRT) versus Einzeitradiochirurgie (SRS) bei Hirnmetastasen. Forum. 2022 Jun;37(3):241–5.

Reardon DA, Brandes AA, Omuro A, Mulholland P, Lim M, Wick A, *et al.* Effect of Nivolumab vs Bevacizumab in Patients With Recurrent Glioblastoma: The CheckMate 143 Phase 3 Randomized Clinical Trial. JAMA Oncol. 2020 Jul 1;6(7):1003–10.

Reuss DavidE. Updates on the WHO diagnosis of IDH-mutant glioma. J Neurooncol. 2023 May;162(3):461–9.

Ruben JD, Dally M, Bailey M, Smith R, McLean CA, Fedele P. Cerebral radiation necrosis: incidence, outcomes, and risk factors with emphasis on radiation parameters and chemotherapy. Int J Radiat Oncol Biol Phys. 2006 Jun 1;65(2):499–508.

Schödel P, Schebesch KM, Brawanski A, Proescholdt M. Surgical Resection of Brain Metastases—Impact on Neurological Outcome. IJMS. 2013 Apr 24;14(5):8708–18.

Seute T, Leffers P, Wilmink JT, ten Velde GPM, Twijnstra A. Response of asymptomatic brain metastases from small-cell lung cancer to systemic first-line chemotherapy. J Clin Oncol. 2006 May 1;24(13):2079–83.

Sneed PK, Mendez J, Vemer-van den Hoek JGM, Seymour ZA, Ma L, Molinaro AM, *et al.* Adverse radiation effect after stereotactic radiosurgery for brain metastases: incidence, time course, and risk factors. J Neurosurg. 2015 Aug;123(2):373–86.

Sperduto PW, Kased N, Roberge D, Xu Z, Shanley R, Luo X, *et al.* Summary Report on the Graded Prognostic Assessment: An Accurate and Facile Diagnosis-Specific Tool to Estimate Survival for Patients With Brain Metastases. JCO. 2012 Feb 1;30(4):419–25.

Stummer W, Reulen HJ, Meinel T, Pichlmeier U, Schumacher W, Tonn JC, *et al.* Extent of resection and survival in glioblastoma multiforme: Identification of and adjustment for bias. Neurosurgery. 2008 Mar;62(3):564–76.

Stupp R, Hegi ME, Mason WP, van den Bent MJ, Taphoorn MJB, Janzer RC, *et al.* Effects of radiotherapy with concomitant and adjuvant temozolomide versus radiotherapy alone on survival in glioblastoma in a randomised phase III study: 5-year analysis of the EORTC-NCIC trial. Lancet Oncol. 2009 May;10(5):459–66.

Suh JH, Kotecha R, Chao ST, Ahluwalia MS, Sahgal A, Chang EL. Current approaches to the management of brain metastases. Nat Rev Clin Oncol. 2020 May;17(5):279–99.

Tabatabai G, Frank B, Möhle R, Weller M, Wick W. Irradiation and hypoxia promote homing of haematopoietic progenitor cells towards gliomas by TGF-beta-dependent HIF-1alpha-mediated induction of CXCL12. Brain. 2006 Sep;129(Pt 9):2426–35.

Terakawa Y, Tsuyuguchi N, Iwai Y, Yamanaka K, Higashiyama S, Takami T, *et al.* Diagnostic accuracy of 11C-methionine PET for differentiation of recurrent brain tumors from radiation necrosis after radiotherapy. J Nucl Med. 2008 May;49(5):694–9.

Tesileanu CMS, Sanson M, Wick W, Brandes AA, Clement PM, Erridge SC, *et al.* Temozolomide and Radiotherapy versus Radiotherapy Alone in Patients with Glioblastoma, IDH-wildtype: Post Hoc Analysis of the EORTC Randomized Phase III CATNON Trial. Clin Cancer Res. 2022 Jun 13;28(12):2527–35.

Thomas RP, Nagpal S, Iv M, Soltys SG, Bertrand S, Pelpola JS, *et al.* Macrophage Exclusion after Radiation Therapy (MERT): A First in Human Phase I/II Trial using a CXCR4 Inhibitor in Glioblastoma. Clin Cancer Res. 2019 Dec 1;25(23):6948–57.

Tsien CI, Pugh SL, Dicker AP, Raizer JJ, Matuszak MM, Lallana EC, *et al.* NRG Oncology/RTOG1205: A Randomized Phase II Trial of Concurrent Bevacizumab and Reirradiation Versus Bevacizumab Alone as Treatment for Recurrent Glioblastoma. J Clin Oncol. 2023 Feb 20;41(6):1285–95.

Tye K, Engelhard HH, Slavin KV, Nicholas MK, Chmura SJ, Kwok Y, *et al.* An analysis of radiation necrosis of the central nervous system treated with bevacizumab. J Neurooncol. 2014 Apr;117(2):321–7.

Vaidya JS, Joseph DJ, Tobias JS, Bulsara M, Wenz F, Saunders C, *et al.* Targeted intraoperative radiotherapy versus whole breast radiotherapy for breast cancer (TARGIT-A trial): an international, prospective, randomised, non-inferiority phase 3 trial. The Lancet. 2010 Jul;376(9735):91–102.

Vellayappan B, Tan CL, Yong C, Khor LK, Koh WY, Yeo TT, *et al.* Diagnosis and Management of Radiation Necrosis in Patients With Brain Metastases. Front Oncol. 2018;8:395.

Verhaak E, Gehring K, Hanssens PEJ, Sitskoorn MM. Health-related quality of life of patients with brain metastases selected for stereotactic radiosurgery. J Neurooncol. 2019 Jul;143(3):537–46.

Vogelbaum MA, Angelov L, Lee SY, Li L, Barnett GH, Suh JH. Local control of brain metastases by stereotactic radiosurgery in relation to dose to the tumor margin. J Neurosurg. 2006 Jun;104(6):907–12.

von Knebel Doeberitz N, Kroh F, Breitling J, König L, Maksimovic S, Graß S, *et al.* CEST imaging of the APT and ssMT predict the overall survival of patients with glioma at the

first follow-up after completion of radiotherapy at 3T. Radiother Oncol. 2023 Jul;184:109694.

Wang L, Jung J, Babikir H, Shamardani K, Jain S, Feng X, *et al.* A single-cell atlas of glioblastoma evolution under therapy reveals cell-intrinsic and cell-extrinsic therapeutic targets. Nat Cancer. 2022 Dec 20;3(12):1534–52.

Weller M, van den Bent M, Preusser M, Le Rhun E, Tonn JC, Minniti G, *et al.* EANO guidelines on the diagnosis and treatment of diffuse gliomas of adulthood. Nat Rev Clin Oncol. 2021 Mar;18(3):170–86.

Wen PY, Van Den Bent M, Youssef G, Cloughesy TF, Ellingson BM, Weller M, *et al.* RANO 2.0: Update to the Response Assessment in Neuro-Oncology Criteria for High- and Low-Grade Gliomas in Adults. JCO. 2023 Nov 20;41(33):5187–99.

Wick W, Dettmer S, Berberich A, Kessler T, Karapanagiotou-Schenkel I, Wick A, *et al.* N2M2 (NOA-20) phase I/II trial of molecularly matched targeted therapies plus radiotherapy in patients with newly diagnosed non-MGMT hypermethylated glioblastoma. Neuro Oncol. 2019 Jan 1;21(1):95–105.

Wick W, Platten M, Meisner C, Felsberg J, Tabatabai G, Simon M, *et al.* Temozolomide chemotherapy alone versus radiotherapy alone for malignant astrocytoma in the elderly: the NOA-08 randomised, phase 3 trial. Lancet Oncol. 2012 Jul;13(7):707–15.

Wick W. *et al.*, Gliome, S2k-Leitlinie, 2021, in: Deutsche Gesellschaft für Neurologie (Hrsg.), Leitlinien für Diagnostik und Therapie in der Neurologie. Online: www.dgn.org/leitlinien (abgerufen am 09.03.2024)

Wilke C, Grosshans D, Duman J, Brown P, Li J. Radiation-induced cognitive toxicity: pathophysiology and interventions to reduce toxicity in adults. Neuro Oncol. 2018 Apr 9;20(5):597–607.

Yamamoto M, Sato Y, Serizawa T, Kawabe T, Higuchi Y, Nagano O, *et al.* Subclassification of Recursive Partitioning Analysis Class II Patients With Brain Metastases Treated Radiosurgically. International Journal of Radiation Oncology*Biology*Physics. 2012 Aug;83(5):1399–405.

Yamamoto M, Serizawa T, Shuto T, Akabane A, Higuchi Y, Kawagishi J, *et al.* Stereotactic radiosurgery for patients with multiple brain metastases (JLGK0901): a multi-institutional prospective observational study. Lancet Oncol. 2014 Apr;15(4):387–95.

Zaiss M, Windschuh J, Paech D, Meissner JE, Burth S, Schmitt B, *et al*. Relaxation-compensated CEST-MRI of the human brain at 7T: Unbiased insight into NOE and amide signal changes in human glioblastoma. Neuroimage. 2015 May 15;112:180-188.

Zeyen T, Paech D, Weller J, Schäfer N, Tzaridis T, Duffy C, *et al.* Undetected pseudoprogressions in the CeTeG/NOA-09 trial: hints from postprogression survival and MRI analyses. J Neurooncol. 2023 Sep;164(3):607–16.

Zhang Z, Liu X, Chen D, Yu J. Radiotherapy combined with immunotherapy: the dawn of cancer treatment. Sig Transduct Target Ther. 2022 Jul 29;7(1):258.

8. Danksagung

Diese Arbeit stellt eine Zusammenschau meines wissenschaftlichen Wirkens in den vergangenen Jahren dar, bildet aufgrund des kumulativen Charakters jedoch nur einen Teil der tatsächlichen Projekte ab. Sicherlich wäre jede einzelne der hier behandelten, wie auch der in dieser Habilitation nicht behandelten Arbeiten nicht möglich gewesen ohne die zahlreiche Unterstützung vieler fantastischer Kollegen und Koautoren. Ich möchte jedem einzelnen von ihnen für die vielen Arbeitsstunden danken, die in Veröffentlichungen geflossen sind, die letztlich meinen Namen an prominenter Stelle trugen. Auf dem gemeinsamen Weg sind viele Freundschaften entstanden, die nicht nur die gemeinsamen Projekte tragen, und hierfür bin ich sehr dankbar.

Mein besonderer Dank gilt meinem damaligen Doktorvater Prof. Dr. Michael Hölzel, der mir die Grundlagen wissenschaftlichen Arbeitens seinerzeit beigebracht und mich seitdem unermüdlich unterstützt hat. Nicht zuletzt waren gute Gespräche mit ihm der Grund für meine Rückkehr nach Bonn 2021. Drei Jahre später kann ich glücklich sagen, dass dies die richtige Entscheidung gewesen war. Ebenso danke ich Prof. Dr. Frank Giordano, dessen Abteilung mich in Bonn schon am ersten Tag freundschaftlich aufgenommen hatte und der von diesem Moment an ein für mich verblüffendes Vertrauen in meine Fähigkeiten hatte und mir ungeahnten Freiraum in der Ausübung meiner wissenschaftlichen Tätigkeit zubilligte. Dies galt insbesondere auch für die GLORIA-Studie, die über viele Jahre hinweg bereits sein Herzensprojekt gewesen war, bevor es meines wurde. Die CXCL12-Inhibition im Glioblastom hat großes Potenzial und ich bin mir sicher, dass wir erst an dessen Oberfläche zu kratzen begonnen haben. Ich danke meiner Chefin Frau Prof. Dr. Eleni Gkika sehr für die Betreuung dieser Arbeit und ihre fortwährende Unterstützung, sodass ich auch unter neuer Leitung meine Forschungsprojekte ungehindert fortführen kann. Ich danke auch PD Dr. Christopher Schmeel für die gute Zusammenarbeit bei unseren gemeinsamen Projekten. Bei Prof. Dr. Martin Stuschke und Prof. Dr. Martin Schuler möchte ich mich für die sehr lehrreiche Zeit in Essen bedanken. Mein Dank geht an das gesamte Team der Klinik für Strahlentherapie und Radioonkologie und des Instituts für Experimentelle Onkologie für ihre Unterstützung. Besonders hervorzuheben sind Frau Dr. Sonia Leonardelli und Frau Dr. Roberta Turiello aus dem IEO sowie Herr Dr. Gustavo Sarria und Herr Dr. Cas Dejonckheere aus der Strahlentherapie. Die

Projekte, die wir gemeinsam in den vergangenen Jahren aufgebaut und durchgeführt haben, bereiteten mir bei aller intensiven Arbeit sehr viel Spaß und haben mich Vieles gelehrt.

Ich danke ferner der Studienstiftung des deutschen Volkes, der Else Kröner-Fresenius-Stiftung, der Novartis-Stiftung für therapeutische Forschung, der Manfred Lautenschläger-Stiftung sowie der Bonner Universitätsgesellschaft für ihre ideelle und materielle Förderung meiner wissenschaftlichen Laufbahn in den vergangenen 10 Jahren.

Ein besonderer Dank geht an die Korrekturleser dieser Arbeit, die ich in der Familie zwangsrekrutiert habe – meinen Schwager Felix Malter, meinen Vater Prof. Dr. Günter Layer sowie meine Brüder Dr. Yannik Layer und Yonah Layer. Ich bedanke mich an dieser Stelle weiterhin bei meinen Freunden und Bekannten für ihre Unterstützung und für ihr Verständnis für mich und mein insbesondere forschungsbedingt oft ausbaufähiges Zeitmanagement, das sich weiter einfach nicht zum Besseren wenden will. Zu guter Letzt gilt mein besonderer Dank auch in dieser Hinsicht meiner Familie. Meinen Eltern, die mich von Kindesbeinen an gefördert und mir all das ermöglicht haben. Meinen Brüdern, ohne die ich nicht der wäre, der ich bin. Meinen Großeltern, die stets an uns glaubten und diese Arbeit nun leider nicht mehr lesen können. Und natürlich meiner Frau Katharina, die mich ohne zu zögern seit nunmehr über zwölf Jahren auf all meinen Schritten begleitet und mich nicht nur bei dieser Arbeit in jeder erdenklichen Form unterstützt hat. Ich freue mich unendlich darauf, unseren Sohn kennenzulernen.

Die Strahlentherapie im Allgemeinen und ihre neuroonkologischen Aspekte im Speziellen sind, zumindest in der Außenwirkung auf Dritte, zuweilen ein eher düsteres und deprimierendes Tätigkeitsfeld. Es mag daher viele überraschen, wenn ich hier schreibe, dass diese Arbeit sehr sinnstiftend und schön sein kann. Ich danke aufrichtig allen Patienten, die in den vergangenen Jahren das Wertvollste überhaupt, ihre Gesundheit, vertrauensvoll in unsere Hände gelegt und an unseren Studien teilgenommen haben. Ihre Willensstärke und Kraft wie auch ihre Positivität sind mir ein Vorbild und Ansporn, weiter für Verbesserungen unserer Therapien zu kämpfen. Den Glauben, dass uns dies gelingt, sind wir ihnen schuldig.

Ich möchte diese Arbeit daher gerne beschließen mit einem weiteren Zitat von Lemony Snicket: “At times the world may seem an unfriendly and sinister place, but believe that there is much more good in it than bad. All you have to do is look hard enough. And what might seem to be a series of unfortunate events may in fact be the first steps of a journey.”